# 520,000 years of environmental change in West Africa

## Thesis

The Open University

# 520,000 years of environmental change in West Africa

**Charlotte S. Miller**
B.Sc. (Hons.) University of Leeds
MPhil. Brunel University

Submitted in accordance with the requirements for the degree of Doctor of Philosophy

July 2013

Date of Submission: 22 August 2013
Date of Award: 10 February 2014.

Department of Environment, Earth and Ecosystems
Centre for Earth, Planetary, Space and Astronomical Research
The Open University
United Kingdom

BRITISH LIBRARY

**IMAGING SERVICES NORTH**

Boston Spa, Wetherby
West Yorkshire, LS23 7BQ
www.bl.uk

# THESIS CONTAINS DAMAGED CD/DVD ROMs

# -UNABLE TO COPY-

# THIS THESIS CONTAINS A CD

# Abstract

Global temperatures are predicted to rise by 2–2.5°C by 2065, profoundly affecting the Earth's environment. The response of ecosystems to past climate fluctuations can inform on how systems will respond in the future. This thesis focuses on Quaternary environmental changes in West Africa, a region important because of its high ecological value and role in the global carbon cycle.

In 2004, the International Continental Drilling Program recovered *c.* 291m of sediments spanning the last *c.* 1 Myr from Lake Bosumtwi (Ghana). Pollen, charcoal and nitrogen isotopes ($\delta^{15}N$) were analysed from the most recent *c.* 150m (*c.* 520 kyr). The latitudinal position and long duration of this core makes it unique for understanding West African monsoon dynamics and vegetation change.

To aid characterisation of the Bosumtwi pollen succession, an atlas of present-day pollen was constructed for 364 pollen and spore taxa.

The pollen record from Bosumtwi reveals dynamic vegetation change over the last *c.* 520 kyr, characterized by eleven biome shifts between savannah and forest. Savannah vegetation is dominated by Poaceae (>55%) associated with Cyperaceae, Chenopodiaceae-Amaranthaceae and Caryophyllaceae. Forest vegetation is palynologically diverse, but broadly characterised by Moraceae, *Celtis*, *Uapaca*, *Macaranga* and *Trema*. Low $\delta^{15}N$ values correspond to forest expansion and these are driven by high lake levels. The timescale indicates that the six periods of forest expansion correspond to global interglacial periods. The record indicates that the wettest climate occurred during the Holocene, and the driest during Marine Isotope Stage 7.

The vegetation and $\delta^{15}N$ records show a strong response to glacial-interglacial variability between 520–320 kyr and 130–0 kyr. Between 320–130 kyr there is a

weaker response to glacial-interglacial cycles probably related to high eccentricity during the peak of the 400-kyr component of eccentricity, with high eccentricity resulting in greater seasonality and ultimately drier conditions.

# Acknowledgements

First and foremost I would like to thank my supervisors William Gosling and Angela Coe, who have provided me with much needed advice and encouragement over the last 3 years 7 months. Additionally, I am also hugely indebted to Dave Kemp (and his love of wiggles), for his guidance on the use of spectral analysis, and for his ability to calm me down through numerous episodes of 'chronology panic'. Without you three, this thesis would not have been possible. I would also like to thank Mabs Gilmour for her assistance with the nitrogen isotope ratio determination, her kindness, patience and willingness to explain even the most basic geochemistry was a god-send!

There are numerous people, both in the department and outside, who I'd like to thank. Firstly I'd like to thank Nats. Without you, especially over the last few months, I would have been lost. You're always willing to help and listen. You were the best (and cleanest) housemate that I could have ever asked for. Secondly, I'd like to thank my office mates: Liz, Anne, Luce (and Nats) for huge amounts of encouragement as well as more tea breaks than I can count. Special thanks go to Jimmy, for friendly games of football, always loosing at squash (ha), beer and banter.

I'd also like to thank the guys from BLC: Steve, Emma P, Emma W and Liv. Thank you for the huge amount of encouragement. Steve 'aka Gym Dad' thank you for the sweaty spin sessions, the pain really took my mind off the thesis. Emma P 'aka Gym Mum', thank you for feeding me and giving me a bed.

Thesis writing in Scotland was made somewhat bearable by Uncle Michael, Auntie Lynne and Oscar. Thank you for all the yummy food, starting my lawn mower for me and taking me fishing (yay!).

Mum, Dad and Grandma your support over the last 27 years has been invaluable. I would like to especially thank my Grandad, whom I dedicate this thesis to. You always believed in me, and look, after 9 years at uni, I've finally finished. Now I can get a 'real' job!

# Table of Contents

## Chapter 4: Geochronology and methods



## Chapter 5: Atlas of the tropical West African pollen flora



## Chapter 6: Quaternary forest associations in lowland tropical West Africa

## List of figures

## List of tables



## List of equations



## CD Appendix

# 1. Introduction

## 1.1. Rationale and research objectives

Evidence that the climate is changing today is overwhelming (IPCC, 2007). Anthropogenic carbon dioxide ($CO_2$) emissions are considered to be the major warming agent having committed the Earth to a global warming of 2.4°C, surpassing the 2°C 'threshold for dangerous anthropogenic interference' regardless of any mitigation procedure (Ramanathan and Feng, 2008). Even with immediate mitigation (capping $CO_2$ and other greenhouse emissions by 2015), followed by 3 % global emission reductions annually thereafter, modelled temperatures would still increase by 2–2.5°C come 2065. Providing the suggested 3 % annual emission reductions are maintained over the next century, the expected temperature change is reduced to *c.* 1°C warming by 2300 (IPCC, 2007). Nevertheless, these emission reductions represent a significant societal challenge, requiring substantially reduced use of fossil fuels, deforestation and agricultural practices. Regardless of policy, society will have to learn how to adapt to global climate change (Buob and Stephan, 2011). According to the fourth Intergovernmental Panel on Climate Change (IPCC) Assessment Report, "the adaptation to climate change occurs through adjustment to reduce the vulnerability or to enhance the resilience of societies in response to observed or expected changes in climate and extreme weather events" (IPCC, 2007). Significant global environmental changes have already occurred; instrumental measurements and time series over the last *c.* 160 years indicate that average surface temperatures have risen globally by *c.* 0.74°C. Changes have also been observed in the amount, intensity, frequency and type of precipitation; for example, more precipitation now falls as rain rather than as snow in northern regions and in some regions there have been increases in the occurrence of both droughts and floods (IPCC, 2007).

The study of sedimentary archives has provided evidence that the climate has varied considerably in the past, without anthropogenic intervention, responding to forces such as the Earth's orbital geometry and plate tectonics, which are themselves in continuous motion (Zachos et al., 2001). In the geological record, the main mechanism for driving temperature change (of a similar magnitude to that which is predicted in the future (±2°C)) is fluctuations in the Earth's orbital parameters; precession, obliquity and eccentricity, which affect the quantity (and distribution) of solar radiation received by the Earth. These oscillations in orbital parameters have caused the Earth to go through a series of transitions from warm (interglacial) to cold (glacial) conditions during the last 2.6 million years (Quaternary). Global temperature change between glacial and interglacial climatic modes is estimated to be *c.* 5°C (Delcourt and Delcourt, 1991). One way in which we can improve our understanding regarding the response of the environment to future high magnitude variations in climate is to examine past records which span periods of comparable magnitude global climate change.

The region of the globe from which we have the least amount of information regarding past climate change is the continental tropics (28°N–28°S); in part, due to the lack of long terrestrial records of past climatic change (Verschuren et al., 2000). Developing an improved understanding of the past climate and environment in the tropics is critical because of the key role the region plays for global climate systems, past hominid evolution and biodiversity.

Africa represents one of the most vulnerable continents to climate change, with this vulnerability intensified by existing socio-economic challenges including, poverty, complex governance, poor infrastructure and technology, societal conflict and ecosystem degradation (IPCC, 2007). The vulnerability of Africa makes it particularly important to improve our understanding of how future climate is likely to affect both the environment and future populations. Extreme climate events such as the Sahel Drought beginning in the 1960's and peaking in the mid-1970s displaced millions of people and is one of the most extreme observed climatic changes in the world

(Nicholson, 2001; Nicholson and Grist, 2001; IPCC, 2007). The Sahel droughts focused scientific attention on better understanding West African monsoon (WAM) variability and extreme climatic events in the historical record (Nicholson, 2009 and references herein).

Additionally, archaeological and genetic studies have unambiguously pointed to Africa as the origin of human populations (Balter, 2002; McDougall et al., 2005). A thorough understanding of how hominid societies responded to past climate change may give us an indication of the future of *Homo sapiens* in the face of global warming.

The grasslands and forests of West Africa may play an important role in the global climate system. Recent studies suggest that the positive feedback triggered by anthropogenic vegetation degradation over West Africa was a significant mechanism for drought persistence during the Sahel droughts (Wang and Eltahir, 2000 and referenes therein). Additionally, quantifying the response of tropical African vegetation to changing global climate conditions is important in predicting future levels of atmospheric carbon dioxide, as West African forests act as both sources, from deforestation (0.2 Pg C $year^{-1}$) and sinks, from forest photosynthesis (+0.4 Pg C year-1; Bousquet et al., 1999; Rayner et al., 1999). The West African forests are regarded as a biodiversity hotspot, featuring a large concentration of endemic species which are likely to experience an exceptional loss of habitat due to future global warming (Myers et al., 2000). In West Africa, the 3–4°C predicted regional warming by 2100 threatens the stability of current vegetation associations (IPCC, 2007), and little is known about the resilience of the natural vegetation to such high magnitude climate change.

Although the Quaternary does not provide a direct analogue for an anthropogenically-induced warm world, it does provide situations where the climate has changed abruptly and global temperatures were warmer than at present. These past periods of warm climate can then be used to help anticipate the response of vegetation to the predicted regional warming. Specifically, there are four periods in the Quaternary which could

provide useful insight into the global system response to predicted climate change. These are Marine Isotope Stage (MIS) 5e (*c.* 130–115 thousand years ago [kyr]), MIS 9 (*c.* 334–301 kyr), MIS 11 (*c.* 424–374 kyr) and MIS 13 (*c.* 528–474 kyr). MIS 5e has long been regarded as a potential analogue for future climatic warming despite orbital configuration dissimilarities (Kukla et al., 1997), with estimates of global temperatures ranging from 0.5–2°C warmer than at present (Montoya et al., 1998); these warm global conditions are directly comparable to the future estimates of global temperature increase (IPCC, 2007). The longest and warmest interglacial interval over the last 500 kyr is considered by some to be MIS 11 (*c.* 424–374 kyr; Howard, 1997). Having a similar orbital configuration to present day, MIS 11 may be a good analogue for future warming (Loutre and Berger, 2003). The deuterium signal from Vostok ice-core records indicate the highest temperatures in Antarctica during the last 500 kyr occur during MIS 9 (Petit et al., 1999), these high temperatures may be analogous to future warming. High amplitude, millennial scale variations in climate have been recorded in ice records during MIS 13 and the transition into MIS 12; consequently MIS 13 may be a key interval to investigate the effects of rapid climatic fluctuations on the environment.

Published terrestrial West African instrumental and palaeoclimatic records cover <28 kyr (Section 2.3; Maley, 1991; Maley and Brenac, 1998) and are therefore insufficient to capture the pattern of vegetation response over the past potential analogues for future global warming provided by previous interglacial periods. Terrestrial records of past vegetation change spanning the most recent global temperature rise of comparable magnitude to the predicted future warming (last glacial-interglacial transition *c.* 21–10 kyr) from West Africa indicate the expansion of forests into previously savannah dominated regions (Maley, 1991; Elenga et al., 1994; Maley and Brenac, 1998). Long marine records offshore western Africa indicate that the pattern of forest expansion with global warming was repeated throughout the latter half of the Quaternary period (Dupont et al., 2000). In this thesis I present the first terrestrial record from West Africa of past climate variability encompassing multiple periods of

known high-magnitude climatic variability. I provide information on the controlling mechanisms of monsoonal rainfall and explore how ecosystems responded to past changes in climate through the vegetation and lake level reconstruction in Lake Bosumtwi (Ghana). Such climate change and ecosystem response is likely to have direct implications for the evolution and migration of modern human populations.

## 1.2. Research Aims

Within this thesis I address three specific research aims:

1. The accurate identification of pollen and spores is imperative when using palynology to reconstruct past vegetation. Research aim 1 is to construct a pollen atlas to be used for the identification of pollen and spores in West Africa, further enabling palynologists working in Africa to identify pollen within sedimentary successions. Although significant African-wide pollen atlases do exist, this atlas will focus on taxa commonly found in tropical West Africa.

2. To predict the pattern of vegetation response in West Africa to future global warming, we can analyse the fossil terrestrial record over past periods of global warmth (*i.e.* interglacials). Research aim 2 is to characterise the palynolgical (floristic) composition of past interglacial vegetation communities in western tropical Africa over the last 520 kyr.

3. Uncertainty exists as to what aspects of climate change are important for instigating biome shifts in West Africa. Research aim 3 is to assess the role of high and low-latitude forcing mechanisms on vegetation and lake level change in western tropical Africa over the last 520 kyr.

## 1.3. Structure of thesis

This thesis examines the fossil pollen and nitrogen isotopes contained within sediment cores obtained from Lake Bosumtwi to reconstruct vegetation and lake moisture

balance over the last *c.* 520 kyr. This introductory chapter is followed by two chapters which provide a detailed background to palaeoenvironmental change (Chapter 2) and the study region (Chapter 3). Methods used within this study are detailed in Chapter 4. The next three chapters are written in the style of manuscripts for publication in international journals and represent the key output and findings of this research. The first paper (Chapter 5) is the tropical West African pollen atlas, which provides a foundation for this thesis, enabling the identification of fossil pollen within the Lake Bosumtwi record. The second paper (Chapter 6) presents the Lake Bosumtwi pollen data over the last *c.* 520 kyr, characterising forest (interglacial) vegetation associations and comparing past forest associations with the modern-day ecoregion vegetation of West Africa. The third paper (Chapter 7) presents the Lake Bosumtwi Poaceae abundance and nitrogen isotope data over the last *c.* 520 kyr; the temporal pattern of biome and lake level change is subsequently characterised. The final chapter of the thesis (Chapter 8) summarises the findings from Chapters 5–7 and draws conclusions on the research aims (Section 1.2).

# 2. Palaeoenvironmental change

## 2.1. Orbital forcing and global climate change

The study of sedimentary successions and ice cores indicate that over the last 500 kyr the Earth has experienced both extreme climatic events and continuous climatic change (Zachos et al., 2001). Since the middle of the nineteenth century, Quaternary climatic change has dominated research on past climate (e.g. Hays et al., 1976; Imbrie et al., 1984). Through the improvement of dating techniques during the 1960's and 70's it was recognised that the climatic variability over the last 500 kyr was driven by high frequency changes in climate ($10^4$ to $10^5$ years) at periodicities near 23, 41 and 100 kyr (Imbrie, 1992), a finding which renewed interest in the Milankovitch theory (Milanković, 1930). It was Milanković who first hypothesized that summer insolation changes at the periods of orbital tilt and precession, which, in turn drive northern hemisphere ice volume, with summer ablation the mechanism connecting forcing and response (Milanković, 1930; Ruddiman, 2006). The three parameters controlling the perturbations in the Earth's orbit are: eccentricity, obliquity and precession.

### *2.1.1 Eccentricity*

Eccentricity is the shape of the Earth's orbit which varies from almost circular (low eccentricity; 0.005) to elliptic (high eccentricity; 0.058; Fig. 2.1A). Eccentricity affects the climate by modulating the amplitude of precession, influencing the strength of the seasons and the total annual/seasonal solar energy budget (Zachos et al., 2001). During times of high eccentricity (more elliptical orbit) the effect of precession on the seasonal cycle is strong. When eccentricity is low (more circular orbit) the Earth experiences smaller seasonal contrasts. The major periodicity of eccentricity is 404 kyr, but shorter periods also average around 100 kyr.

### 2.1.2 Obliquity

Obliquity or tilt of the Earth's axis relative to the plane of the elliptic varies between 22.1° and 24.5° at a periodicity of 41 kyr (Fig. 2.1B). A high angle of tilt increases the seasonal contrast between the hemispheres, leading to cooler winters in both hemispheres and warmer summers. An increase in the meridional gradient of the annual mean insolation, *i.e.* high tilt/seasonality causes a strengthening of the atmospheric and oceanic circulation transporting more heat pole-ward and reducing sea surface temperatures (SSTs) at low-latitudes (Mantsis et al., 2011). The effect of obliquity forcing is greatest at high latitudes, with low latitudes sites experiencing minimal oscillations in insolation. Mean annual insolation forcing at the equator differs by -3 W $m^{-2}$ between times of high and low obliquity, whereas at 90° and 65° insolation differs by 15.4 and 6.5 W $m^{-2}$ respectively (Lee and Poulsen, 2005).

### 2.1.3 Axial precession

Precession is the wobble of the Earth's axis of rotation describing a circle in space, due to the pull of the Moon and Sun on the Earth's equatorial bulge (Zachos et al., 2001). The precession about the Earth's axis takes approximately 23–19 kyr (Fig. 2.1C). Modulated by orbital eccentricity (Fig. 2.1A), precession determines where on the Earth's orbit around the sun the seasons occur, increasing and decreasing the seasonal contrast in the hemispheres. Axial precession is felt strongest at the equator, although the influence of high and low latitude processes on African climate will be discussed further in Section 2.3.2.

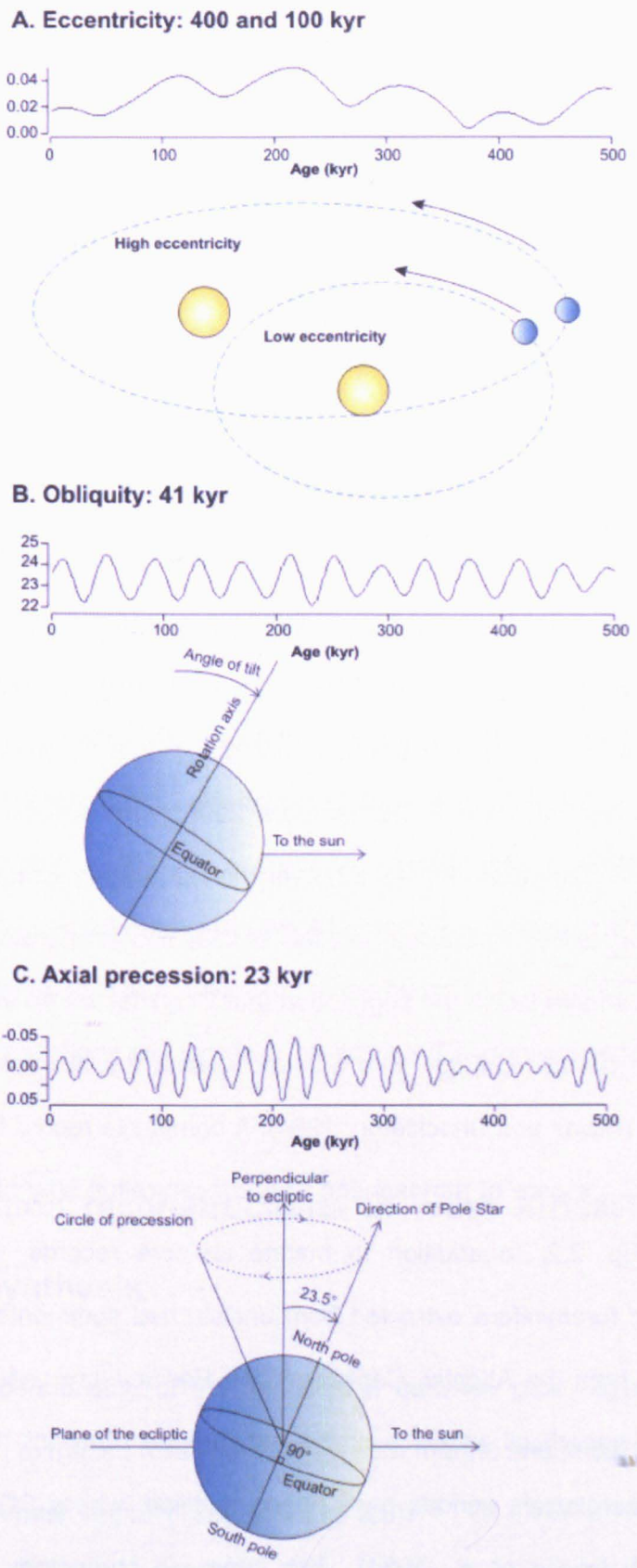


**Fig. 2.1.** Three primary orbital components: eccentricity (400 and 100 kyr), obliquity (41 kyr) and precession (23 and 19 kyr). Orbital configurations are shown for each component (Laskar, 2011). **A).** Eccentricity refers to the shape of the Earth's orbit around the sun from near circular (low eccentricity) to elliptical (high eccentricity). **B).** Obliquity refers to the tilt of the Earth's axis relative to the plane of the elliptical between 22.1° to 24.5°. **C).** Precession refers to the wobble of the Earth's axis with a period of *c.* 26 kyr.

### 2.1.4 Earth system response to orbital variations

The periodic and quasi-periodic oscillations of the Earth's orbital parameters of eccentricity (100 kyr), obliquity (41 kyr) and precession (23 kyr; Fig. 2.1) have manifest themselves as cyclic fluctuations in oxygen isotopes and other palaeoclimate proxy data over last 500 kyr (Hays et al., 1976; Imbrie et al., 1984; Hooghiemstra, 1988; Baker et al., 2001). The orbital oscillations are responsible for the waxing and waning of ice sheets (Berger, 1978), affecting the distribution and amount of incident solar radiation (Imbrie, 1992; Zachos et al., 2001). The concentration of the gases contained within the Vostok ice-core (Antarctica) were subsequently tuned to orbital parameters giving a record of atmospheric gases over the last *c.* 400 kyr (Shackleton, 2000; Bender, 2002). In 2004, the European Project for Ice Coring in Antarctica (EPICA) drilled a second Antarctic core from Dome Concordia (Dome C) producing a climate record covering the last 740 kyr (EPICA members, 2004). Atmospheric $CO_2$ is strongly coupled with Antarctic temperature ($r^2$=0.82) over the last eight glacial cycles. (Petit et al., 1999; Luthi et al., 2008). The close parallels of $CO_2$ and temperature profiles from the Antarctic records have led to the suggestion that $CO_2$ may be an important driving factor for long-term climatic change, with $CO_2$ modulating the direct effects of orbital insolation changes (Pisias and Shackleton, 1984). A composite record from the Vostok and EPICA Dome C ice core of atmospheric $CO_2$ concentration spanning the last 500 kyr is shown in Fig. 2.2. In addition to marine ice-core records, oxygen isotope analyses of pelagic foraminifera extracted from undisturbed sedimentary successions in the deep ocean from the Atlantic, Caribbean and Pacific were used to reconstruct the temperature of superficial waters over the last 300 kyr (Emiliani, 1955). Over the last 500 kyr, six interglacials periods have been identified, where $CO_2$ concentration was high (Fig. 2.2; Imbrie et al., 1984). With improved chronology, the deep sea records now provide an independent climatostratigraphic sequence of which can be compared to ice-cores and terrestrial successions (Lowe and Walker, 1997).

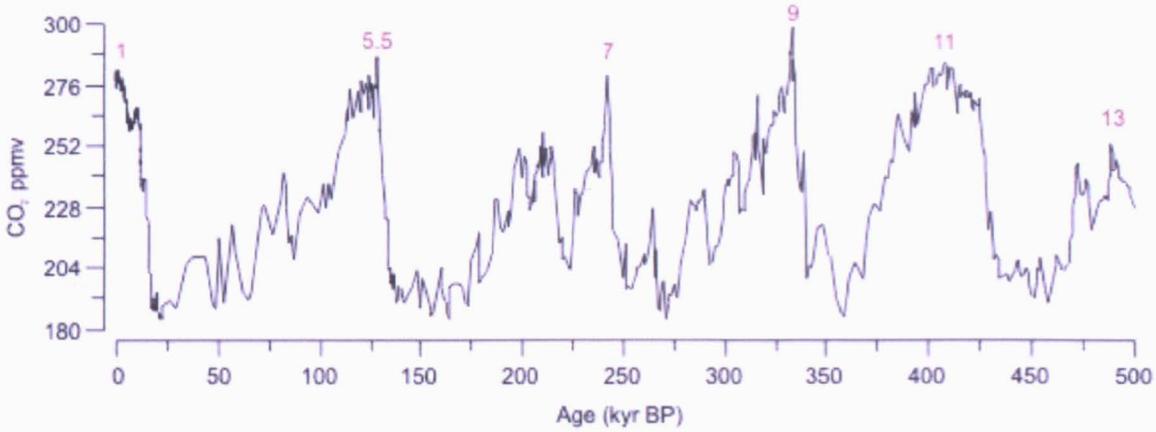


**Fig. 2.2.** Composite $CO_2$ record from Vostok and EPICA Dome C ice cores from 500 kyr to present (Petit et al., 1999; Monnin et al., 2001; Siegenthaler et al., 2005; Luthi et al., 2008). Peaks in $CO_2$ concentration are coincident with interglacial Marine Isotope Stages 1, 5e, 7, 9, 11 and 13; numbers in red indicating timing, based on (Luthi et al., 2008).

## 2.2. Future climate projections in West Africa

Climate projections for the 'business as usual' (A1B) scenario indicate that temperatures in West Africa are expected to rise by 1.9–4.7°C by the end of the century (Christensen, 2007). The precipitation response over the next century is uncertain with multi-model data for the A1B scenario indicating that the precipitation may decrease by up to 9 % but could increase by up to 13 % (IPCC, 2007). If realised, these climate projections will increase pressure on endemic species within the West African region.

## 2.3. Vegetation reconstructions in West Africa: a marine and terrestrial synthesis

To improve understanding of the relationship between past vegetation and climate, previous studies extracted fossil pollen from both marine and terrestrial sediment cores from the West African region (Table 2.1; Fig. 2.3).

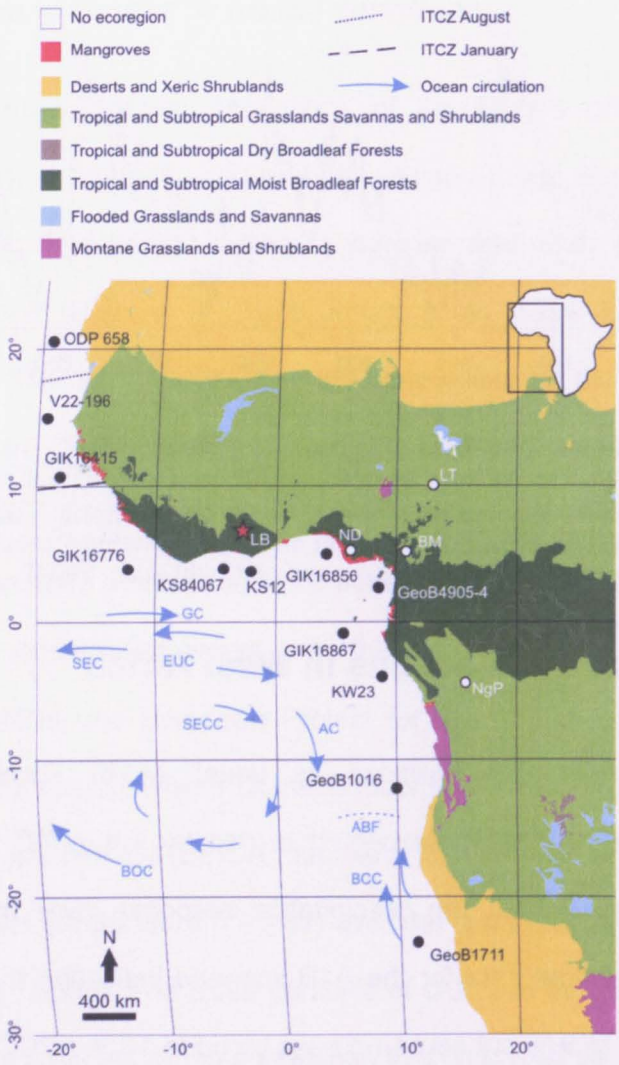


**Fig. 2.3.** Map of the modern vegetation biomes of West Africa (White et al., 1983; Olson et al., 2001) with climatological and oceanographic characteristics as well as the location of Lake Bosumtwi and other records relevant to this study (Table 2.1). LB = Lake Bosumtwi, LT = Lake Tilla, ND = Niger Delta, BM = Barombi Mbo, NgP = Ngamakala Pond; GC = Guinea Current; SEC = South Equatorial Current; EUC = Equatorial Undercurrent; SECC = South Equatorial Counter-Current; AC = Angola Current; BOC = Benguela Ocean Current; BCC = Benguela Coastal Current; ABF = Angola-Benguela-Front. Oceanographic surface currents taken from Dupont et al. (2000). Note ITCZ does not extend over land.

The following section summarises data from the sediment cores listed in Table 2.1 using a series of 'time-slice maps', showing what information is available from each of the MIS during the last *c.* 500 kyr. For each time period fossil pollen data are compared with the modern-day vegetation biomes (Fig. 2.3; Section 3.1.2.1) of West Africa (Olson et al., 2001).

| Site | Location | Depositional setting | Duration (kyr) | Reference |
|---|---|---|---|---|
| GIK 16867 | 2°12'S, 5°6E | Marine | 700–0 | Dupont et al., 1998 |
| GIK 16415 | 9°34'N, 19°05'W | Marine | 700–0 | Dupont and Agwu, 1992 |
| ODP 658 | 20°44.95'N, 18°34.85'W | Marine | >670–0 | Dupont et al., 1989 |
| GIK 16776 | 3°44.1'N, 11°23.9'W | Marine | 400–0 | Jahns et al., 1998 |
| KS84067 | 4°07'35'N 4°06'95'W | Marine | 225–0 | Frédoux, 1994 |
| GeoB1016 | 11°46'S, 11°41'E | Marine | 200–0 | Ning and Dupont, 1997 |
| GIK 16856 | 4°48'N, 3°24'E | Marine | *c.* 150–0 | Dupont and Weinelt, 1996 |
| V22-196 | 13°50'N, 18°57'W | Marine | 140–0 | Lezine, 1991 |
| GeoB1711-4 | 23°18.9'S, 12°22.6'E | Marine | 135–0 | Shi et al., 2001 |
| KW23 | 3°46'S, 9°17'E | Marine | 135–0 | Bengo and Maley, 1991 |
| Niger Delta | 4°33'N, 6°26'E | Delta | 35–0 | Sowunmi, 1981 |
| Lake Barombi-Mbo | 4°67'N, 9°40'E | Lake | 32–0 | Maley and Brenac, 1998 |
| GeoB4905-4 | 2°30'N, 9°23.4'E | Marine | 30–0 | Marret et al., 2013 |
| Lake Bosumtwi | 6°30'N, 1°25'W | Lake | 27.5–0 | Maley, 1991 |
| Ngamakala Pond | 4°4'30S, 15°23'E | Swamp | 24–0 | Elenga et al., 1994 |
| KS12 | 3°52'N 1°56'W | Marine | 22–9 | Lezine and Vergnaud-Grazzini, 1993 |
| Lake Tilla | 10°23'N, 12°08'E | Lake | 17–0 | Salzmann et al., 2002 |

**Table 2.1.** Fossil pollen records from the marine and terrestrial cores of West Africa. Records shown are those covering at least one major climate event (*i.e.* records spanning at least the last *c.* 17 kyr).

### *2.3.1 Past interglacial vegetation in West tropical Africa*

#### *2.3.1.1 West African vegetation during Marine Isotope Stage 13*

Only three marine cores (ODP 658, GIK16415 and GIK16867) provide a vegetation record of MIS 13 (Table 2.1; Fig. 2.3; Fig. 2.4). Site ODP 658 (offshore Mauritania) shows MIS 13 as having high abundances of Poaceae and Chenopodiaceae-Amaranthaceae which are characteristic of the Tropical and Subtropical Grassland biome (Dupont et al., 1989). Core GIK16415 (southwest of Dakar), indicates that the vegetation of early MIS 13 was abundant in ferns and *Uapaca* representing an expansion of the Tropical and Subtropical Moist Broadleaf Forest biome (Dupont and Agwu, 1992). High abundances of taxa from the Montane Grasslands and Shrubland biome are evident in marine core GIK16867 (off Gabon; Dupont et al., 1998).

*2.3.1.2 West African vegetation during Marine Isotope Stage 11*

Only four marine cores (ODP 658, GIK16415, GIK16867 and GIK16776) provide a vegetation record of MIS 11 (Table 2.1; Fig. 2.3; Fig. 2.4). The vegetation during MIS 11 at site ODP 658 contains the high abundances of Poaceae and Chenopodiaceae-Amaranthaceae which are characteristic of the Tropical and Subtropical Grassland biome (Dupont et al., 1989). Additionally, site ODP 658 displays increased abundances of *Rhizophora*, implying high sea level. Site GIK16415 contains an increase in fern spores and *Rhizophora* abundance during late MIS 11 (Dupont and Agwu, 1992). A large expansion of the montane taxa *Podocarpus* is seen in marine cores GIK16867 and GIK16776 (Dupont et al., 1998; Jahns et al., 1998). Pollen influx values are high at site GIK16867 (Dupont et al., 1998).

*2.3.1.3 West African vegetation during Marine Isotope Stage 9*

Only four marine cores (ODP 658, GIK16415, GIK16867 and GIK16776) provide a vegetation record of MIS 9 (Table 2.1; Fig. 2.3; Fig. 2.5). Again site ODP 658 displays high abundances of taxa characteristic of the Tropical and Subtropical Grassland biome (Dupont et al., 1989). Sites GIK16415, GIK16867 and GIK16776 indicate an expansion of the Tropical and Subtropical Moist Broadleaf Forest and the Mangrove biome (Dupont and Agwu, 1992; Dupont et al., 1998; Jahns et al., 1998).

*2.3.1.4 West African vegetation during Marine Isotope Stage 7*

Just five marine cores (ODP 658, GIK16415, GIK16867, GIK16776 and KS84067 provide a vegetation record of MIS 7 (Table 2.1; Fig. 2.3; Fig. 2.5). At site ODP 658 the climate is classed as having 'intermediate humidity' and low trade wind strength, although generally containing taxa characteristic of the Tropical and Subtropical Grassland biome (Dupont et al., 1989). Ferns and *Rhizophora* dominate the vegetation of MIS 7 at sites GIK16776 and GIK16415 (Dupont and Agwu, 1992; Jahns et al., 1998). Sites GIK16415, GIK16867, GIK16776 and KS84067 (off the Ivory Coast) all provide evidence of an expansion of the Tropical and Subtropical Moist Broadleaf

Forest and Mangrove biomes in West Africa during MIS 7 (Dupont and Agwu, 1992; Frédoux, 1994; Dupont et al., 1998; Jahns et al., 1998).

*2.3.1.5 West African vegetation during Marine Isotope Stage 5e*

Eight marine cores (ODP 658, V22-196, GIK16415, KS84067, GIK16856, KW23, GeoB1016 and GeoB1711) provide a record of vegetation during the last interglacial in West Africa (Table 2.1; Fig. 2.3; Fig. 2.6). Sub-stage MIS 5e is missing in sites GIK16867, GIK16776 and GIK16856 (L. Dupont, pers. com). Sites ODP 658 and V22-196 are dominated by taxa typical of the Tropical and Subtropical Grassland biome such as Chenopodiaceae-Amaranthaceae and Poaceae. Marine site GIK16415 contains low pollen concentration but high fern spore abundance (Dupont and Agwu, 1992). Core KS84067, GIK16856 and KW23 record an increase in elements characteristic of the Tropical and Subtropical Moist Broadleaf Forest and Mangrove biome and indicate a retreat in the Montane Grasslands and Shrubland biome during MIS 5e (Fig. 2.6; Bengo and Maley, 1991; Frédoux, 1994; Dupont and Weinelt, 1996).

*2.3.1.6 West African vegetation during the Holocene*

The West African Holocene vegetation is well documented in both terrestrial and marine cores (Table 2.1; Fig. 2.3; Fig. 2.6). Although generally recording high grassland concentrations through the Holocene, GIK16415 records an increase in fern spore percentages and taxa comprising the modern-day Tropical and Subtropical Moist Broadleaf Forest biome at *c.* 15 kyr (Fig. 2.6; Dupont and Agwu, 1992). Sites GIK16856, KS84067, GIK16867 as well as terrestrial records from Lake Bosumtwi and Lake Barombi-Mbo record an increase in taxa from modern-day Tropical and Subtropical Moist Broadleaf Forest biome during the Holocene (Fig. 2.6; Maley, 1991; Frédoux, 1994; Dupont and Weinelt, 1996; Dupont et al., 1998; Maley and Brenac, 1998). Sites KS12 and the Niger Delta indicate the spread of mangrove swamps after the Last Glacial Maximum, into the Holocene but a retreat in their extent toward present day (Sowunmi, 1981; Lezine and Vergnaud-Grazzini, 1993).

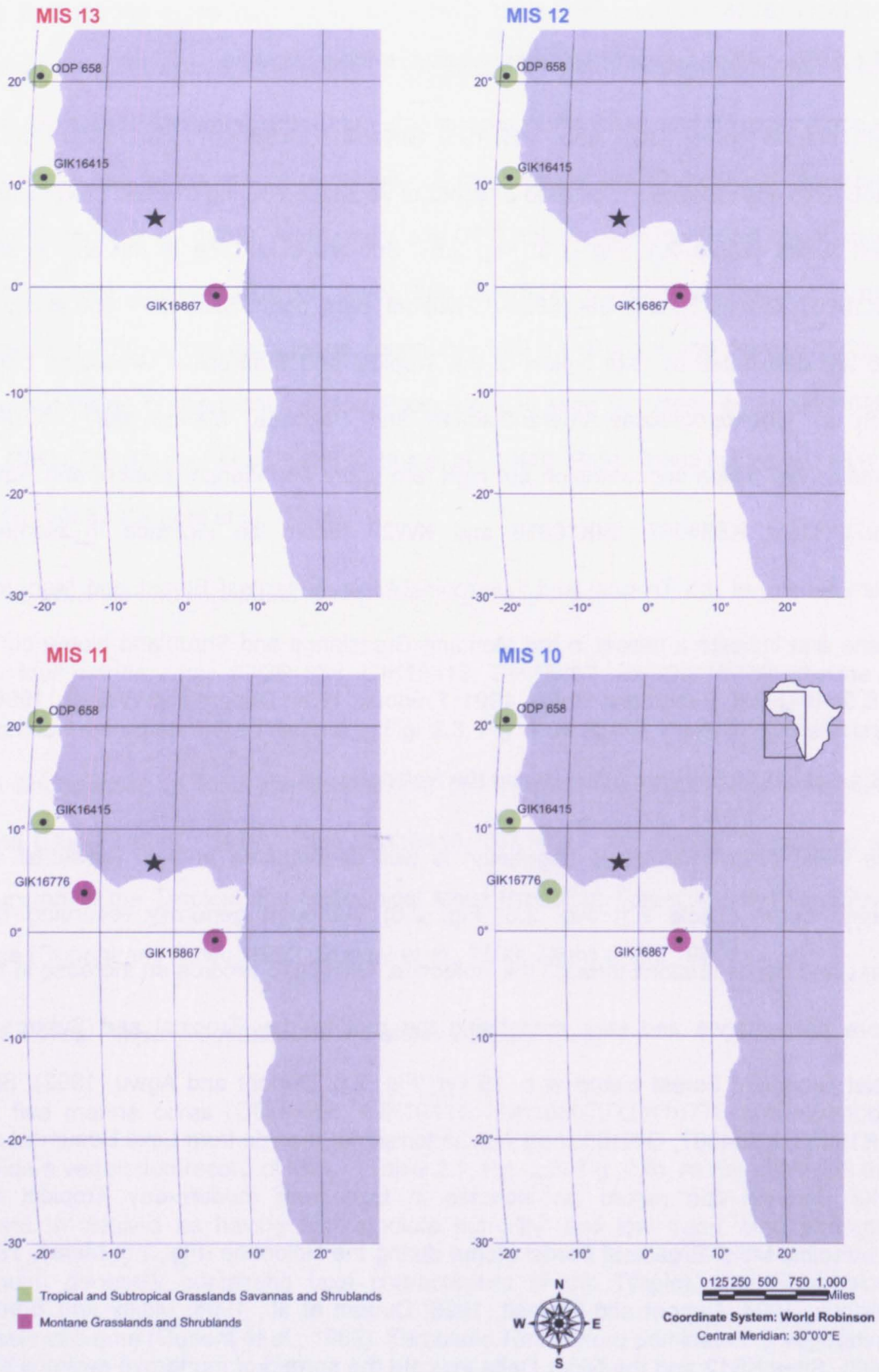


**Fig. 2.4.** Vegetation reconstruction maps based on both marine and terrestrial pollen records from MIS 13 to MIS 10. Red MIS = interglacials. Blue MIS = glacials.

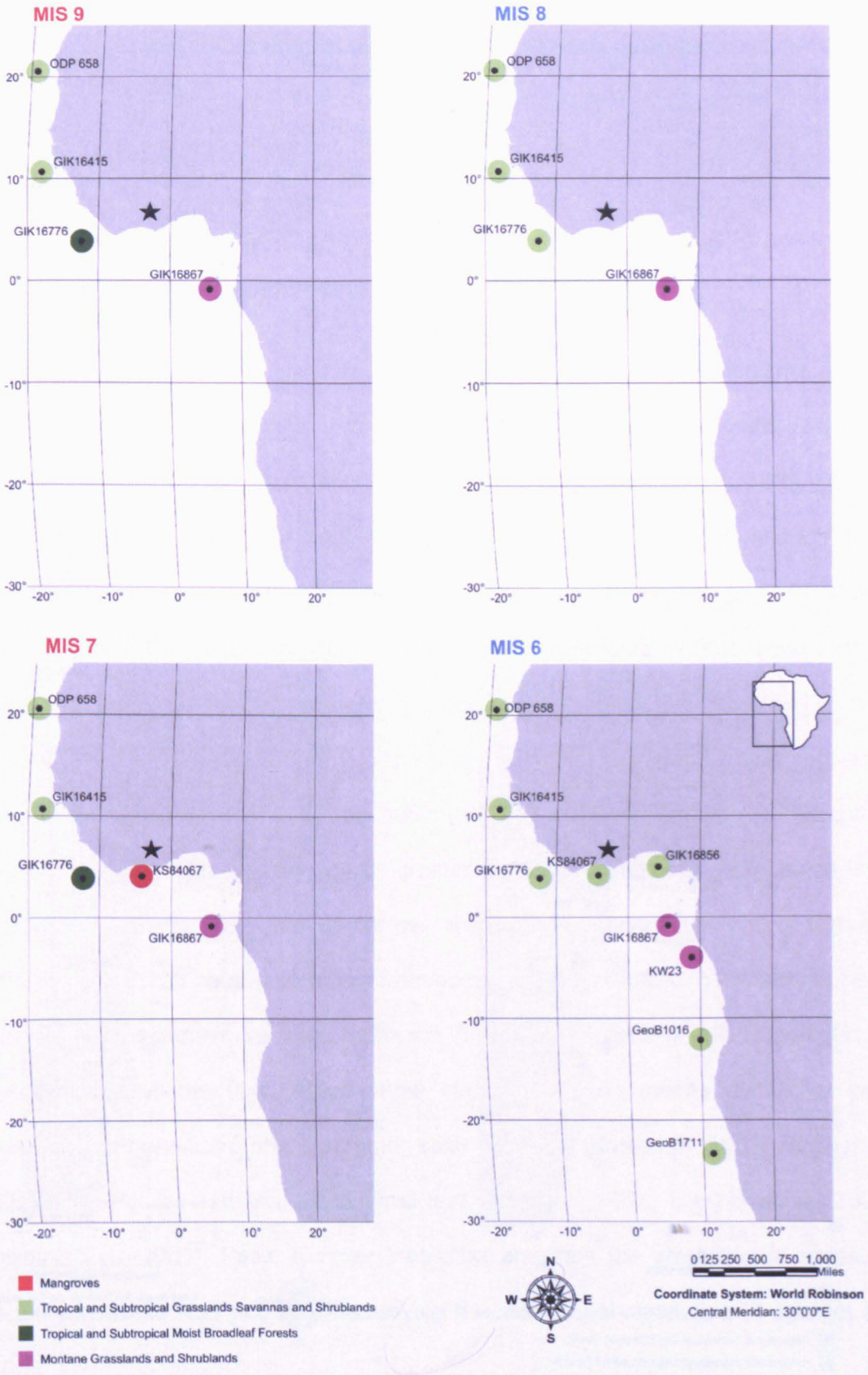


**Fig. 2.5.** Vegetation reconstruction maps based on both marine and terrestrial pollen records from MIS 9 to MIS 6. Red MIS = interglacials. Blue MIS = glacials.

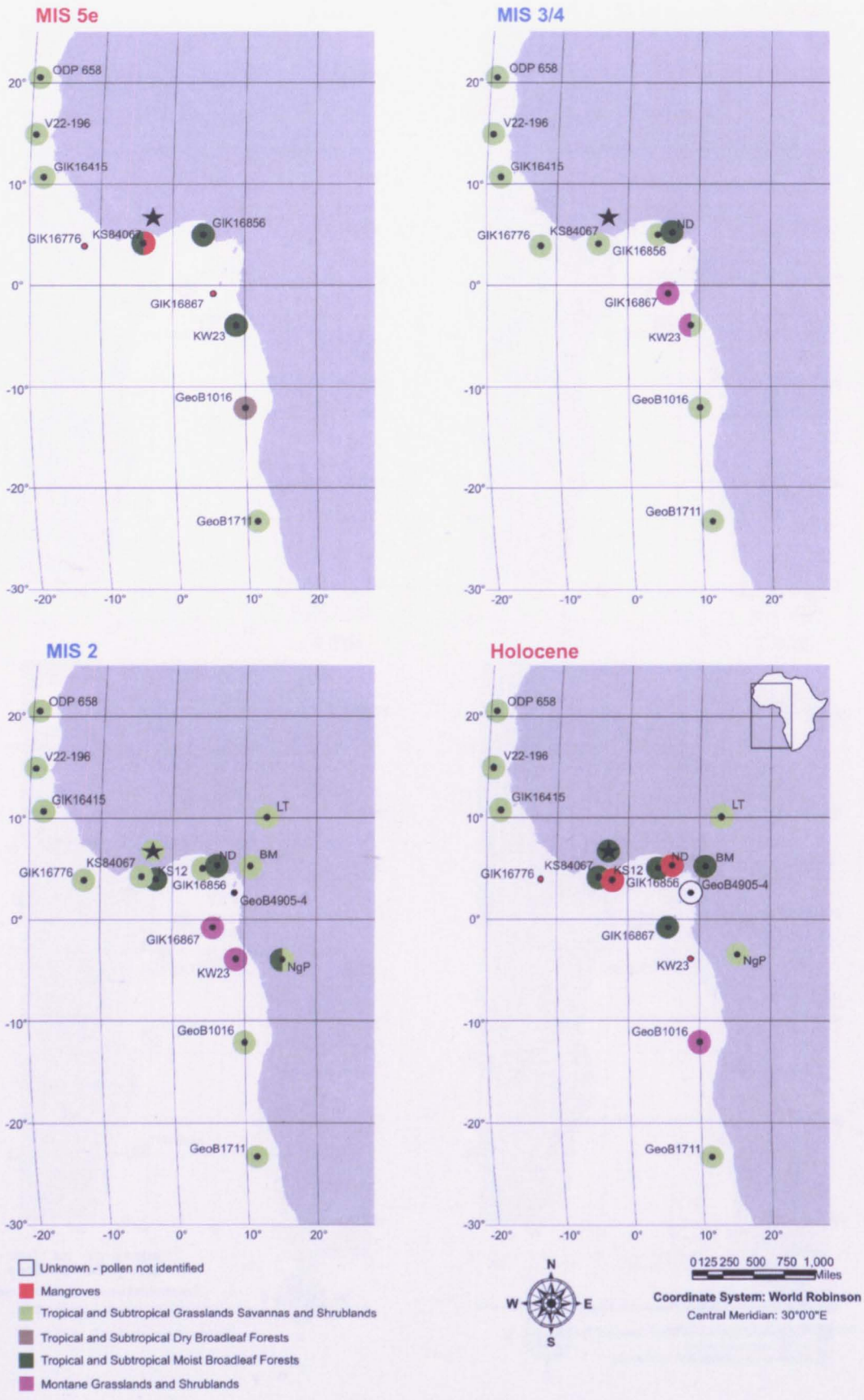


**Fig. 2.6.** Vegetation reconstruction maps based on both marine and terrestrial pollen records from MIS 5e to Holocene. Red MIS = interglacials. Blue MIS = glacials.

### 2.3.2 West African vegetation during past glacial periods

Vegetation associations during past glacial periods show strong similarities, in terms of the restriction of the Tropical and Subtropical Moist Broadleaf Forest and Mangrove biomes and an expansion of the Tropical and Sub-tropical Grasslands Savannas and Shrublands biome (Fig. 2.4–2.6).

### 2.3.3 Theories of palaeoenvironmental change in Africa

Two fundamentally different schools of thought exist as to the mechanisms driving climate change in the tropics; the first suggests that tropical climate responds 'passively' to high-latitude glacial boundary conditions (*e.g.* Dupont et al., 1989; Lezine, 1991), and the second is that tropical climate responds directly to low-latitude solar insolation changes modulated by 23–19 kyr precessional forcing (*e.g.* Prell and Kutzbach, 1987; Clement et al., 2004). Terrestrial environmental responses to climate at low-latitudes are driven by changes in precipitation (deMenocal et al., 1993), with seasonal monsoons dominating climatic variability from annual to glacial-interglacial scale. At low-latitudes, solar insolation heats the continent during the summer months. The heat capacity of the land is much greater than that of the ocean, thus the land becomes warmer and the ocean cooler over the summer months. The strong summer heating over the land causes air inflow from ocean to land, resulting in low atmospheric pressures and a strong summer monsoon (Prell and Kutzbach, 1987). Numerous palaeoclimatic records from Africa show strong monsoon events coinciding with maxima of northern hemisphere summer solar radiation (Kutzbach, 1981; Rossignol-Strick, 1983; Pokras and Mix, 1985; Prell and Kutzbach, 1987; Tuenter et al., 2003; Denison et al., 2005). Peak summer insolation amplifies the atmospheric pressure difference between land and sea intensifying the monsoonal circulation (Ziegler et al., 2010).

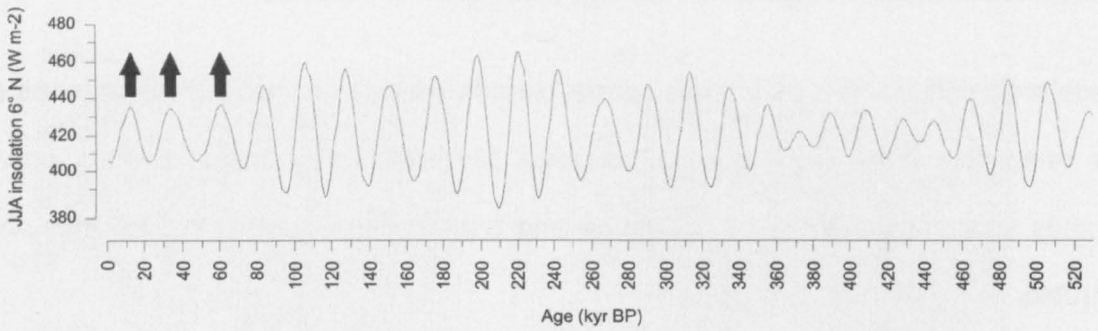


**Fig. 2.7.** Summer (JJA) insolation at 6°N (Paillard et al., 1996). Black arrows indicate peaks in insolation which are associated with times of strong West African monsoon.

### *2.3.4 African climate change and its role in the evolution and dispersal of Homo sapiens*

Evolutionary theory supported by genetics and anatomy of fossil hominids suggest the first appearance of *Homo sapiens* in Africa was at *c.* 190 kyr (McDougall et al., 2005), with modern symbolic behaviour appearing around 135–75 kyr ago (Marean et al., 2007). The global expansion and migration of *Homo sapiens* occurred around 135 kyr (MIS 6) a time of significant global climate change (Hetherington and Reid, 2010). MIS 6, a particularly cold glacial period lasted around 15 kyr, caused ice-sheets to expand across most of Europe and drought throughout Africa and the Mediterranean region (Campo et al., 1982; Dupont and Weinelt, 1996; Dupont et al., 1999; Ayalon et al., 2002; Zhao et al., 2003). Models suggest that during MIS 6 African atmospheric temperatures were 3.75°C cooler and land surfaces almost 4°C cooler than in AD 1800 (Hetherington and Reid, 2010). Seismic reflections and sedimentology indicate intervals of extreme drought between 135–75 kyr in sediment cores from Lake Malawi, Lake Bosumtwi and Lake Tanganyika (Chapter 7; Fig. 7.1) which may have resulted in changing animal and vegetation distribution and decreases in interspecific and intraspecific competition (Scholz et al., 2007; Hetherington and Reid, 2010). For humans, disruption of climate brought about changes in behavioural characteristics leading to the application of novel behaviour and the evolution of the modern hominid (Hetherington and Reid, 2010). Reconstructing climate dynamics on the timescales of

human evolution is of critical importance in understanding the evolutionary drivers and migratory pressures favourable for the development of modern human populations (Dupont, 2011).

## 2.4. Summary

The continent of Africa contains some of the most vulnerable human, animal and vegetation populations to future climate change. Key among these are the tropical forests of West Africa which are highly diverse and play an important role in both the global carbon cycle and global climate systems. If the predicted warming and drying of West Africa over the coming decades is realised, these changes will increase pressure on the endemic species and on human populations within West Africa. One way to better understand the response of tropical ecosystems to climate change is to study the fossil pollen record. Such past studies have demonstrated the response of tropical vegetation over multiple periods of global climate change driven by changes in low-latitude solar insolation and high-latitude glacial boundary conditions. Nevertheless, the lack of long, terrestrial sedimentary archives of past vegetation in West Africa renders it difficult to understand the response of tropical vegetation to global climate change.

# 3. Study region

## 3.1. Tropical West Africa

### *3.1.1 Modern climate*

Both temperature and precipitation in West Africa vary along a rough north-south gradient (36–24 °C, and <600–5000 mm/yr; Fig. 3.1).

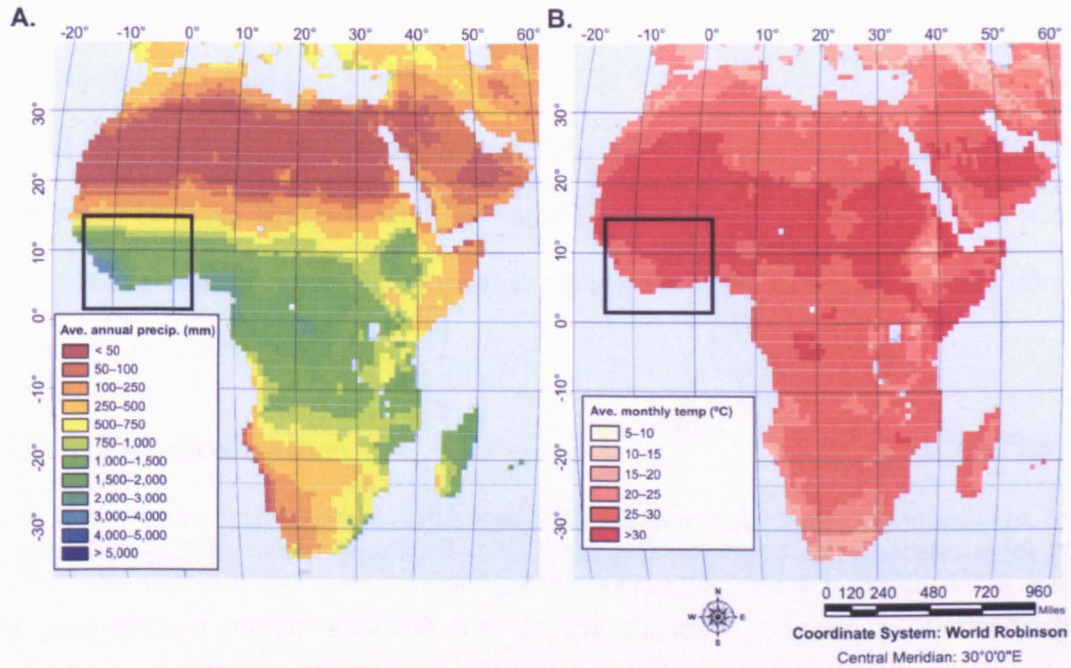


**Fig. 3.1. A**. Map of African average annual precipitation. An average precipitation was calculated for 1961–1990 based on the simulated transient historical data. The result is a 12 month simulated climatology at the scale of the HADCM3 grid. **B).** Map of African average monthly temperature. A 12-month average temperature was calculated for 1961–1990 based on the simulated transient historical data. The result is a 12 month simulated climatology at the scale of the HADCM3 grid. Original data from Carter et al. (2004).

The mechanisms controlling climate in West Africa are the: (i) Intertropical Convergence Zone (ITCZ), and (ii) WAM. During boreal summer, an increase in northern hemisphere summer insolation results in a northward shift in the ITCZ and the development of an area of low pressure over North Africa (Fig. 3.2A). Differential pressure brings moisture eastwards from the Atlantic Ocean to western Africa. In boreal winter, the opposite occurs, with the ITCZ is displaced southwards (Fig. 3.2A). Dry aerosol-rich continental trade winds from the NE (Harmattan) dominate over West

Africa in the winter months. A recent revision of the WAM suggests that the surface ITCZ is *c.* 1000 km north of the rainfall maximum (tropical rainbelt; Fig. 3.2B; Nicholson, 2009). The West African tropical rainbelt is now assumed to be produced by a large core of ascent between the African Easterly Jet (AEJ) and the Tropical Easterly Jet (TEJ; Fig. 3.2B; Nicholson, 2009), producing a column of humid air extending into the upper troposphere (Fig. 3.2B).

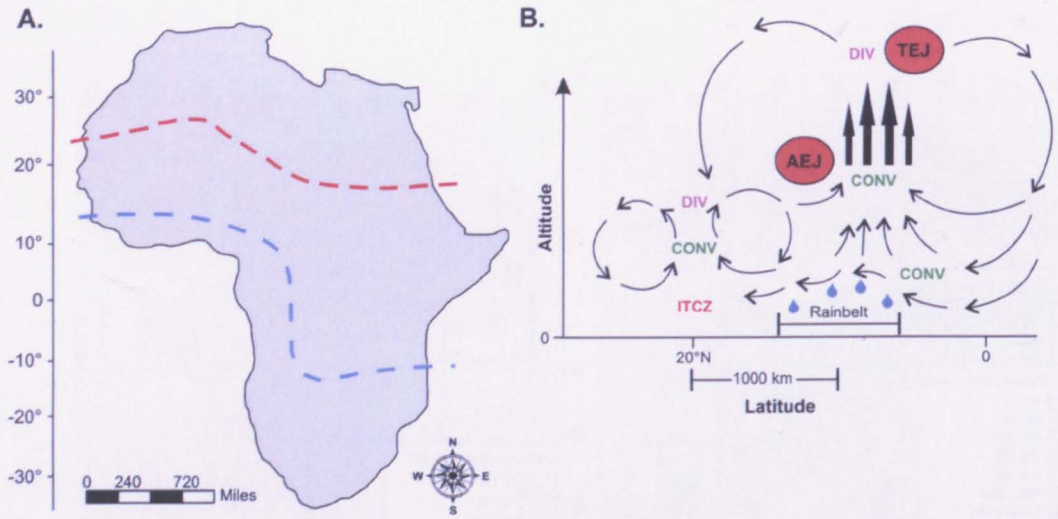


**Fig. 3.2. A).** Map of the mean position of the ITCZ over Africa in August (red dashed line) and January (blue dashed line) based on Goudie (1996). **B).** Development of the WAM (after Nicholson, 2009). CONV = convergence. DIV = divergence. AEJ = African Easterly Jet. TEG = Tropical Easterly Jet.

### *3.1.2 Modern vegetation*

#### *3.1.2.1 Modern-day vegetation nomenclature*

A detailed map of the modern-day vegetation which identifies areas of high biodiversity has recently being developed by Olson et al. (2001). The earth was divided into 14 biomes and a furthermore 867 ecoregions. A biome refers to a major regional group of plant and animal communities adapted to particular climatic conditions (Olson et al., 2001). According to Olson (2001), an ecoregion is defined as: "a relatively large unit of land containing a distinct assemblage of natural communities and species, with boundaries that approximate the original extent of natural communities prior to major land-use change". The scheme compiled by Olson et al. (2001) of ecoregions nested

within biomes provides a comprehensive framework for the discussion of both large scale (continental) and regional vegetation change; therefore, this framework will provide the basis for vegetation discussion throughout this thesis.

*3.1.2.2 Modern-day vegetation in West Africa*

The vegetation of tropical West Africa falls into seven biomes: (i) Deserts and Xeric Shrublands, (ii) Tropical and Subtropical Grasslands, Savannas, and Shrublands, (iii) Tropical and Subtropical Dry Broadleaf Forests, (iv) Tropical and Subtropical Moist Broadleaf Forests, (v) Flooded Grasslands and Savannas, (vi) Montane Grasslands and Shrublands, and (vii) Mangroves (Fig. 2.3; Olson et al., 2001). The savannah and forest biomes constitute the majority of the region, with mangroves limited to coastal regions (Fig. 2.3). These seven biomes are sub-divided into 'ecoregions' which have modern-day vegetation associations that are related to the prevailing climate conditions (Olson et al., 2001).

## 3.2. Lake Bosumtwi

Lake Bosumtwi (6°30' N, 1°25'W; Fig. 2.3), West Africa, was selected for coring in 2004 to gain greater insight into the role of the tropics in triggering, intensifying, and propagating climate changes, as well as to understand the response of tropical vegetation to global climate changes (Koeberl et al., 2005). Lake Bosumtwi is situated in the Ashanti region of southern Ghana in West Africa, 150 km north of the Gulf of Guinea (Fig. 2.3).

### *3.2.1 Lake Bosumtwi modern vegetation*

Lake Bosumtwi is situated in close proximity to the transition between savannah (to the north) and moist forest (to the south; Fig. 2.3); therefore the sediment cores extracted from Lake Bosumtwi are likely to record changes in these vegetation types. Lake Bosumtwi currently lies within the West Guinean Lowland Forest ecoregion (White et al., 1983; Olson et al., 2001). Prior to the degradation of the natural vegetation by

settlement and cultivation, the lake was surrounded by moist semi-deciduous forest (Gill, 1969; Rebelo and Siegfried, 1990), with a dominant canopy comprised of Ulmaceae and Sterculiaceae (Hall and Swaine, 1981; Beuning et al., 2003). Main cultivation crops around Lake Bosumtwi include *Elaeis guineensis* (oil palm), *Musa* sp. (Banana), *Theobroma cacao* (Cocoa) and *Manihot esculenta* (Cassava). Additionally, *Imperata cylindrica* grassland is present on the north-east quadrant of the crater rim, coinciding with the outcrop of the Pepiakese granite (Moon and Mason, 1967).

### *3.2.2 Lake Bosumtwi modern climate*

Average monthly temperature at Lake Bosumtwi ranges from *c.* 23.2°C in August to *c.* 26.8°C in February, with a mean annual temperature of *c.* 26°C. The cooler temperatures in the summer months are due to a decrease in the incoming solar radiation due to increased cloudiness (Shanahan et al., 2007). Humidity varies from *c.* 84.7 % in August to *c.* 75.3 % in January (Turner et al., 1996). Typically, January has the lowest rainfall (*c.* 17 mm) with June having the highest (233.9 mm). The average annual precipitation is 1450 mm (Shanahan et al., 2007).

### *3.2.3 The Bosumtwi meteorite impact crater*

Lake Bosumtwi occupies a 1.08 ±0.04 Myr (Koeberl et al., 1997; Jourdan et al., 2009) meteorite impact crater excavated in metamorphosed rocks belonging to the Birimian Supergroup (2 Gyr; Koeberl et al., 2005). Metagraywackes, metasandstones, shale, mica schists as well as Proterozoic granitoid intrusions and dikes have been observed as lithologies comprising the rim rocks (Wright, 1985). Recent seismic reflection data reveal the presence of a central uplift structure with a diameter of 2 km and a height of 100 m (Scholz et al., 2002). The modern day impact crater has a diameter of *c.* 11 km and a crater rim varying in elevation from 210–460 m above sea level (asl). Presently, Lake Bosumtwi is 8.5 km in diameter (52 $km^2$) and 21 m asl at its deepest point with a present day lake surface elevation of 97 m asl (thus *c.* 74 m water depth). Lake Bosumtwi is hydrologically isolated from the regional aquifer by the bedrock and the

crater walls. The lake is highly stratified, with an anoxic hypolimnion beneath 15–18 m water depth, resulting in anoxic sedimentation, lack of bioturbation and thinly laminated varves (Peck et al., 2004). The closed hydrology of Lake Bosumtwi makes the lake level extremely sensitive to changes in precipitation, cloudiness and temperature (Shanahan et al., 2006).

Since the time of impact, *c.* 294 m of sediment has accumulated in the centre of the basin. The sediments within the lake have originated from erosion of the inside of the crater wall, aeolian transport as well as biological and evaporative processes within the lake.

### *3.2.4 Lake Bosumtwi: past palaeoenvironmental research*

Large fluctuations in Lake Bosumtwi lake level over the last 12 kyr were noted through radiocarbon dating of exposed lacustrine deposits in river gullies around the lake edge (Fig. 3.3; Talbot and Delibrias, 1980; Shanahan et al., 2006). These lake level reconstructions indicate that the lake was much lower than present before 12.69 radiocarbon ($^{14}$C) kyr BP (15.58–14.09 cal kyr BP). After 10.46 $^{14}$C kyr BP (12.84–11.75 cal kyr BP) there was a shift to a deep, stable stratified lake (Talbot and Delibrias, 1980). This lake level highstand allowed for the accumulation of turbidite silts, terminating at 7.8 $^{14}$C kyr BP (9.09–8.29 cal kyr BP) with short-lived rapid lake regression. A well-developed terrace and overflow notch 110 m above present lake level indicates that deep conditions returned shortly after 7.8 $^{14}$C kyr BP. Beach sands 0.5 m above the present lake level indicate a regression around 3.62 $^{14}$C kyr BP (4.24–3.64 cal kyr BP). Additional beach deposits indicate a final lake level highstand 25 m above present lake level at 2.95–1.85 $^{14}$C kyr BP (3.63–1.54 cal kyr BP; Talbot and Delibrias, 1980; Shanahan et al., 2006).

To supplement the early lake level datasets, seven piston cores were retrieved in 1976, to assess mineralogical, sedimentological and palynological change. The longest core (B7) provided a continuous record of palaeoenvironmental change through the Late

Pleistocene-Holocene spanning the last 28 kyr BP. Vegetation reconstructions from Maley (1991) indicate an abrupt transition from arid grasslands (during the last glacial) to wet rainforest vegetation (during the Holocene) at approximately 9.5 cal yrs BP (Fig. 3.4), coinciding with deep lake conditions (Fig. 3.3; Talbot and Delibrias, 1980) and a lithological shift from muddy-silts to dark green laminated muds (Talbot et al., 1984).

Additionally, variations in geochemistry (carbon and nitrogen abundances and the carbon and nitrogen isotopic composition of bulk organic matter) show that during the interval from 9.2 to 3.2 kyr BP the lake was deep with an extremely stable water column (Talbot and Johannessen, 1992). Pollen records indicate a decrease in rainforest around the lake during the late Holocene (Maley, 1991). More recently, detailed investigations based on geomorphological evidence of palaeo-shorelines and exposed sections have provided new constraints on the lake level changes within Lake Bosumtwi (Fig. 3.3; Shanahan et al., 2006).

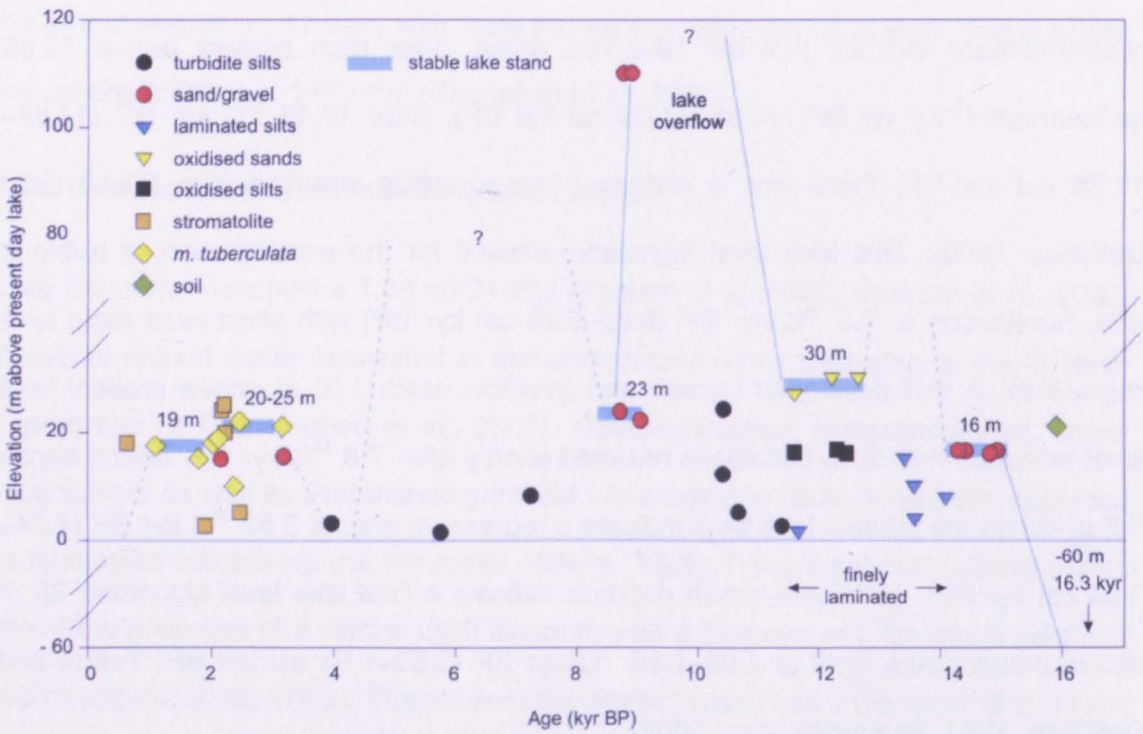


**Fig. 3.3.** The revised lake level reconstruction for Lake Bosumtwi. Symbols indicate the age in calendar years and elevation of the sample above modern lake level. $^{14}C$ dates were calibrated using CALIB 5.0 (Stuiver and Reimer, 2005). Solid blue lines show the reconstructed lake level curve, dashed lines indicate reconstructed lake level curve with greater uncertainty. Blue boxes represent stable lake level, and the location of palaeobeaches of palaeohighstands (Figure re-drawn from Shanahan et al. (2006).

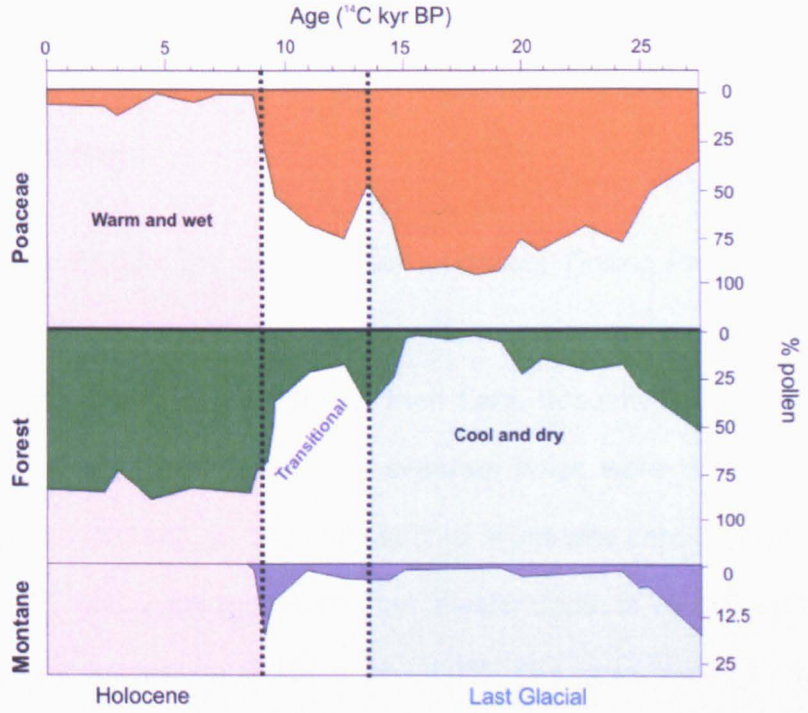


**Fig. 3.4.** Percentage abundance of grass (orange curve), forest (green curve) and montane flora (*Olea hochstetteri*; purple curve) from 28 kyr BP until present. Note $^{14}$C dates are uncalibrated (figure redrawn from Maley, 1991). Blue shading is last glacial, pink shading is Holocene interglacial.

### *3.2.5 The importance of Lake Bosumtwi*

The Lake Bosumtwi impact crater is an ideal site for investigating the impact of global climate change on tropical ecosystems for several reasons:

1. It has been accumulating sediment over the last 1.08 ±0.04 Myr
2. The sediment within the cores of Bosumtwi are mostly fine grained, organic rich, laminated and un-bioturbated, ideal for the preservation of pollen grains
3. It currently lies just *c.* 400 km south of the transition from Sudano-Guinean woodland into grass savannah/woodland; consequently the lake should record fluctuations in the location of vegetation biomes
4. It is hydrologically closed, in terms of both surface and groundwater, and therefore lake level is highly sensitive to changes in both precipitation and evaporation.
5. It lies within the seasonal migration path of the tropical rainbelt, rendering it sensitive to changes in the WAM.

# 4. Geochronology and Methods

## 4.1. Lake drilling

In July and August 2004, the International Continental Drilling Program (ICDP) led an expedition using the GLAD800 lake drilling system to recover 12 sediment cores from 5 core sites arranged in a depth transect from Lake Bosumtwi, Ghana (Fig. 4.1; 4.2; ICDP website). From these 5 sites, 14 separate holes were drilled yielding a total sediment recovery of 1833 m. The longest core taken was core BOS04-5B (hereafter 5B; Fig. 4.1; 4.2), which was recovered from a water depth of 76 m spanning *c.* 294.67 m of sedimentary succession (Peck et al., 2005). The basal sediment layer contains impact-glass bearing lapilli, interpreted to record the final fall-back of material following the meteorite impact that created Lake Bosumtwi (Peck et al., 2005).

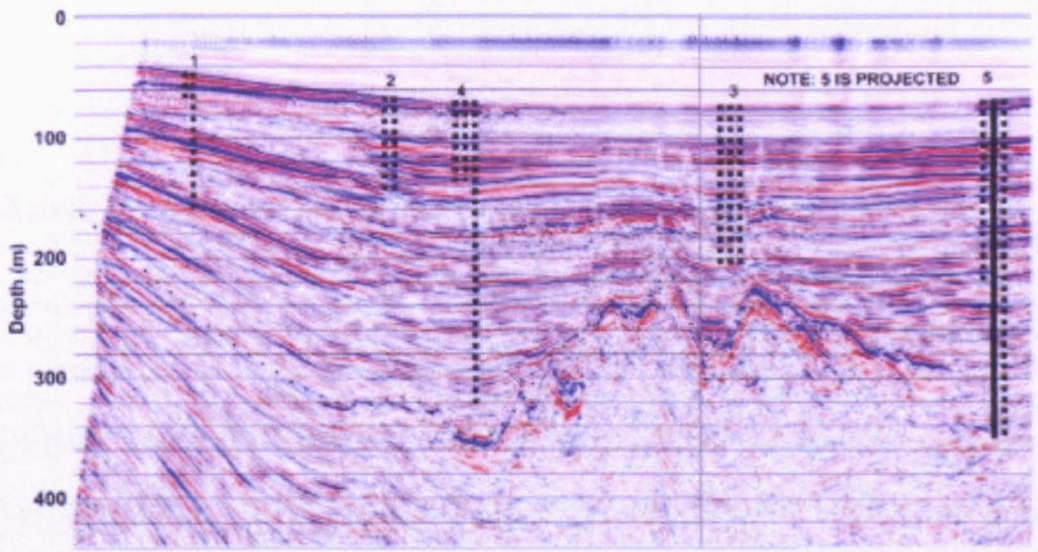


**Fig. 4.1.** Multi-channel seismic reflectance profile of the Lake Bosumtwi sedimentary succession. The dotted line represents the brecciated bedrock of the central uplift feature (Scholz et al., 2002). The vertical black dashed lines indicate the drill holes at the 5 drill sites (Shanahan et al., 2013).

Subsequent to drilling, the cores were shipped to the University of Rhode Island core repository and were split. Prior to destructive analysis the physical properties of the core (density and magnetic susceptibility) were measured at 2-cm intervals using a Geotek multi-sensor core logger. After logging and imaging, u-channel sub-samples

were taken from the cores and measured on a 2-G Enterprises small-access cryogenic magnetometer. The directional parameters (inclination and declination) and the natural remanent magnetisation were measured at 2-cm intervals for the entire length of the core (C. Heil, pers. com.). The cores were sampled at 4 cm resolution for x-ray diffraction, total organic and inorganic carbon and grain size (N. McKay, pers. com.). The physical properties data set was used to splice the 3 drill cores from site 5 together to get a single relative mean core depth (RMCD scale; C. Heil, pers. com.).

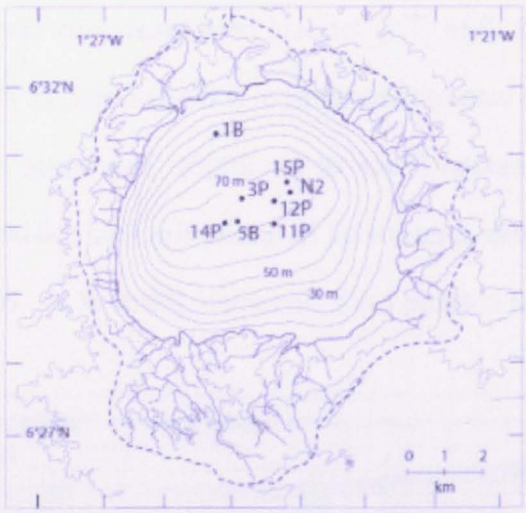


**Fig. 4.2.** Map of the Lake Bosumtwi crater. Dashed line denotes the crater rim. Grey lines are 10 m contours. Black circles indicate the coring sites (Shanahan et al., 2013).

## 4.2. Geochronology

A chronology was established solely for the 5B core based on the linear interpolation between radiocarbon dates (Shanahan et al., 2012) and the basal Ar-Ar date of the impact glass (Fig. 4.3; Koeberl et al., 1997; Jourdan et al., 2009). Previous studies have established 135 independent radiometric age control points from the 5B core (Appendix 1): 127 radiocarbon dates (Shanahan et al., 2012; Shanahan et al., 2013), 1 U-series age (Shanahan et al., 2013), 6 optically stimulated luminescence ages (OSL; Shanahan et al., 2013) and a basal impact glass $^{39}Ar$-$^{40}Ar$ age (Koeberl et al., 1997; Jourdan et al., 2009). Given the good agreement between radiocarbon, U-series and OSL ages, we assume a roughly linear sedimentation rate (Fig. 4.3). Based on a near

linear sedimentation rate the upper 150 m of sediment from core 5B spans the last *c.* 520 kyr.

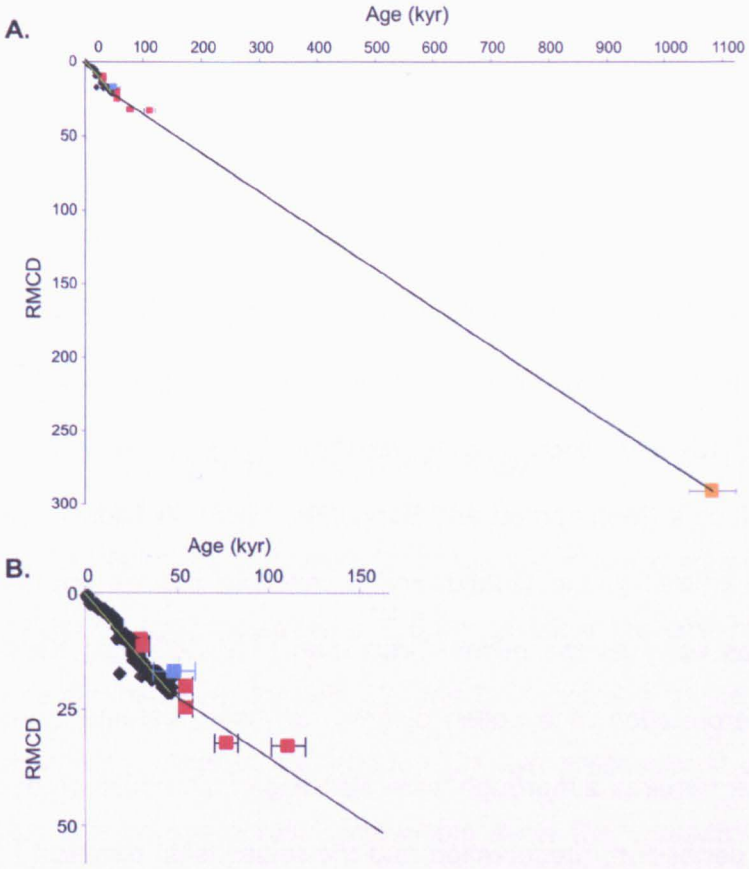


**Fig. 4.3.** Relationship between sediment depth and age for the Lake Bosumtwi 5B sediment core. **A:** The last *c.* 1.08 Myr. **B:** The last *c.* 150 kyr. The black diamonds are radiocarbon ages (<47 kyr BP). Green line indicates the age model constructed using radiocarbon ages (Shanahan et al., 2012); y = 0.0005x – 0.3633. The orange square is the $^{39}Ar$-$^{40}Ar$ age (1.08 ±0.04 Myr). The black line indicates the age model constructed by linear extrapolation from oldest radiocarbon age to impact age derived from $^{39}Ar$-$^{40}Ar$ (Koeberl et al., 1997; Jourdan et al., 2009); y = 0.0003x + 9.2205. The red squares are optical stimulated luminescence ages (Shanahan et al., 2013). The blue square is U-series age (Shanahan et al., 2013).

## 4.3. Palaeoenvironmental proxies

### *4.3.1 Fossil pollen and spores*

#### *4.3.1.1 Concept and justification*

The value of pollen and spore analysis as a tool for reconstructing past vegetation has been well known since its introduction by von Post in 1916 (von Post, 1967). Reconstructing past vegetation is of great value in archaeology and palaeoanthropology since it provides the vegetative setting in which animals and

humans evolved (Moore et al., 1991). The study of past vegetation also provides useful insight when reconstructing past climate change, however possible complications such as local soil influences and human occupation need to be accounted for (Prentice, 1985; Moore et al., 1991).

Pollen analysis has been used to reconstruct vegetation globally, over time with pollen and spores extracted from a range of sedimentary material. Classic examples include; reconstructing vegetation from marine sediment from western equatorial Africa (Jahns et al., 1998), identifying the impact of earthquakes on agriculture in the Dead Sea (Leroy et al., 2010) and reconstructing vegetation over glacial/interglacial transitions from peat in Ethiopia (Mohammed and Bonnefille, 1998). In addition, pollen and spore analysis is not limited to the Quaternary, it can also provide information on global environments as early as the middle-Ordovician (480–360 Myr; Kenrick and Crane, 1997). The interpretation of a pollen diagram to make statements regarding former vegetation cover requires a thorough understanding of the pollen production, dispersal, pollen source, deposition, preservation and the relationship between fossil pollen and former plant communities (Lowe and Walker, 1997).

#### *4.3.1.2 Preservation and identification*

The technique of pollen and spore analysis has proved invaluable in providing information of past environments in Africa. This is primarily due to the high abundance of pollen grains, their wide dispersal and good preservation potential down to the tough nature of the pollen wall. If a pollen grain fails to reach its destination, the cytoplasmatic interior and the intine substances soon perish leaving just the pollen wall (exine; Faegri and Iversen, 1989). The exine, formed of sporopollenin (Kwiatkowski and Lubliner-Mianowska, 1957), is generally well preserved in soils (*e.g.* Bryant, 1986), peat bogs (*e.g.* Mighall et al., 2006), lake sediments (*e.g.* Gasse and Van Campo, 1998), marine sediments (*e.g.* Dupont and Agwu, 1992) as well as ice cores (*e.g.* Liu et al., 2005), speleothems (*e.g.* Brook et al., 2010) and cave deposits (*e.g.* Coles et al., 1989) when

other organic constituents are reduced to structureless unidentifiable substances. In addition, the resistant properties of sporopollenin allow for harsh chemical treatment of samples to oxidise and remove unwanted material which aids in the identification and the concentration of pollen and spores when counting.

The identification of pollen and spores is based on their complex morphological features including number of pores, colps, grain shape and sculpturing (Moore et al., 1991). Identification is based on the use of pollen keys, photographs and laboratory reference material.

*4.3.1.3 Sampling strategy and preparation methodology*

A 0.5 $cm^3$ sediment sample was processed for pollen and spore analyses (Appendix 2). Samples were taken on average every *c.* 2.5 kyr to allow the pattern of vegetation response to be determined over the last 520 kyr by spectral analysis, *i.e.* at least 8 samples per the smallest cycle to be detected (21 kyr, precessional cycle; Weedon, 2003). Additionally this sampling resolution would allow the characterisation of past interglacial vegetation communities. The chronology (Section 4.2) was used to determine the core-section-depth of individual samples in order to request samples from the LacCore Repository.

In total, 217 samples from the upper 150 m of core 5B were analysed for fossil pollen. To determine the pollen count necessary to account for the most variability within the spectrum, one sample (5H-1 0–0.5; *c.* 27.5 kyr) was counted to 1000 pollen grains in increments of 100 (Fig. 4.4; *e.g.* Moore et al., 1991). Although this one pollen sample may not be entirely representative of all pollen samples counted from core BOS04-5B, it is evident that for common pollen types (>1 % of the total pollen sum) a count size of 300 pollen grains is sufficient. However, for minor components (<1 % of the total pollen sum) a much higher count sum of 500 grains is required per sample (Fig. 4.4). The research questions to be addressed within this thesis concern gross vegetation change therefore it was decided that a minimum of 300 pollen grains were to be identified per

sample (excluding aquatics and spores) or when concentrations were low, a minimum of 2000 *Lycopodium* should be counted (*i.e.* concentrations were confirmed as <1392 grains $cm^3$). In most cases 2–4 slides were counted per sample.

The pollen samples extracted from core 5B were prepared using standard techniques (Faegri and Iversen, 1989), with pollen concentrations calculated by adding *Lycopodium* spore tablets (Stockmarr, 1972). All types were digitally photographed using a Nikon eclipse 50i binocular microscope at a magnification of 40x and 100x for special identifications. In total 216 pollen taxa were identified to at least family level and a further 311 pollen types were categorised (Appendix 3a; Appendix 3b). The identification of pollen grains was achieved using the pollen reference collection held at The Open University, UK as well as African pollen reference guides (Chapter 5; Reille, 1995; Gosling et al., 2013).

*4.3.1.4 Fossil pollen ordination: Detrended correspondence analysis*

The multivariate statistical technique of detrended correspondence analsis (DCA) was applied using Psimpoll (Bennett, 2003) in order to highlight ecological gradients within the data set. The technique was used as it elimated the mathematical artifact known as the 'arch effect' of reciprocal averaging (Hill and Gauch, 1980). DCA was performed on: (i) all the pollen samples and including all the pollen/spore taxa reaching an abundance of >2 % of the pollen sum, and (ii) on just the pollen samples occurring within the forest assemblage zones including all taxa >2% of the pollen sum in at least one sample.

*4.3.1.5 Identification of forest zones and the Simpson Diversity Index*

To allow focus on the fossil pollen assemblages which contain higher abundances of forest taxa the fossil pollen diagram was zoned by 'excluding' all samples where grass pollen was >55% of the pollen sum in three consecustive samples. Grass was chosen as the discriminator between forest and savannah formations because of its importance as an indicator of savannah-type vegetation (Hooghiemstra et al., 2006).

The value of >55% was chosen as it represents the overall majority of the vegetation composition. Additionally, the Simpson Index of Diversity (1-D) was calculated for each sample. The calculated value ranges from 0–1, with higher values representing greater diversity. This index represents the probability that two randomly selected individuals from a sample will belong to the same species (Peet, 1974).

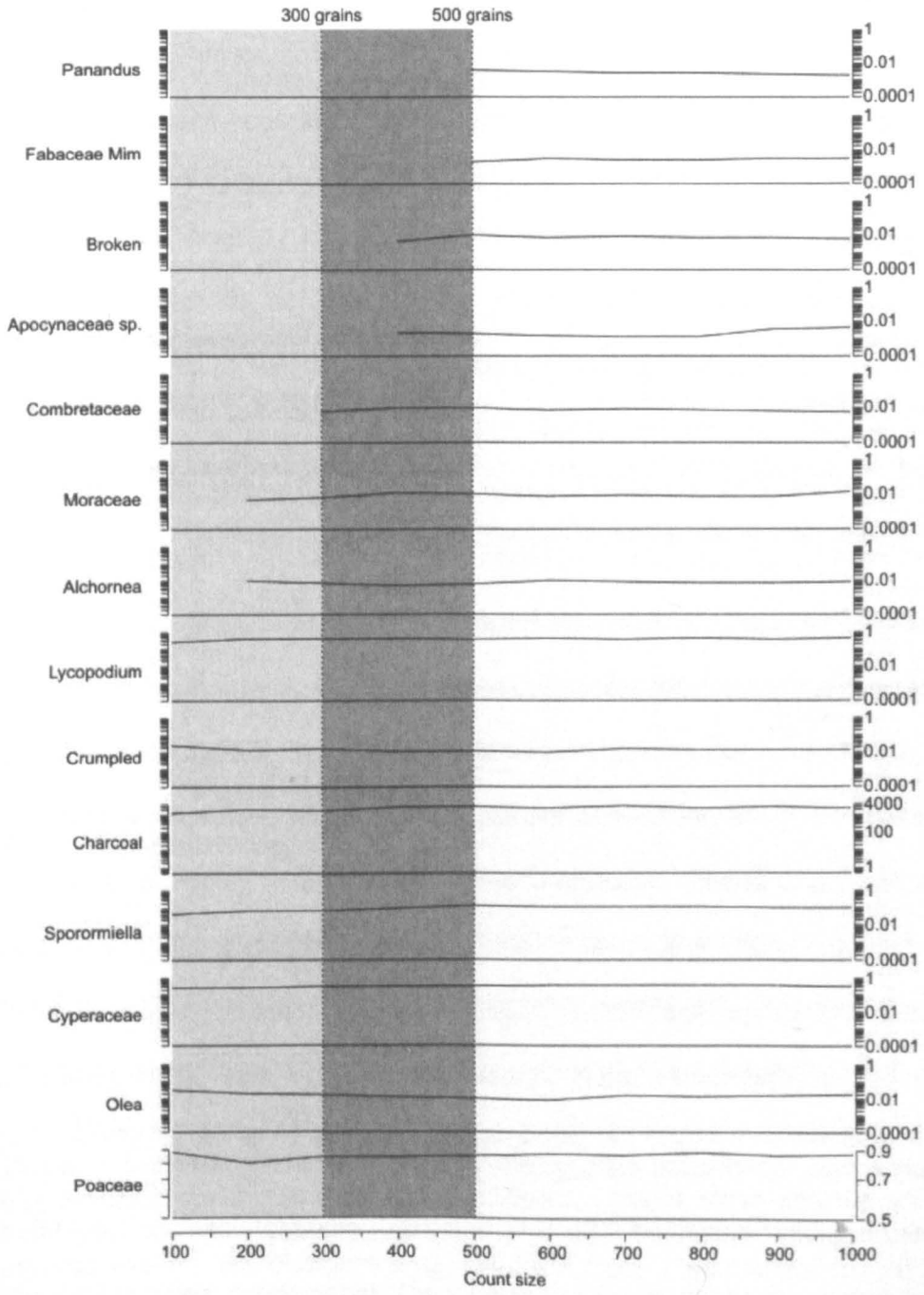


**Fig. 4.4.** The relationship between percentages of pollen, aquatics, damaged and *Lycopodium* marker grains recorded in increments of 100 to a total of 1000 pollen grains from sample 5H-1 0–0.5 (*c.* 27.5 kyr) expressed on a logarithmic scale. Charcoal is expressed as concentration. *Lycopodium* is as percentage of total Lycopodium counted over 1000 pollen grains.

### 4.3.2 Charcoal analysis

#### 4.3.2.1 Concept and justification

Fire plays an important role in the function and maintenance of savannah ecosystems allowing tree-grass coexistence, and preventing canopy closure (Duffin et al., 2008; De Michele et al., 2011). Charcoal analysis is widely used to reconstruct past forest-fire occurrence as well as to study the effects of fire on different ecosystems (Finsinger and Tinner, 2005; Power et al., 2008). In addition, charcoal concentration has been used to assess whether the $CO_2$ released from forest fires affects the global $CO_2$ concentration (Carcaillet et al., 2002).

The analysis of fossil charcoal extracted from lake sediments was developed over half a century ago by Iversen, Waddington and Swain (Clark, 1988). There are various methods used to assess charcoal concentration within a sample; including thin sections, combustion and pollen slides (Finsinger and Tinner, 2005).

In this thesis, charcoal concentration was determined by counting charcoal particles simultaneously with pollen and spores on the same slide. The charcoal counted using this method represents charcoal from regional source areas (Tinner et al., 2000). Charcoal analysts using the pollen-slide technique have yet to decide on a minimum counting sum needed to provide accurate charcoal concentration values, and authors use different minimum counting sums *e.g.* 100 (Tinner et al., 2000) or 200 (Tinner and Conedera, 1995 in Finsinger and Tinner, 2005). Frequently authors fail to reveal the minimum charcoal counting sums used in their studies (Finsinger and Tinner, 2005).

Under the microscope non-charred material can often look similar to charcoal, however using the methodology described (Section 4.3.2.2), charcoal can be identified successfully. A further constraint involves problems with redeposition, sediment mixing, bioturbation, and a lag time between the fire occurrence and charcoal deposition (Duffin et al., 2008). There are still problems concerning defining the distance of the fire

to study site, with some studies indicating decay to zero with increasing distance from fire (Clark et al., 1998) and others suggesting a more complex relationship (Tinner et al., 2006). Additionally, it is crucial to note that charcoal records can also contain low frequency 'background' signals of burning as well as high-frequency 'peak' components and decomposing these two different signals has proved challenging (Higuera et al., 2007).

*4.3.2.2 Sampling strategy and preparation methodology*

Charcoal concentration was determined in the samples counted for pollen and spore analysis, the sampling resolution is detailed in Section 4.3.1.3. Charcoal fragments above 10 µm were counted using a manual cell counter. Charcoal particles were readily identified by their angular structure, opacity and the presence of visible stomata (Clark and Royall, 1995). Charcoal concentration values were calculated by adding a spike of 1 *Lycopodium* spore tablet to samples of known volume (Stockmarr, 1972). In this study, the minimum charcoal counting sum used was 2000. With this high count sum, sufficient precision would certainly be reached (Finsinger and Tinner, 2005). The number of *Lycopodium* counted was recorded at 2000 charcoal fragments in order to calculate charcoal concentration values.

### *4.3.3 Nitrogen isotopes*

Organic matter is an important component of lake sediments. It influences a variety of biogeochemical processes and controls redox conditions within lakes. Together with phosphorus and silicon, nitrogen (N) is one of the key nutrients which limits organic productivity within lake systems (Talbot, 2002). Changes in N sources or the N cycle has dramatic consequences on the production, composition and the accumulation of organic matter. By characterising the N isotopic composition ($\delta^{15}N$) of sediment samples it may be possible to distinguish between the different biogeochemical processes resulting in the production or consumption of nitrate within the lake,

providing important palaeoliminological information which can be related to changes in the global environment (Bernasconi and Barbieri, 1997; Ostrom et al., 1998).

Nitrogen in lacustrine sediments has traditionally been characterised either by weight percent total nitrogen or by the carbon:nitrogen ratio (C/N). Until recently, nitrogen isotope analysis was not used routinely in palaeoliminology due to problems with ambiguous interpretation (Talbot, 2002). In addition to the complexities of the global nitrogen cycle, additional problems exist which complicate the interpretation of N isotopes in lake sediments. Problems with the immobilisation of diagenetically released N from diatom frustules or the selective loss of N downcore may mask the original $\delta^{15}N$ signal within the sediment (Talbot, 2002). The isotopic effect of diagenesis should manifest as an increase in the heavy $\delta^{15}N$ downcore *e.g* Ostrom et al. (1998). In clay rich sediments, positive ammonium ions are readily absorbed onto the negatively charged surfaces of the clay minerals. This results in the selective diffusive loss of $\delta^{14}N$ out of clay-poor sediment horizons whilst the clay-rich horizons retain the isotopically heavier $\delta^{15}N$ (Talbot, 2002). Bulk $\delta^{15}N$ analysis of marine sediment has shown that cleaned marine diatoms contain large amounts of N (Altabet and Francois, 1994). Lake sediments can contain high concentrations of diatoms and thus frustule dissolution during diagenesis could release large amounts of N into the sediment causing changes in the bulk isotopic composition of the sediment (Talbot, 2002). Despite the possibility of attaining ambiguous results from the N isotopes, the proxy may provide important palaeoliminological information unattainable from other proxies.

#### *4.3.3.1 N-isotope methodology*

Nitrogen isotope analyses were performed on 2.5 mg (dry weight) samples of bulk organic matter. The nitrogen isotope composition of 123 decalcified sample residues was determined at a *c.* 5 kyr resolution. Briefly, *c.* 0.6 g sample aliquots were homogenized and treated sequentially with 0.1M and 1M HCl for 24 hr, before being rinsed to neutrality with MilliQ water (18.2 MΩ cm). Each step, involving a change of

reagent or water, was preceded by centrifugation (10 min at 1500 rpm) to prevent the loss of fine material in suspension. The nitrogen isotopic composition ($\delta^{15}N$) of the dried re-homogenized residues was then determined using a Thermo Flash HT elemental analyzer equipped with a Thermo zero-blank device coupled to a Thermo MAT 253 mass spectrometer (EA-MS) held at The Open University. Data are expressed following the guidelines for the reporting of stable isotope measurement results the quantity relative nitrogen $\delta^{15}N$, is defined by the relation:

**Equ. 4.1**.

$$\delta^{15}N_{AIR} = \left( \frac{R(^{15}N/^{14}N)_P}{R(^{15}N/^{14}N)_{AIR}} \right) - 1$$

Where R is the isotope-number ratio, $N(^{15}N)/N(^{14}N)$, of the two isotopes of nitrogen in specimen P, and the equivalent parameters follow for the international measurement standard Air. Standards were run every 8 samples to ensure any uncertainties throughout the run would be identified. All standards run (per day) are shown in Fig. 4.5A, average daily standards are shown in Fig. 4.5B and standards corrected back to the international standard are shown in Fig. 4.5C. All sample isotopic measurements were blank corrected and normalised to the International Atomic Energy Agency (IAEA) no. 3 standard. The average $\delta^{15}N$ of IAEA NO3 and the in-house urea standard was found to be 4.6 ± 0.12 ‰ (1 σ) and -0.9 ± 0.12 ‰ (1 σ) respectively. The measured $\delta^{15}N$ value for IAEA NO3 is within uncertainly of certified published values (4.7 ± 0.2 ‰) demonstrating the accuracy of the protocol. As a true estimate of precision, six aliquots of sample 52E-1 75–75.5 cm (140.6 meters composite depth, *c.* 482.8 kyr) were analyzed, returning a standard deviation of 0.45 ‰ (1 σ). These samples were run on multiple days and consequently represent the uncertainty of the reported $\delta^{15}N$ of organic residues from Lake Bosumtwi.

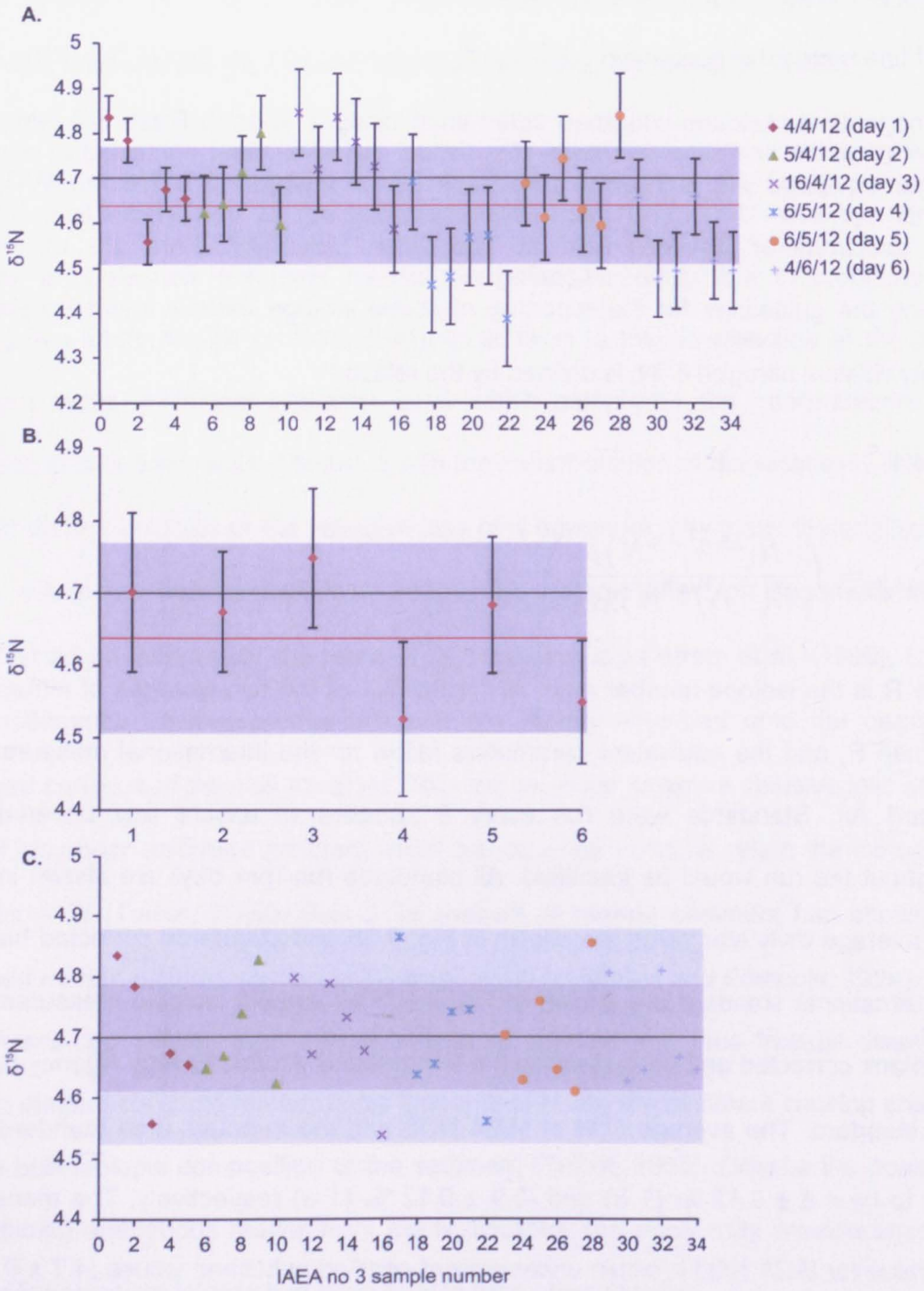


**Fig. 4.5. A).** $\delta^{15}N$ isotopic composition for all IAEA no 3 standards run on each day of analyses. Error bars are to 1 s.d. Red line is the average IAEA no 3 composition run. Black line denotes actual $\delta^{15}N$ isotopic composition. Grey box is the 1 s.d for replicate runs at 0.12 ‰. X-axis is standard sample number. **B).** Average daily $\delta^{15}N$ isotopic composition. Error bars are to 1 s.d. Red line is the average IAEA no 3 composition run. Black line denotes actual $\delta^{15}N$ isotopic composition. X-axis is day standards were run. **C).** $\delta^{15}N$ isotopic composition for all IAEA no 3 standards run on each day of analyses corrected relative to the international standard composition. Black line denotes actual $\delta^{15}N$ isotopic composition and also the average IAEA no 3 composition run. Light grey box is the 2 s.d for replicate runs at 0.17 ‰. Dark grey box is the 1 s.d for replicate runs at 0.09 ‰.

# 5. Atlas of the tropical West African pollen flora

This chapter has been written in the form of a manuscript which has been published in *Review of Palynology and Palaeobotany*. The full reference for this manuscript is:

Gosling, W.D., Miller, C.S., Livingstone, D.L., 2013. Atlas of the tropical West African pollen flora. *Review of Palynology and Palaeobotany.*

**doi:** 10.1016.j.revpalbo.2013.01.003

The accurate identification of fossil pollen and spores is imperative when using palynology to reconstruct past vegetation. In this paper we present a comprehensive tool for identifying the fossil pollen of West Africa and contribute to the existing body of knowledge by presenting *c.* 3000 images and identification keys for 364 pollen and spore taxa commonly found in tropical West Africa. As well as printed plates (Appendix 4), we have added our images to the online searchable Neotropical Pollen database (Bush and Weng, 2007).

My contribution to this publication was the construction of all the fossil pollen identification keys, which makes up the majority of this manuscript (Section 5.4–5.20). This involved describing and 'keying' pollen in order to provide a method of identification for unknown pollen grains. Additionally, whilst adding our pollen images to the existing online Neotropical Pollen Database, I classified the pollen grains by morphology.

## 5.1. Abstract

The accurate and consistent identification of fossil pollen is essential to allow robust inferences to be drawn with regard to past climate and vegetation change. Identifications are best achieved through the direct inspection of reference material. Most substantial reference collections are held at prestigious universities in Europe or the United States of America which can restrict access for researchers trying to

advance palynology in less developed countries. Digital imaging and fast spreading access to the internet means that it is now possible to produce and disseminate high quality images from pollen reference collections. In this paper we contribute to this growing body of work by presenting images of 364 pollen/spore taxa from West Tropical Africa both as printed plates with a key, and within an associated online searchable database.

## 5.2. Introduction

The accurate identification of fossil pollen and spores underpins our ability to reconstruct past vegetation and subsequently infer variation in the Earth's system. Palaeo–palynology can provide, among other things, evidence for past changes in climate (e.g. Overpeck et al., 1990; Davis and Shaw, 2001); biome (*e.g.* Jolly et al., 1998; Tarasov et al., 1998; Williams et al., 2004) and biodiversity (*e.g.* Rull, 1987; Brown, 1999; Odgaard, 1999) across the geological record. At one extreme the incredible resilience of pollen/spore chemistry (sporopollenin) allows palynology to provide evidence for the evolution of plants on timescales of millions of years (*e.g.* Crane et al., 1995; Wikström et al., 2001). Whilst at the other, the influence of human activity upon plants allows the actions of people within the landscape to be traced in the recent past (10-100's years ago; *e.g.* Brugam, 1978; Piperno and Flannery, 2001). The integrity of the information supplied by palynologists to all these areas is reliant on consistent typing or, where possible, identification of the specimens found in the fossil record.

Since its inception morphological identification of pollen grains has been standard practice through comparison with modern material (von Post 1916; reprinted in 1967, von Post, 1967). Subsequently numerous atlases for pollen and spore identification have been produced from across the globe, including: Beug (2004); Colinvaux et al. (1999); Faegri and Iversen (1989); Moore et al. (1991); Reille (1995) and Roubik and Moreno (1991). The proliferation of pollen/spore atlases has facilitated the expansion of

the field of palynology and helped with international standardization of identifications. In addition, as computing power has developed, there has been an increase in the number, and sophistication, of online searchable pollen databases *e.g.* Lézine (2005); Bush and Weng (2007); QPG (2008). However, geographical coverage and access to images for pollen identification remains patchy.

The most substantial atlases for African pollen and spore identification are: (i) in print (Reille, 1995), and (ii) online the African pollen database (Lézine, 2005). Both contain thousands of images of species within hundreds of families, and therefore provide good general coverage of taxa likely to be found in the fossil record. In addition, pollen/spore atlases for specific regions have also been produced, *e.g.* East Africa (Riollet and Bonnefille, 1976), as well as for individual countries: (i) Chad (Maley, 1970), (ii) Ethiopia (Bonnefille, 1971a, 1971b), (iii) Ivory Coast (Ybert, 1979), (iv) Nigeria (Sowunmi, 1973), (v) South Africa (van Zinderen Bakker, 1953, 1956; Van Zinderen Bakker and Coetzee, 1959; Scott, 1982), and (vi) Sudan (El Ghazali, 1993). In this paper we contribute to this body of knowledge by presenting *c.* 3000 images and identification keys for 364 pollen and spore taxa commonly found in tropical West Africa.

## 5.3. Materials and Methods

### *5.3.1 Selection of pollen and spore taxa*

Taxa were selected for inclusion within this tropical West African pollen atlas based upon two criteria: (i) they had been previously identified within fossil records obtained from terrestrial and marine settings within the region (Maley and Livingstone, 1983; Talbot et al., 1984; Lezine and Vergnaud-Grazzini, 1993; Elenga et al., 1994; Frédoux, 1994; Leroy and Dupont, 1994; Dupont et al., 2000), and/or (ii) they had been identified as significant in the regional flora (Hall and Swaine, 1981).

### 5.3.2 Organisation and presentation of images

Images are presented on 129 plates showing both polar and equatorial views of the grain where it was possible to obtain images. Plates are organised by pollen morphology to allow ease of reference when examining fossil pollen material; following (Beug, 2004). In addition, to facilitate interrogation of the images based on botanical classification the family, genera and species of the images are listed in Table 5.1 with reference to plate number. The paper is accompanied by a searchable online database which integrates the images presented here with the *c.* 6000 images of >1000 taxa from the Neotropical Pollen Database (Bush and Weng, 2007). We hope that the combination of our images with those of Bush and Weng (2007) within a freeware format online will promote further expansion by other research groups which will lead to the eventual development of a comprehensive pan–tropical searchable online pollen and spore identification tool.

### 5.3.3 Provenance of specimens and image capture

Images and descriptions of all pollen and spores were obtained from the reference collection of *c.* 30,000 specimens housed within the Department of Biology at Duke University which has been collected and curated by DAL. Reference material was sourced from herbaria and laboratories around the globe; full details for individual specimens can be found on the accompanying online database. Images were obtained using QCapture software (v. 3.1.1) with a QImaging Micropublisher 3.3 RTV camera mounted on a Nikon Eclipse 50i microscope. All images were taken through a Nikon Plan Fluor 40x/0.75 DIC M/N2 objective.

### 5.3.4 Terminology

Terminology follows Punt et al. (2007).

### 5.3.5 Nomenclature

Taxanomic nomenclature follows conventions of Beug (2004).

## 5.4 Polyads

Plates I–III

**Key:**

1. Comprising eight grains 2.
- Comprising twelve grains 3.
- Comprising more than twelve grains 5.

2. Surface psilate (Plate I: 1–3) *Calpocalyx brevibracteatus*
- Surface scabrate (Plate I: 4–6) *Xylia evansii*

3. Polyad diameter less than 40µm 4.
- Polyad diameter greater than 40µm (Plate II: 1–3) *Acacia clavigera*

4. Surface scabrate (Plate I: 7–9) *Acacia seyal*
- Surface psilate (Plate I: 10–12) *Acacia eggelingii*

5. Polyad arrangement non–uniform 6.
- Polyad arrangement uniform (Plate III: 4–6) *Parkia velutina*

6. Polyad diameter less than 110µm (Plate II: 4–6) *Parkia inundabilis*
- Polyad diameter greater than 110µm (Plate III: 1–3) *Parkia bussei*

## 5.5. Tetrads

Plate IV

**Key:**

1. Visible collumnae 2.
- Invisible collumnae (Plate IV: 1–4) *Erica arborea*

2. Surface verrucate (Plate IV: 5–7) *Mimosa strigillosa*
- Surface scabrate (Plate IV: 8–9) *Uvariopsis congensis*

## 5.6. Vesiculate

Plate V, *Podocarpus milanjianus* (Plate V: 1–6)

## 5.7. Inaperturate, including Polypodiaceae

Plates VI–XVI

**Key:**

| | |
|---|---|
| 1. Surface reticulate | 2. |
| - Surface echinate | 6. |
| - Surface psilate | 9. |
| - Surface reticulate | 14. |
| - Surface foveolate (Plate VII : 4–7) | *Trichomanes mandiocanum* |
| - Surface verrucate | 15. |
| - Surface gemmate (Plate VII: 1–3) | *Borassus aethiopum* |
| - Surface perforate (Plate VI: 5–7) | *Acidanthera brevicollis* |
| - Surface scabrate | 16. |
| 2. Equatorial grain shape circular | 3. |
| - Equatorial grain shape suboblate (Plate IX: 9–11) | *Xyris montana* |
| - Equatorial grain shape subprolate (Plate VIII: 10–13) | *Scaphopetalum thonneri* |
| - Equatorial grain shape rectangular (tall) (Plate IX: 1–8) | *Xyris* sp. (x2) |
| 3. Equatorial grain diameter ~9–11µm (Plate X: 1–4) | *Peperomia* sp. |
| - Equatorial grain diameter ~12–18µm (Plate XI: 8–10) | *Tiliacora funifera* |
| - Equatorial grain diameter ~27–33µm (Plate XI: 11–14) | *Scaphopetalum letestui* |
| - Equatorial grain diameter ~40–55µm | 4. |
| - Equatorial grain diameter ~63–77µm | 5. |
| - Equatorial grain diameter ~70–90µm (Plate XII: 7–10) | *Croton macrostachyus* |
| - Equatorial grain diameter ~90–110 (Plate XIII 1–2) | *Dicranolepis usambarica* |
| 4. Wall thickness ~2µm (Plate XII: 1–3) | *Psychotria goetzei* |
| - Wall thickness ~4µm (Plate XII: 4–6) | *Croton gratissimus* |
| 5. Wall thickness ~2µm (Plate XIII 5–7) | *Morinda citrifolia* |
| - Wall thickness ~6µm (Plate XIII: 3–4) | *Tribulus terrestris* |
| 6. Equatorial grain shape circular | 7. |
| - Equatorial grain shape suboblate (Plate VII: 8–11) | *Pycnanthus dinklagei* |
| - Equatorial grain shape oblate (Plate VI: 1–4) | *Illigera rhodantha* |
| - Equatorial grain shape subprolate (Plate VIII: 14–17) | *Pandanus livingstonianus* |
| 7. Equatorial grain diameter ~17–23µm | 8. |
| - Equatorial grain diameter ~36–44µm (Plate XIV: 1–3) | *Iodes kamerunensis* |
| - Equatorial grain diameter ~63–77µm (Plate XIII: 8–10) | *Barteria acuminata* |
| - Equatorial grain diameter ~81–99µm (Plate XIV: 4–7) | *Illigera appendiculata* |
| 8. Wall thickness ~0.5µm (Plate XIV: 8–11) | *Lemna gibba* |
| - Wall thickness ~1.5µm (Plate XV: 1–4) | *Pandanus kirkii* |
| 9. Equatorial grain shape circular | 10. |
| - Equatorial grain shape suboblate | 12. |
| - Equatorial grain shape subprolate | 13. |
| 10. Polar grain shape circular (Plate XI: 1–4) | *Nymphaea caerulea* |
| - Polar grain shape quinquangular | 11. |
| - Polar grain shape triangular (convex) (Plate X: 13–16) | *Nymphaea lotus* |
| 11. Wall thickness ~1µm (Plate VII: 16–19) | *Alternanthera repens* |
| - Wall thickness ~2µm (Plate VII: 12–15) | *Alternanthera nodiflora* |
| 12. Equatorial grain diameter ~35–45µm (Plate XI: 5–7) | *Uvaria kirkii* |

- Equatorial grain diameter ~50–70µm (Plate VIII: 1–6) *Piptostigma mayumbense*

13. Equatorial grain diameter ~50–60µm (Plate X: 11–12) *Lonchitis currori*

14. Wall thickness ~1µm (Plate X: 8–10) *Nephrolepis biserrata*
- Wall thickness ~2µm (Plate X: 5–7) *Nephrolepis exaltata*

15. Equatorial grain shape circular (Plate XVI: 4–10) *Dichrostachys* sp. (x2)
- Equatorial grain shape suboblate (Plate VIII: 7–9) *Dichrostachys unijuga*

16. Equatorial grain diameter ~150–200µm (Plate XV: 5–6) *Tylophora sylvatica*
- Equatorial grain diameter unknown (Plate XVI: 1–3) *Artabotrys likimensis*

## 5.8. Monoporate

Plate XVII

**Key:**

1. Surface scabrate (Plate XVII: 1–2) *Guaduella oblonga*
- Surface reticulate 2.

2. Pore size ~1.5µm (Plate XVII: 6–8) *Typha angustifolia*
- Pore size ~2µm 3.

3. Wall thickness ~1µm (Plate XVII: 3–5) *Typha australis*
- Wall thickness ~1.5µm (Plate XVII: 9–11) *Typha capensis*

## 5.9. Monocolpate

Plates XVIII–XXI

**Key:**

1. Surface psilate 2.
- Surface gemmate (Plate XIX: 6–8) *Borassus aethiopum*
- Surface perforate (Plate XXI: 4–6) *Acidanthera brevicollis*
- Surface foveolate 4.
- Surface scabrate 5.
- Surface echinate 8.
- Surface reticulate 10.

2. Equatorial grain shape rectangular (tall) (Plate XVIII: 1–2) *Raphia ruffia*
- Equatorial grain shape rhombic (tall) (Plate XVIII: 6–8) *Phoenix reclinata*
- Equatorial grain shape circular 3.

3. Polar grain shape triangular (convex) (Plate XX: 4–6) *Nymphaea lotus*
- Polar grain shape circular (Plate XX: 1–3) *Nymphaea caerulea*

4. Equatorial grain shape rectangular (tall) (Plate XIX: 9–10) *Hyphaene natalensis*
- Equatorial grain shape rhombic (tall) (Plate XIX: 11–13) *Hyphaene ventricosa*

| | |
|---|---|
| 5. Equatorial grain shape subprolate | 6. |
| - Equatorial grain shape rectangular (tall) (Plate XVIII: 3–6, Plate XVIII: 17–18, Plate XVIII: 19–21) | *Raphia farinifera* *Calamus erectus* *Calamus gracilis* |
| 6. Polar grain shape triangular (convex) (Plate XVIII: 9–11) | *Elaeis guineensis* |
| - Polar grain shape circular | 7. |
| 7. Collumnae invisible (Plate XX: 7–9) | *Chlorophytum floribundum* |
| - Collumnae visible (Plate XX: 10–11) | *Asparagus falcatus* |
| 8. Wall thinner on pole (Plate XXI: 7–9) | *Aneilema johnstonii* |
| - Wall of even thickness | 9. |
| 9. Equatorial grain size ~50–60µm (Plate XXI: 10–12) | *Commelina africana* |
| - Equatorial grain size ~75–85µm (Plate XXI: 13–15) | *Crinum powellii* |
| - Equatorial grain size ~85–95µm (Plate XXI: 16–18) | *Crinum pauciflorum* |
| 10. Colpus length full | 11. |
| - Colpus length 2/3 (Plate XXI: 1–3) | *Dracaena reflexa* |
| - Colpus length 1/2 (Plate XX: 12–13) | *Dracaena camerooniana* |
| - Colpus length 1/3 | 12. |
| 11. Collumnae invisible (Plate XVIII: 12–14) | *Ancistrophyllum secundiflorum* |
| - Collumnae visible (Plate XIX: 4–5) | *Borassus machadonis* |
| 12. Equatorial grain size ~35–45µm (Plate XIX: 1–3) | *Eremospatha* sp. |
| - Equatorial grain size ~45–55µm (Plate XVIII: 15–16) | *Ancistrophyllum laurentii* |

## 5.10. Syncolporate

Plate XXII

**Key:**

| | |
|---|---|
| 1. Equatorial grain size ~15–20µm (Plate XXII: 7–10) | *Syzygium guineense* |
| - Equatorial grain size ~20–25µm (Plate XXII: 1–3) | *Eugenia michoacanensis* |
| - Equatorial grain size ~30–37µm (Plate XXII: 4–6) | *Myrcia* sp. |

## 5.11. Diporate

Plates XXIII–XXV

**Key:**

| | |
|---|---|
| 1. Equatorial grain shape rectangular (tall) (Plate XXIII: 1–4) | *Musanga smithii* |
| - Equatorial grain shape sub–prolate (Plate XXIII: 5–9) | *Musanga leo-errerae* |
| - Equatorial grain shape sub–oblate | 2. |
| - Equatorial grain shape circular | 4. |

2. Pore shape elliptic (tall) (Plate XXIII: 10–15) *Chlorophora excelsa*
- Pore shape circular 3.

3. Pore morphology thickened pore (Plate XXIII: 16–17) *Antiaris toxicaria*
- Pore morphology plain (Plate XXIII: 18–19) *Ficus ingens*

4. Pore shape irregular (Plate XXIV: 1–5) *Iodes ovalis*
- Pore shape circular with annulus 5.
- Pore shape circular 6.

5. Surface psilate (Plate XXIV: 6–9) *Baissea multiflora*
- Surface scabrate (Plate XXIV: 10–12) *Motandra guineensis*

6. Pore morphology thickened pore (Plate XXIV: 13–19) *Trema orientalis*
- Pore morphology plain 7.

7. Equatorial grain diameter ~18–22µm (Plate XXIV: 20–22) *Trema guinensis*
- Equatorial grain diameter ~63–77 µm (Plate XXV: 1–2) *Morinda citrifolia*

## 5.12. Dicolporate

Plate XXVI

**Key:**

1. Pore size ~10µm (Plate XXVI: 1–6) *Justicia cordata*
- Pore size ~4µm (Plate XXVI: 7–11) *Justicia flava*

## 5.13. Triporate

Plates XXVII–XXXIV

**Key:**

1. Surface granulate (Plate XXVII: 1–7) *Allophylus africanus*
- Surface echinate 2.
- Surface psilate 3.
- Surface reticulate 8.
- Surface scabrate 17.

2. Polar grain diameter ~18–21µm (Plate XXVII: 8–11) *Iodes ovalis*
- Polar grain diameter ~35–45µm (Plate XXVII: 12–14) *Piliostigma reticulatum*
- Polar grain diameter ~50–70µm (Plate XXVIII: 1–3) *Bombax brevicuspe*

3. Polar grain shape circular 4.
- Polar grain shape triangular (convex) 5.

4. Polar grain diameter ~12–16µm (Plate XXVIII: 4–6) *Sesuvium sessile*
- Polar grain diameter ~20–30µm (Plate XXVIII: 10–12) *Baissea multiflora*

5. Pore size ~1–3µm 6.

- Pore size ~4–5µm (Plate XXVIII: 19–21) *Protea susannae*

6. Pore morphology thickened pore (Plate XXVIII: 13–15) *Sabicea floribunda*
- Pore morphology thinning sexine 7.

7. Polar grain diameter ~8–12µm (Plate XXVIII: 7–9) *Coula edulis*
- Polar grain diameter ~18–22µm (Plate XXVIII: 16–18) *Heisteria parvifolia*

8. Pore morphology thickened pore 9.
- Pore morphology slightly extruded 10.
- Pore morphology extruded 11.
- Pore morphology plain 12.
- Pore morphology thinning sexine 15.

9. Polar grain diameter ~25–35µm (Plate XXVIII: 22–24) *Bombax buonopozense*
- Polar grain diameter ~40–50µm (Plate XXIX: 1–6) *Plectronia vulgaris*

10. Polar grain diameter ~14–16µm (Plate XXIX: 10–15) *Lasianthus africanus*
- Polar grain diameter ~45–55µm (Plate XXIX: 16–18) *Kirkia acuminata*
- Polar grain diameter ~60–80µm (Plate XXIX: 7–9) *Ceiba pentandra*

11. Polar grain diameter ~36–44µm (Plate XXX: 1–7) *Vigna fischeri*
- Polar grain diameter ~54–66µm (Plate XXX: 8–10) *Cardiospermum grandiflorum*

12. Polar grain shape circular 13.
- Polar grain shape triangular (convex) 14.

13. Pore size ~3µm (Plate XXX: 11–14) *Triplochiton scleroxylon*
- Pore size ~5µm (Plate XXX: 15–18) *Nesogordonia fertilis*
- Pore size ~6µm (Plate XXX: 19–21) *Entada umbonata*

14. Pore size ~6µm (Plate XXXI: 1–6) *Nesogordonia parvifolia*
- Pore size ~8µm (Plate XXXI: 13–15) *Vigna luteola*
- Pore size ~25µm (Plate XXXI: 16–17) *Psychotria fractinervata*

15. Polar grain diameter ~10–15µm (Plate XXXI: 7–12) *Dichapetalum mossambicense*
- Polar grain diameter ~36–45µm (Plate XXXII: 1–3) *Paullinia pinnata*
- Polar grain diameter ~45–55µm 16.

16. Pore shape circular (Plate XXXII: 4–6) *Entada pursaetha*
- Pore shape elliptic (tall) (Plate XXXII: 7–13) *Protea trichanthera*

17. Polar grain shape circular 18.
- Polar grain shape triangular (convex) 21.

18. Pore shape rectangular (broad) (Plate XXXII: 14–19) *Leptaulus daphnoides*
- Pore shape circular 19.
- Pore shape circular (with annulus) 20.

19. Polar grain diameter ~18–22µm (Plate XXXIII: 1–4) *Celtis zenkeri*
- Polar grain diameter ~27–33µm (Plate XXXIII: 5–7) *Celtis mildbraedii*

20. Pore morphology sunken pore (Plate XXXIII: 8–13) *Anthocleista grandiflora*
- Pore morphology slightly extruded (Plate XXXIII: 14–17) *Hymenocardia acida*

21. Polar grain diameter ~10–15µm (Plate XXXIV: 1–3) *Dichapetalum stuhlmannii*
- Polar grain diameter ~18–24µm 22.

- Polar grain diameter ~40–60µm (Plate XXXIV: 4–7) *Turraeanthus africana*

22. Wall thickness ~0.25µm (Plate XXXIV: 8–9) *Striga forbesii*
- Wall thickness ~1.5µm (Plate XXXIV: 10–14) *Celtis integrifolia*

## 5.14 Tricolpate

Plates XXXV–XXXIX

**Key:**

1. Surface psilate (Plate XXXV: 1–5) *Gunnera chilensis*
- Surface clavate/psilate (Plate XXXVI: 6–11) *Vitex amboniensis*
- Surface scabrate (Plate XXXV: 6–10) *Napoleona imperialis*
- Surface striate (Plate XXXIX: 6–11) *Berlinia grandiflora*
- Surface reticulate 2.

2. Equatorial grain shape rectangular (tall) (Plate XXXVII: 1–6) *Scytopetalum tieghemii*
- Equatorial grain shape rhombic (tall) (Plate XXXVII: 7–12) *Dichostemma* sp.
- Equatorial grain shape circular (Plate XXXVIII: 19–20) *Paramacrolobium coeruleum*
- Equatorial grain shape rhombic (broad) (Plate XXXVIII: 7–12) *Brachystegia leonensis*
- Equatorial grain shape suboblate (Plate XXXVIII: 1–6) *Brachystegia spiciformis*
- Equatorial grain shape prolate 3.
- Equatorial grain shape subprolate 4.

3. Colp length 1 (Plate XXXVI: 1–5) *Leucas calostachys*
- Colp length 2 (Plate XXXVI: 24–26) *Aneulophus africanus*

4. Polar grain shape triangular (convex) 5.
- Polar grain shape circular 6.
- Polar grain shape tri–lobate 8.

5. Equatorial grain diameter ~15–25µm (Plate XXXVII: 13–18) *Cissampelos mucronata*
- Equatorial grain diameter ~40–50µm (Plate XXXIX: 1–5) *Petersia africana*

6. Wall thickness <2 µm (Plate XXXV: 17–21) *Premna maxima*
- Wall thickness >2 µm 7.

7. Equatorial grain diameter ~27–37µm (Plate XXXVI: 18–23) *Tetracera alnifolia*
- Equatorial grain diameter ~40–50µm (Plate XXXV: 22–27) *Premna resinosa*

8. Wall thickness ~2µm (Plate XXXVI: 12–17) *Vitex doniana*
- Wall thickness~ 3µm (Plate XXXV: 11–16) *Farsetia stenoptera*
- Wall thickness ~10µm (Plate XXXVIII: 13–18) *Afzelia bracteata*

## 5.15. Tricolporate

Plates XL–CXIV

**Key:**

| | |
|---|---|
| 1. Equatorial grain shape circular | 2. |
| - Equatorial grain shape oblate (Plate XL: 1–6) | *Gerrardina foliosa* |
| - Equatorial grain shape perprolate (Plate XL: 7–11) | *Thecacoris gymnogyne* |
| - Equatorial grain shape prolate | 3. |
| - Equatorial grain shape rectangular (tall) | 4. |
| - Equatorial grain shape rhombic (broad) | 5. |
| - Equatorial grain shape rhombic (tall) | 6. |
| - Equatorial grain shape sub–oblate | 7. |
| - Equatorial grain shape sub–prolate | 8. |
| - Equatorial grain shape undetermined | 87. |
| | |
| 2. Surface psilate | 11. |
| - Surface reticulate | 12. |
| - Surface scabrate | 13. |
| - Surface striate (Plate XL: 12–17) | *Vepris uguenensis* |
| | |
| 3. Surface psilate | 27. |
| - Surface reticulate | 28. |
| - Surface striate | 37. |
| | |
| 4. Surface psilate | 9. |
| - Surface reticulate | 10. |
| - Surface scabrate | 40. |
| | |
| 5. Surface psilate (Plate XLI: 1–10) | *Alchornea floribunda* |
| - Surface clavate/pilate (Plate XLI: 11–16) | *Ilex mitis* |
| - Surface reticulate | 42. |
| - Surface scabrate | 43. |
| | |
| 6. Surface psilate | 44. |
| - Surface striate | 46. |
| - Surface reticulate | 49. |
| - Surface scabrate (Plate LXXVIII: 4–7) | *Daniella oliveri* |
| | |
| 7. Surface psilate | 53. |
| - Surface striate (Plate XLII: 1–7) | *Crudia bracteata* |
| - Surface reticulate | 54. |
| - Surface scabrate (Plate XLII: 8–14) | *Parinari curatellifolia* |
| | |
| 8. Surface echinate | 60. |
| - Surface psilate | 62. |
| - Surface reticulate | 65. |
| - Surface scabrate | 80. |
| - Surface striate | 85. |
| | |
| 9. Pore shape circular (Plate XLIII: 1–6) | *Diospyros mespiliformis* |
| - Pore shape elliptic (broad) (Plate XLIII: 7–9) | *Lotus chazaliei* |
| - Pore shape lalongate (Plate XLIII: 10–16) | *Canarium schweinfurthii* |
| - Pore shape lolongate (Plate XLIV: 1–14) | *Heliotropium* sp. x2 |
| | |
| 10. Pore shape circular | 39. |
| - Pore shape elliptic (tall) (Plate XLV: 1–6) | *Balanites glaber* |
| | |
| 11. Pore shape circular | 14. |

- Pore shape elliptic (broad) (Plate XLV: 7–12) *Centroplacus glaucinus*

12. Pore shape circular (Plate XLV: 13–18) *Indigofera leptoclada*
- Pore shape circular with annulus 15.
- Pore shape concave 16.
- Pore shape lalongate (Plate XLVI: 1–8) *Millettia psilopetala*
- Pore shape rectangular (broad) 18.
- Pore shape lolongate 21.
- Pore shape rhombic (tall) (Plate XLVI: 9–16) *Argomuellera macrophylla*
- Pore shape squared 23.
- Pore shape elliptic (tall) (Plate XLVII: 1–6) *Balanites aegyptiacus*
- Pore shape irregular (Plate XLVII: 7–12) *Martretia quadricornis*
- Pore shape undetermined (Plate XLVIII: 1–3) *Cliffortia nitidula*

13. Pore shape circular 26.
- Pore shape rectangular (broad) (Plate XLVIII: 4–9) *Parinari holstii*
- Pore shape lalongate (Plate XLVIII: 10–15) *Macaranga schweinfurt*
- Pore shape lolongate (Plate XLVIII: 16–22) *Prunus africana*

14. Pore morphology with an operculum (Plate XLIX: 1–8) *Alchornea cordifolia*
- Pore morphology sunken pore (Plate XLIX: 9–12) *Medusandra richardsiana*

15. Pore morphology thickened pore (Plate XLIX: 14–18) *Commiphora campestris*
- Pore morphology sunken pore (Plate L: 1–7) *Commiphora scheffleri*

16. Pore morphology thickened pore (Plate L: 8–16) *Erythrococca bongensis*
- Pore morphology sunken pore 17.
- Pore morphology slightly extruded (Plate LI: 1–5) *Amanoa strobilacea*
- Pore morphology extruded (Plate LI: 6–12) *Discoglypremna caloneura*

17. Pore position mid–wall (Plate LII: 1–8) *Entada abyssinica*
- Pore position corner (Plate LII: 9–15) *Baphia massaiensis*

18. Pore morphology thickened pore 19.
- Pore morphology sunken pore 20.

19. Colpus length full (Plate LIII: 1–6) *Mallotus wrayi*
- Colpus length >2/3 (Plate LIII: 7–12) *Fagara macrophylla*

20. Polar grain shape circular (Plate LIII: 13–18) *Olea hochstetteri*
- Polar grain shape triangular (convex) (Plate LIV: 1–8) *Ixora aneimenodesma*

21. Wall thickness even 22.
- Wall thinner on pole (Plate LIV: 9–16) *Anthostema aubryanum*

22. Polar grain shape tri–lobate (Plate LV: 1–7) *Agelaea heterophylla*
- Polar grain shape circular (Plate LV: 8–15) *Adenia nicobarica*

23. Visible collumnae 24.
- Invisible collumnae (Plate LVI: 1–3) *Salacia kraussii*

24. Polar grain shape tri–lobate (Plate LVI: 4–8) *Maytenus senegalensis*
- Polar grain shape triangular (convex) 25.

25. Equatorial grain diameter ~17–25µm (Plate LVI: 9–14) *Hippocratea affinis*
- Equatorial grain diameter ~25–35µm (Plate LVII: 1–8) *Hippocratea africana*

26. Pore morphology extruded (Plate LVII: 9–14) *Grandidiera boivinii*
- Pore morphology slightly extruded (Plate LVIII: 1–8) *Cynometra alexandri*

27. Pore shape lalongate (Plate LVIII: 9–13) *Calantica jalbertii*
- Pore shape rhombic (broad) (Plate LVIII: 14–20) *Blighia wildemaniana*

28. Colpus length full 29.
- Colpus length >2/3 35.

29. Pore shape circular 30.
- Pore shape concave 31.
- Pore shape elliptic (tall) 32.
- Pore shape lalongate 33.
- Pore shape rhombic (broad) (Plate LIX: 1–6) *Corchorus fascicularis*
- Pore shape squared (Plate LIX: 7–13) *Strephonema pseudocola*
- Pore shape undetermined 34.

30. Equatorial grain diameter ~18–22µm (Plate LX: 1–6) *Crossopteryx febrifuga*
- Equatorial grain diameter ~45–55µm (Plate LX: 7–9) *Cissus petiolata*

31. Pore morphology sunken pore (Plate LXI: 1–6) *Ritchiea capparoides*
- Pore morphology thinning sexine (Plate LX: 10–17) *Spondianthus preussii*

32. Pore morphology plain (Plate LXI: 7–13) *Blighia unijugata*
- Pore morphology slightly extruded (Plate LXII: 1–7) *Cissus quadrangularis*

33. Pore morphology plain (Plate LXII: 8–13) *Grewia bicolor*
- Pore morphology sunken pore (Plate LXIII: 1–5) *Vepris humbertii*

34. Pore morphology plain (Plate LXIII: 6–11) *Rubus scheffleri*
- Pore morphology slightly extruded (Plate LXIV: 1–6) *Drypetes gerrardii*

35. Pore shape circular (Plate LXIV: 7–11) *Flacourtia indica*
- Pore shape concave 36.
- Pore shape elliptic (broad) (Plate LXIV: 12–17) *Avicennia nitida*
- Pore shape irregular (Plate LXV: 1–6) *Dasylepis assinensis*
- Pore shape rectangular (broad) (Plate LXV: 7–15) *Hannoa* sp. (x2)
- Pore shape rhombic (tall) (Plate LXV: 16–21) *Ormocarpum kirkii*

36. Pore morphology thickened (Plate LXVI: 1–7) *Maesobotrya hirtella*
- Pore morphology extruded (Plate LXVI: 8–14) *Cassipourea flanaganii*

37. Pore shape elliptic (tall) (Plate LXVI: 15–20, LXVII: 1–4) *Lannea* sp. (x2)
- Pore shape lolongate 38.

38. Pore morphology thinning sexine (Plate LXVII: 5–9) *Isoberlinia angolensis*
- Pore morphology plain (Plate LXVIII: 1–5) *Isoberlinia doka*

39. Pore morphology thinning sexine (Plate LXVIII: 6–12) *Scytopetalum tieghemii*
- Pore morphology sunken pore (Plate LXIX: 1–7) *Euphorbia hypericifolia*

40. Pore shape elliptic (tall) (Plate LXIX: 8–13) *Pterocarpus abyssinicus*
- Pore shape lolongate (Plate LXIX: 14–19) *Pterocarpus lucens*
- Pore shape rectangular (broad) 41.

41. Colpus length 2/3 (Plate LXX: 1–7) *Dodonaea viscosa*

- Colpus length 1/3 LXX: 8–13) *Tabernaemontana ventricosa*

42. Pore shape circular (Plate LXXI: 1–6) *Sterculia tragacantha*
- Pore shape concave (Plate LXXI: 7–12) *Prosopis africana*
- Pore shape lalongate (Plate LXXII: 1–8) *Hagenia abyssinica*
- Pore shape rectangular (broad) (Plate LXXII: 9–16) *Monotes kerstingii*

43. Visible collumnae (Plate LXXIII: 1–6) *Copaifera gorskiana*
- Invisible collumnae (Plate LXXIII: 7–12) *Pygeum africanum*

44. Pore shape concave (Plate LXXIII: 13–18) *Acridocarpus macrocalyx*
- Pore shape lolongate 45.

45. Wall thickness even (Plate LXXIV: 1–7) *Guibourtia arnoldiana*
- Wall thicker on pole (Plate LXXIV: 8–14) *Griffonia simplicifolia*

46. Pore morphology thinning sexine (Plate LXXV: 1–6) *Lannea humilis*
- Pore morphology sunken pore 47.
- Pore morphology plain 48.

47. Colpus length full (Plate LXXV: 7–12) *Sclerocarya birrea*
- Colpus length >2/3 (Plate LXXVI: 1–6) *Spondias mombin*

48. Pore shape elliptic (tall) (Plate LXXVII: 1–6) *Berlinia bifoliolata*
- Pore shape rhombic (broad) (Plate LXXVII: 7–12) *Teclea villosa*

49. Pore shape circular 50.
- Pore shape elliptic (broad) 51.
- Pore shape rhombic (broad) 52.
- Pore shape zonorate (Plate LXXVIII: 1–3) *Corchorus trilocularis*

50. Pore morphology thinning sexine (Plate LXXIX: 1–6) *Aubrevillea platycarpa*
- Pore morphology sunken pore (Plate LXXX: 1–6) *Caloncoba angolensis*

51. Pore morphology thinning sexine (Plate LXXX: 7–12) *Avicennia officinalis*
- Pore morphology sunken pore (Plate LXXXI: 1–7) *Culcasia dinklagei*

52. Pore morphology plain (Plate LXXXI: 8–12) *Hildegardia barteri*
- Pore morphology sunken pore (Plate LXXXII: 1–7) *Zizyphus mauritiana*

53. Pore morphology plain (Plate XXII: 7–10) *Syzygium guineense*
- Pore morphology thinning sexine (Plate LXXXII: 8–13) *Dialium guianense*
- Pore morphology extruded (Plate LXXXII: 14–17) *Irvingia smithii*

54. Pore shape circular 55.
- Pore shape elliptic (broad) 58.
- Pore shape elliptic (tall) (Plate LXXXII: 18–23) *Mitragyna inermis*
- Pore shape irregular 59.
- Pore shape lalongate (Plate LXXXIII: 1–7) *Tetrorchidium didymostemon*
- Pore shape squared (Plate LXXXIII: 8–13) *Gaertnera paniculata*
- Pore shape rectangular (broad) (Plate LXXXIV: 1–3) *Uapaca bojeri*

55. Pore morphology extruded (Plate LXXIX: 7–10) *Cardiospermum corindum*
- Pore morphology thinning sexine 56.
- Pore morphology sunken pore 57.

56. Polar grain shape triangular (convex) (Plate LXXXIV: 4–10) *Pericopsis angolensis*

- Polar grain shape triangular (straight) (Plate LXXXIV: 11–18) *Rhynchosia memnonia*

57. Wall thickness even (Plate LXXXV: 1–8) *Piptadenia africana*
- Wall thinner on pole (Plate LXXXV: 9–14) *Brachystegia spiciformis*

58. Pore morphology sunken pore (Plate LXXXVI: 1–20) Sapindaceae sp. (x3)
- Pore morphology thinning sexine (Plate LXXXVII: 1–6) *Sesbania goetzei*
- Pore morphology extruded (Plate LXXXVII: 7–14) *Ixora brachypoda*

59. Visible collumnae (Plate LXXXVIII: 1–6) *Rhynchosia* sp.
- Invisible collumnae (Plate LXXXVIII: 7–13) *Prosopis alpataco*

60. Pore shape concave (Plate LXXXIX: 1–7) *Centaurea perrottetii*
- Pore shape rectangular (broad) (Plate XC: 1–5) *Centaurea dimorpha*
- Pore shape elliptic (tall) 61.

61. Wall thickness even (Plate XCI: 1–7) *Artemisia judaica*
- Wall thinner on pole (Plate XCI: 8–13) *Artemisia* sp.

62. Pore shape circular 90.
- Pore shape circular with annulus (Plate XCI: 14–19) *Tabernaemontana retusa*
- Pore shape concave 63.
- Pore shape elliptic (broad) 64.
- Pore shape rectangular (broad) (Plate XCII: 1–5) *Lophira alata*
- Pore shape rectangular (tall) (Plate XCII: 6–13) *Trichodesma africanum*
- Pore shape rhombic (broad) (Plate XCII: 14–19) *Diospyros austroafricana*

63. Pore morphology sunken pore (Plate XCIII: 1–7) *Diospyros abyssinica*
- Pore morphology thinning sexine (Plate XCIII: 8–13) *Afrolicania elaeosperma*

64. Colpus length 2/3 (Plate XCIII: 14–16) *Casearia engleri*
- Colpus length1/2 (Plate XCIV: 1–3) *Neolemonniera clitandrifolia*

65. Pore shape circular 66.
- Pore shape concave 69.
- Pore shape elliptic (broad) 70.
- Pore shape elliptic (tall) 72.
- Pore shape irregular 75.
- Pore shape lalongate 77.
- Pore shape lolongate 79.
- Pore shape rectangular (broad) (Plate XCIV: 4–10) *Elaeodendron buchananii*
- Pore shape rectangular (tall) (Plate XCV: 1–6) *Euphorbia engleri*
- Pore shape rhombic (broad) (Plate XCVI: 1–7) *Rhizophora mangle*
- Pore shape undetermined (Plate XCVI: 8–15) *Euphorbia cussonioides*

66. Pore morphology sunken pore 67.
- Pore morphology thinning sexine (Plate XCVII: 1–6) *Rhektophyllum congense*

67. Pore position mid–wall (Plate XCVII: 7–13) *Securinega virosa*
- Pore position corner 68.

68. Equatorial grain diameter ~27–33µm (Plate XCVII: 14–17) *Detarium senegalense*
- Equatorial grain diameter ~50–60µm (Plate XCVIII: 1–7) *Cola nitida*

69. Pore morphology sunken pore (Plate XCVIII: 8–14) *Rhizophora mucronata*
- Pore morphology thinning sexine (Plate XCIX: 1–7) *Ritchiea fragariodora*

- Pore morphology slightly extruded (Plate XCIX: 8–13) *Millettia oblata*

70. Pore morphology sunken pore 71.
- Pore morphology extruded (Plate C: 1–8) *Cassine parvifolia*
- Pore morphology slightly extruded (Plate C: 9–15) *Nauclea esculenta*

71. Equatorial grain diameter ~25–30µm (Plate C: 16–23) *Maesobotrya barteri*
- Equatorial grain diameter ~30–40µm (Plate CI: 1–6) *Cola millenii*

72. Pore morphology thickened (Plate CI: 7–12) *Cola gigantea*
- Pore morphology extruded (Plate CII: 1–8) *Bridelia micrantha*
- Pore morphology slightly extruded (Plate CII: 9–14) *Euphorbia grandicornis*
- Pore morphology plain 73.

73. Pore position mid–wall (Plate CIII: 1–7) *Anthostema senegalense*
- Pore position corner 74.

74. Extine type tectate (Plate CIII: 8–14) *Ormocarpum sennoides*
- Extine type semitectate (Plate CIV: 1–7) *Salacia pyriformis*

75. Pore morphology sunken pore 76.
- Pore morphology thickened (Plate CIV: 8–13) *Grewia glandulosa*

76. Polar grain shape circular (Plate CV: 1–6) *Lotus arabicus*
- Polar grain shape triangular (convex) (Plate CV: 7–14) *Uapaca heudelotii*

77. Pore position corner (Plate CV: 15–20) *Vepris gossweileri*
- Pore position mid–wall 78.

78. Pore size ~8µm (Plate CVI: 1–6) *Zanthoxylum procerum*
- Pore size ~2µm (Plate CVI: 7–12) *Odyendea gabunenesis*

79. Pore morphology sunken pore (Plate CVI: 13–20) *Convolvulus trabutianus*
- Pore morphology thinning sexine (Plate CVII: 1–8) *Millettia tanaensis*
- Pore morphology plain (Plate CVII: 9–15) *Oncoba dentata*

80. Pore shape concave (Plate CVII: 16–23) *Detarium le–testui*
- Pore shape elliptic (broad) 81.
- Pore shape irregular (Plate CVIII: 1–7) *Kiggelaria africana*
- Pore shape lalongate 83.
- Pore shape lolongate 84.
- Pore shape rectangular (broad) (Plate CVIII: 8–12) *Sarcophrynium brachystachyum*

81. Pore morphology extruded 82.
- Pore morphology thinning sexine (Plate CVIII: 13–20) *Cassia longiracemosa*

82. Wall thickness ~3µm (Plate CIX: 1–7) *Tephrosia nana*
- Wall thickness ~1µm (Plate CIX: 8–14) *Tephrosia elata*

83. Pore morphology plain (Plate CIX: 15–19) *Dissomeria crenata*
- Pore morphology sunken pore (Plate CX: 1–8) *Homalium buchholzii*

84. Colpi width ~15µm (Plate CX: 9–14) *Cassia burttii*
- Colpi width ~ 35µm (Plate CX: 15–20) *Copaifera carrissoana*

85. Pore shape circular 86.
- Pore shape lalongate (Plate CXI: 1–7) *Vepris eugeniifolia*

- Pore shape lolongate (Plate CXII: 1–6) *Hymenostegia afzelii*

86. Equatorial grain diameter ~27–33µm (Plate CXI: 8–15) *Cynometra pedicellata*
- Equatorial grain diameter ~35–50µm (Plate CXI: 16–20) *Aphloia theiformis*

87. Pore morphology plain 88.
- Pore morphology sunken pore (Plate CXII: 7–9) *Placodiscus amaniensis*
- Pore morphology thickened 89.

88. Polar grain shape triangular (convex) (Plate CXII: 10–12) *Nauclea diderrichii*
- Polar grain shape tri–lobate (Plate CXIII: 1–3) *Microdesmis* sp.

89. Visible collumnae (Plate CXIII: 6–7) *Rinorea oblongifolia*
- Invisible collumnae (Plate CXIII: 4–5) *Rinorea welwitschii*

90. Pore morphology sunken pore (Plate CXIII: 8–15) *Pericopsis laxiflora*
- Pore morphology thinning sexine (Plate CXIV: 1–6) *Baphia obovata*

## 5.16. Stephanoporate

Plate CXV, *Funtumia latifolia* (Plate CXV: 1–3)

## 5.17. Stephanocolpate

Plates CXVI–CXX

**Key:**

1. Full length of grain 2.
- 2/3 the full length of grain 3.
- 1/2 the full length of grain 4.
- < 1/3 the full length of grain (Plate CXVI: 1–7) *Borreria densiflora*
- Colpi length undetermined
(Plate CXVI: 8–9, *Borreria ruelliae*
Plate CXVI: 10–11) *Sesamum indicum*

2. Equatorial grain shape subprolate (Plate CXVII: 1–4) *Afzelia quanzensis*
- Equatorial grain shape rectangular (broad) (Plate CXVIII: 1–6) *Diodia scandens*

3. Equatorial grain shape circular (Plate CXIX: 1–5) *Mitracarpus hirtus*
- Equatorial grain shape suboblate (Plate CXIX: 6–9) *Sesamum angustifolium*

4. Surface baculate (Plate CXX: 1–6) *Diodia aulacosperma*
- Surface reticulate (Plate CXX: 7–14) *Mitracarpus verticillatus*

## 5.18. Stephanocolporate

Plates CXXI–CXXII

**Key:**

1. Polar grain shape elliptic (Plate CXXI: 1–7) *Atroxima afzeliana*
- Polar grain shape circular (Plate CXXII: 1–7) *Securidaca longepedunculata*

## 5.19. Heterocolporate

Plate CXXIII

**Key:**

1. Pore shape elliptic (tall) (Plate CXXIII: 1–6) *Combretum aculeatum*
- Pore shape elliptic (broad) (Plate CXXIII: 7–12) *Terminalia brownii*
- Pore shape rectangular (broad) (Plate CXXIII: 13–17) *Combretum gueinzii*
- Pore shape concave 2.
- Pore shape squared (Plate CXXIII: 18–23) *Terminalia aemula*

2. Pore morphology extruded (Plate CXXIII: 24–29) *Guiera senegalensis*
- Pore morphology sunken pore (Plate CXXIII: 30–35) *Pteleopsis diptera*

## 5.20. Periporate

Plates CXXIV–CXXIX

**Key:**

1. Pore shape irregular 2.
- Pore shape circular 4.
- Pore shape circular with annulus 8.
- Pore shape elliptic broad (Plate CXXIV: 1–4) *Plantago lanceolata*

2. Surface pattern reticulate 3.
- Surface pattern scabrate (Plate CXXIV: 5–8) *Celosia stuhlmanniana*
- Surface pattern verrucate (Plate CXXV: 1–3) *Calystegia sepium*
- Surface pattern psilate (Plate CXXV: 4–6) *Costus spectabilis*

3. Pore section plain (Plate CXXIV: 9–14) *Celosia* sp. (x2)
- Pore section thinning sexine (Plate CXXIV: 15–18) *Drymaria cordata*

4. Surface pattern reticulate 5.
- Surface pattern echinate 6.

5. Equatorial grain diameter ~27–33µm (Plate CXXIV: 19–22) *Plantago major*
- Equatorial grain diameter ~36–44µm (Plate CXXVI: 1–3) *Plantago palmata*
- Equatorial grain diameter ~90–110µm (Plate CXXVI: 4–7) *Dicranolepis oligantha*

6. Equatorial grain diameter ~20–30µm (Plate CXXVII: 1–4) *Bosqueia manongarivensis*
- Equatorial grain diameter ~60–80µm (Plate CXXVII: 5–8) *Ipomoea donaldsonii*
- Equatorial grain diameter ~80–120µm 7.

7. Wall thickness ~5µm (Plate CXXVIII: 5–6) *Hewittia sublobata*
- Wall thickness ~12µm (Plate CXXIX: 1–2) *Ipomoea ochracea*

8. Equatorial grain diameter ~35–45µm (Plate CXXVIII: 1–4) *Lynchnis* sp.
- Equatorial grain diameter ~45–55µm (Plate CXXIX: 3–6) *Cerastium indicum*

## 5.21. Acknowledgements

The authors would like to thank the two reviewers for constructive comments which improved the quality of this manuscript. Collection and collation of the pollen images, development of the keys and preparation of this manuscript was funded by awards from the Royal Society (International Travel grant, #TG090002, WDG and DAL) and the Natural Environments Research Council (New Investigator Award, #NE/G000824/1,WDG; and studentship #M82525J, CSM).

| Family | Species | Plate |
|---|---|---|
| Acanthaceae | *Avicennia nitida* | LXIV |
| Acanthaceae | *Avicennia officinalis* | LXXX |
| Acanthaceae | *Justicia cordata* | XXVI |
| Acanthaceae | *Justicia flava* | XXVI |
| Achariaceae | *Caloncoba angolensis* | LXXX |
| Achariaceae | *Dasylepis assinensis* | LXV |
| Achariaceae | *Grandidiera boivinii* | LVII |
| Achariaceae | *Kiggelaria africana* | CVIII |
| Aizoaceae | *Sesuvium sessile* | XXVIII |
| Amaranthaceae | *Alternanthera nodiflora* | VII |
| Amaranthaceae | *Alternanthera repens* | VII |
| Amaranthaceae | *Celosia patentiloba* | CXXIV |
| Amaranthaceae | *Celosia stuhlmanniana* | CXXIV |
| Amaranthaceae | *Celosia trigyna* | CXXIV |
| Amaryllidaceae | *Crinum pauciflorum* | XXI |
| Amaryllidaceae | *Crinum powellii* | XXI |
| Anacardiaceae | *Lannea humilis* | LXXV |
| Anacardiaceae | *Lannea stuhlmannii* | LXVI |
| Anacardiaceae | *Lannea triphylla* | LXVII |
| Anacardiaceae | *Sclerocarya birrea* | LXXV |
| Anacardiaceae | *Spondias mombin* | LXXVI |
| Annonaceae | *Artabotrys likimensis* | XVI |
| Annonaceae | *Piptostigma mayumbense* | VIII |
| Annonaceae | *Uvaria kirkii* | XI |
| Annonaceae | *Uvariopsis congensis* | IV |
| Aphloiaceae | *Aphloia theiformis* | CXI |
| Apocynaceae | *Baissea multiflora* | XXIV |
| Apocynaceae | *Baissea multiflora* | XXVIII |
| Apocynaceae | *Funtumia latifolia* | CXV |
| Apocynaceae | *Motandra guineensis* | XXIV |
| Apocynaceae | *Tabernaemontana retusa* | XCI |
| Apocynaceae | *Tabernaemontana ventricosa* | LXX |
| Apocynaceae | *Tylophora sylvatica* | XV |
| Aquifoliaceae | *Ilex mitis* | XLI |
| Araceae | *Culcasia dinklagei* | LXXXI |
| Araceae | *Lemna gibba* | XIV |

| | | |
|---|---|---|
| Araceae | *Rhektophyllum congense* | XCVII |
| Arecaceae | *Ancistrophyllum laurentii* | XVIII |
| Arecaceae | *Ancistrophyllum secundiflorum* | XVIII |
| Arecaceae | *Borassus aethiopum* | VII |
| Arecaceae | *Borassus aethiopum* | XIX |
| Arecaceae | *Borassus machadonis* | XIX |
| Arecaceae | *Calamus erectus* | XVIII |
| Arecaceae | *Calamus gracilis* | XVIII |
| Arecaceae | *Elaeis guineensis* | XVIII |
| Arecaceae | *Eremospatha* sp. | XIX |
| Arecaceae | *Hyphaene natalensis* | XIX |
| Arecaceae | *Hyphaene ventricosa* | XIX |
| Arecaceae | *Phoenix reclinata* | XVIII |
| Arecaceae | *Raphia farinifera* | XVIII |
| Arecaceae | *Raphia ruffia* | XVIII |
| Asparagaceae | *Asparagus falcatus* | XX |
| Asparagaceae | *Chlorophytum floribundum* | XX |
| Asparagaceae | *Dracaena camerooniana* | XX |
| Asparagaceae | *Dracaena reflexa* | XXI |
| Asteraceae | *Artemisia judaica* | XCI |
| Asteraceae | *Artemisia* sp. | XCI |
| Asteraceae | *Centaurea dimorpha* | XC |
| Asteraceae | *Centaurea perrottetii* | LXXXIX |
| Boraginaceae | *Heliotropium bacciferum* | XLIV |
| Boraginaceae | *Heliotropium subulatum* | XLIV |
| Boraginaceae | *Trichodesma africanum* | XCII |
| Boraginaceae | *Trichomanes mandiocanum* | VII |
| Brassicaceae | *Farsetia stenoptera* | XXXV |
| Burseraceae | *Canarium schweinfurthii* | XLIII |
| Burseraceae | *Commiphora campestris* | XLIX |
| Burseraceae | *Commiphora scheffleri* | L |
| Cannabaceae | *Celtis integrifolia* | XXXIV |
| Cannabaceae | *Celtis mildbraedii* | XXXIII |
| Cannabaceae | *Celtis zenkeri* | XXXIII |
| Cannabaceae | *Trema guinensis* | XXIV |
| Cannabaceae | *Trema orientalis* | XXIV |
| Capparaceae | *Ritchiea capparoides* | LXI |
| Capparaceae | *Ritchiea fragariodora* | XCIX |
| Cardioteridaceae | *Leptaulus daphnoides* | XXXII |
| Caryophyllaceae | *Cerastium indicum* | CXXIX |
| Caryophyllaceae | *Drymaria cordata* | CXXIV |
| Caryophyllaceae | *Lychnis* sp. | CXXVIII |
| Celastraceae | *Cassine parvifolia* | C |
| Celastraceae | *Elaeodendron buchananii* | XCIV |
| Celastraceae | *Hippocratea affinis* | LVI |
| Celastraceae | *Hippocratea africana* | LVII |
| Celastraceae | *Maytenus senegalensis* | LVI |
| Celastraceae | *Salacia kraussii* | LVI |
| Celastraceae | *Salacia pyriformis* | CIV |
| Centroplacaceae | *Centroplacus glaucinus* | XLV |
| Chrysobalanaceae | *Afrolicania elaeosperma* | XCIII |
| Chrysobalanaceae | *Parinari curatellifolia* | XLII |
| Chrysobalanaceae | *Parinari holstii* | XLVIII |
| Combretaceae | *Combretum aculeatum* | CXXIII |
| Combretaceae | *Combretum gueinzii* | CXXIII |
| Combretaceae | *Guiera senegalensis* | CXXIII |

| | | |
|---|---|---|
| Combretaceae | *Pteleopsis diptera* | CXXIII |
| Combretaceae | *Strephonema pseudocola* | LIX |
| Combretaceae | *Terminalia aemula* | CXXIII |
| Combretaceae | *Terminalia brownii* | CXXIII |
| Commelinaceae | *Aneilema johnstonii* | XXI |
| Commelinaceae | *Commelina africana* | XXI |
| Connaraceae | *Agelaea heterophylla* | LV |
| Convolvulaceae | *Calystegia sepium* | CXXV |
| Convolvulaceae | *Convolvulus trabutianus* | CVI |
| Convolvulaceae | *Hewittia sublobata* | CXXVIII |
| Convolvulaceae | *Ipomoea donaldsonii* | CXXVII |
| Convolvulaceae | *Ipomoea ochracea* | CXXIX |
| Costaceae | *Costus spectabilis* | CXXV |
| Davalliaceae | *Nephrolepis biserrata* | X |
| Davalliaceae | *Nephrolepis exaltata* | X |
| Dichapetalaceae | *Dichapetalum mossambicense* | XXXI |
| Dichapetalaceae | *Dichapetalum stuhlmannii* | XXXIV |
| Dilleniaceae | *Tetracera alnifolia* | XXXVI |
| Dipterocarpaceae | *Monotes kerstingii* | LXXII |
| Ebenaceae | *Diospyros abyssinica* | XCIII |
| Ebenaceae | *Diospyros austroafricana* | XCII |
| Ebenaceae | *Diospyros mespiliformis* | XLIII |
| Ericaceae | *Erica arborea* | IV |
| Erythroxylaceae | *Aneulophus africanus* | XXXVI |
| Euphorbiaceae | *Alchornea cordifolia* | XLIX |
| Euphorbiaceae | *Alchornea floribunda* | XLI |
| Euphorbiaceae | *Anthostema aubryanum* | LIV |
| Euphorbiaceae | *Anthostema senegalense* | CIII |
| Euphorbiaceae | *Argomuellera macrophylla* | XLVI |
| Euphorbiaceae | *Croton gratissimus* | XII |
| Euphorbiaceae | *Croton macrostachyus* | XII |
| Euphorbiaceae | *Dichostemma* sp. | XXXVII |
| Euphorbiaceae | *Discoglypremna caloneura* | LI |
| Euphorbiaceae | *Erythrococca bongensis* | L |
| Euphorbiaceae | *Euphorbia cussonioides* | XCVI |
| Euphorbiaceae | *Euphorbia engleri* | XCV |
| Euphorbiaceae | *Euphorbia grandicornis* | CII |
| Euphorbiaceae | *Euphorbia hypericifolia* | LXIX |
| Euphorbiaceae | *Macaranga schweinfurt* | XLVIII |
| Euphorbiaceae | *Mallotus wrayi* | LIII |
| Euphorbiaceae | *Martretia quadricornis* | XLVII |
| Euphorbiaceae | *Tetrorchidium didymostemon* | LXXXIII |
| Fabaceae (Ceasalpiniodeae) | *Afzelia bracteata* | XXXVIII |
| Fabaceae (Ceasalpiniodeae) | *Afzelia quanzensis* | CXVII |
| Fabaceae (Ceasalpiniodeae) | *Berlinia bifoliolata* | LXXVII |
| Fabaceae (Ceasalpiniodeae) | *Berlinia grandiflora* | XXXIX |
| Fabaceae (Ceasalpiniodeae) | *Brachystegia leonensis* | XXXVIII |
| Fabaceae (Ceasalpiniodeae) | *Brachystegia spiciformis* | XXXVIII |
| Fabaceae (Ceasalpiniodeae) | *Brachystegia spiciformis* | LXXXV |
| Fabaceae (Ceasalpiniodeae) | *Cassia burttii* | CX |
| Fabaceae (Ceasalpiniodeae) | *Cassia longiracemosa* | CVIII |
| Fabaceae (Ceasalpiniodeae) | *Copaifera carrissoana* | CX |
| Fabaceae (Ceasalpiniodeae) | *Copaifera gorskiana* | LXXIII |
| Fabaceae (Ceasalpiniodeae) | *Crudia bracteata* | XLII |
| Fabaceae (Ceasalpiniodeae) | *Cynometra alexandri* | LVIII |
| Fabaceae (Ceasalpiniodeae) | *Cynometra pedicellata* | CXI |

| | | |
|---|---|---|
| Fabaceae (Ceasalpiniodeae) | *Daniella oliveri* | LXXVIII |
| Fabaceae (Ceasalpiniodeae) | *Detarium le-testui* | CVII |
| Fabaceae (Ceasalpiniodeae) | *Detarium senegalense* | XCVII |
| Fabaceae (Ceasalpiniodeae) | *Dialium guianense* | LXXXII |
| Fabaceae (Ceasalpiniodeae) | *Griffonia simplicifolia* | LXXIV |
| Fabaceae (Ceasalpiniodeae) | *Guibourtia arnoldiana* | LXXIV |
| Fabaceae (Ceasalpiniodeae) | *Hymenostegia afzelii* | CXII |
| Fabaceae (Ceasalpiniodeae) | *Isoberlinia angolensis* | LXVII |
| Fabaceae (Ceasalpiniodeae) | *Isoberlinia doka* | LXVIII |
| Fabaceae (Ceasalpiniodeae) | *Paramacrolobium coeruleum* | XXXVIII |
| Fabaceae (Ceasalpiniodeae) | *Piliostigma reticulatum* | XXVII |
| Fabaceae (Faboideae) | *Baphia massaiensis* | LII |
| Fabaceae (Faboideae) | *Baphia obovata* | CXIV |
| Fabaceae (Faboideae) | *Indigofera leptoclada* | XLV |
| Fabaceae (Faboideae) | *Lotus arabicus* | CV |
| Fabaceae (Faboideae) | *Lotus chazaliei* | XLIII |
| Fabaceae (Faboideae) | *Millettia oblata* | XCIX |
| Fabaceae (Faboideae) | *Millettia psilopetala* | XLVI |
| Fabaceae (Faboideae) | *Millettia tanaensis* | CVII |
| Fabaceae (Faboideae) | *Ormocarpum kirkii* | LXV |
| Fabaceae (Faboideae) | *Ormocarpum sennoides* | CIII |
| Fabaceae (Faboideae) | *Pericopsis angolensis* | LXXXIV |
| Fabaceae (Faboideae) | *Pericopsis laxiflora* | CXIII |
| Fabaceae (Faboideae) | *Pterocarpus abyssinicus* | LXIX |
| Fabaceae (Faboideae) | *Pterocarpus lucens* | LXIX |
| Fabaceae (Faboideae) | *Rhynchosia memnonia* | LXXXIV |
| Fabaceae (Faboideae) | *Rhynchosia* sp. | LXXXVIII |
| Fabaceae (Faboideae) | *Sesbania goetzei* | LXXXVII |
| Fabaceae (Faboideae) | *Tephrosia elata* | CIX |
| Fabaceae (Faboideae) | *Tephrosia nana* | CIX |
| Fabaceae (Faboideae) | *Vigna fischeri* | XXX |
| Fabaceae (Faboideae) | *Vigna luteola* | XXXI |
| Fabaceae (Mimosoideae) | *Acacia clavigera* | II |
| Fabaceae (Mimosoideae) | *Acacia eggelingii* | I |
| Fabaceae (Mimosoideae) | *Acacia seyal* | I |
| Fabaceae (Mimosoideae) | *Aubrevillea platycarpa* | LXXIX |
| Fabaceae (Mimosoideae) | *Calpocalyx brevibracteatus* | I |
| Fabaceae (Mimosoideae) | *Dichrostachys cinerea* | XVI |
| Fabaceae (Mimosoideae) | *Dichrostachys glomerata* | XVI |
| Fabaceae (Mimosoideae) | *Dichrostachys unijuga* | VIII |
| Fabaceae (Mimosoideae) | *Entada abyssinica* | LII |
| Fabaceae (Mimosoideae) | *Entada pursaetha* | XXXII |
| Fabaceae (Mimosoideae) | *Entada umbonata* | XXX |
| Fabaceae (Mimosoideae) | *Mimosa strigillosa* | IV |
| Fabaceae (Mimosoideae) | *Parkia bussei* | III |
| Fabaceae (Mimosoideae) | *Parkia inundabilis* | II |
| Fabaceae (Mimosoideae) | *Parkia velutina* | III |
| Fabaceae (Mimosoideae) | *Piptadenia africana* | LXXXV |
| Fabaceae (Mimosoideae) | *Prosopis africana* | LXXI |
| Fabaceae (Mimosoideae) | *Prosopis alpataco* | LXXXVIII |
| Fabaceae (Mimosoideae) | *Xylia evansii* | I |
| Gentianaceae | *Anthocleista grandiflora* | XXXIII |
| Gerrardinaceae | *Gerrardina foliosa* | XL |
| Gunneraceae | *Gunnera chilensis* | XXXV |
| Hernandiaceae | *Illigera appendiculata* | XIV |
| Hernandiaceae | *Illigera rhodantha* | VI |

| | | |
|---|---|---|
| Icacinaceae | *Iodes kamerunensis* | XIV |
| Icacinaceae | *Iodes ovalis* | XXIV |
| Icacinaceae | *Iodes ovalis* | XXVII |
| Iridaceae | *Acidanthera brevicollis* | VI |
| Iridaceae | *Acidanthera brevicollis* | XXI |
| Irvingiaceae | *Irvingia smithii* | LXXXII |
| Kirkiaceae | *Kirkia acuminata* | XXIX |
| Lamiaceae | *Leucas calostachys* | XXXVI |
| Lamiaceae | *Premna maxima* | XXXV |
| Lamiaceae | *Premna resinosa* | XXXV |
| Lamiaceae | *Vitex amboniensis* | XXXVI |
| Lamiaceae | *Vitex doniana* | XXXVI |
| Lecythidaceae | *Napoleona imperialis* | XXXV |
| Lecythidaceae | *Petersia africana* | XXXIX |
| Lecythidaceae | *Scytopetalum tieghemii* | XXXVII |
| Lecythidaceae | *Scytopetalum tieghemii* | LXVIII |
| Lindsaeaceae | *Lonchitis currori* | X |
| Malpighiaceae | *Acridocarpus macrocalyx* | LXXIII |
| Malvaceae | *Bombax brevicuspe* | XXVIII |
| Malvaceae | *Bombax buonopozense* | XXVIII |
| Malvaceae | *Ceiba pentandra* | XXIX |
| Malvaceae | *Cola gigantea* | CI |
| Malvaceae | *Cola millenii* | CI |
| Malvaceae | *Cola nitida* | XCVIII |
| Malvaceae | *Corchorus fascicularis* | LIX |
| Malvaceae | *Corchorus trilocularis* | LXXVIII |
| Malvaceae | *Grewia bicolor* | LXII |
| Malvaceae | *Grewia glandulosa* | CIV |
| Malvaceae | *Hildegardia barteri* | LXXXI |
| Malvaceae | *Nesogordonia fertilis* | XXX |
| Malvaceae | *Nesogordonia parvifolia* | XXXI |
| Malvaceae | *Scaphopetalum letestui* | XI |
| Malvaceae | *Scaphopetalum thonneri* | VIII |
| Malvaceae | *Sterculia tragacantha* | LXXI |
| Malvaceae | *Triplochiton scleroxylon* | XXX |
| Marantaceae | *Sarcophrynium brachystachyum* | CVIII |
| Meliaceae | *Turraeanthus africana* | XXXIV |
| Menispermaceae | *Cissampelos mucronata* | XXXVII |
| Menispermaceae | *Tiliacora funifera* | XI |
| Moraceae | *Antiaris toxicaria* | XXIII |
| Moraceae | *Bosqueia manongarivensis* | CXXVII |
| Moraceae | *Chlorophora excelsa* | XXIII |
| Moraceae | *Ficus ingens* | XXIII |
| Myricaceae | *Myrica* sp. | XXII |
| Myristicaceae | *Pycnanthus dinklagei* | VII |
| Myrtaceae | *Eugenia michoacanensis* | XXII |
| Myrtaceae | *Syzygium guineense* | XXII |
| Nymphaeaceae | *Nymphaea caerulea* | XI |
| Nymphaeaceae | *Nymphaea caerulea* | XX |
| Nymphaeaceae | *Nymphaea lotus* | X |
| Nymphaeaceae | *Nymphaea lotus* | XX |
| Ochnaceae | *Lophira alata* | XCII |
| Olacaceae | *Coula edulis* | XXVIII |
| Olacaceae | *Heisteria parvifolia* | XXVIII |
| Oleaceae | *Olea hochstetteri* | LIII |
| Orobanchaceae | *Striga forbesii* | XXXIV |

| | | |
|---|---|---|
| Pandaceae | *Microdesmis* sp. | CXIII |
| Pandanaceae | *Pandanus kirkii* | XV |
| Pandanaceae | *Pandanus livingstonianus* | VIII |
| Passifloraceae | *Adenia nicobarica* | LV |
| Passifloraceae | *Barteria acuminata* | XIII |
| Pedaliaceae | *Sesamum angustifolium* | CXIX |
| Pedaliaceae | *Sesamum indicum* | CXVI |
| Periscaceae | *Medusandra richardsiana* | XLIX |
| Phyllanthaceae | *Amanoa strobilacea* | LI |
| Phyllanthaceae | *Bridelia micrantha* | CII |
| Phyllanthaceae | *Hymenocardia acida* | XXXIII |
| Phyllanthaceae | *Maesobotrya barteri* | C |
| Phyllanthaceae | *Maesobotrya hirtella* | LXVI |
| Phyllanthaceae | *Securinega virosa* | XCVII |
| Phyllanthaceae | *Spondianthus preussii* | LX |
| Phyllanthaceae | *Thecacoris gymnogyne* | XL |
| Phyllanthaceae | *Uapaca bojeri* | LXXXIV |
| Phyllanthaceae | *Uapaca heudelotii* | CV |
| Piperaceae | *Peperomia* sp. | X |
| Plantaginaceae | *Plantago lanceolata* | CXXIV |
| Plantaginaceae | *Plantago major* | CXXIV |
| Plantaginaceae | *Plantago palmata* | CXXVI |
| Poaceae | *Guaduella oblonga* | XVII |
| Podocarpaceae | *Podocarpus milanjianus* | V |
| Polygalaceae | *Atroxima afzeliana* | CXXI |
| Polygalaceae | *Securidaca longepedunculata* | CXXI |
| Proteaceae | *Protea susannae* | XXVIII |
| Proteaceae | *Protea trichanthera* | XXXII |
| Putranjivaceae | *Drypetes gerrardii* | LXIV |
| Rhamnaceae | *Zizyphus mauritiana* | LXXXII |
| Rhizophoraceae | *Cassipourea flanaganii* | LXVI |
| Rhizophoraceae | *Rhizophora mangle* | XCVI |
| Rhizophoraceae | *Rhizophora mucronata* | XCVIII |
| Rosaceae | *Cliffortia nitidula* | XLVIII |
| Rosaceae | *Hagenia abyssinica* | LXXII |
| Rosaceae | *Prunus africana* | XLVIII |
| Rosaceae | *Pygeum africanum* | LXXIII |
| Rosaceae | *Rubus scheffleri* | LXII |
| Rubiaceae | *Borreria densiflora* | CXVI |
| Rubiaceae | *Borreria ruelliae* | CXVI |
| Rubiaceae | *Crossopteryx febrifuga* | LX |
| Rubiaceae | *Diodia aulacosperma* | CXX |
| Rubiaceae | *Diodia scandens* | CXVIII |
| Rubiaceae | *Gaertnera paniculata* | LXXXIII |
| Rubiaceae | *Ixora aneimenodesma* | LIV |
| Rubiaceae | *Ixora brachypoda* | LXXXVII |
| Rubiaceae | *Lasianthus africanus* | XXIX |
| Rubiaceae | *Mitracarpus hirtus* | CXIX |
| Rubiaceae | *Mitracarpus verticillatus* | CXX |
| Rubiaceae | *Mitragyna inermis* | LXXXII |
| Rubiaceae | *Morinda citrifolia* | XIII |
| Rubiaceae | *Morinda citrifolia* | XXV |
| Rubiaceae | *Nauclea diderrichii* | CXII |
| Rubiaceae | *Nauclea esculenta* | C |
| Rubiaceae | *Plectronia vulgaris* | XXIX |
| Rubiaceae | *Psychotria fractinervata* | XXXI |

| | | |
|---|---|---|
| Rubiaceae | *Psychotria goetzei* | XII |
| Rubiaceae | *Sabicea floribunda* | XXVIII |
| Rutaceae | *Fagara macrophylla* | LIII |
| Rutaceae | *Teclea villosa* | LXXVII |
| Rutaceae | *Vepris eugeniifolia* | CXI |
| Rutaceae | *Vepris gossweileri* | CV |
| Rutaceae | *Vepris humbertii* | LXII |
| Rutaceae | *Vepris uguenensis* | XL |
| Rutaceae | *Zanthoxylum procerum* | CVI |
| Salicaceae | *Calantica jalbertii* | LVIII |
| Salicaceae | *Casearia engleri* | XCIII |
| Salicaceae | *Dissomeria crenata* | CIX |
| Salicaceae | *Flacourtia indica* | LXIV |
| Salicaceae | *Homalium buchholzii* | CX |
| Salicaceae | *Oncoba dentata* | CVII |
| Sapindaceae | *Allophylus africanus* | XXVII |
| Sapindaceae | *Blighia unijugata* | LXI |
| Sapindaceae | *Blighia wildemaniana* | LVIII |
| Sapindaceae | *Cardiospermum corindum* | LXXIX |
| Sapindaceae | *Cardiospermum grandiflorum* | XXX |
| Sapindaceae | *Chytranthus obliquinervis* | LXXXVI |
| Sapindaceae | *Chytranthus sacleuxii* | LXXXVI |
| Sapindaceae | *Dodonaea viscosa* | LXX |
| Sapindaceae | *Lecaniodiscus cupanioides* | LXXXVI |
| Sapindaceae | *Paullinia pinnata* | XXXII |
| Sapindaceae | *Placodiscus amaniensis* | CXII |
| Sapotaceae | *Neolemonniera clitandrifolia* | XCIV |
| Simaroubaceae | *Hannoa klaineana* | LXV |
| Simaroubaceae | *Hannoa undulata* | LXV |
| Simaroubaceae | *Odyendea gabunenesis* | CVI |
| Thymelaeaceae | *Dicranolepis oligantha* | CXXVI |
| Thymelaeaceae | *Dicranolepis usambarica* | XIII |
| Typhaceae | *Typha angustifolia* | XVII |
| Typhaceae | *Typha australis* | XVII |
| Typhaceae | *Typha capensis* | XVII |
| Urticaceae | *Musanga leo-errerae* | XXIII |
| Urticaceae | *Musanga smithii* | XXIII |
| Violaceae | *Rinorea oblongifolia* | CXIII |
| Violaceae | *Rinorea welwitschii* | CXIII |
| Vitaceae | *Cissus petiolata* | LX |
| Vitaceae | *Cissus quadrangularis* | LXII |
| Xyridaceae | *Xyris aristata* | IX |
| Xyridaceae | *Xyris montana* | IX |
| Xyridaceae | *Xyris welwitschii* | IX |
| Zygophyllaceae | *Balanites aegyptiacus* | XLVII |
| Zygophyllaceae | *Balanites glaber* | XLV |
| Zygophyllaceae | *Tribulus terrestris* | XIII |

**Table 5.1.** List of pollen species shown on plates ordered alphabetically by family, genus and species. Plates can be found in Appendix 4 (on CD).

# 6. Quaternary forest associations in lowland tropical West Africa

This chapter has been written as an invited review manuscript which has been published in *Quaternary Science Reviews*. The full reference for this manuscript is:

Miller, C.S., Gosling, W.D., 2013. Quaternary forest associations in lowland tropical West Africa. *Quaternary Science Reviews* 84, 7–25.

Full methodological details are provided in Chapter 4. The presented data are tabulated in Appendix 5 and will be made available online via the Pangaea database. References are made to previous chapters to avoid repetition for the adaptation into thesis format. My contribution to this manuscript was the counting and identification of pollen grains, as well as the interpretation of data, and the writing of the manuscript.

## 6.1. Abstract

Terrestrial fossil pollen records are frequently used to reveal the response of vegetation to changes in both regional and global climate. Here we present a fossil pollen record from sediment cores extracted from Lake Bosumtwi (West Africa). This record covers the last *c.* 520 thousand years (kyr) and represents the longest terrestrial pollen record from Africa published to date. The fossil pollen assemblages reveal dynamic vegetation change which can be broadly characterized as indicative of biome shifts between savannah and woodland. Savannah formations are heavily dominated by grass (Poaceae) pollen (>55%) typically associated with Cyperaceae, Chenopodiaceae-Amaranthaceae and Caryophyllaceae. Woodland formations are palynologically more diverse than the savannah, with the key taxa occurring in multiple forest zones being Moraceae, *Celtis*, *Uapaca*, *Macaranga* and *Trema*. The fossil pollen data indicate that over the last *c.* 520 kyr the vegetation of West Africa mainly belonged to the savanna biome; however six periods of forest expansion are evident which most likely

correspond to global interglacial periods. A comparison of the forest assemblage composition within each interglacial suggests that the Holocene (11–0 kyr) forest occurred under the wettest climate, while the forest which occurred at the time of Marine Isotope Stage 7 probably occurred under the driest climate.

## 6.2. Introduction

Today West Africa contains highly diverse grasslands and forests (Myers et al., 2000) which play an important role in the global carbon cycle (Lewis et al., 2009) and climate systems (Wang and Eltahir, 2000). The distribution and composition of tropical West African vegetation is strongly linked to the prevailing climate (Holdridge et al., 1971). However, over the coming decades regional climate models suggest that temperatures will increase and precipitation regimes, such as the West African Monsoon, will alter (Christensen et al., 2007). The response of vegetation to the projected climate changes remains uncertain. One way in which we can improve our understanding of the relationship between vegetation and climate is to examine fossil vegetation records which span periods of global climate change of a comparable magnitude.

The most recent period of time which spans a similar magnitude climate fluctuation to those projected for the future is the last glacial-interglacial transition; *c.* 21–10 thousand years (kyr) ago (Jolly et al., 1998; Annan and Hargreaves, 2013). At the last glacial-interglacial transition, West African terrestrial records of past vegetation change, indicate the expansion of forests into previously savannah dominated regions (Maley, 1991; Elenga et al., 1994; Maley and Brenac, 1998). Continuously deposited sediments recovered from offshore West African marine locations in the Gulf of Guinea (*e.g.* Dupont and Agwu, 1992; Dupont et al., 1998; Jahns et al., 1998) and the tropical Atlantic (*e.g.* Dupont et al., 1989; Lézine and Casanova, 1991), indicate that the pattern of forest expansion occurred repeatedly and coincident with periods of warmer global climate during the latter half of the Quaternary period (Dupont, 2011), *i.e.* forests were more extensive in West Africa during interglacial periods. However, interpretation of the

composition of specific vegetation associations from marine fossil pollen records is inherently difficult due to: (i) wide pollen source areas (river and wind bourn input), (ii) complex oceanic transport pathways, including offshore water currents (Dupont et al., 2000), and (iii) low pollen concentrations within the sediments (*e.g.* Frédoux, 1994). Consequently, marine pollen records are representative of a large, but not accurately defined source area.

In this paper we present the first fossil pollen data from the landmark Lake Bosumtwi sediment core to provide an overview of tropical West African vegetation change during the last 520 kyr. We focus this study on exploring the palynological (floristic) composition of six past forest stages. Based upon correlation of the Bosumtwi forest (BF) stages with fossil pollen records from the marine (*e.g.* Dupont et al., 1989; Dupont and Agwu, 1992; Frédoux, 1994; Dupont and Weinelt, 1996; Dupont et al., 1998; Jahns et al., 1998), and in line with independent age estimates (Koeberl et al., 1997; Jourdan et al., 2009; Shanahan et al., 2012; Shanahan et al., 2013) we interpret the six forest zones as most likely equivalent to the last six interglacial periods (Marine Isotope Stages [MIS] 13, 11, 9, 7, 5e and 1). The past forest assemblages are then related to the modern day vegetation of West Africa. To place the Lake Bosumtwi findings in a broader context we go on to synthesise previously published fossil pollen work from tropical West Africa into regional vegetation maps. The 'time-slice' past vegetation maps produced are used to discuss West African continental-scale changes in vegetation distribution.

Today the grasslands and forests of tropical West Africa are highly diverse (Myers et al., 2000) and play important roles in both the global carbon cycle (Lewis et al., 2009) and climate systems (Wang and Eltahir, 2000). In West Africa, the 3–4°C predicted regional warming by 2100 threatens the stability of current vegetation associations (Christensen, 2007). However, little is known about the resilience of the natural vegetation to such high magnitude climate change. One way in which we can improve our understanding of the relationship between vegetation and climate is to examine

fossil vegetation records which span periods of global climate change of a comparable magnitude.

The most recent period of time which spans a similar magnitude climate fluctuation to those predicted for the future is the last glacial-interglacial transition; *c.* 21–10 kyr (Jolly et al., 1998; Annan and Hargreaves, 2013). At the last glacial-interglacial transition, West African terrestrial records of past vegetation change, indicate the expansion of forests into previously savannah dominated regions (Maley, 1991; Elenga et al., 1994; Maley and Brenac, 1998). Continuously deposited sediments recovered from offshore marine locations nearby, in the Gulf of Guinea (*e.g.* Dupont and Agwu, 1992; Dupont et al., 1998; Jahns et al., 1998) and the tropical Atlantic (*e.g.* Dupont et al., 1989; Lézine and Casanova, 1991), provide information on vegetation change over multiple glacial-interglacial cycles (>670 kyr). A comparison of fossil pollen and oxygen isotope data obtained from the marine records indicate that the pattern of forest expansion occurred repeatedly and coincident with periods of warmer global climate during latter half of the Quaternary period (Dupont, 2011), *i.e.* forests were more extensive in West Africa during global interglacial periods. However, interpretation of the composition of specific vegetation associations from marine fossil pollen records is inherently difficult due to wide pollen source areas, complex transport pathways (Dupont et al., 2000), as well as low pollen concentrations within the sediments (*e.g.* Frédoux, 1994). In this paper we present the first fossil pollen data from a terrestrial study site in West Africa that spans multiple glacial-interglacial cycles. The fossil pollen record is from a long sediment core extracted from Lake Bosumwti (Ghana; Koeberl et al., 2005; Shanahan et al., 2013). The new fossil pollen data allow the assessment of the compositional differences during six periods of forest expansion in lowland tropical West Africa over the last *c.* 520 kyr. Based upon correlation with fossil pollen records from the marine (*e.g.* Dupont et al., 1989; Dupont and Agwu, 1992; Frédoux, 1994; Dupont and Weinelt, 1996; Dupont et al., 1998; Jahns et al., 1998) and in line with independent age estimates (Koeberl et al., 1997; Jourdan et al., 2009; Shanahan et al., 2012; Shanahan et al.,

2013) we interpret the six forest zones as most likely equivalent to the last six interglacial periods (Marine Isotope Stages [MIS] 13, 11, 9, 7, 5e and 1).

### *6.2.1 Tropical West Africa*

#### *6.2.1.1 Modern vegetation*

Seven vegetation biomes have been recognised in tropical West Africa: (i) Deserts and Xeric Shrublands, (ii) Tropical and Subtropical Grasslands, Savannas and Shrublands, (iii) Tropical and Subtropical Dry Broadleaf Forests, (iv) Tropical and Subtropical Moist Broadleaf Forests, (v) Flooded Grasslands and Savannas, (vi) Montane Grasslands and Shrublands, and (vii) Mangroves (Fig. 6.1; White et al., 1983; Olson et al., 2001). The two most extensive biomes in tropical West Africa are the 'Tropical and Subtropical Grasslands, Savannas and Shrublands' and the 'Tropical and Subtropical Moist Broadleaf Forests' with a further two, 'Montane Grasslands and Shrublands' and 'Mangroves' limited to small areas at high altitude and along the coast respectively (Fig. 6.1). These four biomes have been sub-divided into fourteen 'ecoregions' that have characteristic vegetation associations which are, in turn, related to the prevailing climate conditions (Table 6.1; Olson et al., 2001).

| Biome | Ecoregion | Vegetation | Climate |
|---|---|---|---|
| **Tropical and Subtropical Grasslands, Savannah and Shrublands** | Sahelian Acacia Savanna | Continuous **grass cover**, including: *Cenchrus biflorus*, *Schoenefeldia gracilis*, and *Aristida stipoides*.<br><br>Woody species: ***Acacia*** *tortilis*, *A. laeta*, *Commiphora africana*, *Balanities aegyptica* and *Boscia senegalensis*. | Temperature: 33–36°C (monthly mean)<br><br>Precipitation: <600 mm/yr<br><br>Dry season: 6–8 months (May-September) |
| | West Sudanian Savanna | **Grass understory**, principally *Hyparrhenia*.<br><br>Dry woody species: *Anogneissus* spp. with ***Acacia*** spp., *Balanites aegyptiaca*, ***Combretum*** *glutinosum*, *Commiphora africana*, *Prosopis africana*, *Tamarindus indica* and *Ziziphus mucronata*. | Temperature: 30–33°C (monthly mean)<br><br>Precipitation: 600–1,000 mm/yr<br><br>Dry season: |

| | | | |
|---|---|---|---|
| | | Wet woody species: *Afzelia africana*, *Burkea africana*, ***Combretum*** spp. and *Terminalia* spp. | several months |
| | Guinean Forest-savanna Mosaic | Woody species: *Afzelia Africana*, *Aningeria altissima*, *A. robusta*, *Aubrevillea kerstingii*, *Chrysophyllum perpulchrum*, *Cola gigantea*, *Hildegardia barteri*, *Khaya grandifolia*, *Mansonia altissima*, *Morus mesozygia*, *Nesogordonia papaverifera*, *Pterygota macrocarpa*, *Annona senegalensis*, *Borassus aethiopum*, *Bridelia ferruginea*<br><br>**Principal grasses**: *Andropogon* sp., *Pennisetum unsetum*, *Brachiaria brizantha* etc.<br><br>The Guinean Forest-savanna Mosaic ecoregion boundaries follow the 'mosaic of lowland rain forest and secondary grassland' vegetation unit of White (1983), for an extensive list of species within this ecoregion see (White et al., 1983). | Precipitation: 1600–2000 mm/yr<br><br>Dry season: 4–5 months |
| | East Sudanian savanna | Trees: *Anogeissus leiocarpus*, *Kigelia aethiopica*, ***Acacia*** *seyal*, ***Combretum***, *Terminalia*, *Boswellia papyrifera*, ***Lannea*** *schimperi* and *Stereospermum kunthianum*.<br><br>Grasses: *Oxytenanthera abyssinica*, *Hyparrhenia*, *Cymbopogon*, *Echinochloa*, *Sorghum* and *Pennisetum* | Temperature: 18–33°C<br><br>Precipitation: 600–1000 mm/yr |
| | Northern Congolian Forest Savanna Mosaic | Gallery forest: *Berlinia grandiflora*, *Cola laurifolia*, *Cynometra vogelii*, *Diospyros elliotii*, *Parinari congensis* and *Pterocarpus santalinoides*, *Gilbertiodendron dewevrei*.<br><br>Dry forest: *Afzelia africana*, *Aningeria altissima*, *Chrysophyllum perpulchrum*, *Cola gigantea*, *Morus mesozygia* and *Khaya grandifoliola*.<br><br>Wet forest: *Piptadeniastrum africanum* and *Sterculia (Eriobroma) oblonga*, *Canarium schweinfurthii*, *Ricinodendron heudelotii* and *Terminalia superba*.<br><br>Wooded grasslands: *Afzelia africana*, *Butyrospermum paradoxum*, *Daniellia oliveri*, *Maranthes polyandra*, ***Parkia*** *biglobosa*, *Piliostigma thonningii*, *Psuedocedrela kotschyi*, *Pterocarpus erinaceus*, *Stereospermum kunthianun* and *Terminalia* sp., *Annona senegalensis*, *Burkea africana*, ***Combretum*** *collinum*, ***Hymenocardia*** *acida*, *Pariniari curatelifolia*, *Stereospernum kunthianum*, *Strychnos* sp. and Vitex sp. | Temperature: 18–31°C<br><br>Precipitation: 1,200 –1,600 mm/yr |
| **Tropical and Subtropical Moist** | Eastern Guinean forests | ***Lophira***, *Heritiera*, *Cynometra*, *Entandrophragma utile*, *Khaya ivorensis*, *Triplochiton scleroxylum*, *Hymenostegia afzelii*, *Diospyros mespiliformis*, *Anogeissus* | Temperature: 22–34°C<br><br>Precipitation: |

| | | | |
|---|---|---|---|
| **Broadleaf Forests** | | *leiocarpus*, *Millettia thonningii*, *Drypetes parvifolia*, Malvaceae, Sterculiaceae, **Ulmaceae** and **Moraceae**, **Mimosaceae** and **Caesalpiniaceae**, *Milicia excelsa*, *Triplochiton scleroxylon*, *Antiaris africana*, *Diospyros mespiliformis*, *Afzelia africana*, and *Ceiba pentandra*, *Cola grandifolia*, *Vitex* sp., ***Celtis*** sp., *Khaya grandifolia*, and ***Holoptelea*** sp. | 1000–2500 mm/pa<br><br>Dry season: 4–5 months |
| | Guinean montane forest | > 800 m asl: *Parinari excelsa*, *Gaertnera paniculata*, *Garcinia polyantha* and ***Syzygium*** *staudtii.*<br><br>Rocky outcrops: *Afrotrilepis pilosa*, *Disa welwitschii*, *Osbeckia porteresii*, *Polystachya microbambusa* and *Swertia mannii.*<br><br>Humid valleys: ***Uapaca*** *togoensis*, *Cola lateritia* var. *maclaudii*, *Parinari excelsa*, *Piptadeniastrum africanum* and *Canarium schweinfurthii*, *Guarea cedrata*, *Heritiera utilis*, *Triplochiton scleroxylon.*<br><br>Specialised: *Ochna membranacea*, *Caloncoba echinata*, *Morus mesozygia*, *Ramusatia vivipara.*<br><br>Frequent fire: Trees: ***Lophira*** *lanceolata*, ***Parkia*** *biglobosa* and *Pterocarpus erinaceus*. **Grasses**: *Anadelphia leptocoma*, *Andropogon tectorum* and *Hyparrhenia diplandra.*<br><br>Sub-montane shrub savanna: ***Syzygium*** spp., *Kotschya ochreata* var. *ochreata*, *Monechma depauperatum*, *Dissotis elliotii*, *Dissotis fructicosa*, *Cyathea manniana*, *Cyathea dregei.* Herbaceous plants and grasses: *Ctenium newtonii*, *Loudetia kagerensis*, *Wedelia Africana*, *Hyparrhenia chrysargyra*, *Rhytachne rottboellioides.*<br><br>>1375 m, shrubs: ***Syzygium*** *guineense* var. *macrocarpum*, *Tetracera alnifolia*, *Canthium henriquesianum*, *Hibiscus noldeae*. Grasses and herbs: *Samanea* sp., *Eupatorium africanum*, *Vernonia purpurea* and *Hypolytrum cacuminum.*<br><br>Sub-montane gallery forests: *Parinari excelsa*, *Cyathea camerooniana* and *Marattia fraxinea*, *Oxythenanthera abyssinica*, *Anthonotha macrophylla*, *Amphimas pterocarpoides*, *Daniella thurifera*, ***Ficus*** *congensis*, *Terminalia ivorensis*, *Allanblackia floribunda* and *Musanga cecropioides*, *Whitfieldia lateritia*, *Clematis grandiflora*, *Sopubia ramosa*, *Anisopappus africanum*, *Lonchitis currovi* and *Ouratea squamosa.*<br><br>Pioneer species: *Harungana* | Temperature: 33–10°C<br><br>Precipitation: 1,600–2400 mm/yr |

| | | | |
|---|---|---|---|
| | | *madagascariensis* and ***Trema guineensis*** | |
| | Western Guinean Lowland forests | Tree: *Dacroydes klaineana*, *Strombosia glaucenscens*, *Allanblackia floribunda*, *Coula edulis*, ***Diospyros*** *sanza-minika*.<br><br>Evergreen forests plant associations: *Anthonotha* sp., *Erythrophleum ivorense*, *Klainedoxa gabonensis*, ***Parkia*** *bicolor*, *Parinari excelsa* and *Piptadeniastrum africanum*, ***Calpocalyx*** *aubrevillei*, *Dialium* sp., *Heritiera utilis*, ***Lophira*** *alata* and *Sacoglottis gabonensis*, *Gilbertiodendron preusii*, *Parinari excelsa* or *Tetraberlinia tubmaniana*.<br><br>Moist evergreen forest: *Heritiera utilis*, *Cryptosepalum tetraphyllum*, *Erythrophleum ivorense* and ***Lophira*** *alata*, *Klainedoxa gabonensis*, ***Uapaca*** *guineensis*, *Oldfieldia africana*, *Brachystegia leonensis* and *Piptadeniastrum africanum*<br><br>Semi-deciduous forests: ***Celtis*** sp., *Mansonia latissima*, *Milicia excelsa*, *Nesogordonia papaverifera*, *Sterculia rhinopetala* and *Pterygota macrocarpa*, *Entandrophragma* sp., *Khaya* sp, *Anthonotha fragrans*, *Bridelia grandis*, *Daniella thurifera*, *Parinari excelsa*, ***Parkia*** *bicolor*, ***Pycnanthus*** *angolensis*, *Terminalia superba* and *Terminalia ivorensis*, *Khaya senegalensis*, *Erythrophleum* sp., *Terminalia* sp., *Chlorophora regia* and *Antiaris excelsa*. | Temperature: 33–12°C<br><br>Precipitation: 3300 mm/yr<br><br>Dry season: 3 months (December-February) |
| | Nigerian Lowland Forests | Moist region: **Leguminosae** family (*Brachystegia* sp., *Cylicodiscus gabunensis*, *Gossweilerodendron balsamiferum*, *Piptadeniastrum africanum*), and the **Meliaceae** family (*Entandrophragma* sp., *Guarea* sp., *Khaya ivorensis*, *Lovoa trichilioides*)<br><br>Dry region: Sterculiaceae (*Cola* sp., *Mansonia altissima*, *Nesogordonia papaverifera*, *Pterygota* sp., *Sterculia* sp., *Triplochiton scleroxylon*), **Moraceae** (*Antiaris africana*, ***Ficus*** sp., *Milicia excelsa*), **Ulmaceae** (***Celtis*** sp., ***Holoptelea*** *grandis*). | Precipitation: 2500–1500 mm/yr<br><br>Dry season: 3 months (December-February) |
| | Niger Delta Swamp Forests | Strong seasonal variations: ***Lophira*** *alata*, ***Pycnanthus*** *angolensis*, *Ricinodendron heudelotii*, *Sacoglottis gabonensis*, ***Uapaca*** sp., *Hallea ledermannii*, ***Albizia*** *adianthifolia*, *Irvingia gabonensis*, *Klainedoxa gabonensis*, *Treculia Africana*, ***Ficus*** *vogeliana*, *Calamus deerratus*.<br><br>Continuous water-logged forest: **Euphorbiaceae** (***Uapaca*** sp., *Klaineanthus gaboniae*, *Anthostema aubreyanum*, | Temperature: 28°C (monthly mean)<br><br>Precipitation: 4000 mm/yr<br><br>Dry season: 2 months (January and February) |

| | | | |
|---|---|---|---|
| | | ***Macaranga*** sp.) Annonaceae (*Xylopia* sp., *Hexalobus crispiflorus*) Guttiferae (*Symphonia globulifera*, *Pentadesma buteraceae*), **Rubiaceae** (*Hallea ledermannii*, *Rothmannia* sp.), Myristicaceae (*Coelocaryon preussii*, ***Pycnanthus*** *marchalianus*), and Ctenolophonaceae (*Ctenolophon englerianus*).<br><br>In dry sections: ***Lophira*** *alata*, *Sacoglottis gabonensis*, *Irvingia gabonensis*, *Klainedoxa gabonensis*, *Alstonia boonei*, *Ctenolophon englerianus*, *Klaineanthus gaboniae*, *Raphia* sp, *Oxystigma mannii* (Ceasalpinioideae), *Diospyros preussii*, *Ouratea* sp., *Massularia acuminata*, *Monodora myristica*, *Homalium* sp., ***Alchornea*** *cordifolia*.<br><br>Palms: *Eremospatha* and *Podococcus* sp. | |
| | Cross-Sanaga-Bioko Coastal Forests | Annonaceae, **Leguminosae**, Euphorbiaceae, Rubiaceae and Sterculiaceae, ***Medusandra*** sp. | Temperature: 33–15°C<br><br>Precipitation: >10,000 mm/yr<br><br>Dry season: none, low seasonality |
| **Montane Grasslands and Shrublands** | Jos Plateau Forest-grassland Mosaic | Tree species: *Isoberlinea doka*, *Vitex doniana*, ***Lannea*** *schimperi*, ***Syzygium*** *guineense*, *Berlinea* sp, *Carissa edulis*, *Dalbergia hostilis*, *Diospyros abyssinica*, *D. ferrea*, *Dodonaea viscosa*, *Euphorbia desmondii*, *E. kamerunica*, *E. poissonii*, ***Ficus*** *glumosa*, *Kleinia cliffordiana*, ***Rhus*** *longipes*, *R. natalensis*, *Ochna schweinfurthiana*, ***Olea*** *capensis*, *Opilia celtidifolia*, and *Pachystela brevipes*. | Temperature: 15.5–30.5°C<br><br>Precipitation: 1500–2000 mm/yr |
| **Mangrove** | Guinean mangrove | ***Rhizophora*** mangle, *R. harrisonii*, *R. racemosa*, *Avicennia germanians* and *Laguncularia racemosa*. | Precipitation: 750–6000 mm/yr |
| | Central African mangrove | *R. racemosa*, *R. mangle*, and *R. harrisonii*, *A. germinans*, *L. racemosa* and introduced species, *Nypa fruticans*. | |

**Table 6.1.** Modern vegetation of tropical West Africa. The ecoregions shown are only those which contain taxa identified within the Lake Bosumtwi fossil pollen record (data from Olson et al. 2001 and White et al. 1983). Bolded taxa represent those present within the Lake Bosumtwi fossil pollen record.

*6.2.1.2 Prevailing climate*

Temperature and precipitation in tropical West Africa vary along an approximately north-south gradient (36–24 °C, and <600–6000 mm/yr). The Intertropical Convergence Zone (ITCZ), the tropical rainbelt and the West African Monsoon govern the climate in West Africa. The tropical rainbelt lies *c.* 1000 km (or 10°) south of the surface ITCZ (Nicholson, 2009). During boreal summer, an increase in northern hemisphere summer (June–August) insolation results in a northward shift in the ITCZ and the development of an area of low pressure over North Africa. Differential pressure brings moisture eastwards from the Atlantic Ocean to western Africa (SW monsoon). In boreal winter, the opposite occurs, with the ITCZ displaced southwards. Dry, aerosol-rich, continental January trade winds from the NE dominate over West Africa in the winter months (December–February).

## *6.2.2 Lake Bosumtwi*

*6.2.2.1 Physical setting and hydrology*

Lake Bosumtwi (6°30'N, 1°25'W) occupies a 1.08 ±0.04 Myr (Koeberl et al., 1997; Jourdan et al., 2009) meteorite impact crater in metamorphosed rocks belonging to the Precambrian-age Birimian Supergroup (Koeberl et al., 2007). The impact crater has a diameter of *c.* 11 km with a crater rim which varies in elevation from 210–460 m above sea level (asl). Since the time of impact *c.* 294 m of sediment has accumulated in the centre of the basin (Koeberl et al., 2005). The sedimentary deposits within the lake have originated from erosion of the inside of the crater wall, vegetation within the crater, long distance aeolian transport and biological and evaporative processes within the lake.

Today, Lake Bosumtwi is 8.5 km in diameter (52 $km^2$) with the lake floor at 21 m asl at its deepest point and with a present day lake surface elevation of 97 m asl (thus *c.* 74 m water depth). Lake Bosumtwi is hydrologically isolated from the regional aquifer by

the bedrock and the crater walls. The lake is highly stratified, with an anoxic hypolimnion beneath 15–18 m water depth, resulting in anoxic sedimentation with thinly laminated varves (Peck et al., 2004). The closed hydrology of Lake Bosumtwi makes the lake level extremely sensitive to changes in precipitation, cloudiness and temperature (Shanahan et al., 2006).

*6.2.2.2 Surrounding vegetation*

Lake Bosumtwi is ideally situated for the study of past vegetation in lowland tropical West Africa because of its proximity to the transition between savannah (to the north) and moist forest to the south (Fig. 6.1). Today, Lake Bosumtwi lies within the 'Tropical and Subtropical Moist Broadleaf Forest' biome (Fig. 6.1; Olson et al., 2001). Prior to the degradation of the natural vegetation by human settlement and cultivation, the lake was surrounded by moist semi-deciduous forest (Gill, 1969; Rebelo and Siegfried, 1990), with a dominant canopy comprised of trees from the Ulmaceae and Sterculiaceae families (Hall and Swaine, 1981; Beuning et al., 2003). The main crops cultivated around the lake today are *Elaeis guineensis* (oil palm), *Musa* sp. (Banana), *Theobroma cacao* (Cocoa) and *Manihot esculenta* (Cassava). There is a natural area of *Imperata cylindrica* grassland which occurs on the north-east quadrant of the crater rim, coinciding with the outcrop of the Pepiakese granite which intruded into the Birimian metasediments (Moon and Mason, 1967).

*6.2.2.3 Climatic conditions*

Lake Bosumtwi lies directly in the path of the migration of the ITCZ and the associated tropical rainbelt (Nicholson, 2009), and therefore the sediment cores from Lake Bosumtwi are likely to record change within these climate systems. Average monthly temperatures at Lake Bosumtwi range from *c.* 23°C in August to *c.* 27°C in February, with a mean annual temperature of *c.* 26°C. The cooler temperatures in the summer months are due to a decrease in the incoming solar radiation caused by increased cloudiness (Shanahan et al., 2007). Humidity varies from *c.* 85 % in August to *c.* 75 %

in January (Turner et al., 1996). January typically has the lowest rainfall (*c.* 17 mm) with June having the highest (*c.* 234 mm). The average annual precipitation is *c.* 1450 mm (Shanahan et al., 2007).

*6.2.2.4 Palaeoenvironmental change*

The published past vegetation reconstruction from Lake Bosumtwi covers the last *c.* 28 kyr and indicates an abrupt transition at *c.* 9.5 kyr $^{14}$C yr BP from grasslands (during the last glacial) to forest vegetation during the Holocene (Maley, 1991). Abundant taxa identified from the last glacial period include Poaceae, Chenopodiaceae-Amaranthaceae, *Olea* sp. and Cyperaceae. Poaceae is typical of the 'Tropical and Subtropical Grasslands, Savannah and Shrublands' biome, *Olea* sp. characteristic of 'Montane Grasslands and Shrublands', and Cyperaceae, a marginal plant which may thrive under low lake level conditions. The Holocene is characterised by arboreal taxa such as *Alchornea*, *Celtis*, Moraceae, *Lannea* and *Uapaca* associated with the 'Tropical and Subtropical Moist Broadleaf Forest' biome.

Carbon isotope ($\delta^{13}$C) analysis of coarse fraction bulk organic sediments from the Lateglacial period in Lake Bosumtwi range from -11.5‰ to -19.6‰, which have been interpreted to reflect a dominance of $C_4$ (grassland) plants (Talbot and Johannessen, 1992); an interpretation supported by the high percentages of Poaceae (grass) pollen grains (Maley, 1991). The transition into the Holocene is marked by a negative 20‰ shift in the $\delta^{13}$C which has been interpreted as indicative of a change to $C_3$-dominated (forest) vegetation (Talbot and Johannessen, 1992). The switch from savannah to forest at *c.* 9.5 $^{14}$C yr BP coincides with the onset of deep lake conditions (Talbot and Delibrias, 1980) and a lithological shift from muddy-silts to dark green laminated organic muds (Talbot et al., 1984).

Lake Bosumtwi lake level reconstructions based on the radiocarbon dating of exposed lacustrine deposits in the river gullies around the crater indicate that the lake was much lower than present before *c.* 15.6–14.1 cal kyr BP (Talbot and Delibrias, 1980). After *c.*

12.8–11.8 cal kyr BP thick successions of turbidite silts are interpreted to represent a shift to a deep, stable, stratified lake (Talbot and Delibrias, 1980). A well-developed terrace and overflow notch (at *c.* 110 m above present lake level) indicates that the lake overtopped the crater from *c.* 11.6–8.8 cal kyr BP. Beach sands *c.* 0.5 m above the present lake level indicate a regression before *c.* 4.2–3.6 cal kyr BP. Additional beach deposits show a most recent lake level highstand *c.* 25 m above present lake level between *c.* cal 3.6–1.5 kyr BP (Talbot and Delibrias, 1980; Shanahan et al., 2006).

Millennial and sub-millennial scale climate changes have also been identified from the Lake Bosumtwi sediments. Magnetic hysteresis measurements spanning the last *c.* 26 kyr have been used to suggest that: (i) during the last glacial period the input of aeolian dust into the lake was high and (ii) during the Holocene there were millennial-scale fluctuations in dust input. The changes in dust input at Lake Bosumtwi are thought to be related to changes in Atlantic Sea Surface Temperature (SST) and glacial boundary conditions (Peck et al., 2004); with cooler SST leading to a reduction in evaporation and moisture needed to fuel the West African monsoon, leading to reduced vegetation cover and more dust production. In addition, high resolution elemental data (Al, Si, K, Ca, Ti, Mn and Fe), as a proxy for the terrigenous sediment component, spanning *c.* 2.7 kyr from Lake Bosumwti identified annual laminations which indicate intervals of severe drought, thought to be related to changes in monsoon intensity driven by fluctuations in Atlantic SST and the Atlantic Multidecadal Oscillation (Shanahan et al., 2009).

## 6.3. Materials and methods

### *6.3.1 Sediment recovery and age*

In 2004, an expedition led by the International Continental Scientific Drilling Program (PI's C. Koeberl; B. Milkereit; J. Overpeck; C. Scholz) raised 1833 m of sediment from

14 separate drill holes from Lake Bosumtwi (Ghana). The longest continuous core recovered was from site 5, core BOS04-5B (hereafter 5B), located in the deepest part of the lake (*c.* 74 m water depth), totalling 294.67 m of sedimentary succession (Koeberl et al., 2007).

Previous studies have established 135 independent radiometric age control points from the 5B core: 127 radiocarbon dates (Shanahan et al., 2012; Shanahan et al., 2013), 1 U-series age (Shanahan et al., 2013), 6 optically stimulated luminescence ages (Shanahan et al., 2013) and a basal impact glass Ar-Ar age (Koeberl et al., 1997; Jourdan et al., 2009). The good agreement between the previously published independent age estimates suggest that the upper 150 m of sediment from core 5B used in this study spans the last *c.* 520 kyr (Fig 4.3).

### *6.3.2 Fossil pollen analysis*

To reconstruct past vegetation change in tropical West Africa during the last half million years we analysed 217 samples, at an average temporal resolution of 2.4 kyr from the upper 150 m of core 5B for fossil pollen. The pollen samples were prepared using standard techniques (Faegri and Iversen, 1989), with pollen concentrations calculated with reference to known abundances of the exotic marker *Lycopodium* (Stockmarr, 1972). Pollen sums of >300 terrestrial grains were achieved wherever possible; however, in samples with low pollen concentration (*i.e.* with pollen sums from 15–175, and concentrations <1392 grains $cm^{-3}$) counting ceased when 2000 exotic *Lycopodium* spores had been counted. The identification of pollen grains was achieved using the pollen reference collection held at The Open University, UK, as well as African pollen reference guides (Reille, 1995; Lézine., 2005; Gosling et al., 2013).

### *6.3.3 Identification and analysis of forest assemblage zones*

Visual inspection of the summary fossil pollen data for the entire *c.* 520 kyr record was initially used to identify periods of dominance by forest (vs. savannah) taxa. To allow

focus on the fossil pollen assemblages which contain a higher percentages of forest taxa we then zoned the diagram by excluding all samples where grass (Poaceae) pollen was >55 % of the pollen sum in three consecutive samples. Grass was chosen as the discriminator between forest and savannah type vegetation because of its high representation in the fossil pollen record, and its importance as an indicator of savannah-type vegetation (Maley, 1991; Hooghiemstra et al., 2006). Fossil pollen diagrams were then plotted to show the detailed assemblages within each of the forest assemblage zones. All pollen diagrams were produced using C2 software (Juggins, 2005).

Statistical comparison of fossil pollen assemblages was achieved using the detrended correspondence analysis (DCA) function in Psimpoll (Bennett, 2003). DCA was performed on: (i) all pollen samples and including all pollen/spore taxa reaching an abundance of >2 % of the pollen sum in at least one sample (43 taxa; taxon scores), and (ii) on just the pollen samples occurring within the forest assemblage zones including all taxa >2 % of the pollen sum in at least one sample (22 taxa; sample scores).

Additionally, the Simpson's Index of Diversity (1-D) was calculated for each sample; the calculated value ranges from 0-1, with higher values representing greater diversity. The index represents the probably that two randomly selected individuals from a sample will belong to the same species (Peet, 1974).

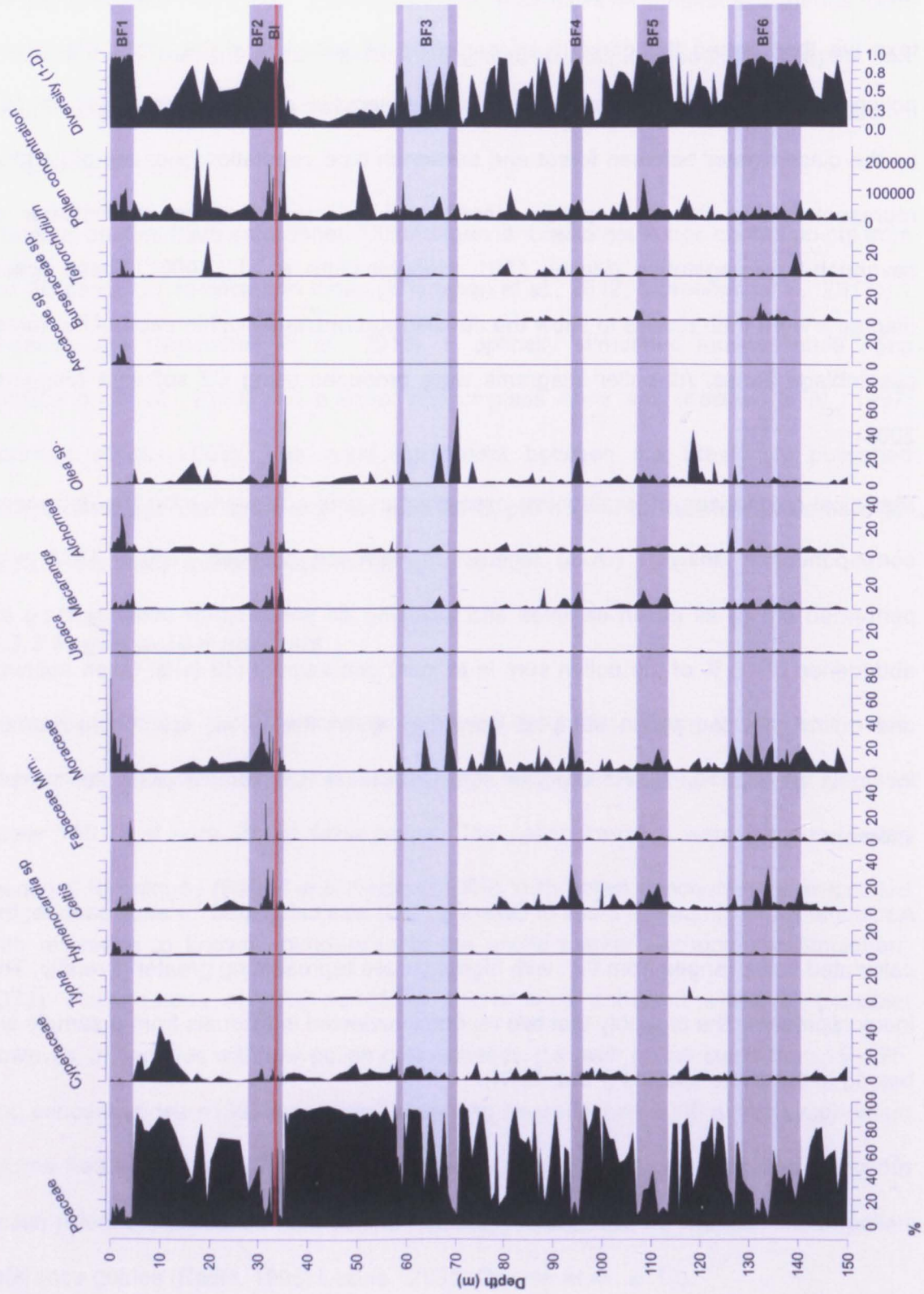


**Fig. 6.1.** Pollen abundance diagram (displaying pollen >10 % of the total pollen sum) from 150–0 m depth (520 kyr BP to present). Horizontal dark-grey bars indicate ≥3 adjacent samples with <55 % Poaceae. Dark and pale-grey bars are Bosumtwi forest zones (BF). Red bar is the barren interval (BI). Pollen concentration is in grains $cm^{-3}$.

## 6.4. Results

In total, 216 pollen taxa were identified to at least family level and a further 311 pollen types were identified, but remain as unknowns. Out of 217 samples, 100 samples were included in the six separate stratigraphic zones containing 'forest assemblages' (Fig. 6.2–4). These six Bosumtwi forest assemblages are discussed below and are named Bosumtwi forest (BF) zones 6-1.

### 6.4.1 Bosumtwi forest assemblage zones

*6.4.1.1 Bosumtwi forest zone 6 (BF6; 140.6–125.62 m); 24 pollen samples.*

Zone BF6 (Fig. 6.2a) is characterised by Moraceae (mean 14 %), *Celtis* (mean 7.2 %), *Alchornea* (mean 2.8 %), *Macaranga* (mean 2.8 %) and Fabaceae Mimosaceae (mean 2.2 %). Percentages of Poaceae are high (<67 %) but fluctuate throughout zone BF6. The aquatic *Menyanthes trifoliata* increases to 6.9 % within zone BF6. *Celtis* and Moraceae increase to 33 % and 48.1 % respectively. The mean pollen concentration in zone BF6 is 20,193 grains $cm^{-3}$ and the mean Simpson diversity value (1-D) for the pollen assemblage is 0.83 (Fig. 6.2a).

*6.4.1.2 Bosumtwi forest zone 5 (BF5; 111.25–105.45 m); 8 pollen samples.*

Zone BF5 (Fig. 6.2b) is characterised by *Celtis* (mean 8.6 %), Moraceae (mean 7.5 %), *Macaranga* (mean 7 %), *Alchornea* (mean 3.3 %) and *Pycnanthus* (mean 0.8 %). Cyperaceae percentages are low (<2.7 %) for the duration of zone BF5. Vegetation composition throughout BF5 is relatively stable. Burseraceae reaches a maximum percentage of 8.9 % towards the end of BF5. The mean pollen concentration in zone BF5 is 41,160 grains $cm^{-3}$ and the mean Simpson diversity (1-D) for the pollen assemblage is 0.92 (Fig. 6.2b).

*6.4.1.3 Bosumtwi forest zone 4 (BF4; 95.95–93.57 m); 4 pollen samples.*

Zone BF4 (Fig. 6.3a) is characterised by *Celtis* (mean 16.8 %) Moraceae (mean 15 %), *Olea* sp. (mean 10.2 %), *Macaranga* (mean 4.9 %) and *Alchornea* (mean 3.1 %). The base of zone BF4 is determined by a decrease in both Poaceae and Cyperaceae percentages to 49.6 % and 0 % (Fig. 6.3a). The percentage of Moraceae and *Celtis* increase through zone BF4 and reach maxima (36 % and 35.3 %) at the top of the zone (Fig. 6.3a). The mean pollen concentration in zone BF4 is 28,570 grains $cm^{-3}$ and the mean Simpson diversity (1-D) for the pollen assemblage is 0.83 (Fig. 6.3a).

*6.4.1.4 Bosumtwi forest zone 3 (BF3; 70.3–58.05 m); 23 pollen samples.*

Zone BF3 (Fig. 6.3b) contains high percentages of *Olea* sp. and Moraceae at mean percentages of 9.3 % and 8.3 % respectively. Zone BF3 contains large fluctuations in pollen percentages, but generally contains a decrease in Poaceae and an increase in arboreal taxa. The zone is divided into three sub-stages. The first sub-stage (70.3–68.6 m) contains a rapid decrease in Poaceae percentage from 93–7.2 % and a maximum in *Olea* sp. percentage (59.5 %) at 70.3 m, followed by an increase in Moraceae percentages (46.5 %) at 68.6 m. The second sub-stage (68.6–59.45 m) contains highly variable Poaceae pollen percentages (93.5–24.3 %). Cyperaceae percentage is low but constant throughout (0.6–11.7 %). Moraceae reaches a maximum percentage of 32.7 % at 63.6 m. The third sub-stage (59.45–58.25 m) is characterised by low percentages of Poaceae (>27 %) and Cyperaceae (>0.7 %) and high percentages of *Olea* sp. (<32 %) and Moraceae (<22 %). The mean pollen concentration in zone BF3 is 31,705 grains $cm^{-3}$ and the mean Simpson diversity (1-D) for the pollen assemblage is 0.52 (Fig. 6.3b).

*6.4.1.5 Bosumtwi forest zone 2 (BF2; 35.85–28.1 m); 26 pollen samples.*

Zone BF2 (Fig. 6.4a) is characterised by Moraceae (mean 13.2 %), *Celtis* (mean 6.6 %), *Macaranga* (mean 6.6 %), *Alchornea* (mean 3 %), Fabaceae Papilionoideae (mean 2.3 %), Fabaceae Mimosaceae (mean 1.83 %), *Uapaca* (mean 1.7 %) and *Holoptelea* (mean 0.3 %). Prior to BF2 there is a prolonged period of savannah stability (>80 %

Poaceae; Fig. 6.4a). At the base of zone BF2 *Olea* sp. reaches its maximum percentage over the last *c.* 520 kyr (71 %) and pollen concentration increases to 234,117 grains $cm^{-3}$. Zone BF2 is characterized by an abrupt decrease in Poaceae percentages from 61 to 5.6 % at 35.05 m. Poaceae percentages recover between 33.85–32.9 m, however total pollen concentration decreases to *c.* 90 grains $cm^{-3}$, rendering these samples effectively barren (BI; Fig. 2; Fig 5a). The mean pollen concentration in zone BF2 is 43,427 grains $cm^{-3}$ and the mean Simpson diversity (1-D) for the pollen assemblage is 0.86 (Fig. 6.4a).

*6.4.1.6 Bosumtwi forest zone 1 (BF1; 4.8–0 m); 15 pollen samples.*

Prior to BF1, Poaceae percentages reached 91 % (Fig. 6.4b) and *Typha* and Cyperaceae were key components of the vegetation assemblage. *Olea* sp. has maxima at 16.6 m and 4.8 m (>10 %) but is reduced (to <2 %) in zone BF1. Cyperaceae has a maximum of 44 % at 10 m but is reduced (to <1 %) in zone BF1. Zone BF1 (Fig. 6.4b) contains high percentages of Moraceae (mean 18.9 %), *Alchornea* (mean 8.8 %), *Celtis* (mean 4.2 %), *Macaranga* (mean 3.7 %), *Trema* (mean 2.3 %), *Hymenocardia* (mean 3.6 %), Fabaceae Mimosaceae (mean 1.5 %) and *Holoptelea* (mean 1.2 %). Percentages of *Alchornea*, Arecaceae and *Tetrorchidium* show maxima of 31 %, 17 % and 14 % respectively at 2.2 m. *Trema* is present throughout BF1 but increases to 8 % at 1.8 m. Moraceae is a major component of the zone BF1 assemblage, reaching maximum percentages of 77 % at core-top exceeding any value over the last 520 kyr. The mean pollen concentration in zone BF1 is 52,205 grains $cm^{-3}$ and the mean Simpson diversity value (1-D) for the pollen assemblage is 0.91 (Fig. 6.4b).

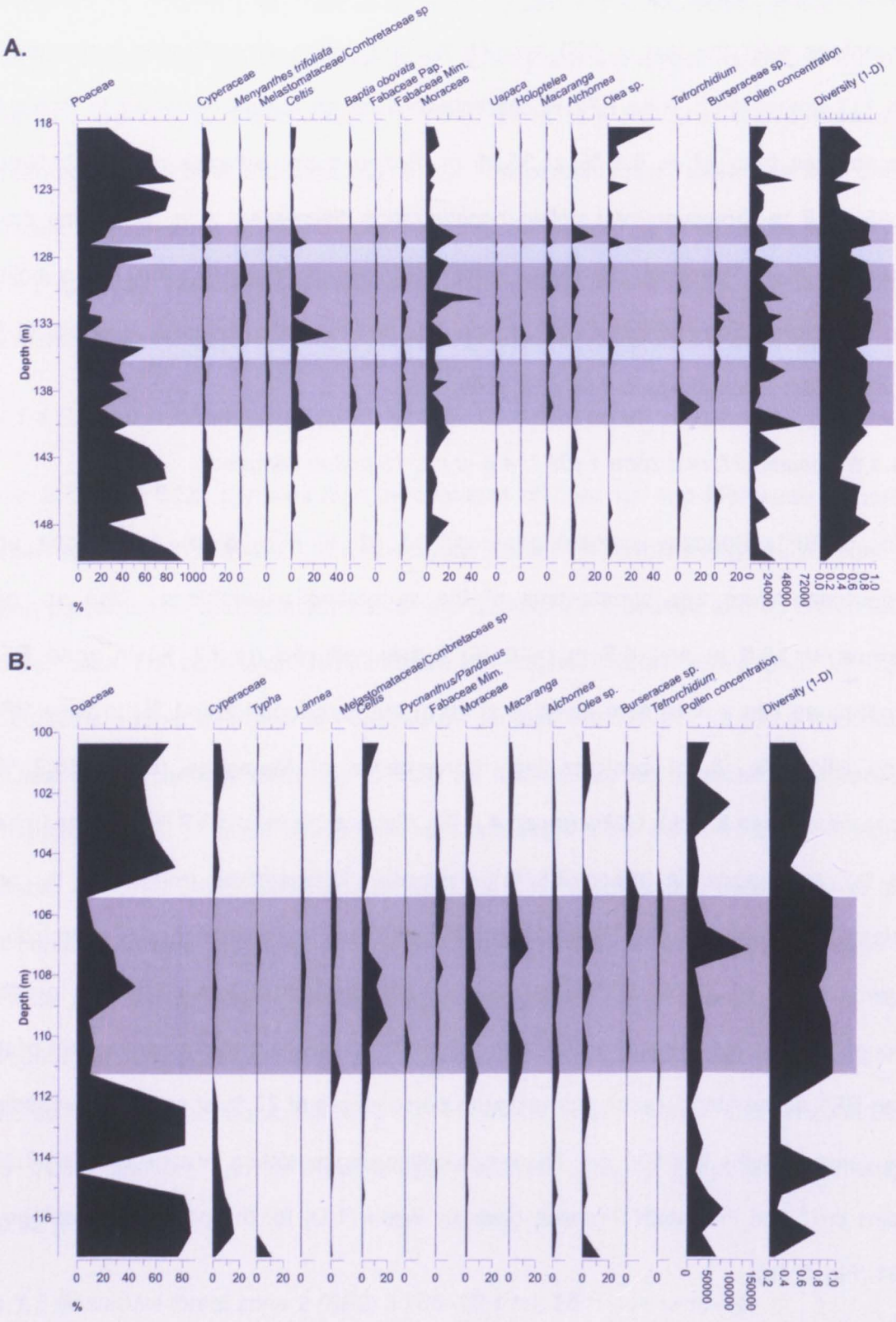


**Fig. 6.2.** Pollen abundance diagram (displaying pollen >3 % of the total pollen sum). **A)** BF6 (140.6–125.62 m depth; MIS 13). **B)** BF5 (111.25–105.45 m; MIS 11). Horizontal dark-grey bars indicate ≥3 adjacent samples with <55 % Poaceae. Dark and pale-grey bars are Bosumtwi forest zones (BF). Pollen concentration is in grains $cm^{-3}$.

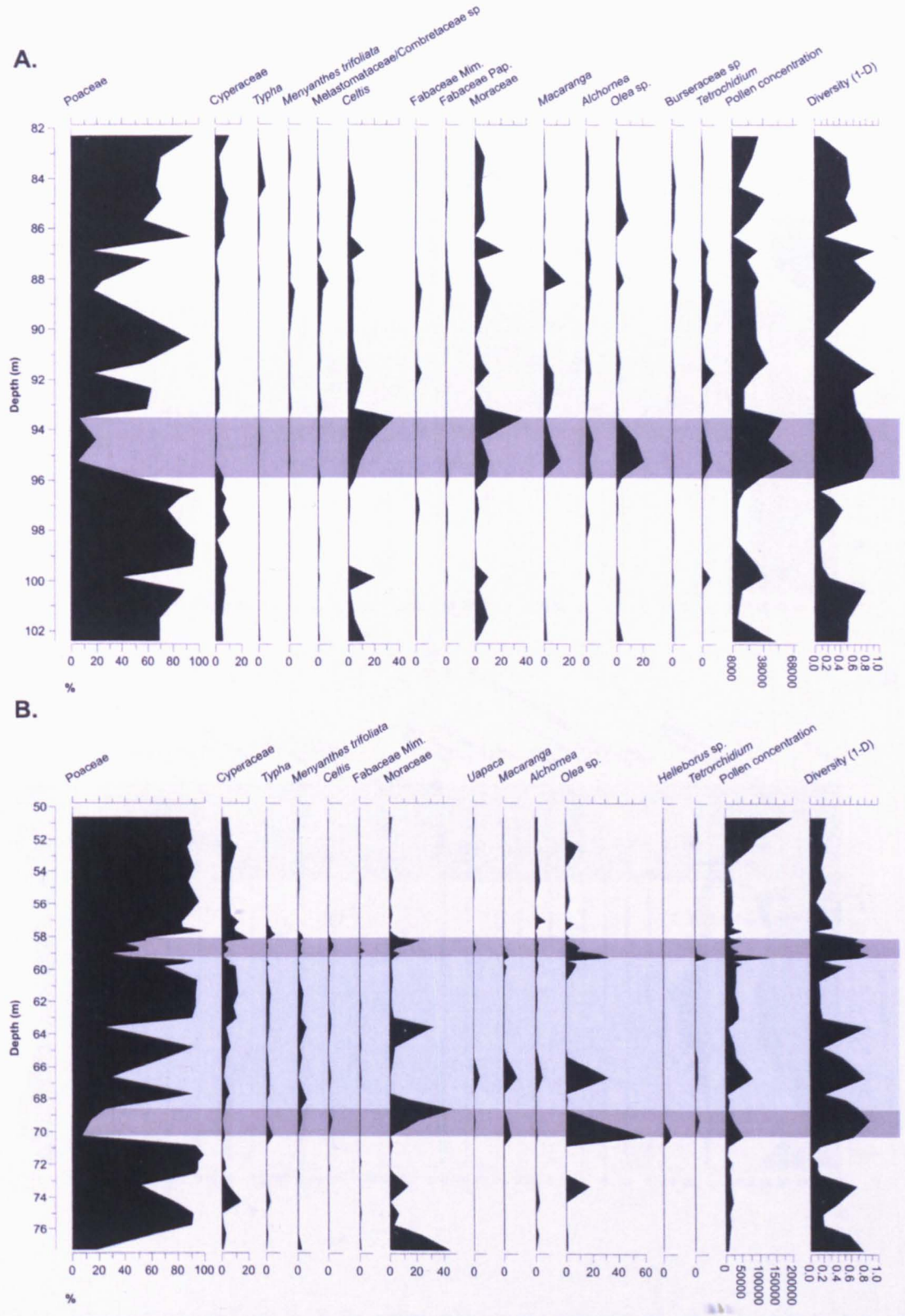


**Fig. 6.3.** Pollen abundance diagram (displaying pollen >3 % of the total pollen sum). **A)** BF4 (95.95–93.57 m; MIS 9). **B)** BF3 (70.3–58.05 m; MIS 7). Horizontal dark-grey bars indicate ≥3 adjacent samples with <55 % Poaceae. Dark and pale-grey bars are Bosumtwi forest zones (BF). Pollen concentration is in grains $cm^{-3}$.

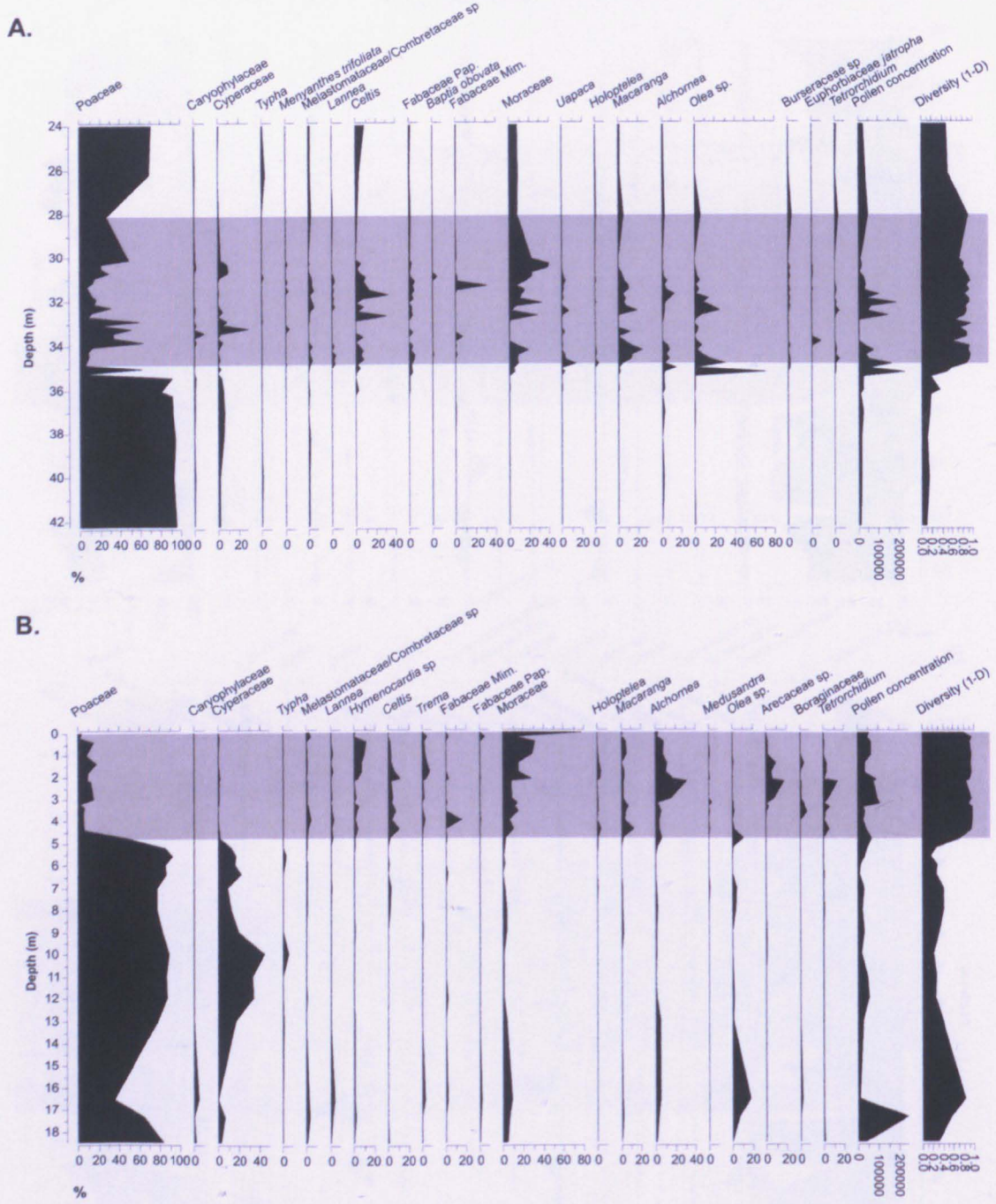


**Fig. 6.4.** Pollen abundance diagram (displaying pollen >3 % of the total pollen sum). **A)** BF2 (35.85–28.1 m; MIS 5e). **B)** BF1 (4.8–0 m; Holocene). Horizontal dark-grey bars indicate ≥3 adjacent samples with <55 % Poaceae. Dark and pale-grey bars are Bosumtwi forest zones (BF). Pollen concentration is in grains $cm^{-3}$.

### 6.4.2 Fossil pollen ordination

Detrended correspondence analysis (DCA) was applied to the pollen assemblages (Fig. 6.5).

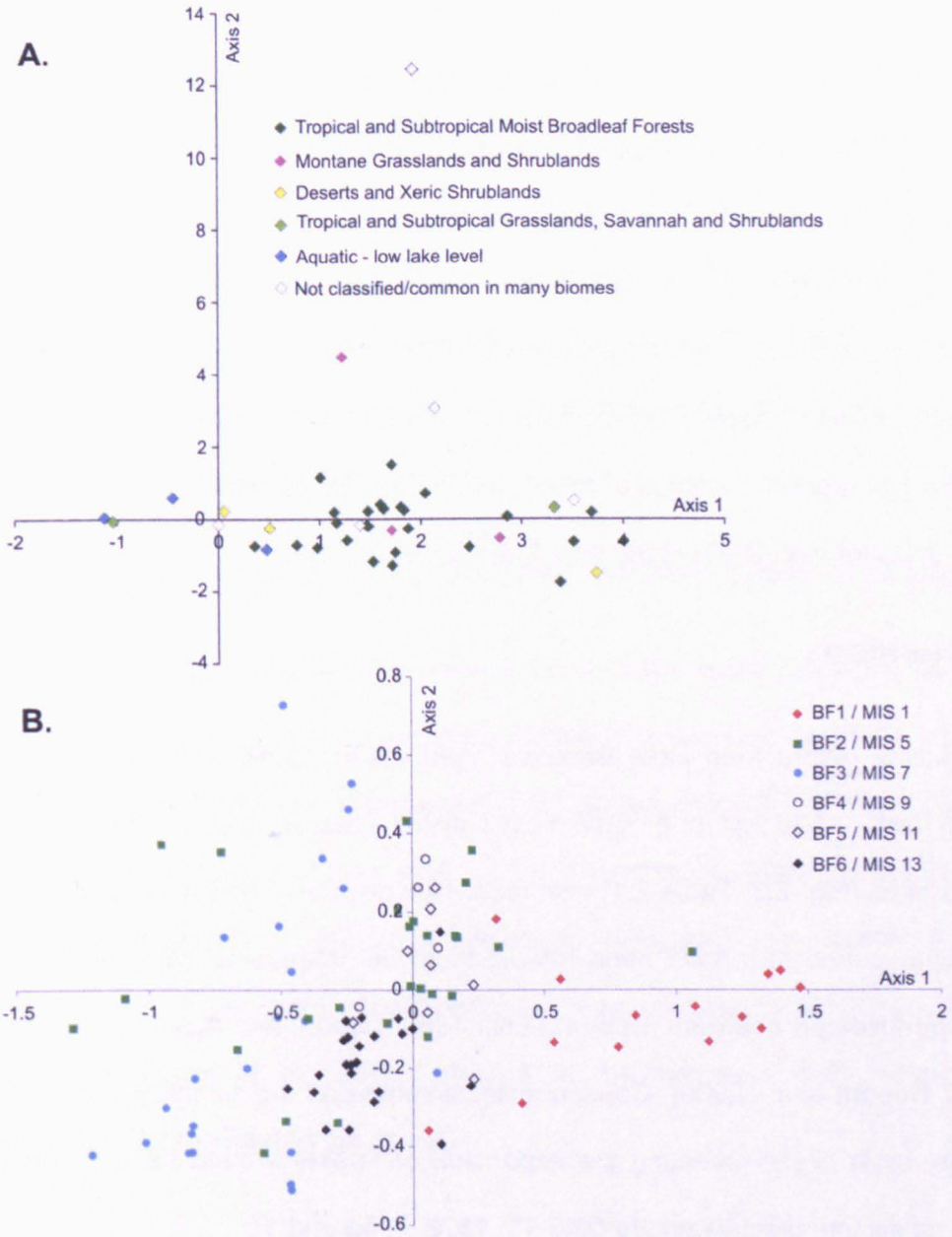


**Fig. 6.5.** Fossil pollen DCA ordination of Lake Bosumtwi data. **A)** Ordination of Lake Bosumtwi fossil pollen DCA taxon scores axis 1 vs. axis 2. Axis 1 represents most of the ecological variance (eigenvalue (EV) 0.44), axis 2 EV is 0.21. DCA was performed on all pollen/spore taxa reaching abundance of >2 % of the pollen sum in at least one sample. In total, 43 pollen/spore taxa were included from 217 samples. Ecological biome classifications follows Olson et al., (2001). **B)** Ordination of Lake Bosumtwi forest zone DCA sample scores. DCA was performed using Psimpoll (Bennett, 2003). For the DCA taxon scores ordination plot which is labelled with individual taxon names see Appendix 7.

Rare taxa were downweighted (using the function in Psimpoll) as this lowers (but does not remove) the influence of low percentage species on the DCA results (Bennett, 2003). DCA was performed on all pollen/spore taxa comprising >2 % of the pollen sum in at least one sample. Pollen taxon scores were grouped into vegetation biomes according to Olson et al. 2001 (Fig. 6.5a; Appendix 6, Table S1). Generally, taxon scores of Poaceae, Chenopodiaceae-Amaranthaceae, and Caryophyllaceae plot toward the negative on axis 1. Taxon scores of *Uapaca*, *Macaranga*, *Celtis* and *Trema* plot positive on axis 1 (Fig. 6.5a). All sample scores from zone BF1 plot positive on axis 1 (Fig. 6.5b). Sample scores from zone BF2 are widely dispersed, having both positive and negative values along axis 1 (Fig. 6.5b). Zone BF3 sample scores plot solely (apart from one sample) with negative scores on axis 1 (Fig. 6.5b). Sample scores from both BF4 and BF5 plot around the origin of axis 1 and 2. Zone BF6 sample scores are highly condensed and plot negative on both axis 1 and 2 (Fig. 6.5b).

## 6.5. Discussion

The fossil pollen record from Lake Bosumtwi contains six forest assemblage zones through the last *c.* 520 kyr (Fig. 6.1). Fossil pollen records obtained from nearby marine core sites (Fig. 2.3; Table 2.1) also record six periods of forest expansion over the same time period that have been related to global interglacial climates through parallel oxygen isotope analyses (Dupont et al., 1989; Dupont and Agwu, 1992; Jahns et al., 1998; Dupont et al., 2000). Consequently, we interpret the six forest zones (BF) identified as, most likely, reflecting the expansion of forests around Lake Bosumtwi during the last six interglacial periods (MIS 13, 11, 9, 7, 5e and 1).

The diameter of Lake Bosumtwi (*c.* 8.5 km) means that *c.* 80 % of the pollen accumulating in the sediments is likely to be mainly derived from the regional landscape (greater than several hundred meters from the basin). The remaining *c.* 20 % is likely to be comprised of local (<20 m) and extralocal (from plants between 20 and several hundred meters from the edge of the lake) sources (Jacobson and Bradshaw,

1981). The constrained nature of the Lake Bosumtwi basin (meteorite impact crater) means that even with a dramatic change in lake level (+/- 100 m; Shanahan et al., 2006) there cannot have been a large change in lake diameter (lake bottom 6 km diameter, crater rim 11 km diameter). Consequently, the relative proportion of local vs. long distance pollen entering the lake due to fluctuations in lake level is likely to have remained relatively constant. However, it is possible that the source area for the long distance pollen input has varied in the past due to changes in the relative strength of the trade winds (*i.e.* Hooghiemstra, 1989), the type of vegetation surrounding the lake (Bradshaw, 1981) as well as and rainfall variations, with frequent rain washing the pollen out from the air (Hooghiemstra, 1988). Despite the large pollen catchment area for Lake Bosumtwi the regional picture is significantly smaller than the super-regional input into the marine sediments.

### *6.5.1 Forest assemblage zones and their modern vegetation associations*

A comparison of the Lake Bosumtwi fossil pollen taxa identified over the last *c.* 520 kyr with modern day vegetation associations (Table 6.1) indicate that the majority of the fossil pollen taxa found are represented in the various modern day ecoregions of West Africa (Fig. 6.6; Table 6.1; Olson et al., 2001). However, the pollen record indicates that plant associations are of variable composition in time, with little resemblance between modern and past vegetation composition. Comparing the climatic range of (multiple) ecoregions (Olson et al., 2001) allowed an estimation of both temperature and precipitation for the past forest zones.

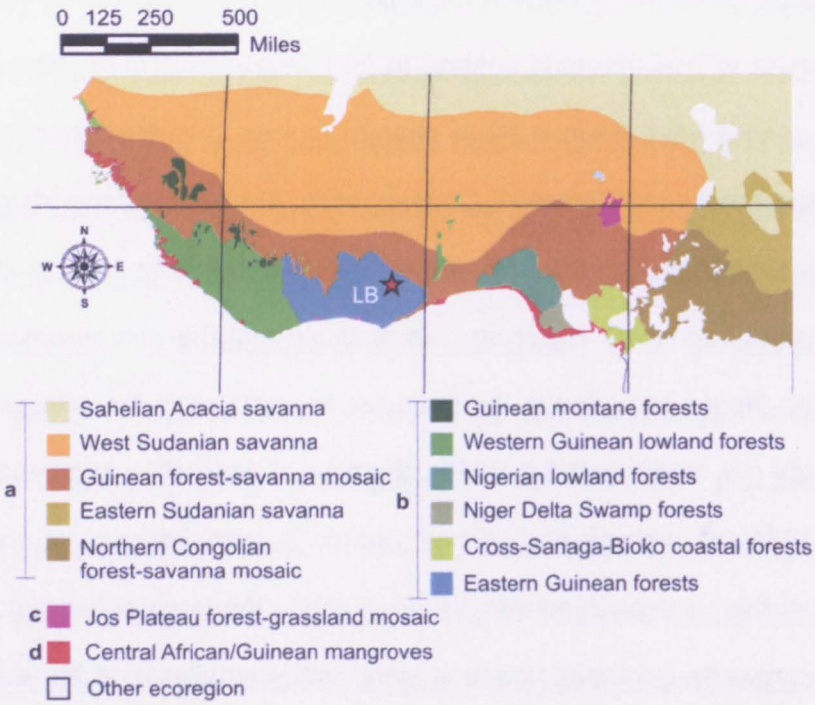


**Fig. 6.6.** Map of present-day ecoregions of West Africa which contain taxa identified within the Lake Bosumtwi fossil pollen record (Table 6.1). Ecoregions are grouped into biomes: **a)** Tropical and Subtropical Grasslands, Savannah and Shrublands; **b)** Tropical and Subtropical Moist Broadleaf Forests; **c)** Montane Grasslands and Shrublands; **d)** Mangroves. Map adapted from Olson et al. (2001). LB = Lake Bosumtwi.

*6.5.1.1 BF6; MIS 13 equivalent*

Taxa associated with zone BF6 include: *Celtis*, *Uapaca*, *Macaranga*, *Alchornea*, *Holoptelea*, Moraceae and Fabaceae species (Fig. 6.2a). Today, *Celtis* and *Uapaca* are associated with the 'Western Guinean Lowland Rainforest' ecoregion. *Celtis* is also present in the modern-day 'Eastern Guinean Lowland Rainforest' ecoregion along with *Holoptelea*, Moraceae and Fabaceae species. *Macaranga*, *Uapaca* and *Alchornea* are characteristic of the 'Niger Delta Swamp Forest' ecoregion. *Holoptelea*, Moraceae and *Celtis* are also currently found within the dry northern part of the 'Nigerian Lowland Forest' ecoregion. Fabaceae species are also found within the moist regions of the 'Nigerian Lowland Forest' ecoregion.

Given the close association between the most highly abundant fossil pollen taxa and modern day ecoregion vegetation we suggest that the vegetation within zone BF6 was similar to that of the modern 'Western Guinean Lowland Rainforest', 'Eastern Guinean

Lowland Rainforest' and the 'Nigerian Lowland Forest' ecoregions. Assuming little change in species climatic tolerances over the late Quaternary, the vegetation association identified in the fossil pollen assemblage suggests that precipitation during zone BF6 was probably *c.* 1000–3300 mm/yr, with seasonal temperatures ranging from *c.* 22–34°C.

*6.5.1.2 BF5; MIS 11 equivalent*

Taxa associated with BF5 include *Celtis*, Moraceae, *Macaranga*, *Alchornea* and *Pycnanthus* (Fig. 6.2b). Today, *Alchornea* and *Macaranga* are characteristic of vegetation within the 'Niger Delta Swamp Forest' ecoregion. *Celtis* and *Pycnanthus/Panandus* are common within the 'Western Guinean Lowland Rainforest' and 'Eastern Guinean Lowland Rainforest' ecoregion. Moraceae is characteristic of the 'Nigerian Lowland Forest', the 'Western Guinean Lowland Rainforest' and the 'Eastern Guinean Lowland Rainforest' ecoregions.

The high frequency of both Moraceae and *Celtis* suggest the vegetation assemblage within zone BF5 is most closely related to the vegetation found in the 'Western Guinean Lowland Rainforest' and 'Eastern Guinean Lowland Rainforest' ecoregions today, suggesting precipitation was 1000–3300 mm/yr and with seasonal temperatures ranging from 12–34°C.

*6.5.1.3 BF4; MIS 9 equivalent*

Main taxa associated with zone BF4 are Moraceae, *Celtis*, *Olea* sp., *Macaranga* and *Alchornea* (Fig. 6.3a). *Celtis*, *Alchornea* and *Macaranga* are characteristic of the 'Niger Delta Swamp Forest' and the 'Western Guinean Lowland Rainforest' ecoregions. Moraceae is abundant in the 'Nigerian Lowland Forest', the 'Western Guinean Lowland Rainforest' and the 'Eastern Guinean Lowland Rainforest' ecoregions. *Olea* sp. is found in the montane forests associated with the 'Jos Plateau Forest-grassland Mosaic' ecoregion.

The high percentage of *Celtis* and Moraceae suggests that the vegetation around Lake Bosumtwi during zone BF4 was similar to that of the present day 'Western Guinean Lowland Rainforest' and 'Eastern Guinean Lowland Rainforest' ecoregion, indicating past precipitation of 1000–3300 mm/yr, and seasonal temperatures ranging from 12–34°C. However, high percentages of the montane taxa *Olea* sp. support generally cooler conditions allowing the downslope migration and expansion of montane forests (*i.e.* Maley, 1991).

*6.5.1.4 BF3; MIS 7 equivalent*

The main fossil pollen components of zone BF3 are *Olea* sp., Moraceae, *Alchornea*, *Macaranga* and Poaceae (Fig. 6.3b). Moraceae is abundant in the 'Nigerian Lowland Forest' and the 'Western Guinean Lowland Rainforest' ecoregions. *Olea* sp. is associated with the montane 'Jos Plateau Forest-grassland Mosaic' ecoregion. Additionally, *Alchornea* and *Macaranga* are taxa characteristic of the 'Niger Delta Swamp forest' ecoregion. Poaceae is characteristic of savannah ecoregions, such as the 'Sahelian Acacia Savanna', the 'West Sudanian Savanna' and the 'Guinean Forest-savanna Mosaic' ecoregions. The high but fluctuating percentages of Poaceae (24.3–93.5%) during the second sub-zone within zone BF3 (68.6–59.45 m) implies an expansion and contraction of the savannah ecoregions.

The high percentages of Poaceae, Moraceae, *Alchornea* and *Macaranga* in zone BF3 suggest that the vegetation around Lake Bosumtwi was similar to the present day vegetation further east (Fig. 6.6) from the 'Guinean Forest-savanna Mosaic' and the 'Nigerian Lowland Forest' ecoregion. Consequently, we infer that average precipitation during zone BF3 was from 1500–2500 mm/yr.

*6.5.1.5 BF2; equivalent MIS 5e*

In zone BF2 the main fossil pollen taxa identified were Moraceae, *Celtis*, *Macaranga*, *Alchornea*, Fabaceae Papilionoideae, Fabaceae Mimosaceae, *Uapaca* and *Holoptelea*

(Fig. 6.4a). Poaceae and Melastomataceae/Combretaceae percentages are low within zone BF2. Today the characteristic pollen taxa are found in high percentages in the vegetation of the 'Niger Delta Swamp Forest', 'Western Guinean Lowland Rainforest', 'Eastern Guinean Lowland Rainforest' and the 'Nigerian Lowland Forest' ecoregions. The elevated percentage of Moraceae and the high mean diversity (1-D 0.86) during zone BF2 suggests that the vegetation around Lake Bosumtwi was most probably similar to the 'Nigerian Lowland Forest' or 'Western Guinean Lowland Rainforest' ecoregions, with high precipitation ranging from 1500–3300 mm/yr and seasonal temperatures ranging from 12–33 °C.

*6.5.1.6 BF1; equivalent Holocene*

Zone BF1 is characterised by Moraceae, *Alchornea*, *Celtis*, *Macaranga*, *Trema*, *Hymenocardia*, Fabaceae Mimosaceae and *Holoptelea* (Fig. 6.4b). Taxa which are currently associated with the 'Niger Delta Swamp Forest', the 'Western Guinean Lowland Rainforest', the 'Eastern Guinean Lowland Rainforest' and the 'Nigerian Lowland Forest' ecoregions. *Hymenocardia* is today found within the 'Northern Congolian Forest Savanna Mosaic' ecoregion, *Medusandra* within the 'Cross-Sanaga-Bioko Coastal Forests' ecoregion and *Trema* within the 'Guinean Montane Forest' ecoregion. Although *Trema* is represented in the modern-day 'Guinean Montane Forest' ecoregion, it represents secondary forest species, often present after degradation. Increased percentages of *Trema* after 1.8 m (mid-Holocene) could be related to increased environmental disturbance by humans. The high diversity (1-D 0.91) and lack of dominance by one diagnostic taxon makes it difficult to provide an estimate of past climate conditions during BF1.

### *6.5.2 Comparison of forest vegetation assemblages*

The weighting of the pollen taxon scores along DCA axis 1 is interpreted as characterising shifts between forest and savannah biomes (Fig. 6.5a). We have linked

DCA axis 1 to biome shift (and moisture availability) because characteristic savannah taxa are separated from characteristic forest taxa.

The comparison between just the forest assemblages reveals clear compositional differences between zones (Fig. 6.5b). The contrasting vegetation composition between BF1 (Holocene) and BF3 (MIS 7) is clearly shown by the DCA ordination of sample scores, with samples from the Holocene plotting positive and samples from MIS 7 plotting negative on axis 1. The positive Holocene DCA scores suggest the climate was significantly wetter than the climate during MIS 7. Samples from BF2 (MIS 5e) have both positive and negative scores on axis 1 of the DCA ordination, indicating that climate varied substantially throughout this period. The sample scores of BF6 (MIS 13), BF5 (MIS 11) and BF4 (MIS 9) plot around the origin of the DCA ordination (Fig. 6.5b), containing either taxa with both positive and negative DCA scores or solely taxa which plot near the origin of the DCA ordination (Fig. 6.5a). Samples from BF6 (MIS 13) are clustered together, indicating low variability and that the samples within this forest zone all contain similar species, in comparable abundances.

The transition into all forest zones at Lake Bosumtwi is marked by an increase in pollen concentration and diversity (Fig. 6.2–5). Higher pollen concentrations during forest zones are likely to be the result of either a decreased sedimentation rate, as seen at *c.* 50 kyr BP when lake levels were exceptionally high (Shanahan et al., 2012), or alternatively, an increase in pollen production. The highest pollen diversity values occurred during BF5 (MIS 11), while samples from BF2 (MIS 5e) contained taxa from a range of different modern ecoregions.

Significant peaks in the montane taxa *Olea* sp. mark transitions into BF3 (MIS 7; *c.* 59 %), BF2 (MIS 5e; *c.* 30 %) and BF1 (Holocene; *c.* 12 %). Maley, (1991) state that the occurrence of *Olea* sp. in MIS 2 at Lake Bosumtwi is an indicator of *c.* 3–4°C cooling. In our new record, the occurrence of *Olea* sp. throughout all forest zones, with the exception of the BF1 (Holocene), suggests that the climate within BF1 (Holocene) was

either significantly warmer than previous forest zones or that climatic cooling is not solely responsible for the occurrence of *Olea* sp. within the fossil pollen record.

Zone BF1 (Holocene) has the lowest percentage of Poaceae when compared with any other period during the last 520 kyr (Fig. 6.1). In the absence of Poaceae, BF1 is characterized by a highly diverse pollen assemblage comprised of taxa belonging to modern forest ecoregions with relatively high rainfall (1500–4000 mm/yr). Both zones BF1 (Holocene) and BF5 (MIS 11) have similarly high pollen assemblage diversity values. The lowest diversity values of all the forest zones over the last *c.* 520 kyr occurred during BF3 (MIS 7).

Our study indicates that BF1 (Holocene) is unlike any other previous forest zone over the last *c.* 520 kyr and appears to be characterised by higher percentages of taxa such as *Alchornea* and Moraceae indicating a much wetter environment in West Africa during the last *c.* 11 kyr. Additionally, BF3 (MIS 7) is dissimilar to any other forest zone as it contains higher percentages of Poaceae and Cyperaceae suggesting that climate in West Africa was significantly drier at this time. Other forest zones are either comprised of taxa from numerous modern day ecoregions (BF2; MIS 5e), indicating that climate varied substantially, or taxa representing 'average vegetation composition' with no climatic extremes and low climatic variability (BF6, BF5, BF4; MIS 13, MIS 11, MIS 9).

### *6.5.3 West African forest vegetation associations*

To place the Lake Bosumtwi sediments in a wider regional context and gain a broader picture of West African vegetation during previous interglacials we present a comparison of our findings with terrestrial and marine records from the region, covering at least one major climate event (*i.e.* records spanning at least the last *c.* 17 kyr; Table 2.1). The key pollen taxa identified within each fossil pollen record during the interpreted interglacial periods was compared to the modern-day vegetation biomes of Olson et al. (2001) and classified according to the dominant vegetation

components. The maps produced each cover an individual interglacial period (Fig. 2.4–6). Each map shows the location of the fossil pollen records spanning that 'time-slice' and indicate the vegetation biome at that time for each location by colour code.

*6.5.3.1 West African vegetation during Marine Isotope Stage 13*

Three marine cores (ODP 658, GIK16415 and GIK16867) and the Lake Bosumtwi core provide a vegetation record of MIS 13 (BF6; Table 2.1; Fig. 2.3; Fig. 2.4). During MIS 13, site ODP 658 (offshore Mauritania) records high concentrations of Chenopodiaceae-Amaranthaceae and Poaceae which are characteristic of the 'Tropical and Subtropical Grassland' biome (Dupont et al., 1989). The late part of MIS 13 is missing from core GIK16415 (southwest of Dakar), but the early part records an increase in fern and *Uapaca* percentages. Both site GIK16415 and Lake Bosumtwi provide evidence for an expansion of the 'Tropical and Subtropical Moist Broadleaf Forest' biome during MIS 13 (BF6; Dupont and Agwu, 1992). Marine core GIK16867 (off Gabon) records generally high concentrations of taxa from the 'Montane Grasslands and Shrubland' biome although the percentages of mangrove and forest appear to decline with Poaceae percentages relatively high but fluctuating through the course of MIS 13 (Dupont et al., 1998). High montane taxa within marine core GIK16867 contrasts with the low montane taxa percentages evidenced at Lake Bosumtwi (BF6). Core GIK16867 and Lake Bosumtwi may sample pollen from two separate montane regions (Fig. 2.3) with a retreat in the West African afromontane forest north east of Lake Bosumtwi and an advance in the West African afromontane forest south east of site GIK16867 (Fig. 2.3). Parallels can be drawn between zones BF6 (MIS 13) and BF1 (Holocene) both from records derived from Lake Bosumtwi and core GIK16867; with both MIS 13 and Holocene forests containing similar percentages of montane taxa. Taken together these observations suggest both interglacials, in West Africa, had similar temperatures.

*6.5.3.2 West African vegetation during Marine Isotope Stage 11*

Four marine cores (ODP 658, GIK16415, GIK16867, GIK16776) and the Lake Bosumtwi core provide a vegetation record of MIS 11 (BF5; Table 2.1; Fig. 2.3; Fig. 2.4). Site ODP 658 again records high concentrations of Chenopodiaceae-Amaranthaceae and Poaceae which are characteristic of the 'Tropical and Subtropical Grassland' biome (Dupont et al., 1989). During MIS 11 at site ODP 658 taxa such as *Pinus*, *Ephedra* and Asteraceae, which are transported exclusively by the NE trade winds, decrease (Dupont et al., 1989). Additionally, site ODP 658 displays increased percentages of *Rhizophora*, implying increased river discharge (Dupont, 2011) and high sea level; supporting recent estimates of a *c.* 13 m eustatic sea level rise during MIS 11 (Roberts et al., 2012). Early MIS 11 is missing from core GIK16415, however late MIS 11 displays an increase in fern spores and *Rhizophora* percentage (Dupont and Agwu, 1992). High fern spores indicate an increase in canopy cover, characteristic of the modern day 'Tropical and Subtropical Moist Broadleaf Forest' biome. The vegetation around Lake Bosumtwi during BF5 (MIS 11) consisted of taxa belonging to the 'Tropical and Subtropical Moist Broadleaf Forest' biome. The percentage of montane taxa (*Olea* sp.) at Bosumtwi is low throughout BF5 (MIS 11), contrary to the large expansion of the montane taxa *Podocarpus* seen in marine cores GIK16867 and GIK16776 (off Liberia; Fig. 2.3; Jahns, 1996; Dupont et al., 1998).

High pollen concentration values during BF5 (MIS 11), evidenced at Lake Bosumtwi and GIK16867, as well as decreased trade wind indicators at ODP 658 imply that the high pollen influx is most likely related to an increase in pollen production and not an intensification of atmospheric circulation. High pollen production during interglacial periods is evidenced in many other records across the globe (*e.g.* Hanselman et al., 2005; Fréchette et al., 2006). High pollen productivity in tropical forests (*i.e.* interglacials) and low productivity in savannah (*i.e.* glacials) has also been demonstrated in modern pollen trapping studies (Gosling et al., 2009).

*6.5.3.3 West African vegetation during Marine Isotope Stage 9*

Four marine cores (ODP 658, GIK16415, GIK16867, GIK16776) and the Lake Bosumtwi core provide a vegetation record of MIS 9 (BF4; Table 2.1; Fig. 2.3; Fig. 2.5). Site ODP 658 again records high percentages of taxa characteristic of the 'Tropical and Subtropical Grassland' biome (Dupont et al., 1989), although there is a strong delayed response in the vegetation to increased moisture availability at the beginning of MIS 9 and an early response in the vegetation to decreased moisture availability at the end of MIS 9 (Dupont et al., 1989). Core GIK16415, displays an increase in fern spores and *Rhizophora* percentage (Dupont and Agwu, 1992); indicating an expansion of both the 'Tropical and Subtropical Moist Broadleaf Forest' and the 'Mangrove' biomes. At site GIK16867, although dominated by montane taxa, MIS 9 is characterised by an increase in the percentage of *Alchornea*, *Uapaca*, *Celtis* and *Rhizophora* (Dupont et al., 1998), inferred to represent an expansion of the 'Tropical and Subtropical Moist Broadleaf Forest' and the 'Mangrove' biomes. During MIS 9, site GIK16776 records an increase in taxa representative of the modern 'Tropical and Subtropical Moist Broadleaf Forest' biome, with increased fern spores and low pollen influx, possibly related to reduced atmospheric circulation (Jahns et al., 1998). At Lake Bosumtwi, MIS 9 is characterised by taxa from the 'Tropical and Subtropical Moist Broadleaf Forest' biome, supporting findings from the marine records.

*6.5.3.4 West African vegetation during Marine Isotope Stage 7*

Five marine cores (ODP 658, GIK16415, GIK16867, GIK16776 and KS84067) and the Lake Bosumtwi core provide a vegetation record of MIS 7 (BF3; Table 2.1; Fig. 2.3; Fig. 2.5). Site ODP 658 shows high percentages of taxa during MIS 7 characteristic of the 'Tropical and Subtropical Grassland' biome (Dupont et al., 1989). During MIS 7, sites GIK16776 and GIK16415 show a decrease in Poaceae and an increase in ferns and *Rhizophora* (Dupont and Agwu, 1992; Jahns et al., 1998). Site GIK16867 indicates

MIS 7 as having high percentages of *Alchornea*, *Uapaca*, *Celtis* and *Rhizophora*. Site KS84067 indicates that MIS 7 contained high percentages of *Alchornea*, *Uapaca*, *Lannea*, *Macaranga* and *Rhizophora*. Sites GIK16867, GIK16776 and KS84067 all provide evidence of an expansion of the 'Tropical and Subtropical Moist Broadleaf Forest' and 'Mangrove' biomes in West Africa during MIS 7. Mangrove swamps were abundant along the Guinean coast during MIS 7 as a response to eustatic sea level rise and increased freshwater discharge (Frédoux, 1994; Shi and Dupont, 1997; Jahns et al., 1998).

Although the vegetation during BF3 (MIS 7) at Lake Bosumtwi was similar the 'Tropical and Subtropical Moist Broadleaf Forest' biome it was also highly unstable, with the expansion and contraction of savannah-type vegetation. Globally selected records also show high amplitude fluctuations within MIS 7, where at times climate conditions reverted back to full glacial (Lang and Wolff, 2011). Low vegetation diversity values at Lake Bosumtwi (BF3) coupled with high climatic instability, evidenced globally during MIS 7, support model evidence that rapid fluctuations between climatic extremes decreases biodiversity (Fjeldsaå et al., 1997).

*6.5.3.5 West African vegetation during Marine Isotope Stage 5e*

Eight marine cores (ODP 658, V22-196, GIK16415, KS84067, GIK16856, KW23, GeoB1016 and GeoB1711) and the Lake Bosumtwi core provide a record of vegetation during the last interglacial in West Africa (BF1; Table 2.1; Fig. 2.3; Fig. 2.6). The vegetation record of sub-stage MIS 5e is absent in sites GIK16867 and GIK16776 and partially disturbed in GIK16856 due to sediment slumping (L. Dupont, pers. com). The fossil pollen record of MIS 5e from ODP 658 and V22-196 is dominated by taxa such as Chenopodiaceae-Amaranthaceae and Poaceae typical of the 'Tropical and Subtropical Grassland' biome. Marine site GIK16415 although dominated by savannah taxa, contains low pollen, but high fern spore percentages. Vegetation compositional data from GIK16415 is inferred to represent a shift in the northern limit of the 'Tropical

and Subtropical Moist Broadleaf Forest' biome from 6°N during MIS 6 to 10°N during MIS 5e (Hooghiemstra and Agwu, 1988). Core KS84067, GIK16856 and KW23 record an increase in Euphorbiaceae, Caesalpiniaceae, *Celtis*, *Lophira, Alchornea, Uapaca* and *Rhizophora* as well as a decrease in montane elements (*Podocarpus)* implying an expansion of the 'Tropical and Subtropical Moist Broadleaf Forest' and 'Mangrove' biomes and a retreat in the 'Montane Grasslands and Shrubland' biome during MIS 5e (Fig. 2.3; Bengo and Maley, 1991; Lézine and Casanova, 1991; Frédoux, 1994; Dupont and Weinelt, 1996). Although low pollen concentrations during MIS 5e are recorded in core GeoB1711-4, high percentages of *Alchornea*, *Brachystegia*, *Burkea* and *Bridelia* indicate that the vegetation may have been similar to either the 'Tropical and Subtropical Grassland Savannas and Shrublands biome' or the 'Tropical and Subtropical Moist Broadleaf Forest' biome. Site GeoB1016 records high percentages of *Alchornea* and *Brachystegia* and low percentages of Poaceae indicating an expansion of the 'Tropical and Subtropical Moist Broadleaf Forest' and 'Tropical and Subtropical Dry Broadleaf Forests' biome and a retreat of the 'Tropical and Subtropical Grassland Savannas and Shrublands' biome.

The current absence of a detailed chronology for the 5B core does not allow discussion regarding each sub-stage of the last interglacial period and such work awaits a more refined timescale (J. Overpeck, pers. com.). During BF2 (MIS 5e) the vegetation around Lake Bosumtwi is dominated by taxa from the 'Nigerian Lowland Forest' and the 'Western Guinean Lowland Rainforest' ecoregions, both within the 'Tropical and Subtropical Moist Broadleaf Forest' biome.

*6.5.3.6 West African vegetation during the Last glacial-Holocene transition*

The transition from the Lateglacial to the Holocene is well documented in both marine and terrestrial records from West Africa (Table 2.1; Fig. 2.3; Fig. 2.6) although the timing appears to differ slightly between sites. In the marine, the Lateglacial-Holocene transition occurred at: GIK16415 (*c.* 15 kyr BP; Hooghiemstra and Agwu, 1988),

GIK16856 (*c.* 14 kyr BP; Dupont et al., 2000), GeoB1016 (*c.* 13–10 kyr BP; Fig. 2.3; Dupont et al., 2000) and KS12 (*c.* 12 kyr BP; Lezine and Vergnaud-Grazzini, 1993; Dupont et al., 2000). Although generally recording high grass percentages through the Holocene, GIK16415 records an increase in fern spore percentages and taxa comprising the modern-day 'Tropical and Subtropical Moist Broadleaf Forest' biome at *c.* 15 kyr BP (Dupont and Agwu, 1992). Sites GIK16856, KS84067 and GIK16867 show an increase in taxa from the modern-day 'Tropical and Subtropical Moist Broadleaf Forest' biome during the Holocene (Frédoux, 1994; Dupont and Weinelt, 1996; Dupont et al., 1998). Sites KS12 and the Niger Delta indicate the spread of mangrove swamps after the Last Glacial Maximum but a retreat in their extent toward the present day (Sowunmi, 1981; Lezine and Vergnaud-Grazzini, 1993). The terrestrial record from Lake Tilla (Nigeria) shows an increase in taxa such as *Celtis*, *Lannea*, *Alchornea*, *Hymenocardia* and *Uapaca* from the 'Tropical and Subtropical Moist Broadleaf Forest' biome *c.* 10 kyr BP at the Lateglacial-Holocene transition (Salzmann et al., 2002). Lake Barombi Mbo (Cameroon) displays an increase in taxa such as *Lophira*, *Pycnanthus* and *Uapaca* from the 'Tropical and Subtropical Moist Broadleaf Forest' biome at *c.* 13 kyr BP (Fig. 2.3; Maley and Brenac, 1998). Humid conditions are evidenced in the Niger Delta, with high *Rhizophora* percentages interpreted as an increase in freshwater discharge at *c.* 12 kyr BP (Fig. 2.3; Sowunmi, 1981). In this study, the glacial-Holocene transition at Lake Bosumtwi is also marked by an increase in taxa associated with the modern-day 'Tropical and Subtropical Moist Broadleaf Forest' biome at *c.* 11 kyr BP.

*6.5.3.7 West African evidence of Early Holocene vegetation*

Three terrestrial and eleven marine pollen records (BF1; Table 2.1; Fig. 2.3; Fig. 2.6) indicate that the 'Tropical and Subtropical Moist Broadleaf Forest' biome expanded during the early Holocene and was more diverse than at present. Marine transgression during the early Holocene resulted in *Rhizophora* expansion along the coasts of the Gulf of Guinea and in inland lagoons (Dupont et al., 2000; Salzmann and Hoelzmann, 2005). Prior to 4.5–3.4 kyr BP, during the early Holocene, there is no evidence for the

presence of the 'Guineo Forest Savannah-mosaic' ecoregion which forms the present-day Dahomey Gap (Fig. 6.6; Salzmann and Hoelzmann, 2005). Nevertheless, our data from Lake Bosumtwi indicates little change in forest composition during the early BF1 (Holocene). High percentages of *Alchornea*, Arecaceae and *Tetrorchidium* at 2.2 m (mid-Holocene) at Lake Bosumtwi suggests forest expansion similar to conditions experienced in the Sanaga Basin (Fig. 2.3; Marret et al., 2008; Marret et al., 2013) and that drier conditions became pronounced after *c.* 5.5 kyr BP (Lezine and Cazet, 2005). The most significant change in vegetation composition in the Holocene around Lake Bosumtwi occurred *c.* 500 years ago with the sudden increase in Moraceae percentage from 12 to 77 %. This sudden increase in arboreal taxa may relate to recent human activities or possibly a global increase in tropical moisture availability, as documented in other records of hydrological change such as Dongge Cave (southern China; Wang et al., 2005) and in the Arabian Sea (Anderson et al., 2002; Gupta et al., 2003).

## 6.6. Conclusions

Pollen and spores extracted from the uppermost *c.* 150 m of core 5B from Lake Bosumtwi (West Africa) provide a record of vegetation dynamics over the last *c.* 520 kyr. During the last *c.* 520 kyr the vegetation of West Africa mainly belonged to the 'Tropical and Subtropical Grasslands Savannas and Shrublands' biome (Fig. 2.3); however six distinct zones can be identified where savannah vegetation was reduced and the vegetation was more characteristic of the 'Tropical and Subtropical Moist Broadleaf Forest' biome (Fig. 2.3; Fig. 6.1). A comparison with nearby marine core sites, which also record six periods of forest expansion over the same time period, suggests that the six forest assemblage zones identified at Lake Bosumtwi most likely relate to global interglacial periods (MIS 13, 11, 9, 7, 5e and 1).

The six forest assemblage zones identified were floristically distinct, possibly relating to different climatic conditions during each interglacial period. Key taxa associated with the Lake Bosumtwi equivalent MIS 13 include *Celtis*, *Uapaca*, *Macaranga*, *Alchornea*,

*Holoptelea*, Moraceae and Fabaceae species. *Celtis*, Moraceae, *Macaranga*, *Alchornea* and *Pycnanthus* were dominant at Lake Bosumtwi during MIS 11. Main taxa associated with the equivalent MIS 9 were Moraceae, *Celtis*, *Olea* sp., *Macaranga* and *Alchornea*. The main fossil pollen components of the equivalent MIS 7 were *Olea* sp., Moraceae, *Alchornea*, *Macaranga* and Poaceae. In MIS 5e Moraceae, *Celtis*, *Macaranga*, *Alchornea*, Fabaceae Papilionoideae, Fabaceae Mimosaceae, *Uapaca* and *Holoptelea* were dominant. The Holocene vegetation is characterised by Moraceae, *Alchornea*, *Celtis*, *Macaranga*, *Trema*, *Hymenocardia*, Fabaceae Mimosaceae and *Holoptelea*.

The DCA ordination of the fossil pollen assemblages from Lake Bosumtwi highlights the contrasting vegetation composition between the Holocene and MIS 7 and suggests that the Holocene was significantly wetter than any other interglacial period over the last *c.* 520 kyr. MIS 7 had the lowest diversity of any interglacial, most likely due to generally drier climate conditions. Conversely, high climatic stability may have resulted in the high diversity values evident during the Holocene and MIS 11. Although the diversity values suggest that MIS 11 was similarly diverse to the Holocene, the DCA ordination of sample scores indicate that MIS 11 was also significantly drier. Sub-stage MIS 5e contained a range of both wet and dry samples, suggesting intervals of drought superimposed on a generally wet climate.

The Holocene has the lowest percentages of Poaceae throughout and instead is highly diverse and comprised of taxa belonging to modern forest ecoregions. Our study indicates that the Holocene is unique when compared to other interglacials over the last *c.* 520 kyr. The Holocene appears to be characterised by species indicating that the climate of West Africa was much wetter during the last *c.* 11 kyr BP. This finding has direct implications for conservation management and ecologists working to protect the present day endemic species within these fragile tropical ecosystems. For the first time it is now evident that prior to 11 kyr BP, the vegetation of tropical West Africa was unlike that of today and probably occurred under drier than modern climate conditions.

Given predictions of increasingly drier regional climates in West Africa over the coming decades (Christensen, 2007), the interglacial flora of MIS 7 may prove a good analogue for future forest associations in West Africa.

## 6.7. Acknowledgements

We thank A.L. Coe, N. Ludgate and D. Kemp for pertinent discussion during the construction of this manuscript. We thank T. Shanahan and N. Mckay for assistance with Lake Bosumtwi chronology. Additionally, we thank the reviewer Henry Hooghiemstra, whose expertise greatly improved this manuscript at review. This research was funded by the NERC/The Open University Charter studentship (NE/H525054/1, CSM) and NERC New Investigator Award (NE/G000824/1, WDG). The data reported in this paper is archived on the PANGAEA database (www.pangaea.de).

# 7. Vegetation and climate change in tropical West Africa over the last *c.* 520,000 years

This chapter has been written in the form of a manuscript and is ready to be submitted as a report to Science. Submission of this manuscript has been put on hold following a request from the lead Principal Investigators of the Lake Bosumtwi coring project (ICDP website) this is to allow them to first submit another manuscript later in the summer. It is anticipated that the full reference for this manuscript will be:

Miller, C.S., Gosling, W.D., Kemp. D.B., Coe, A.L., Gilmour, I., 2013. Vegetation and climate change in tropical West Africa over the last *c.* 520,000 years.

Full methodological details are provided in Chapter 4 and Appendix 6. The presented data are tabulated in Appendix 5 and will be made available online via the Pangaea database. Supplementary information has been incorporated into the text and references are made to previous chapters to avoid repetition for the adaptation into thesis format. My contribution to this manuscript was the counting and identification of all pollen grains, the acquisition of all $\delta^{15}N$ data and the writing of the manuscript.

## 7.1. Abstract

The longest terrestrial record of past vegetation and moisture balance from Africa reveals the response of tropical vegetation to changes in global climate over the last *c.* 520,000 years. The Bosumtwi impact crater (W. Africa) formed 1 million years ago, subsequently accumulated *c.* 290 m of sediment. We demonstrate that variations in grass pollen abundance (0–99 %) through the upper 150 m of this record shows eleven major biome shifts between savannah and woodland. Variations in $\delta^{15}N$ (+2 to +14 ‰) suggest the highest lake levels coincided with intervals of woodland expansion. The shifts between savannah and woodland occurred on both glacial-interglacial (100,000 year) and millennial timescales, and were likely controlled by both high and low latitude

mechanisms. Climatic changes recorded in the Lake Bosumtwi record coincide with key events in the migration of early *Homo sapiens* populations.

## 7.2. Main text

Today tropical West Africa is a region of global ecological importance (Myers et al., 2000) that is being impacted by a rapidly growing human population (Shanahan et al., 2013) and is vulnerable to naturally driven periodic multi-decadal drought (Shanahan et al., 2012). Evidence from the recent geological record (Quaternary) and predictions from climate models (Maley, 1991; Shackleton et al., 2003; Fréchette et al., 2006; Cowling et al., 2008; Dupont, 2011) indicate that climate change has triggered switches between woodland (>55 % tree cover) and savannah biomes in West Africa in the past. The magnitude of Quaternary temperature change is comparable with predicted change (1.9–4.7°C) for West Africa in the coming decades (IPCC, 2007). However, uncertainty exists surrounding what aspects of climate change are important for instigating biome shifts in the region (*e.g.* atmospheric $CO_2$ concentration, temperature, precipitation, seasonality) and whether other landscape-scale factors (*e.g.* fire) also play an important role.

Terrestrial sedimentary successions spanning multiple glacial-interglacial cycles are globally scarce, and in Africa, just three such records have been recovered (Fig. 7.1). Lake Malawi and Lake Tanganyika are situated 330 km apart in East Africa while Lake Bosumtwi is the only record in West Africa (6°30'N, 1°25'W; Fig. 7.1).

The Lake Bosumtwi impact crater is an ideal site for investigating long-term past vegetation and climatic change because it: i) has been accumulating sediment over the last 1.08 ±0.04 Myr (Koeberl et al., 2007), ii) currently lies just *c.* 400 km south of the transition into the savannah/woodland biome (Olson et al., 2001), iii) is hydrologically closed, in terms of both surface and groundwater, and therefore lake level is highly sensitive to changes in moisture balance (Talbot and Delibrias, 1980), and iv) lies within the seasonal migration path of the tropical rainbelt (Fig. 3.2; Nicholson and Grist,

2001). Lake level and surrounding vegetation is sensitive to changes in the strength of the West African monsoon (Shanahan et al., 2008), which is itself driven by changes in orbital parameters (Dupont, 2011). Here we investigate the response of West African terrestrial vegetation and local lake system dynamics through the major climate changes of the past *c.* 520,000 years from a multi-proxy analysis of the upper 150 m of the Bosumtwi sedimentary succession.

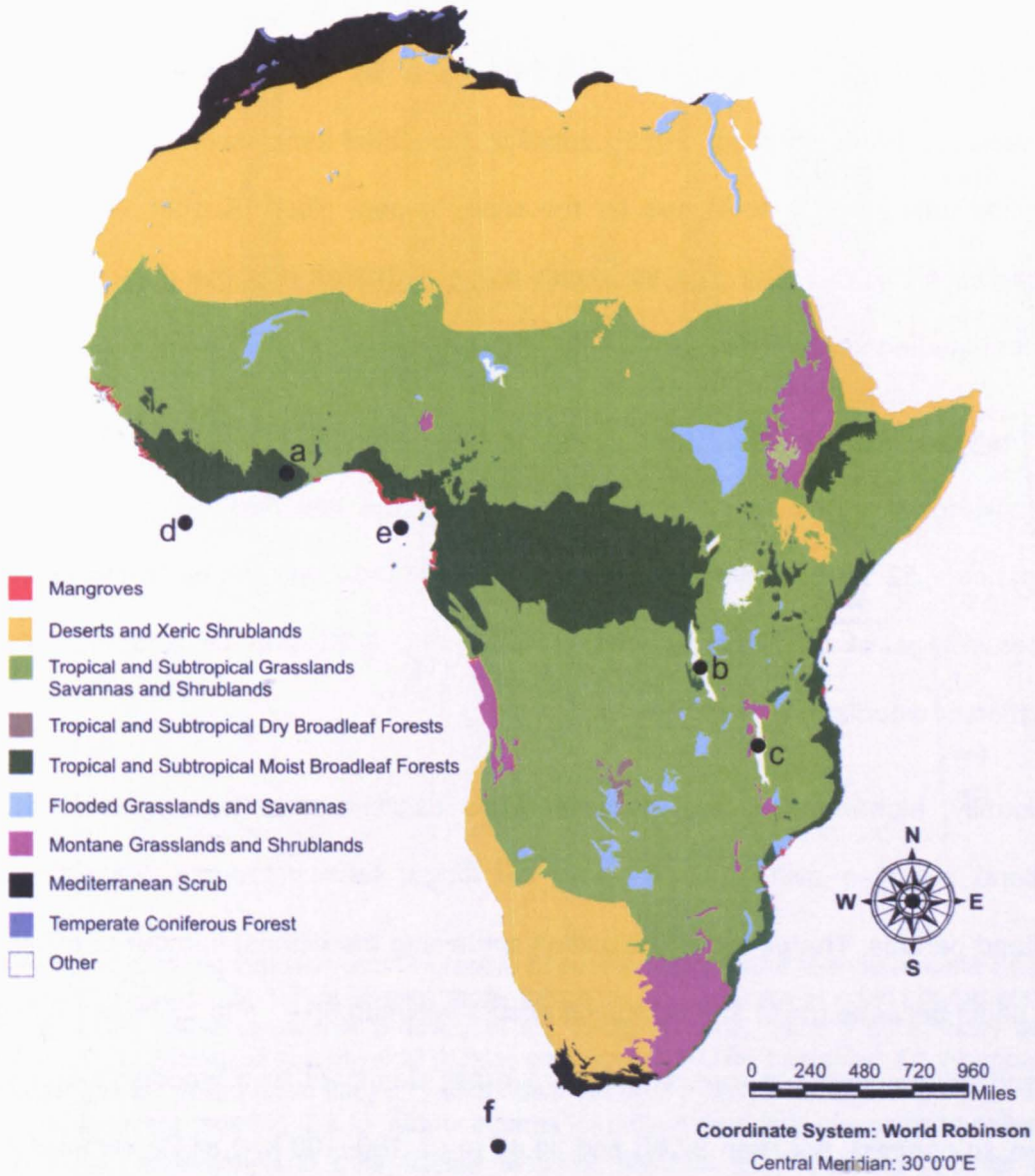


**Fig. 7.1.** Distribution of modern vegetation biomes across Africa (modified from Olson et al. 2001). Sites mentioned in the text are marked. Lakes: Bosumtwi **(a)**, Lake Tanganyika (Felton et al., 2007) **(b),** and Lake Malawi (Scholz et al., 2007) **(c).** Marine cores: GIK 16776 (Jahns et al., 1998) **(d),** MD03-2707 (Weldeab et al., 2007) **(e),** and ODP 1089 (Cortese et al., 2007) **(f).**

In 2004, 1833 m of sediment were recovered from 14 separate drill holes from Lake Bosumtwi by the International Continental Drilling Program (Koeberl et al., 2007). In this study we have used core BOS04-5B (hereafter 5B), which was recovered from the deepest part of the lake (74 m) and yielded the longest, most continuous, sedimentary succession (294.67 m in length; Koeberl et al., 2007). To reconstruct past biome shifts, fire frequency and moisture balance changes we conducted pollen, charcoal, and nitrogen stable isotope analysis on the upper 150.7 m of core 5B (Appendix 6).

Chronological control within our record from core 5B has been attained through radiocarbon (Shanahan et al., 2012), optically stimulated luminescence (Shanahan et al., 2013) and a basal Ar-Ar age for the crater impact glass (Koeberl et al., 1997; Jourdan et al., 2009). Our age vs. depth model indicates that the upper 150 m of sediment studied spans the last *c.* 520 kyr (Fig. 4.3).

Our analyses indicate that grass pollen is the dominant component of the Lake Bosumtwi fossil pollen record for the majority of the last 520 kyr (mean relative abundance = 52 %). However, six prolonged periods (>54 kyr) can be identified where the percentage of grass is reduced (<55 %; Fig. 7.2C and D) and the relative proportion of woodland taxa increased.

Additionally, higher frequency, millennial scale oscillations between grassland and woodland are also evident during both the longer term prolonged grassland and woodland periods. The period of deposition containing the highest number of millennial scale shifts between grass and woodland occurs between 96.41 and 57.65 m (320–180 kyr) and encompasses a transition from a grass dominant to a woodland dominant system. In contrast, between 57.65 and 35.45 m (*c.* 180–100 kyr) all 22 samples from this interval contain >80 % Poaceae indicating that the climate was very stable with no short term shifts. Total pollen/spore concentration is high throughout the core (<245,000 grains $cm^{-3}$) except for 33.85–32.90 m, which is effectively barren (1,400–90 grains $cm^{-3}$).

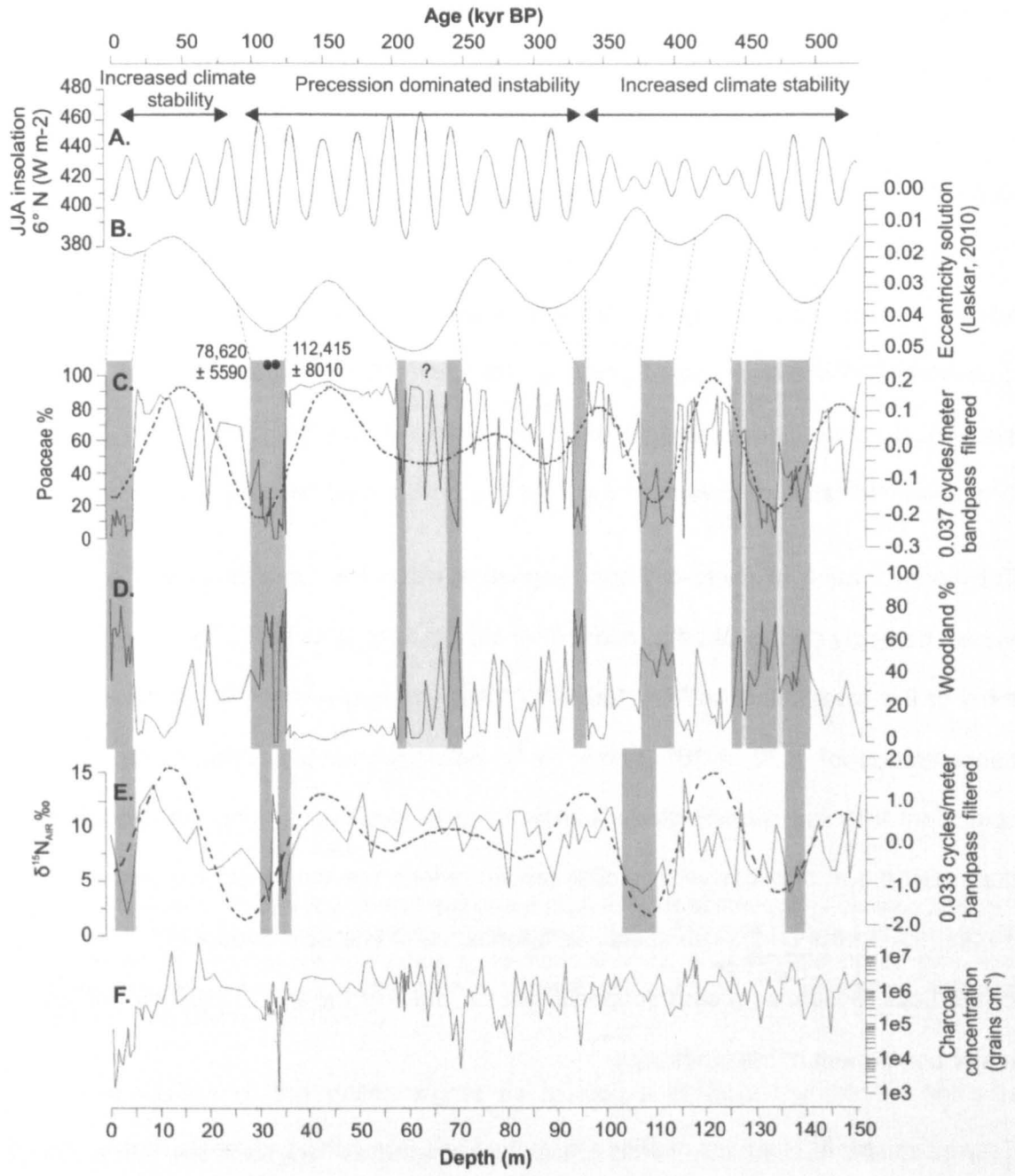


**Figure 7.2.** Orbital periodicities and the record of past environmental change at Lake Bosumtwi obtained from the upper 150 m of sediments from core 5B. Variance in orbital parameters: **A).** Summer (JJA) insolation at 6°N (Paillard et al., 1996), and **B).** La2010 eccentricity solution (Laskar, 2011). Biological and physical proxies obtained from Lake Bosumtwi: **C).** Abundance of Poaceae (grass) pollen [solid line] and data filtered at 0.033 [dashed line] to highlight variance at *c.* 100 kyr scale (see Fig. 7.5 for further information), **D).** Abundance of woodland pollen taxa, **E).** $\delta^{15}N_{AIR}$ [solid line] and data filtered at 0.033 [dashed line] (see Fig. 7.5 for further information), and **F).** charcoal concentration. Vertical grey bars indicate ≥3 adjacent samples with <55 % Poaceae (C and D), and $\delta^{15}N$ <+6.19 (E). Filtering of Poaceae abundance and $\delta^{15}N_{AIR}$ was carried out using a Gaussian filter (0.026 bandwidth) to highlight variance in the data and likely orbital control. Black circles are optically stimulated luminescence dates take from core BOS04-5B (Shanahan et al., 2013).

To characterize major vegetation change (biome shifts) around Lake Bosumtwi from our record we examined the fossil pollen/spore record (Fig. 7.3) using detrended correspondence analysis (DCA; Bennett, 2003). The weighting of the pollen species along DCA axis 1 is interpreted as characterising shifts between woodland and savannah biomes (Fig. 7.3). We link DCA axis 1 to biome shift because characteristic savannah taxa (*e.g.* Poaceae, Amaranthaceae, Cyperaceae) are separated from characteristic woodland taxa (*e.g. Alchornea*, *Celtis*, *Macaranga*). Switches in biome are broadly characterized by the anti-phasing of high abundances (>55 %) of grass (Poaceae, indicative of savannah; Fig. 7.2C) with woodland taxa (Fig. 7.2D).

The concentration of micro-charcoal fragments within the Lake Bosumtwi sediments varies markedly throughout the record (0–2.5 x $10^7$ fragments $cm^{-3}$; Fig. 7.2F). Through most of the studied interval, *i.e.* 150–4.8 m (520–10 kyr) charcoal is abundant (mean concentration of 1.69 x $10^5$ grains $cm^{-3}$); notwithstanding a brief barren interval, coincident with the palynologically barren interval. However, during the deposition of the upper 4.8 m of sediment charcoal concentrations are low (mean concentrations of 11,260 fragments $cm^{-3}$). The sustained abundance of charcoal throughout the majority of the Lake Bosumtwi record suggests that for most of the last *c.* 520 kyr fire was a major component of the landscape.

Organic matter $\delta^{15}N$ values obtained from the Lake Bosumtwi sediments range from +2 to +14‰ (Fig. 7.2E). Five periods can be identified when the nitrogen isotope composition of organic matter decreased consistently, $\delta^{15}N$ <+6.2 ‰, for 3 consecutive samples (Fig. 7.2E). The decrease in $\delta^{15}N$ is consistent with increased N fixation by cyanobacteria within the lake. Today, cyanobacteria are the main component of N fixation in tropical African lakes and dominate when dissolved inorganic nitrogen (DIN) becomes limited (Talbot and Johannessen, 1992; Talbot, 2001). Limitation of DIN in Lake Bosumtwi is thought to have occurred during periods of water column stability and stratification, occurring during times of either high lake level or reduced wind stress

(Talbot, 2001). We therefore interpret the decrease in $\delta^{15}N$ as broadly indicative of deeper lake conditions.

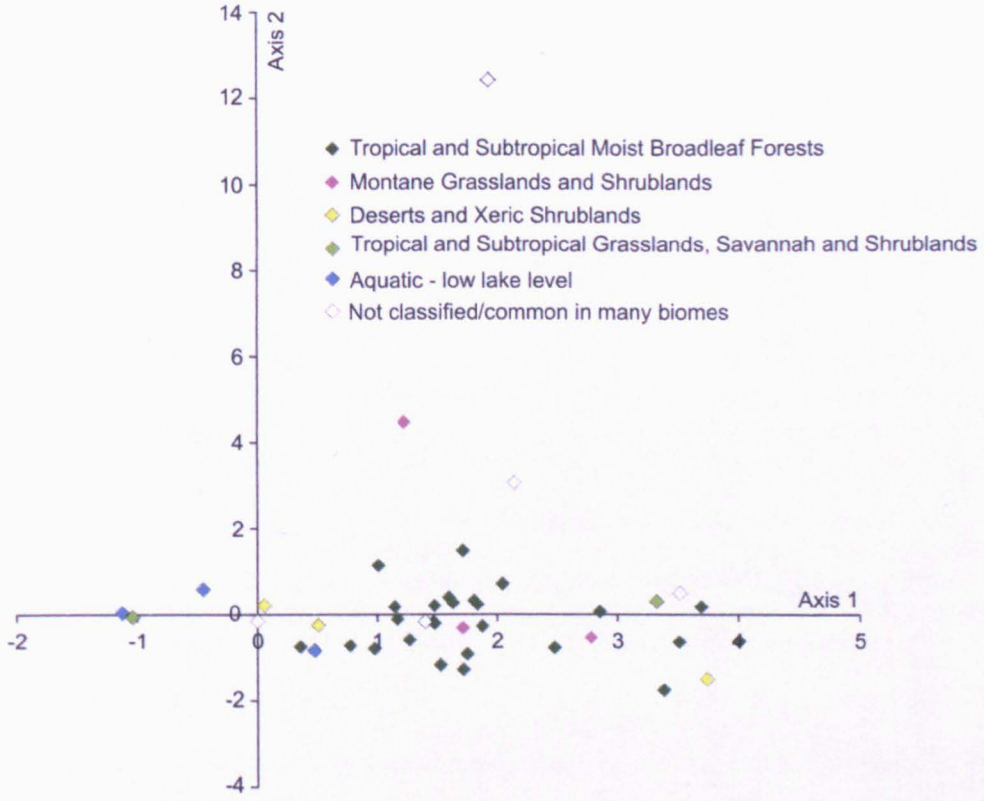


**Fig. 7.3.** Ordination of Lake Bosumtwi fossil pollen DCA species scores axis 1 vs. axis 2. Axis 1 represents most of the ecological variance (eigenvalue (EV) 0.44), axis 2 EV is 0.21. DCA was performed on all pollen/spore taxa reaching abundance of >2 % of the total pollen sum in at least one sample. In total 43 pollen/spore taxa were included from 217 samples. Ecological groupings follow Olson et al. (2001).

Our interpretation of the pollen signal as indicative of terrestrial biome shifts is supported by the relationships between woodland pollen and deeper lake level (Fig. 7.2D and Fig. 7.2E); with woodland taxa flourishing when more moisture is available.

The temporal pattern of biome and lake level change in our Bosumtwi record through the last *c.* 520 kyr suggest that major ecological and climate oscillations occur in phase with *c.*100 kyr glacial-interglacial cycles, which in turn have an underlying orbital control (Fig. 7.2; Fig. 7.4). Spectral analysis of the savannah (Poaceae pollen) and $\delta^{15}N$ data reveals evidence in both proxy records for enhanced variance at a frequency of *c.*100 kyr supporting this inference (Fig. 7.5). Indeed, a similar orbital control on fossil pollen and sea surface temperature (SST) has been recognised from nearby marine sediment

cores (Jahns et al., 1998; Cortese et al., 2007; Weldeab et al., 2007), suggesting an important connection between high latitude climate oscillations and the West African monsoon (Fig. 7.4).

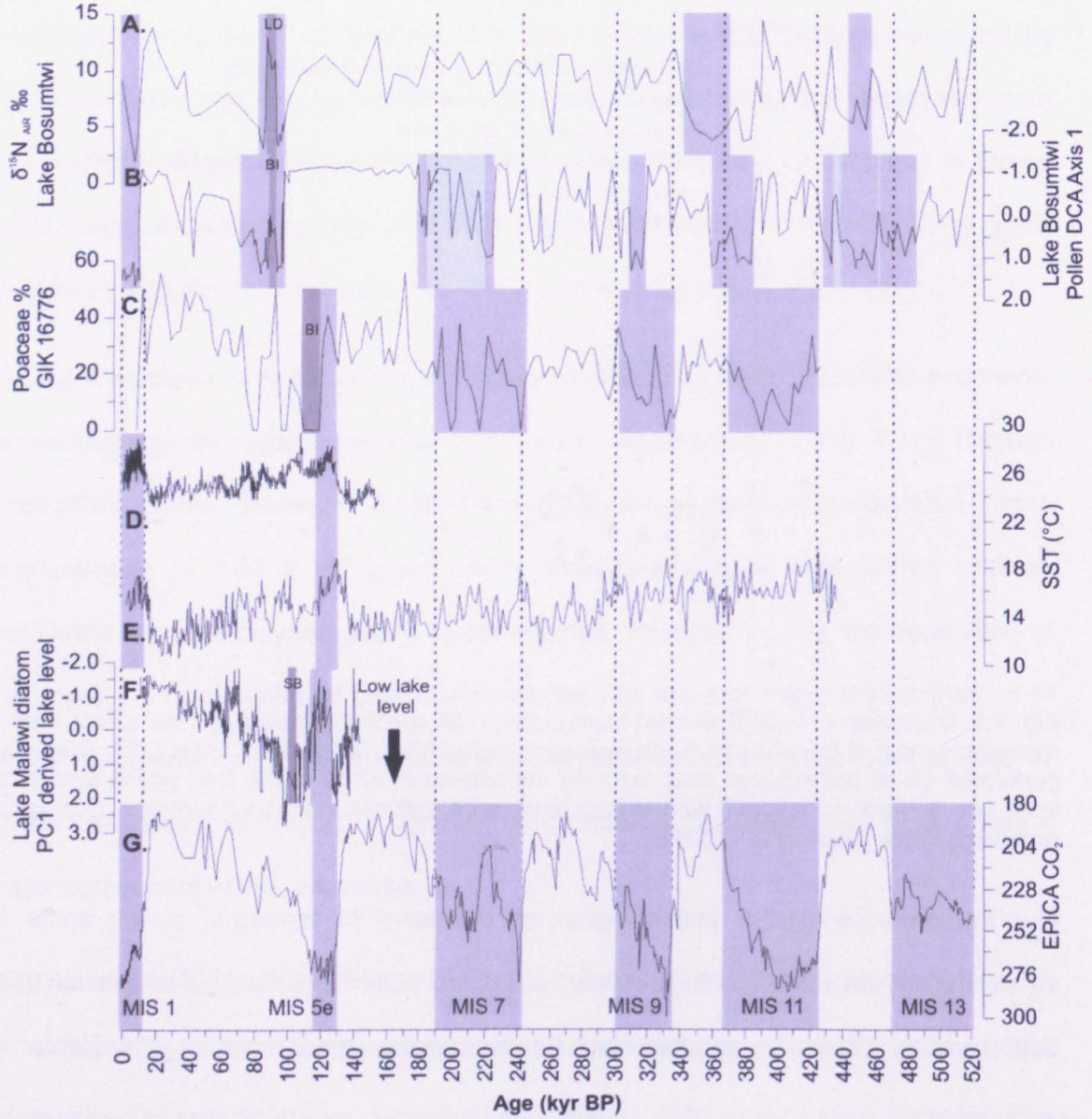


**Fig. 7.4.** Comparison of Lake Bosumtwi lake level and biome shifts with regional and global records. Lake Bosumtwi: **A).** Lake level (derived from $\delta^{15}N_{AIR}$), and **B).** Biome shift (pollen DCA Axis 1). Other records of: **C).** Vegetation change (Poaceae %; Jahns et al., 1998), **D).** SSTs from Gulf of Guinea (Weldeab et al., 2007), **E).** SSTs from southern Atlantic Ocean (Cortese et al., 2007), **F).** Lake level, Lake Malawi (Stone et al., 2011), and **G).** Global $CO_2$ (Petit et al., 1999; Monnin et al., 2001; Raynaud et al., 2005; Siegenthaler et al., 2005; Luthi et al., 2008). LD= lake desiccation. BI= barren interval. SB= sand bed. Light grey bars indicate interpreted marine isotope warm stages in each record. Dark grey bars indicate intervals of extreme drought.

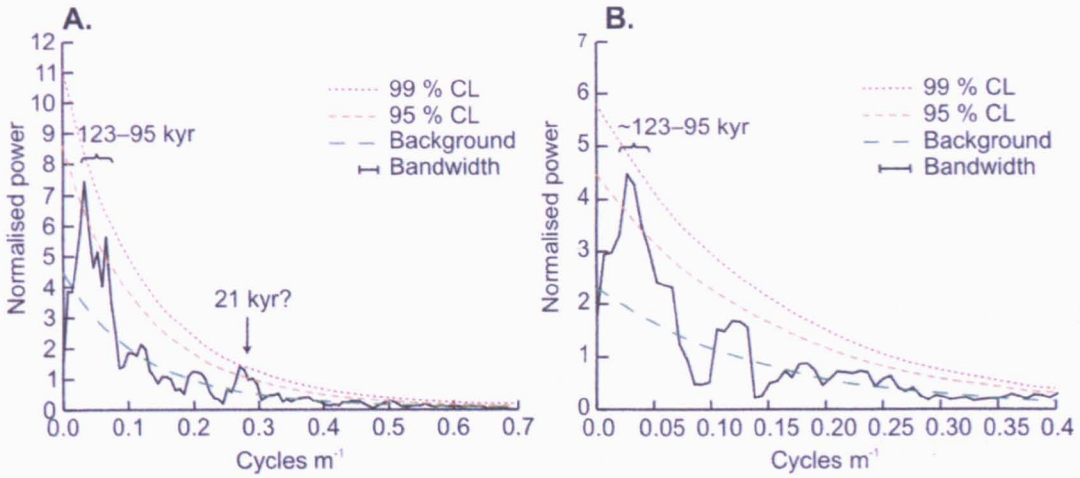


**Fig. 7.5.** Spectral analysis results of Lake Bosumtwi data. **A).** Poaceae %, and **B).** nitrogen isotopes ($\delta^{15}N$). The Poaceae and $\delta^{15}N$ datasets reveal evidence for low frequency cyclicity with high statistical significance (at bandwidths of 15–31 m and 25–38 m respectively) with 95 % and 99 % confidence levels (CL) shown. Filtered versions of the datasets (filter frequency = 0.033, *i.e.* 30.3 m wavelength) shown in Fig. 7.2C and Fig. 7.2E highlight this statistically verified variability and support the inference that the cycles correspond to orbital eccentricity (95–123 kyr). Spectra were calculated on quadratic detrended, linearly interpolated Poaceae % and nitrogen isotope data using multi-taper spectral analysis as outlined in Weedon (2003), 4 tapers used. Confidence intervals were determined using the robust methodology of Mann and Lees, (1996) based on a second order polynomial fit to the median smoothed spectra.

Throughout the majority of the Lake Bosumtwi record (*c.* 520–320 and 130–0 kyr) vegetation/climate at the *c.* 100 kyr scale appears strongly coupled to orbital eccentricity (Fig. 7.2). Periods of globally warmer temperatures (Fig. 7.4G) are associated with low savannah abundances, whereas colder conditions are associated with high savannah abundances (Fig. 7.4B). We suggest that the influence of high latitude glaciation on low latitude vegetation and climate was probably through the concomitant fluctuations in Atlantic SSTs (Fig. 7.4D–7.4E), which resulted in the latitudinal displacement of the tropical rainbelt (deMenocal et al., 1993; Weldeab et al., 2007; Dupont, 2011). Importantly however, through the central portion of the Lake Bosumtwi record *c.* 96–44 m (*c.* 320–130 kyr) the link between 100 kyr eccentricity and vegetation/climate change appears weakened. In this interval 400 kyr eccentricity was high (Fig. 7.2A), and the strength of orbital precession (which is modulated by eccentricity) was similarly enhanced, thus promoting enhanced seasonality and potentially accounting for the break down in the high latitude control of tropical vegetation and climate. An increasingly seasonal climate causes fuel build-up during

wet boreal summers and increased fuel flammability during dry boreal winters, promoting drought and annual fires which ultimately maintain savannah (Daniau et al., 2013). The absence of charcoal and pollen/spores between 33.85–32.9 m supports previous suggestions that the lake dried out completely for an undetermined period of time sometime between 112 and 79 kyr. Severe lake level low stands between *c.* 135–75 kyr are also evidenced within the sediments of Lake Malawi and Lake Tanganyika (Fig. 6.1; Scholz et al., 2007).

We have shown that West African vegetation, moisture balance and fire frequency over the last 520 kyr was governed by two factors which control the WA monsoon system. Both high-latitude forcing, through fluctuations in North Atlantic SSTs, and low-latitude insolation are key factors in driving the WA monsoonal precipitation.

The palaeoenvironmental reconstructions show several significant climatic events that may have been important in the evolution and migration of early *Homo sapien* populations. Large-scale shifts in climate (*e.g.* 320–180 kyr) are thought to alter the ecological structure and increase selection pressures, leading to faunal turnover (deMenocal, 2004). The culmination of the climatic instability at *c.* 180 kyr roughly coincides with the first appearance of *Homo sapiens* in Africa at *c.* 190 kyr (McDougall et al., 2005). Climatic stability occurs both during the Holocene and during the period of extended savannah (*c.* 180–100 kyr). The stability during the Holocene is thought to have been a major factor influencing the development of society and agriculture (Feynman and Ruzmaikin, 2007; J. Rockström et al., 2009). Moreover, Holocene climatic stability may have increased the role of humans in manipulating, or even suppressing, the natural fire regime, leading to unusually low charcoal production (Fig. 7.2F). It is possible that the climatic stability we observe from *c.* 180–100 kyr may have been a key interval in hominid evolution enabling species diversification. The abrupt onset of severely arid conditions (*c.* 112–78 kyr) identified by complete lake desiccation at Lake Bosumtwi, Lake Malawi and Lake Tanganyika (Fig. 6.1; Scholz et al., 2007) demonstrate that the drought was an African-wide climatic phenomenon. In response

to the extreme drought within the African continental interior *Homo sapiens* may have developed an adaptation to living in coastal environments (Walter et al., 2000). We suggest here that the severe drought evidenced from the Lake Bosumtwi record may have driven the apparent sudden migration of *Homo sapiens* populations out of Africa (Hetherington and Reid, 2010) along the Red Sea coast and into the Levant by 100 kyr BP (Grün and Stringer, 1991).

Over the last 520 kyr savannah and woodland ecosystems in West Africa have experienced dramatic transient shifts to alternative states, modulated by both global temperature and regional precipitation fluctuations. The climate shifts evident from the Lake Bosumtwi record may have influenced early human migration and evolution. Our data help to constrain the requisite climatic changes needed to drive biome change in West Africa and provide a natural analogue to future climate change scenarios in the region.

Future human-induced temperature change via increased atmospheric greenhouse gases is likely to result in a reorganisation of vegetation biomes in West Africa; however, associated changes in precipitation (seasonality) may play a greater role in driving the vegetation biome shift, having both a social and economic impact.

## 7.3. Acknowledgments

We thank G. Izon and N. Ludgate for pertinent discussion during the drafting of this manuscript and M. Gilmour for assistance with $\delta^{15}N$ data acquisition. This research was funded by the NERC/The Open University Charter studentship (NE/H525054/1, CSM) and NERC New Investigator Award (NE/G000824/1, WDG). The data reported in this paper is archived on the PANGAEA database (www.pangaea.de).

# 8. Conclusions and further work

A fossil pollen, charcoal and bulk sediment nitrogen isotope record, spanning the last 520 kyr was determined in sediment cores extracted from Lake Bosumtwi (Ghana). The three research aims outlined in Chapter 1 have been addressed as follows:

1. Construct an atlas of modern day pollen types to be used for the identification of Quaternary and present day pollen and spores in West Africa (Section 8.1.1): Chapter 5 presents an atlas consisting of *c.* 3000 images and keys of 364 pollen and spore types commonly found in both terrestrial and marine sediments from West Africa. This atlas enabled the identification of the common fossil pollen types found within the studied Lake Bosumtwi sedimentary succession. This chapter has been published in *Review of Palynology and Palaeobotany.*

2. Characterise past interglacial vegetation communities in tropical West Africa over the last *c.* 520 kyr: In Chapter 6, fossil pollen data have been used to assess the vegetation and the compositional differences during six past periods of forest expansion in lowland tropical West Africa. This chapter has been published as a paper to *Quaternary Science Reviews.*

3. Determine the role of orbital forcing on environmental change in tropical West Africa over the last *c.* 520 kyr: In Chapter 7 variations in the nitrogen isotopic composition ($\delta^{15}N$) of bulk sediment and summary pollen data (abundance of Poaceae vs. woodland taxa, and multivariate analysis of the full pollen set) are used to characterize the major environmental changes. Comparison with previously published records allowed the Lake Bosumtwi data to be placed within a regional and global context. The wider perspective then allowed inferences to be drawn with regard to the influence of variability in the Earth's

orbital parameters on environmental change in tropical West Africa. Chapter 7 is written in the form of a manuscript to be submitted to *Science*.

This chapter summaries the key findings from this thesis (Section 8.1) and details how each specific research aim has been met. Section 8.2 explores in further detail the mechanisms controlling vegetation and hydrological change at Lake Bosumtwi as well as presenting the Lake Bosumtwi data in a regional context. Sections 8.3 and 8.4 discuss the limitations of this thesis and identify potential areas for future further work.

## 8.1. Summary of findings

### *8.1.1 Atlas of the tropical West African pollen flora*

To allow the accurate identification of fossil pollen and spores extracted from the Lake Bosumtwi sediment cores it was first necessary to construct a reference for identifying the fossil pollen of West Africa. Although substantial African pollen atlases do exist (*e.g.* Reille, 1995; Lézine, 2005), they are not specifically focused on the diverse vegetation of tropical West Africa. In Chapter 5 (Gosling et al., 2013), we contribute to the existing body of knowledge by presenting *c.* 3000 images and comprehensive identification keys for 364 modern pollen and spore taxa commonly found within tropical West Africa. The photographed pollen and spores were obtained from the reference collection housed within the Department of Biology at Duke University, collected and curated by D. Livingstone. Additionally, pollen taxa were morphologically classified and added to the Neotropical Pollen Database (Bush and Weng, 2007). The atlas and key presented in Chapter 5 allowed for the accurate identification of fossil pollen taxa within the Lake Bosumtwi record and therefore underpins all the results presented in Chapter 6 and Chapter 7. A higher success rate in the identification of highly diverse fossil pollen from the tropics allowed the reconstruction of past vegetation associations at these low latitudes over periods where climate differs from that of today. The reconstruction of vegetation from long records provides a

contribution towards understanding how tropical vegetation will respond to predicted future climate change.

### *8.1.2 Late Quaternary interglacial forest associations in lowland tropical West Africa*

In West Africa, the 3–4°C predicted regional warming by 2100 has the potential to threaten the stability of current vegetation associations (Christensen, 2007). Despite this, little is known about the resilience of the natural vegetation in West Africa to such high magnitude climate change. Consequently, understanding the resilience of tropical rainforests in the face of contemporary climate warming is critical as tropical rainforests are important due to their: (1) high ecological value (Myers et al., 2000), (2) role as a store of global carbon (Lewis et al., 2009), and (3) function within global climate systems (Nicholson et al., 1998). To improve our understanding of the possible response of tropical vegetation in the face of contemporary global warming, the fossil pollen record was examined over the last *c.* 520 kyr, spanning periods where global temperatures were significantly higher than at present.

Importantly, the last *c.* 520 kyr includes the last glacial-interglacial transition (*c.* 21–11 kyr BP) which is thought to represent a time when global temperatures rose by a comparable magnitude (*c.* 5°C; Delcourt and Delcourt, 1991; Annan and Hargreaves, 2013) to those predicted in the coming century. At the last glacial-interglacial transition, marine and terrestrial pollen records from West Africa indicate an expansion of forests during the interglacial into regions previously dominated by savannah (Maley, 1991; Elenga et al., 1994; Maley and Brenac, 1998). Marine cores from offshore West Africa indicate that this pattern of vegetation response occurred repeatedly for the latter half of the Quaternary (>670 kyr), indicating that the expansion of tropical rainforests occurred in association with globally warmer (interglacial) periods. Interpreting the composition of regional (10s–100s kms) interglacial vegetation associations from marine records is difficult, due to complications caused by large (extra-regional; 100s–

100s kms) source areas and complex pollen transport pathways (Dupont et al., 2000). Records derived from terrestrial settings source pollen more locally, allowing detailed examination of the composition of regional vegetation associations.

West African terrestrial palaeoenvironmental records span the last <*c.* 28 kyr; consequently, the last glacial-interglacial is the only example of the impact of high magnitude climate change on the environment in West Africa. The Lake Bosumtwi record allows us to test whether the environmental response seen at the last glacial-interglacial transition is repeated over multiple global climate transitions in the past.

In this study I present the first full fossil pollen data set from a long sediment core extracted from Lake Bosumtwi (Ghana). The results indicate that over the last *c.* 520 kyr the vegetation of West Africa was dominated by savannah-type taxa punctuated by six periods of forest expansion. Pollen records from marine cores offshore West Africa also display six periods of forest expansion. Parallel oxygen isotope analyses within these cores suggest that these six periods of forest expansion correspond to the last six interglacial periods; Marine Isotope Stages (MIS) 13, 11, 9, 7, 5e and 1 (Holocene). Additional evidence from independent age estimates from the Lake Bosumtwi core 5B indicate that the six periods of forest expansion are again, most likely equivalent to MIS 13, MIS 11, MIS 9, MIS 7, MIS 5e and the Holocene. The characterisation of the fossil pollen identified within each of the Lake Bosumtwi forest zones enabled the comparison with modern day ecoregions (Olson et al., 2011), to: (1) assess the variability within tropical West African forest vegetation associations, and (2) provide an indication of probable palaeoclimate conditions (*e.g.* precipitation and temperature).

Detrended correspondence analysis (DCA) of sample scores enabled a comparison of the vegetation composition within each forest zone (Fig. 6.5b). The DCA analysis indicates that forest zone 1 (Holocene) is unlike any other forest zone identified during the last *c.* 520 kyr. The Holocene forest association is characterised by higher abundances of taxa such as *Alchornea* and Moraceae which suggest a relatively wetter

environment prevailed in West Africa during the last *c.* 11 kyr. Forest zone 3 (MIS 7) is also distinct from other identified forest zones, containing higher abundances of Poaceae and Cyperaceae. The MIS 7 forest vegetation association is interpreted as having a more open canopy relative to other forest zones which suggests that during this period climate in West Africa was dry. Forest zone 2 (MIS 5e) contains taxa from a range of modern day ecoregions, with both savannah and forest taxa indicating that MIS 5e was a period when the climate was highly variable. Forest zones 6, 5 and 4 (MIS 13, MIS 11 and MIS 9) have a similar pollen assemblage composition with no climatic extremes when compared to MIS 7, 5e and 1.

The pollen data presented (Chapter 6) suggests that that prior to *c.* 11 kyr the climate of West Africa was much drier than observed at present. Future projections indicate a <9 % decrease in West African precipitation (Christensen, 2007). Data from 73 % of multi-models, predict an increase in the dry season water deficit in western equatorial Africa, which will be amplified as global temperatures increase (James et al., 2013). This drying is hypothesised to be related to a northward displacement of the ITCZ (James et al., 2013). Conversely, in the Congo Basin, atmosphere-only general circulation model simulations predict no future change in the risk of low precipitation (Otto et al., 2013). Presently, the African equatorial rainforests are close to the hydrological limit to maintain closed canopy forest (Lewis et al., 2009). The projected drying itself may result in the forests becoming more open and more fire prone, although interactions with future increased temperatures and higher atmospheric $CO_2$ concentrations ultimately makes it difficult to predict the resilience of the rainforests. Future reductions in precipitation may cause vegetation assemblages to trend toward that reconstructed at Lake Bosumtwi during MIS 7; advocating MIS 7 as a possible analogue for future forest associations in West Africa.

### *8.1.3 Vegetation and climate change in tropical West Africa over the last c. 520,000 years*

Vegetation response to the 100 kyr eccentricity cycle is well established at both mid and high latitudes (*e.g.* Tzedakis et al., 1997); however at low-latitudes, the pattern of response is more complex, with both precession (*c.* 21 kyr) and eccentricity (*c.* 400 and 100 kyr) cycles likely to exert influence on vegetation composition (Pokras and Mix, 1987; Clement et al., 2004; Scholz et al., 2007).

Pollen and nitrogen isotope ($\delta^{15}N$) ratios from bulk sediment were determined from sediment cores extracted from Lake Bosumtwi, to reconstruct both vegetation and lake level change over the last *c.* 520 kyr. Spectral analysis was then used to detect any cyclic component and infer any underlying orbital control on the vegetation and lake level change.

Variations in grass pollen abundance (0–99 %) document eleven major biome shifts oscillating between savannah and woodland over the last *c.* 520 kyr. Variations in $\delta^{15}N$ of bulk sediment (+2 to +14‰) suggest the highest lake levels coincided with the intervals of forest expansion.

The temporal pattern of biome and lake level change suggest that these oscillations occur in phase with *c.* 100 kyr glacial-interglacial cycles, although the strength of the 100 kyr signal varies throughout the record. Spectral analysis of the Poaceae pollen (savannah taxon) and $\delta^{15}N$ data support this interpretation and reveal evidence in both proxy records for enhanced variance at a frequency of *c.* 100 kyr. The influence of the high-latitude 100 kyr glacial-interglacial cycle on low latitude vegetation was most likely through fluctuations in Atlantic sea surface temperatures (SST), exerting control on the strength of the West African Monsoon.

From 320–130 kyr BP the vegetation around Lake Bosumtwi was unstable, abruptly fluctuating from periods of savannah to rainforest. Additionally, throughout this interval,

the Lake Bosumtwi lake level is stable but low. These results suggest a de-coupling between the 100 kyr high-latitude forcing and tropical vegetation from *c.* 320–130 kyr BP, inferred to have been the product of strengthened orbital precession, enhancing seasonality, promoting drought and maintaining savannah.

The new data also suggest a period of climate stability from *c.* 180–100 kyr. This interval is co-incident with the first appearance of *Homo Sapiens* in Africa at *c.* 190 kyr. The climatic stability may have promoted favourable conditions for the evolution and migration of hominid populations.

## 8.2 Mechanisms for West African vegetation and lake level change

The new pollen and geochemical records presented in Chapter 7 suggest that overall biome shifts and lake level fluctuations correspond with the 100 kyr component of orbital eccentricity (Section 8.1.3). In this section the relationship between orbital forcing and environmental change in West Africa is explored in greater detail, permitting the new findings (Chapter 7) to be put within a wider context and allowing the role of high-latitude forcing as a mediator of the strength of the West African Monsoon to be investigated. The locations of sites discussed are shown in Fig. 8.1.

### *8.2.1 Orbital eccentricity: 100 and 400-kyr components*

Between 520–320 kyr and 130–0 kyr the vegetation assemblage and inferred lake level change at Lake Bosumtwi show strong 100 kyr cyclicity (Fig. 8.2A, G, H).

Numerous other African palaeoclimate records indicate dry conditions during glacial maxima; such as an increase in wind-blown dust at ODP 658 (Fig. 8.1F; Tiedemann et al., 1989) and an increase in the abundance of savannah pollen components in marine cores *e.g.* GIK16856 and GIK16776 (Fig. 8.1E and Fig. 8.1F; Dupont and Weinelt, 1996; Jahns et al., 1998). High and low latitude climates are coupled with fluctuations in Atlantic SSTs; higher Atlantic SSTs cause increased evaporation and thus increase

the moisture available for fuelling the West African Monsoon (Camberlin et al., 2001; Nicholson and Grist, 2001). Cold SST (*i.e* Heinrich Events), limit evaporation, ultimately weakening the West African Monsoon, resulting in drought at Lake Bosumtwi (Peck et al., 2004; Shanahan et al., 2009).

For the majority of the Lake Bosumtwi record (*c.* 520–320 and 130–0 kyr BP) the vegetation and hydrological changes observed correlate with the 100 kyr component of the eccentricity cycle (Fig. 8.2). The fossil pollen assemblages from MIS 13, 11, 5e and 1 are comparable to taxa typifying the modern day Tropical and Subtropical Moist Broadleaf Forest biome (Fig. 2.3). Nitrogen isotope ratios also reveal high lake levels in West Africa during MIS 13, 11, 5e and 1 (Fig. 8.2).

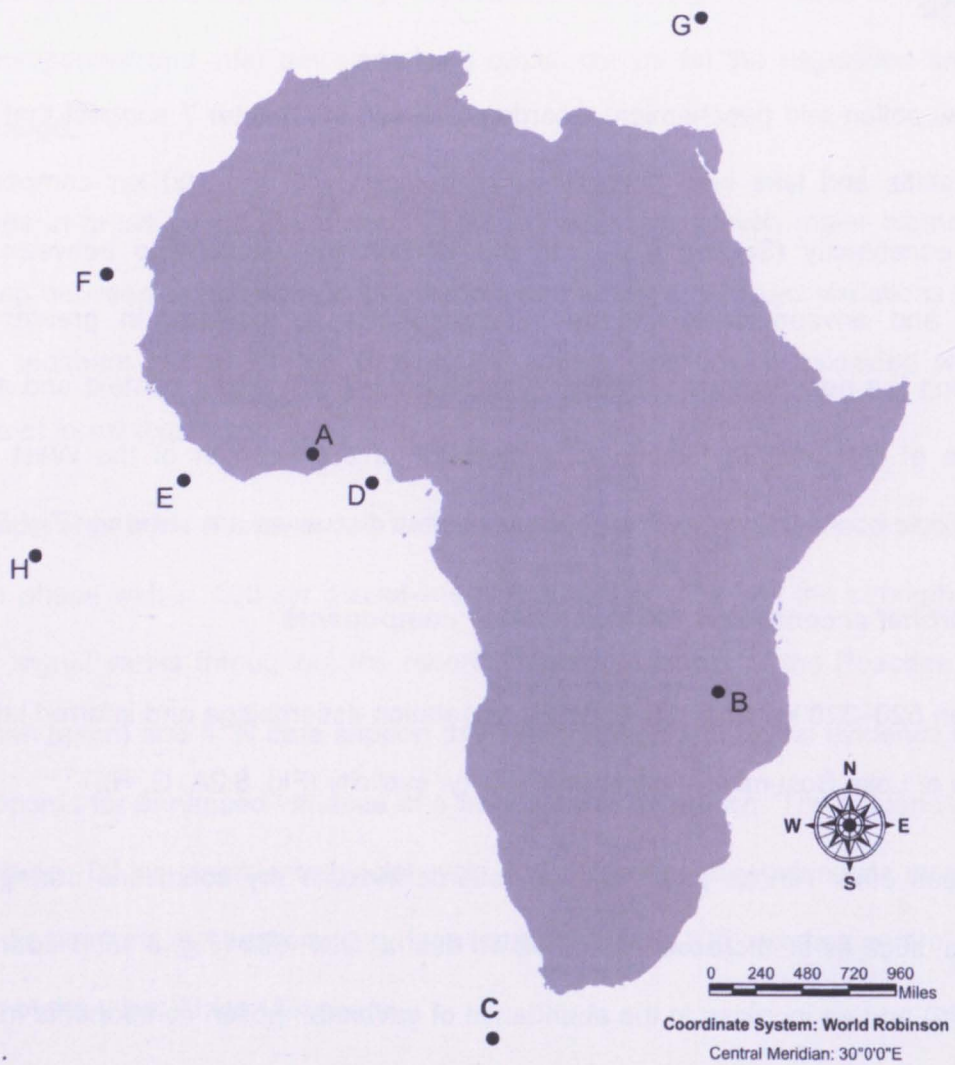


**Fig. 8.1.** Location map of cores pertinent to this discussion. **A).** Lake Bosumtwi (this study). **B).** Lake Malawi (Scholz et al., 2007). **C).** ODP 1089 (Cortese et al., 2007). **D).** GIK16856 (Dupont and Weinelt, 1996). **E).** GIK16776 (Jahns et al., 1998). **F).** ODP 658 (Sarnthein and Tiedemann, 1989). **G).** ODP 967 (Larrasoaña et al., 2003). **H).** Core V30-40 (Pokras and Mix, 1987).

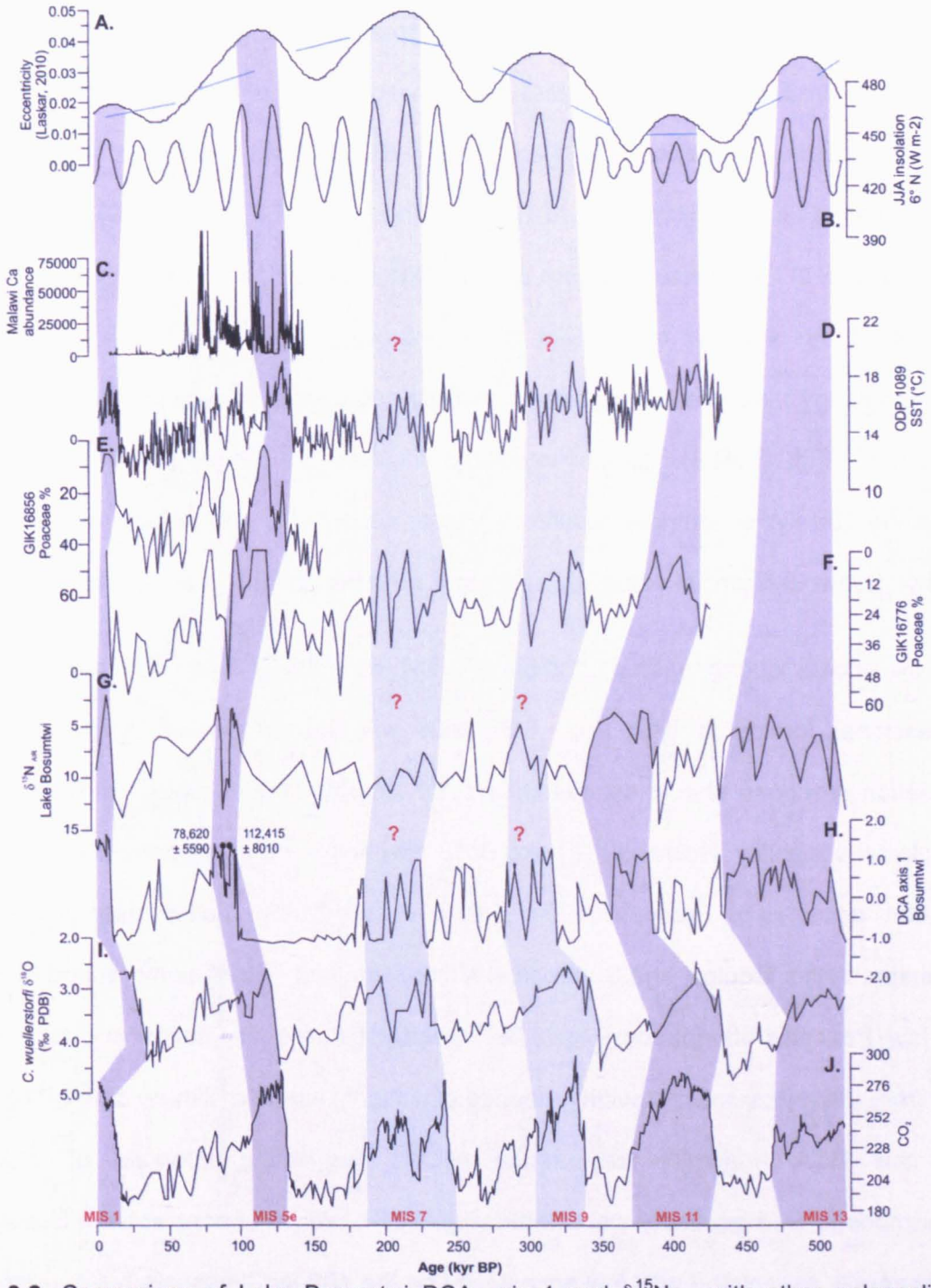


**Fig. 8.2.** Comparison of Lake Bosumtwi DCA axis 1 and $\delta^{15}N_{AIR}$ with other palaeoclimate records. **A).** 100 kyr eccentricity solution (the blue dashed line is the 400 kyr component of eccentricity; Laskar et al., 2010). **B).** Summer insolation at 6°N (Paillard et al., 1996). **C).** Lake Malawi Ca abundance, indicating intervals of calcium carbonate precipitation, which occurs during severe lake lowstands and periods of high salinity (Scholz et al., 2007). **D).** Radiolarian derived SST estimates from Site 1089, ODP Leg 177 (Cortese et al., 2007). **E).** Poaceae abundance from core GIK16856 (Dupont and Weinelt, 1996). **F).** Poaceae abundance from core GIK 16776 (Jahns et al., 1998). **G).** $\delta^{15}N_{AIR}$ from Lake Bosumtwi (this study). **H).** Pollen DCA axis 1 from Lake Bosumtwi (this study). **I).** $\delta^{18}O_{SW}$ from ODP 658, representing the ice volume/sea level component of benthic foraminifera $\delta^{18}O$ (Sarnthein and Tiedemann, 1989). **J).** Composite $CO_2$ record from Vostok and EPICA Dome C ice cores (Petit et al., 1999; Monin et al., 2001; Siegenthaler et al., 2005; Luthi et al., 2008). Dark grey bars indicate warm marine isotope stages in each record. Light grey bars indicate less prominent warm marine isotope stages. Black circles are optically stimulated luminescence dates taken from core BOS04-5B (Shanahan et al., 2013).

The pattern of vegetation and lake level response to 100 kyr glacial-interglacial variability from 320–130 kyr BP is less pronounced in the Lake Bosumtwi record (Fig. 8.2). This pattern of response is also seen in SST records from Site 1089, where glacial-interglacial variability appears muted during MIS 9 and 7 (Fig. 8.2D). Vegetation and lake level at Lake Bosumtwi from 320–130 kyr show a close correspondence to the maxima of the 400 kyr component of eccentricity, with high 400 kyr eccentricity corresponding to increased vegetation instability and low lake levels at Lake Bosumtwi (Fig. 8.3A; Fig, 8.3H–I). As eccentricity modulates the amplitude of precession, increased 400 kyr eccentricity results in greater seasonality and reduced influence of 100 kyr glacial-interglacial variability at tropical latitudes (Scholz et al., 2007).

MIS 5e occurs during a time of high 400 kyr eccentricity when the amplitude of precessional forcing is high (Fig. 8.3), thus with the presented hypothesis, the vegetation response should be muted and not strongly coupled with 100 kyr glacial-interglacial variability. However, at Lake Bosumtwi and in nearby marine cores, off the Guinean coast (*e.g.* Frédoux, 1994; Jahns et al., 1998), pollen data reveal an expansion in the Tropical and Subtropical Moist Broadleaf Forest biome during MIS 5e (*i.e.* low Poaceae abundance; Fig. 8.3). Nevertheless the vegetation and lake level data from Lake Bosumtwi provide evidence of a highly variable climate during MIS 5e, with the DCA ordination of sample scores suggesting intervals of drought superimposed on a generally wet climate (Fig. 6.5B). Wet conditions at Lake Bosumtwi are generally associated with low eccentricity on the 400-kyr timescale but correspond to high eccentricity on the 100 kyr timescale (Fig. 8.3). The following section will discuss how the West African Monsoon is controlled by changes in orbital eccentricity.

### *8.2.2 The 100 kyr component of eccentricity and the West African Monsoon*

Annual precipitation at Lake Bosumtwi today has a bimodal distribution with maximum precipitation during the early summer and the autumn, associated with the annual migration of the ITCZ and the tropical rainbelt (Fig. 8.4; Fig. 8.5).

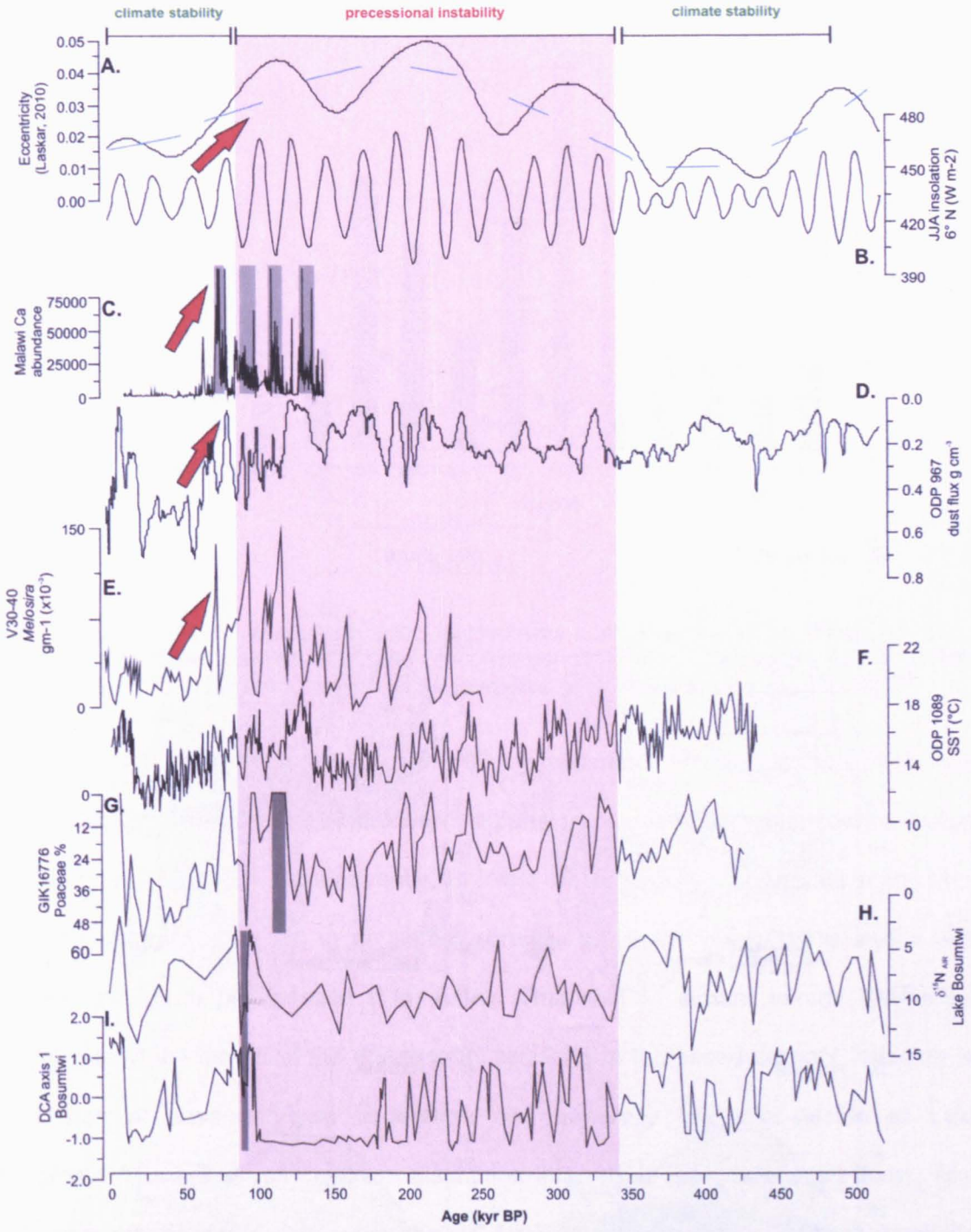


**Fig. 8.3.** Comparison of Lake Bosumtwi DCA axis 1 and $\delta^{15}N_{AIR}$ of bulk sediment with other palaeoclimate records and their relationship with eccentricity maxima (higher amplitude precessional variability). **A).** 100 kyr eccentricity solution (the blue dashed line is the 400 kyr component of eccentricity; Laskar et al., 2010). **B).** Summer insolation at 6°N (Paillard et al., 1996). Red arrow indicates increased amplitude of the precessional signal. **C).** Lake Malawi Ca abundance. Red arrow indicates increased abundance of intervals of calcium carbonate precipitation, which occurs during severe lake lowstands and periods of high salinity (Scholz et al., 2007). **D).** Down-core variations of aeolian dust from site ODP 967 (Larrasoaña et al., 2003; Trauth et al., 2009). Red arrow indicates decreased aridity. **E).** Abundances of *Melosira* sp. per gram ($x10^{-5}$) in core V30-40 (Pokras and Mix, 1987). Red arrow indicates drying of the African continental interior. **F).** Radiolarian derived SST estimate from Site 1089, ODP Leg 177 (Cortese et al., 2007). **G).** Poaceae % from core GIK 16776 (Jahns et al., 1998). **H).** $\delta^{15}N_{AIR}$ from Lake Bosumtwi (this study). **I).** Pollen DCA axis 1 from Lake Bosumtwi (this study). Pink box indicates the period of precessional instability (high 400 kyr eccentricity). Dark grey bars indicate barren intervals (or low lake level interpreted from $\delta^{15}N_{AIR}$).

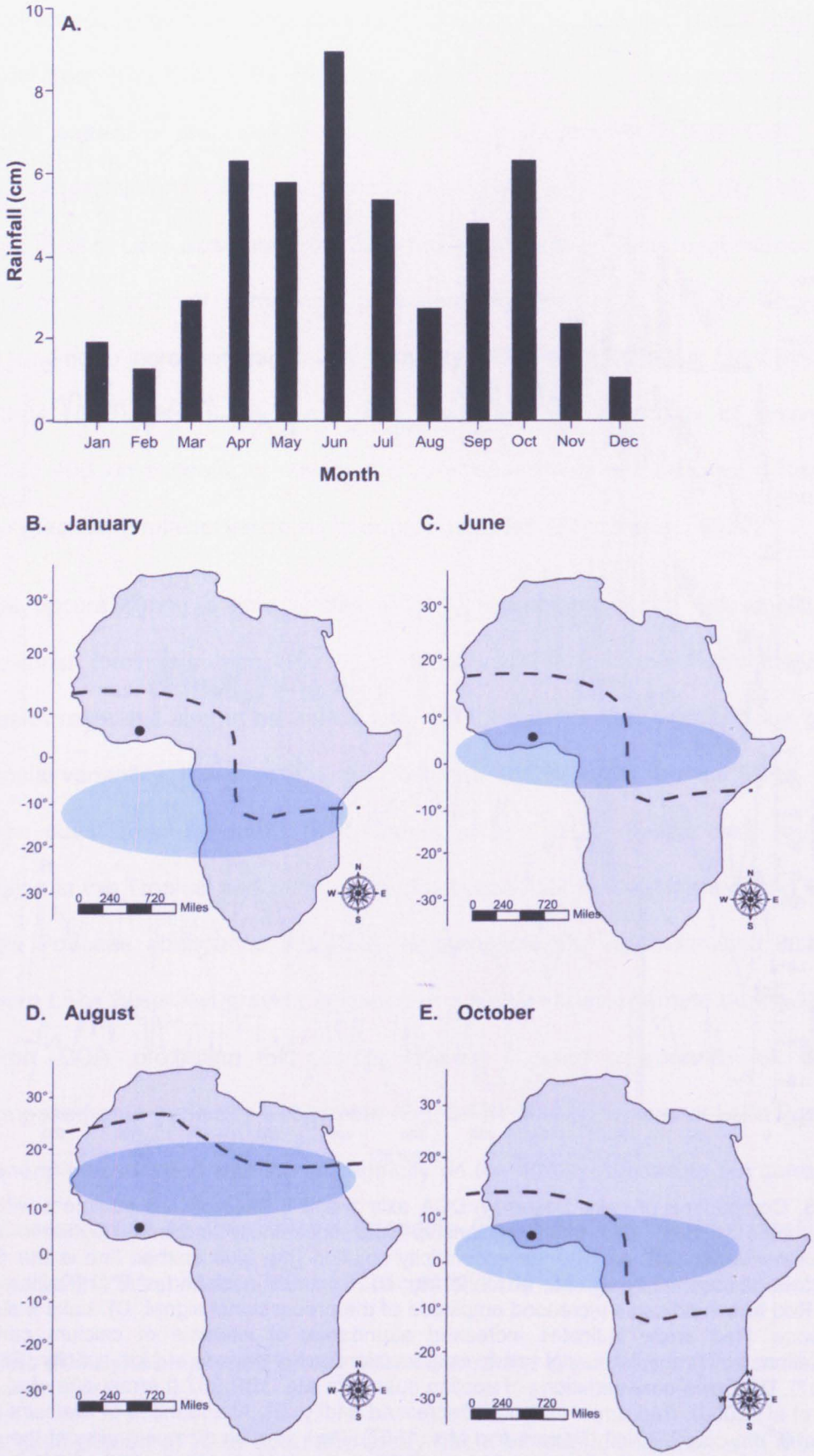


**Fig. 8.4. A).** Average annual precipitation data from Kumasi (35 km NE of Lake Bosumtwi) from 1945–2000. Figure adapted from (Shanahan et al., 2006). Position of the ITCZ and tropical rainbelt (blue shading) in January **(B)**, June **(C)**, August **(D)** and October **(E).** Black circle is Lake Bosumtwi.

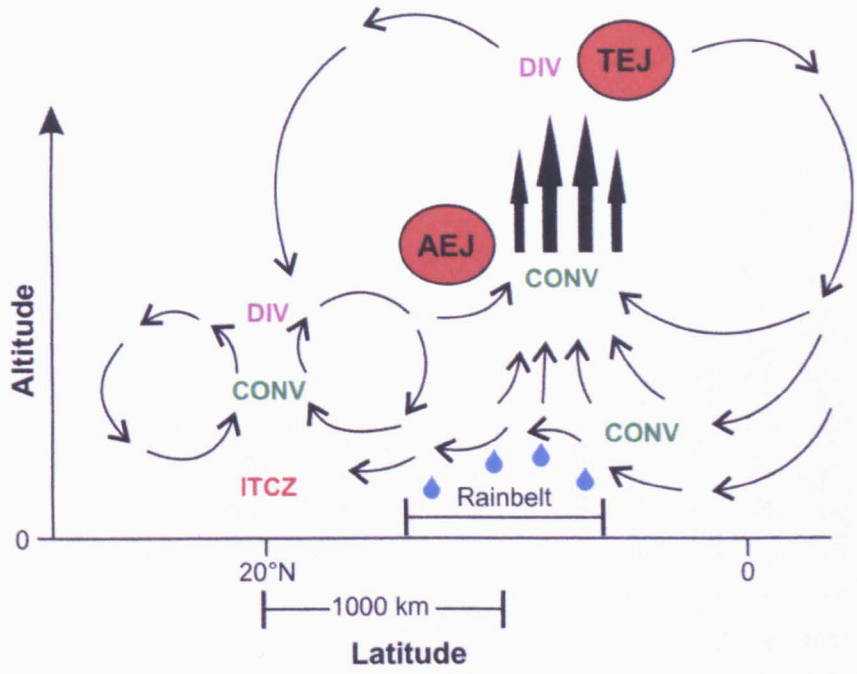


**Fig. 8.5.** Schematic representation of the mechanisms controlling the West African Monsoon, adapted from Nicholson (2009). CONV = convergence. DIV = divergence. AEJ = African Easterly Jet. TEG = Tropical Easterly Jet. Note tropical rainbelt is 1000 km south of ITCZ.

During the last interglacial period, high 100 kyr eccentricity forcing is thought to have caused an intensification and northward expansion of the African monsoonal system (Nikolova et al., 2012). Consequently, in West Africa, the monsoon was most likely shifted northward, resulting in an earlier summer maximum precipitation and a later autumn maximum precipitation (Fig. 8.6A). This shift in annual rainfall distribution would extend the length of the dry season, resulting in increased drought, causing an expansion of savannah-type vegetation and generally low lake levels at Lake Bosumtwi. The annual precipitation distibution inferred at Lake Bosumtwi during high 100 kyr eccentricity (Fig. 8.6), when the ITCZ was displaced northward, appears similar to the average precipitation measurements today from meterological stations to the south, with a single rainy season and a long dry season (Fig. 8.7). High 100 kyr eccentricity forcing (during 400 kyr eccentricity maxmia), northward expansion of the African monsoon resulting in an extended dry season provides a mechanism for the drought intervals at Lake Bosumtwi during MIS 5e and dry unstable conditions from 320–130 kyr BP (Fig. 8.3). Nevertheless, it is unclear why extreme drought (and lake desiccation) is only evidenced during MIS 5e.

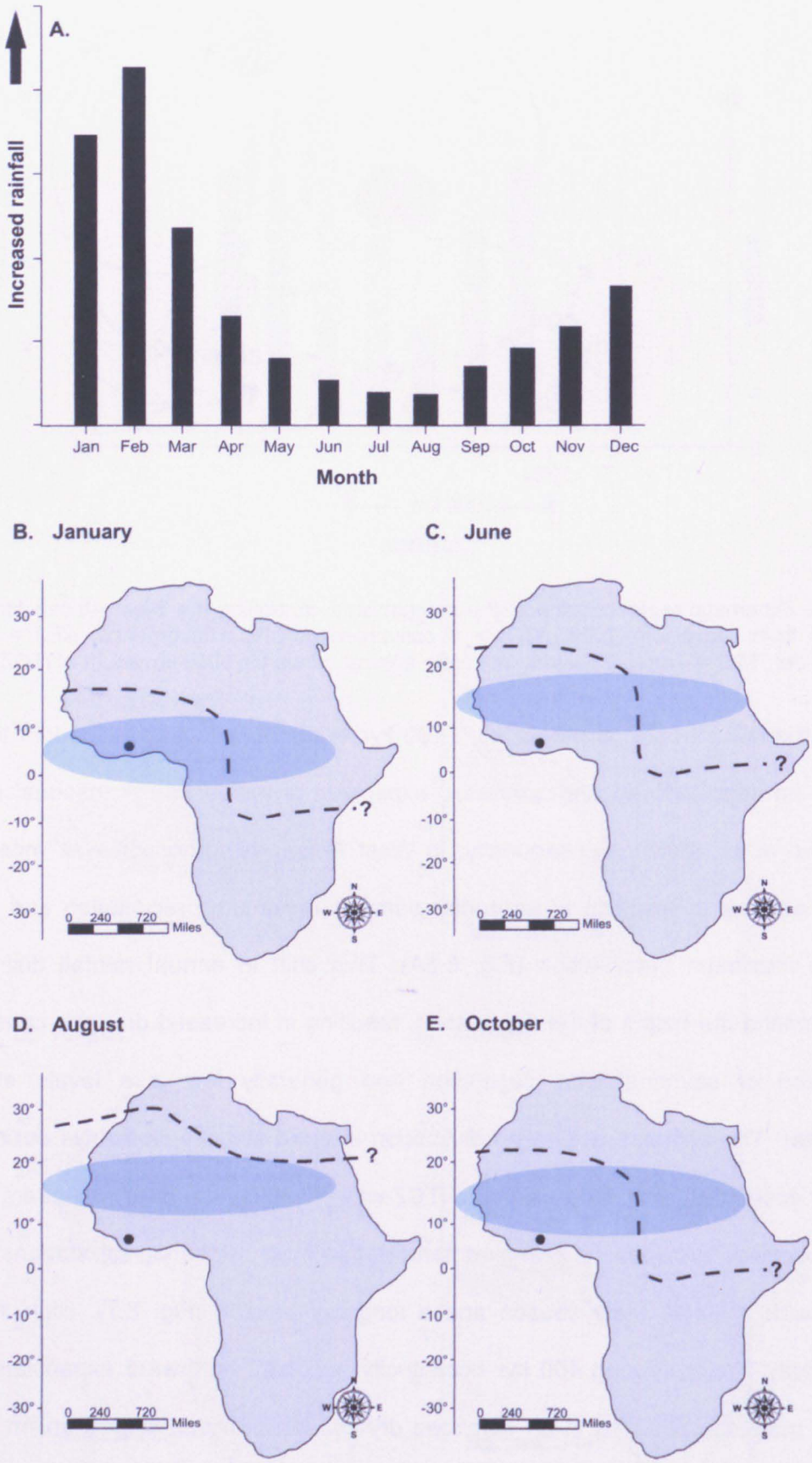


**Fig. 8.6. A).** Inferred annual precipitation distribution in West Africa during eccentricity maxima. The increase in the length of the dry season is a result of northward migration of the ITCZ and the associated shift in the tropical rainbelt. Position of the inferred ITCZ and tropical rainbelt (blue shading) during times of eccentricity maxima in January **(B)**, June **(C)**, August **(D)** and October **(E)**. Black circle is the location of Lake Bosumtwi.

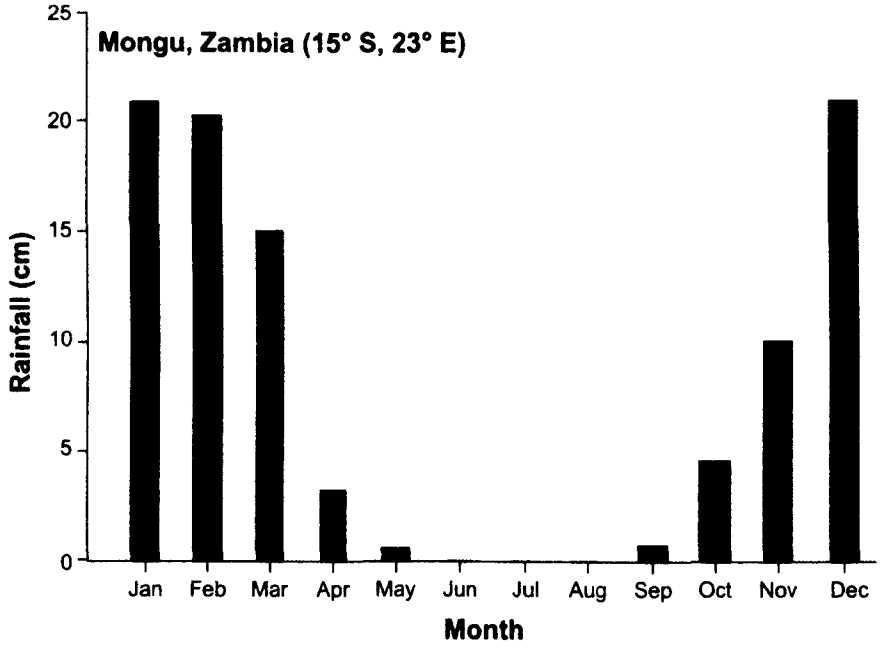


**Fig. 8.7.** Average annual precipitation data from Mongu (Zambia; *c.* 6000 km SE of Lake Bosumtwi), showing one wet season and a long dry season. Data from: www.weather-and-climate.com.

These dry conditions evidenced at Lake Bosumtwi from 320–130 kyr BP seem to occur at both insolation minima and maxima (Fig. 8.3). Other studies suggest high lake levels across North Africa coincide with maximum insolation (Street-Perrott and Grove, 1976; Kutzbach and Street-Perrott, 1985; Street-Perrott and Perrott, 1993; Gasse, 2000). Geomorphological lake level reconstructions from Lake Bosumtwi indicate that the deepest lake conditions, since the Last Glacial Maximum, occurred between 11–8.8 kyr BP, when Lake Bosumtwi overflowed, coinciding with summer insolation maxima *c.* 10 kyr BP (Shanahan et al., 2006). An explanation for generally dry conditions during the whole precessional cycle, during high 400 kyr eccentricity, may be due to an increase in the amplitude of the seasonal cycle. Tropical forests are presently found in areas which have little seasonal variation with rainfall spread throughout the year, whilst savannah vegetation dominates in regions which experience lower yearly rainfall and longer dry seasons (Forseth, 2012). An increase in seasonality could explain the expansion of savannah vegetation, climate instability, generally low lake levels and a weakening of the strength of 100 kyr glacial-interglacial cyclicity evidenced at Lake Bosumtwi from 320–130 kyr BP, during high 400 kyr eccentricity.

### *8.2.3 Other proxy evidence for climatic instability at 400-kyr eccentricity maxima*

Enhanced climatic variability and a weaker 100 kyr component of eccentricity during periods of high 400 kyr eccentricity is seen in other African records (Fig. 8.2; Fig. 8.3). Sediment cores extracted from Lake Malawi (East Africa; Fig. 8.1B) provide evidence for increased climatic instability relating to high precessional forcing from 135–75 kyr BP (Fig. 8.3C; Scholz et al., 2007). High Ca abundance, related to low lake level and high salinity coincides with enhanced precessional-scale variability (Fig. 8.3C). Additionally, peaks in Ca abundance also occur during times of insolation minima, when the length of the dry season was extended (Fig. 8.3C). Increased abundance (and variability) of the freshwater diatom *Melosira* sp. in core V30-40, offshore equatorial Africa (Fig. 8.1), indicates increased aolian transport from tropical Africa due to increased desertification prior to *c.* 75 kyr BP, again coinciding with the increased amplitude of precession (Fig. 8.3E). A sub-millennial resolution radiolarian based SST record from core ODP 1089 (off SW Africa) shows rapid SST fluctuations during both glacial and interglacial intervals, with the SST response to warming during MIS 9 and MIS 7 less pronounced than during MIS 5e and MIS 1 (Fig. 8.3F). Nevertheless, according to the presented hypothesis, MIS 11, which occurs during an interval of climatic stability (low 400 kyr eccentricity), should be well represented as a period of interglacial warmth in core ODP 1089, however this is not the case. Site ODP 1089, as well as other SST records off SW Africa (*e.g.* TN057-6; Hodell et al., 2000) show intermediate and stable SST during MIS 11 (Fig. 8.3F). A possible explanation for the lack of temperature response in these offshore SW African records during MIS 11 is oceanic cooling as a result of increased North Atlantic Deep Water Formation (*e.g.* Crowley, 1992; Manabe and Stouffer, 1997).

Vegetation and lake level data from Lake Bosumtwi suggest that during 400 kyr eccentricity maxima the African monsoon may migrate northwards, increasing the length of the dry season in West Africa (Section 8.2.2). If the monsoon does migrate northwards during intervals of high 400 kyr eccentricity, then palaeorecords from North

Africa should show a strengthening of the North African monsoon, during these intervals of 400-kyr eccentricity maxima. High-resolution variations of Saharan dust deposition in the eastern Mediterraean Sea, from core ODP 967, indicate low dust production during both 100 kyr and 400 kyr eccentricity maxima. During periods of eccentricity maxima (highest amplitude of insolation maxima), the greening of the Sahara may have lead to a decrease in dust flux over the Eastern Mediterranean Sea (J. Larrasoaña, pers. com; Trauth et al., 2009), related to an enhanced northward penetration of the African summer monsoon, providing support to the presented hypothesis (Fig. 8.3D; Larrasoaña et al., 2003).

## 8.3 Limitations

The African pollen atlas (Chapter 5) aided the identification of the common taxa recovered from within the Lake Bosumtwi sediments, nevertheless, in hyper-diverse samples 311 rare taxa remain unidentified (Appendix 4b). Pollen from herbariums or collected directly from the modern vegetation surrounding Lake Bosumtwi may further improve our ability to identify some of these rare taxa.

Understanding the relationship between the modern pollen 'rain' and vegetation in West Africa is crucial in interpreting the fossil pollen record. To help further our understanding of how different vegetation types are represented in the fossil pollen record, W. Gosling and I set up pollen traps in 2011 within a range of vegetation study plots, belonging to the Forestry Research Institute of Ghana. These pollen traps will be replaced annually and are the focus of a PhD studentship at The Open University beginning in October 2013.

The main limitation of the research presented was the lack of a robust independent chronology derived solely from Lake Bosumtwi core 5B. Future planned improvements in chronology are inevitable and further discussed in Section 8.4.5

## 8.4 Further work

The research presented in this thesis raises a number of new research questions. These are introduced in Sections 8.4.1–8.4.5.

### *8.4.1 Expanding the record back to c. 1 myr*

A key finding from this thesis is the probable break-down in the link between high-latitude forcing and tropical vegetation (and lake level) response during times of high 400 kyr eccentricity (increased amplitude precessional forcing; *e.g* c. 320–130 kyr BP; Fig. 8.3). The increase in the strength of orbital precession, enhances seasonality, promoting drought, leading to millennial scale vegetation fluctuations, which are on timescales that are important for life. Further investigation of the coupled vegetation and nitrogen isotope record over multiple periods of high amplitude precession (Fig. 8.8) would indicate whether a similar relationship between vegetation response and orbital parameters is observed from 1000–520 kyr BP thus allowing this hypothesis to be refuted or supported.

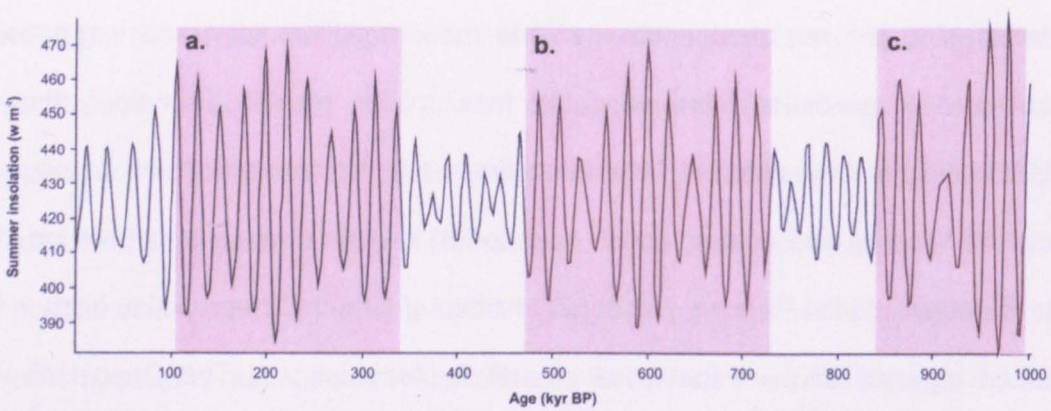


**Fig. 8.8.** Summer insolation at 6°N (Paillard et al., 1996). Red shading indicates periods of high amplitude insolation (eccentricity maxima). **A)** *c.* 320–130 kyr BP. **B)** *c.* 730–475 kyr BP. **C)** *c.* 1000–840 kyr BP.

### *8.4.2 Establishing an independent chronology*

The results of this study indicate that both vegetation and lake level respond to the Earth's orbital cyclicity. Increasing the sampling resolution for both pollen and nitrogen

isotopes (<1,500 years) would allow the application of refined cyclostratigraphic methodologies. The recognition of orbital signals in high resolution nitrogen isotope data may allow us to directly tie our data to well constrained records over the same time period (*e.g.* ice core climate data from EPICA and Vostok (Petit et al., 1999; Monnin et al., 2001; Siegenthaler et al., 2005; Luthi et al., 2008), and orbital insolation solutions (Paillard, 1996). A high resolution chronology for the whole 1 million year Lake Bosumtwi record would allow us to establish the precise timing of vegetation changes associated with global climate change, as well as to further tie the Lake Bosumtwi vegetation record to other proxy records from nearby marine sites offshore West Africa (*e.g.* SST; Weldeab et al., 2007).

### *8.4.3 A high resolution vegetation record*

A higher resolution vegetation record (<1,500 years) would allow us to further investigate the transitions into and out of forest zones (interglacial periods) allowing the sequence of vegetation change to be observed and potentially calculate rates of change. Determining how vegetation has changed and the rate of which it has responded to changing global climate conditions may give us an indication of the likely nature and speed of the response of West African tropical vegetation in the face of future climate change. Additionally, high resolution sampling of both pollen and nitrogen isotopes would reveal further information on the details of the relationship between increased West African moisture availability and summer insolation maxima.

### *8.4.4 Investigation of the MIS 5e 'mega-drought'*

Better chronological constraints of the Lake Bosumtwi sediment core, would allow us to identify the exact timing of the African-wide 'megadroughts' (*e.g.* Scholz et al., 2007). These droughts are manifest as unconformities within the sedimentary record and are reported to occur at *c.* 74.2 kyr BP at Lake Malawi, *c.* 97.3 kyr BP at Lake Tanganyika and *c.* 77.9 kyr BP at Lake Bosumtwi (Scholz et al., 2007). The Lake Bosumtwi age vs. depth model used in this thesis (Fig. 4.3) indicates the drought at Lake Bosumtwi

occurred in the middle of our interpreted MIS 5e. The drought interval within the Lake Bosumtwi sedimentary succession contains low concentrations of both pollen and charcoal, possibly due to the oxidation of organic materials, as well as an increase in the $\delta^{15}N$ composition of organic matter, inferred to represent low lake levels, and a loss of palynomorphs within the sediment.

Interestingly, nearby marine cores offshore West Africa (GIK16867 and GIK16776; Fig. 2.3) also have this pollen-barren interval during MIS 5e (Dupont and Agwu, 1992; Jahns et al., 1998). High resolution pollen analysis of the annual laminations immediately prior and post the 'mega-drought' would provide an indication of the response of tropical vegetation to a drying climate and assess how vegetation recovers after a period of severe climatic deterioration.

The position of the 'mega-drought' within MIS 5e is interesting. Although high solar insolation plus an extended dry season provides a mechanism for the complete desiccation at Lake Bosumtwi during MIS 5e, previous studies indicate a strengthening of monsoonal rainfall due to insolation maxima at the peak of MIS 5e (Branonnot et al., 2008). High insolation during MIS 5e made a significant contribution to the melting of the Greenland Ice Sheet (van de Berg et al., 2011). Studies have shown that the Atlantic Meridional Overturning Circulation (AMOC) is likely to slow down in response to freshening due to the melting of the Greenland Ice Sheet (Weijer et al., 2012). A potential decrease in AMOC during the peak of MIS 5e may be responsible for drought at Lake Bosumtwi. Additionally, millennial-scale drought events during the last 25 kyr BP evidenced in the sediment cores from Lake Bosumtwi have previously been related to periods of reduced AMOC (Shanahan et al., 2006). Conversely, these recent droughts were associated with reduced SST (Vizy and Cook, 2002), which is unlikely during MIS 5e, with $U^{K}_{37}$ SST reconstructions from site ODP 658 (Fig. 8.2i) indicating SST were *c.* 24°C, at least *c.* 3°C warmer than peak Holocene temperatures (Maslin et al., 1996). This thesis highlights the need for both tighter chronological constraint and further research into the causes of the African 'megadroughts'.

### *8.4.5 Future improvements in Lake Bosumtwi chronology*

The Lake Bosumtwi research team have been working on the chronology for core 5B since 2004 (Overpeck et al., in prep). All data in this thesis have been plotted against depth as well as an age generated from our simple age vs. depth model (Fig. 4.3). Both pollen and nitrogen isotope data are tabulated against depth (as well as core, section, depth) in Appendix 5. Improvements in chronology will allow us to re-plot our data against a refined age model, and allow comparison of the vegetation and nitrogen isotope data with other proxy data emerging from members of the Lake Bosumtwi research team. Nevertheless, a comparison of the Lake Bosumtwi vegetation and lake level data with vegetation records from nearby marine cores has enabled the identification of glacial-interglacial cycles. Improvements in chronology are unlikely to drastically alter the placement of the identified MISes within the Lake Bosumtwi record.

## 8.5 Summary

As well as constructing a pollen atlas to aid in the identification of fossil pollen (research aim 1), the vegetation history of tropical West Africa over the last *c.* 520 kyr has been reconstructed (research aim 2). Additionally, the West African vegetation composition of the last six interglacial periods have been compared and contrasted (research aim 2). By investigating the temporal pattern of vegetation and lake level change, the role of orbital forcing in driving changes at Lake Bosumtwi has been established (research aim 3). Future improvements of the Lake Bosumtwi chronology, as well as investigating vegetation and lake level change in the early part of the Lake Bosumtwi core (1000–520 kyr BP) will allow the newly presented hypotheses to be tested. Additionally, comparison of reconstructed vegetation at Lake Bosumtwi with newly emerging ICDP vegetation data from long sediment cores from Lake Malawi (Fig. 8.1; S. Ivory, pers. com) will allow the reconstruction of both the West and East African monsoonal systems over periods of past global climate warmth, ultimately

providing information on the future of both these monsoonal systems in the face of contemporary climate warming.

# 9. References

Altabet, M.A., Francois, R., 1994. The use of nitrogen isotopic ratio for reconstruction of past changes in surface ocean nutrient ulilization, In: Zahn, R. (Ed.), Carbon cycling in the glacial ocean: constraints on the ocean's role in global change. Springer-Verlag, Berlin, pp. 281–306.

Anderson, D.M., Overpeck, J.T., Gupta, A.K., 2002. Increase in the Asian SW Monsoon during the past centuries. Science 297, 596.

Annan, J.D., Hargreaves, J.C., 2013. A new global reconstruction of temperature changes at the Last Glacial Maximum. Climate of the Past 9, 367–376.

Ayalon, A., Bar-Matthews, M., Kaufman, A., 2002. Climatic conditions during marine oxygen isotope stage 6 in the eastern Mediterranean region from the isotopic composition of speleothems of Soreq Cave, Israel. Geology 30, 303–306.

Baker, P.A., Rigsby, C.A., Seltzer, G.O., Fritz, S.C., Lowenstein, T.K., Bacher, N.P., Veliz, C., 2001. Tropical climate changes at millennial and orbital timescales on the Bolivian Altiplano. Nature 409, 698–701.

Balter, M., 2002. What Made Humans Modern? Science 295, 1219–1225.

Bender, M.L., 2002. Orbital tuning chronology for the Vostok climate record supported by trapped gas composition. Earth and Planetary Science Letters 204, 275–289.

Bengo, M., Maley, J., 1991. Analyses des flux pollinitiques sur la marge sud du Golfe de Guinée depuis 135000 ans. Comptes Rendus de l'Académie des Sciences 313, 843–849.

Bennett, K.D., 2003. Documentation for psimpoll 4.10 and pscomb 1.03: C programs for plotting pollen diagrams and analysing pollen data. Quaternary Geology, University of Uppsala.

Berger, A., 1978. Long-term variations of daily insolation and Quaternary climatic change. Journal of Atmospheric Science 35, 2362–2367.

Bernasconi, S.M., Barbieri, A., 1997. Carbon and nitrogen isotope variations in sedimenting organic matter in Lake Lugano.

Beug, H.G., 2004. Leitfaden der Pollenbestimmung für Mitteleuropa und angrenzende Gebiete. Verlag Dr, Friedrich Pfeil.

Beuning, K.R.M., Talbot, M.R., Livingstone, D.A., Schmukler, G., 2003. Sensitivity of carbon isotopic proxies to paleoclimatic forcing: A case study from Lake Bosumtwi, Ghana, over the last 32,000 years. Global Biogeochemical Cycles 17, 32–31.

Bonnefille, R., 1971a. Atlas des pollens d'Ethiopie principales especes des forests de montagne. Pollen et Spore 13, 15–72.

Bonnefille, R., 1971b. Atlas des pollens d'Ethiopie. Adansonia 11, 463–518.

Bousquet, P., Ciais, P., Peylin, P., Ramonet, M., Monfray, P., 1999. Inverse modeling of annual atmospheric CO2 sources and sinks: 1. Method and control inversion. Journal of Geophysical Research: Atmospheres 104, 26161–26178.

Branonnot, P., Marzin, C., Gregoire, L., Mosquet, E., Marti, O., 2008. Monsoon response to changes in Earth's orbital parameters: comparisons between simulations of the Eemian and of the Holocene. Climate of the Past 4, 281–294.

Bradshaw, R.H.W., 1981. Modern pollen representation factors for woods in south-east England. Journal of Ecology 69, 45–70.

Brook, G.A., Scott, L., Railsback, L.B., Goddard, E.A., 2010. A 35 ka pollen and isotope record of environmental change along the southern margin of the Kalahari from a stalagmite and animal dung deposits in Wonderwerk Cave, South Africa. Journal of Arid Environments 74, 870–884.

Brown, A.G., 1999. Biodiversity and Pollen Analysis: Modern Pollen Studies and the Recent History of a Floodplain Woodland in S. W. Ireland. Journal of Biogeography 26, 19–32.

Brugam, R.B., 1978. Pollen indicators of land-use change in southern Connecticut. Quaternary Research 9, 349–362.

Bryant, V.M., 1986. The Palynology of Archaeological Sites, 1985, Geoffrey W. Dimbleby, Academic Press, Inc. 176 + xii p., $45.00. Geoarchaeology 1, 311–312.

Buob, S., Stephan, G., 2011. To mitigate or to adapt: How to confront global climate change. European Journal of Political Economy 27, 1–16.

Bush, M.B., Weng, C., 2007. Introducing a new (freeware) tool for palynology. Journal of Biogeography 34, 377–380.

Camberlin, P., Janicot, S., Poccard, I., 2001. Seasonality and atmospheric dynamics of the teleconnection between African rainfall and tropical sea-surface temperature: Atlantic vs. ENSO. International Journal of Climatology 21, 973–1005.

Campo, E.V., Duplessy, J.C., Rossignol-Strick, M., 1982. Climatic conditions deduced from a 150-kyr oxygen isotope-pollen record from the Arabian Sea. Nature 296, 56–59.

Carcaillet, C., Almquist, H., Asnong, H., Bradshaw, R.H.W., Carrión, J.S., Gaillard, M.J., Gajewski, K., Haas, J.N., Haberle, S.G., Hadorn, P., Müller, S.D., Richard, P.J.H., Richoz, I., Rösch, M., Sánchez Goñi, M.F., von Stedingk, H., Stevenson, A.C., Talon, B., Tardy, C., Tinner, W., Tryterud, E., Wick, L., Willis, K.J., 2002. Holocene biomass burning and global dynamics of the carbon cycle. Chemosphere 49, 845–863.

Carter, T.R., Jones, P.D., Hulme, M., New, M., 2004. A comprehensive set of high-resolution grids of monthly climate for Europe and the globe: The observed record (1901–2000) and 16 scenarios (2001–2100). Tyndall Working Paper 55.

Christensen, J.H., Hewitson, B., Busuioc, A., Chen, A., Gao, X., Held, R., Jones, R., Kolli, R.K., Kwon, W.K., Laprise, R., Magana Rueda, V., Mearns, L., Menendez, C. G., Räisänen, J., Rinke, A., Sarr, A. , Whetton, P., Arritt, R., Benestad, R., Beniston, M. , Bromwich, D., Caya, D., Comiso, J., de Elia, R. and Dethloff, K., 2007. Regional climate projections, Climate Change, 2007: The Physical Science Basis. Contribution of Working group I to the Fourth Assessment Report of the Intergovernmental Panel on Climate Change. University Press, Cambridge.

Clark, J., Royall, P.D., 1995. Particle-Size Evidence for Souce Areas of Charcoal Accumulation in Late Holocene Sediments of Eastern North American Lakes. Quaternary Research. 43, 80–89.

Clark, J.S., 1988. Particle motion and the theory of charcoal analysis: source area, transport, deposition, and sampling. Quaternary Research 30, 67–80.

Clark, J.S., Lynch, J.A., Stocks, B.J., Goldammer, J.G., 1998. Relationships between charcoal particles in air and sediments in west-central Siberia. The Holocene 8, 19–29.

Clement, A.C., Hall, A., Broccoli, A.J., 2004. The importance of precessional signals in the tropical climate. Climate Dynamics 22, 327–341.

Coles, G.M., Hunt, C.O., Jenkinson, R.D.S., 1989. Taphonomy and the Palynology of Cave Deposits. Cave Science 16, 83–90.

Colinvaux, P.A., De Oliveira, P.E., Moreno, J.E., 1999. Amazon pollen manual and atlas. Harwood Academic Press., New York.

Cortese, G., Abelmann, A., Gersonde, R., 2007. The last five glacial-interglacial transitions: A high-resolution 450,000-year record from the subantarctic Atlantic. Paleoceanography 22, PA4203.

Cowling, S.A., Cox, P.M., Jones, C.D., Maslin, M.A., Peros, M., Spall, S.A., 2008. Simulated glacial and interglacial vegetation across Africa: Implications for species phylogenies and trans-African migration of plants and animals. Global Change Biology 14, 827–840.

Crane, P.R., Friis, E.M., Pedersen, K.R., 1995. The origin and early diversification of angiosperms. Nature 374, 27–33.

Crowley, T.J., 1992. North Atlantic Deep Water cools the southern hemisphere. Paleoceanography 7, 489–497.

Daniau, A.-L., Sánchez Goñi, M.F., Martinez, P., Urrego, D.H., Bout-Roumazeilles, V., Desprat, S., Marlon, J.R., 2013. Orbital-scale climate forcing of grassland burning in southern Africa. Proceedings of the National Academy of Sciences.

Davis, M., Shaw, R.G., 2001. Range Shifts and Adaptative Responses to Quaternary Climate Change. Science 292, 673–979.

De Michele, C., Accatino, F., Vezzoli, R., Scholes, R.J., 2011. Savanna domain in the herbivores-fire parameter space exploiting a tree–grass–soil water dynamic model. Journal of Theoretical Biology 289, 74–82.

Delcourt, H.R., Delcourt, P.A., 1991. Quaternary Ecology: A Paleoecological Perspective. Chapman and Hall.

deMenocal, P.B., 2004. African climate change and faunal evolution during the Pliocene–Pleistocene. Earth and Planetary Science Letters 220, 3–24.

deMenocal, P.B., Ruddiman, W.F., Pokras, E.M., 1993. Influences of High- and Low-Latitude Processes on African Terrestrial Climate: Pleistocene Eolian Records from Equatorial Atlantic Ocean Drilling Program Site 663. Paleoceanography 8, 209–242.

Denison, S.M., Maslin, M.A., Boot, C., Pancost, R.D., Ettwein, V.J., 2005. Precession-forced changes in South West African vegetation during Marine Isotope Stages 101–100 (~2.56–2.51 Ma). Palaeogeography, Palaeoclimatology, Palaeoecology 220, 375–386.

Duffin, K.I., Gillson, L., Willis, K.J., 2008. Testing the sensitivity of charcoal as an indicator of fire events in savanna environments: quantitative predictions of fire proximity, area and intensity. The Holocene 18, 279–291.

Dupont, L., 2011. Orbital scale vegetation change in Africa. Quaternary Science Reviews 30, 3589–3602.

Dupont, L., Beug, H.J., Stalling, H., Tiedemann, R., 1989. First palynological results from site 658 at 21°N off northwest Africa: Pollen as climate indicators, In: Ruddiman, W., Sarnthein M., et al. (Ed.), Proceedings of the Ocean Drilling Program, Scientific Results.

Dupont, L., Schneider, R., Schmüser, S., Jahns, S., 1999. Marine-terrestrial interaction of climate changes in West Equatorial Africa of the last 190,000 years. Palaeoecology of Africa 26, 61–84.

Dupont, L.M., Agwu, C.O.C., 1992. Latitudinal shifts of forest and savanna in N. W. Africa during the Brunhes chron: further marine palynological results from site M 16415 (9°N, 19°W). Vegetation History and Archaeobotany 1, 163–175.

Dupont, L.M., Jahns, S., Marret, F., Ning, S., 2000. Vegetation change in equatorial West Africa: Time-slices for the last 150 ka. Palaeogeography, Palaeoclimatology, Palaeoecology 155, 95–122.

Dupont, L.M., Marret, F., Winn, K., 1998. Land-sea correlation by means of terrestrial and marine palynomorphs from the equatorial East Atlantic: phasing of SE trade

winds and the oceanic productivity. Palaeogeography, Palaeoclimatology, Palaeoecology 142, 51–84.

Dupont, L.M., Weinelt, M., 1996. Vegetation history of the savanna corridor between the Guinean and the Congolian rain forest during the last 150,000 years. Vegetation History and Archaeobotany 5, 273–292.

El Ghazali, G.E.B., 1993. A study on the pollen flora of Sudan. Review of Palaeobotany and Palynology 76, 99–345.

Elenga, H., Schwartz, D., Vincens, A., 1994. Pollen evidence for Late Quaternary vegetation and inferred climate changes in Congo. Palaeogeography Palaeoclimatology Palaeoecology 109, 345–346.

Emiliani, C., 1955. Pleistocene temperatures. Journal of Geology 63, 538–578.

EPICA members, 2004. Eight glacial cycles from an Antarctic ice core. Nature 429, 623–628.

Faegri, K., Iversen, J., 1989. Textbook of pollen analysis, 4th ed. Wiley, Chichester.

Felton, A.A., Russell, J.M., Cohen, A.S., Baker, M.E., Chesley, J.T., Lezzar, K.E., McGlue, M.M., Pigati, J.S., Quade, J., Curt Stager, J., Tiercelin, J.J., 2007. Paleolimnological evidence for the onset and termination of glacial aridity from Lake Tanganyika, Tropical East Africa. Palaeogeography, Palaeoclimatology, Palaeoecology 252, 405–423.

Feynman, J., Ruzmaikin, A., 2007. Climate stability and the development of agricultural societies. Climatic Change 84.

Finsinger, W., Tinner, W., 2005. Minimum count sums for charcoal concentration estimates in pollen slides: accuracy and potential errors. The Holocene 15, 293–297.

Fjeldsaå, J., Ehrlich, D., Lambin, E., Prins, E., 1997. Are biodiversity 'hotspots' correlated with current ecoclimatic stability? A pilot study using the NOAA-AVHRR remote sensing data. Biodiversity & Conservation 6, 401–422.

Forseth, I., 2012. Terrestrial Biomes. Nature Education Knowledge 3.

Fréchette, B., Wolfe, A.P., Miller, G.H., Richard, P.J.H., de Vernal, A., 2006. Vegetation and climate of the last interglacial on Baffin Island, Arctic Canada. Palaeogeography, Palaeoclimatology, Palaeoecology 236, 91–106.

Frédoux, A., 1994. Pollen analysis of a deep-sea core in the Gulf of Guinea: vegetation and climatic changes during the last 225,000 years B.P. Palaeogeography, Palaeoclimatology, Palaeoecology 109, 317–330.

Gasse, F., 2000. Hydrological changes in the African tropics since the last glacial maximum. Quaternary Science Reviews 19, 189–211.

Gasse, F., Van Campo, E., 1998. A 40,000-yr Pollen and Diatom Record from Lake Tritrivakely, Madagascar, in the Southern Tropics. Quaternary Research 49, 299–311.

Gill, H.E., 1969. A ground-water reconnaissance of the Republic of Ghana, with a description of geohydrologic provinces. USGS Water Supply Paper 1757–K.

Gosling, W.D., Mayle, F.E., Nicholas, J., Killeem, T.J., 2009. Differentiation between neotropical rainforest, dry forest and savannah ecosystem by their modern pollen spectra and implications for the fossil pollen record. Review of Palaeobotany & Palynology 153, 70–85.

Gosling, W.D., Miller, C.S., Livingstone, D.A., 2013. Atlas of the tropical West African pollen flora. Review of Palaeobotany & Palynology 199, 1–136.

Goudie, A.S., 1996. Climate: past and present., In: Adams, W.M., Goudie, A.S., Orme, A.R. (Eds.), The Physical Geography of Africa, Oxford, pp. 34–59.

Grün, R., Stringer, C.B., 1991. Electron spin resonance dating and the evolution of modern humans. Archaeometry 33, 153–199.

Gupta, A.K., Anderson, D.M., Overpeck, J.T., 2003. Abrupt changes in the Holocene Asian southwest monsoon and their links to the north Atlanic. Nature 421, 354–357.

Hall, J.B., Swaine, M.D., 1981. Distribution and Ecology of Vascular Plants in a Tropical Rain Forest. Forest Vegetation in Ghana. The Hague, Junk.

Hanselman, J.A., Gosling, W.D., Ralph, G.M., Bush, M.B., 2005. Contrasting histories of MIS 5e and the Holocene from Lake Titicaca (Bolivia/Peru). Journal of Quaternary Science 20, 663–670.

Hays, J.D., Imbrie, J., Shackleton, N.J., 1976. Variations in the Earth's orbit: Pacemaker of the ice ages. Science 194, 1121–1132.

Hetherington, R., Reid, R.G.B., 2010. The Climate Connection: Climate Change and Modern Human Evolution. Cambridge University Press.

Higuera, P.E., Peters, M.E., Brubaker, L.B., Gavin, D.G., 2007. Understanding the origin and analysis of sediment-charcoal records with a simulation model. Quaternary Science Reviews 26, 1790–1809.

Hill, M.O., Gauch, H.G. 1980. Detrended correspondence qnalysis: An improved ordination technique. Vegetatio 42, 47–58.

Hodell, D.A., Charles, C.D., Ninnemann, U.S., 2000. Comparison of interglacial stages in the South Atlantic sector of the southern ocean for the past 450 kyr: implifications for Marine Isotope Stage (MIS) 11. Global and Planetary Change 24, 7–26.

Holdridge, L.R., Grenke, W.C., Hatheway, W.H., Liang, T., Tosi, J.A. 1971. Forest environments in tropical life zones: A pilot study. Pergamon Press, Oxford.

Hooghiemstra, H., 1988. Palynological records from northwest African marine sediments: a general outline of the interpretation of the pollen signal. Philosophical Transactions of the Royal Society of London 318, 431–449.

Hooghiemstra, H., 1988. The orbital-tuned marine oxygen isotope record applied to the middle and Late Pleistocene pollen record of Funza (Colombian Andes). Palaeogeography, Palaeoclimatology, Palaeoecology 66, 9–17.

Hooghiemstra, H., Agwu, C.O.C., 1988. Changes in the vegetation and trade winds in equatorial northwest Africa 140,000–70,000 yr B.P. as deduced from two marine pollen records. Palaeogeography, Palaeoclimatology, Palaeoecology 66, 173–184, 193–204, 211–213.

Hooghiemstra, H., 1989. Variations of the NW African trade wind regime during the last 14,000 years: changes in pollen flux evidenced by marine sediment records. In: Leinen, M., Sarnthein, M. (Eds.), Palaeoclimatology and Palaeometeorology:

Modern and Past Patterns of Global Atmospheric Transport. Kluwer, Dordrecht, 733–770.

Hooghiemstra, H., Lezine, A.-M., Leroy, S.A.G., Dupont, L., Marret, F., 2006. Late Quaternary palynology in marine sediments: A synthesis of the understanding of pollen distribution patterns in the NW African setting. Quaternary International 148, 29–44.

Howard, W.H., 1997. A warm future in the past. Nature 388, 418–419.

ICDP website, I.B., http://www.icdp-online.org/front_content.php?idcat=391

Imbrie, J., 1992. On the structure and origin of major glaciation cycles 1. Linear responses to Milankovitch forcing. Paleoceanography 7, 701–738.

Imbrie, J.D., Hays, J., Martinson, D.G., McIntyre, A., Mix, A., Morley, J.J., Pisias, N.G., Prell, W.L., Shackleton, N.J., 1984. The orbital theory of Pleistocene climate: support from a revised chronology of the marine 18O record., In: Berger, A.L., Imbrie, J., Hays, J., Kukla, G., Saltzman, B. (Eds.), Milankovitch and Climate. Reidel, Dordrecht, Netherlands, pp. 269–305.

IPCC, 2007. Climate Change 2007: The physical science basis. Contribution of Working Group I to the Fourth Assessment Report of the Intergovernmental Panel on Climate Change. Cambridge Univiersity Press, Cambridge & New York.

Jacobson, J.G.L., Bradshaw, R.H.W., 1981. The selection of sites for paleovegetational studies. Quaternary Research 16, 80–96.

James, R, Washington, R., Rowell, D.P., 2013. Implications of global warming for the climate of African rainforests. Philosophical Transactions of the Royal Society 368.

Jahns, S., Hüls, M., Sarnthein, M., 1998. Vegetation and climate history of west equatorial Africa based on a marine pollen record off Liberia (site GIK 16776) covering the last 400,000 years. Review of Palaeobotany and Palynology 102, 277–288.

Jahns, S., 1996. Vegetation history and climate changes in West Equatorial Africa during the Late Pleistocene and Holocene, based on a marine pollen diagram from the Congo fan. Vegetation History and Archaeobotany 5, 207–213.

Jolly, D., Harrison, S.P., Damnati, B., Bonnefille, R., 1998. Simulated climate and biomes of Africa during the late quaternary: comparison with pollen and lake status data. Quaternary Science Reviews 17, 629–657.

Jolly, D., Prentice, I.C., Bonnefille, R., Ballouche, A., Bengo, M., Brenac, P., Buchet, G., Burney, D., Cazet, J.-P., Cheddadi, R., Edorh, T., Elenga, H., Elmoutaki, S., Guiot, J., Laarif, F., Lamb, H., Lezine, A.-M., Maley, J., Mbenza, M., Peyron, O., Reille, M., Reynaud-Farrera, I., Riollet, G., Ritchie, J.C., Roche, E., Scott, L., Ssemmanda, I., Straka, H., Umer, M., Van Campo, E., Vilimumbalo, S., Vincens, A., Waller, M., 1998. Biome reconstruction from pollen and plant macrofossil data for Africa and the Arabian peninsula at 0 and 6000 years. Journal of Biogeography 25, 1007–1027.

Jourdan, F., Renne, P.R., Reimold, W.U., 2009. An appraisal of the ages of terrestrial impact structures. Earth and Planetary Science Letters 286, 1–13.

Juggins, S., 2005. C2 Program version 1.5. Department of Geography, University of Newcastle, Newcastle upon Tyne, UK.

Kenrick, P., Crane, P.R., 1997. The origin and early evolution of plants on land. Nature 389, 33–39.

Koeberl, C., Bottomley, R., Glass, B.P., Storzer, D., 1997. Geochemistry and age of Ivory Coast tektites and microtektites. Geochimica et Cosmochimica Acta 61, 1745–1772.

Koeberl, C., Milkereit, B., Overpeck, J.T., Scholz, C.A., Amoako, P.Y.O., Boamah, D., Danuor, S.K., Karp, T., Kueck, J., Hecky, R.E., King, J.W., Peack, J.A., 2007. An international and multidisciplinary drilling project into a young complex impact structure: The 2004 ICDP Bosumtwi Crater Drilling Project- An overview. Meteoritics and Planetary Science 42, 483–511.

Koeberl, C., Peck, J., King, J.W., Milkereit, B., Overpeck, J.T., Scholz, C.A., 2005. The ICDP Lake Bosumtwi drilling project: a first report. Scientific Drilling 1, 23–27.

Kukla, G., McManus, J.F., Rousseau, D.-D., Chuine, I., 1997. How long and how stable was the last interglacial? Quaternary Science Reviews 16, 605–612.

Kutzbach, J., 1981. Monsoon Climate of the Early Holocene: Climate Experiment with the Earth's Orbital Parameters for 9000 Years Ago. Science 214, 59–61.

Kutzbach, J.E., Street-Perrott, F.A., 1985. Milankovitch forcing of fluctuations in the level of tropical lakes from 18 to 0 kyr BP. Nature 317, 130–134.

Kwiatkowski, A., Lubliner-Mianowska, K., 1957. Badanie skladu chemicznego pylku II. Acta Societatis Botanicorum Poloniae 26, 501–514.

Lang, N., Wolff, E.W., 2011. Interglacial and glacial variability from the last 800 ka in marine, ice and terrestrial archives. Climate of the Past 7, 361–380.

Larrasoaña, J.C., Roberts, A.P., Rohling, E.J., Winklhofer, M., Wehausen, R., 2003. Three million years of monsoon variability over the northern Sahara. Climate Dynamics 21, 689–698.

Laskar, J., Fienga, A., Gastineau, M., Manche, H., 2011. La2010: a new orbital solution for the long-term motion. Astronomy and Astrophysics 532.

Lee, S.Y., Poulsen, C.J., 2005. Tropical Pacific climate response to obliquity forcing in the Pleistocene. Paleoceanography 20, PA4010.

Leroy, S., Dupont, L., 1994. Development of vegetation and continental aridity in northwestern Africa during the Late Pliocene: the pollen record of ODP site 658. Palaeogeography, Palaeoclimatology, Palaeoecology 109, 295–316.

Leroy, S.A.G., Marco, S., Bookman, R., Miller, C.S., 2010. Impact of earthquakes on agriculture during the Roman–Byzantine period from pollen records of the Dead Sea laminated sediment. Quaternary Research 73, 191–200.

Lewis, S.L., Lopez-Gonzalez, G., Sonke, B., Affum-Baffoe, K., Baker, T.R., Ojo, L.O., Phillips, O.L., Reitsma, J.M., White, L., Comiskey, J.A., Djuikouo K, M.-N., Ewango, C.E.N., Feldpausch, T.R., Hamilton, A.C., Gloor, M., Hart, T., Hladik, A., Lloyd, J., Lovett, J.C., Makana, J.-R., Malhi, Y., Mbago, F.M., Ndangalasi, H.J., Peacock, J., Peh, K.S.-H., Sheil, D., Sunderland, T., Swaine, M.D., Taplin, J., Taylor, D., Thomas, S.C., Votere, R., Wöll, H., 2009. Increasing carbon storage in intact African tropical forests. Nature 457, 1003–1006.

Lezine, A.-M., 1991. West African paleoclimates during the last climatic cycle inferred from an Atlantic deep-sea pollen record. Quaternary Research 35, 456–463.

Lézine, A.-M., Casanova, J., 1991. Correlated oceanic and continental records demonstrate past climate and hydrology of North Africa (0–140 ka). Geology 19, 307–310.

Lezine, A.-M., Cazet, J.-P., 2005. High-resolution pollen record from core KW31, Gulf of Guinea, documents the history of the lowland forests of West Equatorial Africa since 40,000 yr ago. Quaternary Research 64, 432–443.

Lézine, A.M., 2005. African Pollen Database, http://medias.obs-mip.fr/apd/accueil.htm.

Lezine, A.M., Vergnaud-Grazzini, C., 1993. Evidence of forest extension in West Africa since 22,000 BP: A pollen record from the eastern tropical Atlantic. Quaternary Science Reviews 12, 203–210.

Liu, K.-b., Reese, C.A., Thompson, L.G., 2005. Ice-core pollen record of climatic changes in the central Andes during the last 400 yr. Quaternary Research 64, 272–278.

Loutre, M.F., Berger, A., 2003. Marine Isotope Stage 11 as an analogue for the present interglacial. Global and Planetary Change 36, 209–217.

Lowe, J.J., Walker, M.J.C., 1997. Reconstructing Quaternary environments (2nd edition). Longman, London.

Luthi, D., Le Floch, M., Bereiter, B., Blunier, T., Barnola, J.-M., Siegenthaler, U., Raynaud, D., Jouzel, J., Fischer, H., Kawamura, K., Stocker, T.F., 2008. High-resolution carbon dioxide concentration record 650,000–800,000 years before present. Nature 453, 379–382.

Maley, J., 1970. Contributions a l'etude du Bassin tchadien Atlas de pollens du Tchad. Bulletin du Jardin botanique national de Belgique 40, 29–48.

Maley, J., 1991. The African rain forest vegetation and palaeoenvironments during the late Quaternary. Climate Change 19, 79–98.

Maley, J., Brenac, P., 1998. Vegetation dynamics, palaeoenvironmenal and climatic changes in the forests of western Cameroon during the last 28,000 years B.P. Review of Palaeobotany and Palynology 99, 157–187.

Maley, J., Livingstone, D.A., 1983. Extension d'un element montagnard dans le sud du Ghana (Afrique de l'Ouest) au Pleistocene superieur et a l'Holocene inferieur: premieres donnees polliniques. Comptes Rendus des Seances - Academie, Serie II 296, 1287–1292.

Manabe, S., Stouffer, R.J., 1997. Coupled ocean-atmosphere model response to freshwater input: Comparison to Younger Dryas Event. Paleoceanography 12, 321–336.

Mann, M., Lees, J., 1996. Robust estimation of background noise and signal detection in climatic time series. Climatic Change 33, 409–445.

Mantsis, D.F., Clement, A.C., Broccoli, A.J., Erb, M.P., 2011. Climate Feedbacks in Response to Changes in Obliquity. Journal of Climate 24, 2830–2845.

Marean, C.W., Bar-Matthews, M., Bernatchez, J., Fisher, E., Goldberg, P., Herries, A.I.R., Jacobs, Z., Jerardino, A., Karkanas, P., Minichillo, T., Nilssen, P.J., Thompson, E., Watts, I., Williams, H.M., 2007. Early human use of marine resources and pigment in South Africa during the Middle Pleistocene. Nature 449, 905–908.

Marret, F., Kim, S.-Y., Scourse, J., 2013. A 30,000 kyr record of land–ocean interaction in the eastern Gulf of Guinea. Quaternary Research.

Marret, F., Scourse, J., Kennedy, H., Ufkes, E., Jansen, J.H.F., 2008. Marine production in the Congo-influenced SE Atlantic over the past 30,000 years: A novel dinoflagellate-cyst based transfer function approach. Marine Micropaleontology 68, 198–222.

Maslin, M., Sarnthein, M., Knaack, J.J., 1996. Subtropical Eastern Atlantic climate during the Eemian. Naturwissenschaften 83, 122–126.

McDougall, I., Brown, F.H., Fleagle, J.G., 2005. Stratigraphic placement and age of modern humans from Kibish, Ethiopia. Nature 433, 733–736.

Mighall, T.M., Martínez Cortizas, A., Biester, H., Turner, S.E., 2006. Proxy climate and vegetation changes during the last five millennia in NW Iberia: Pollen and non-pollen palynomorph data from two ombrotrophic peat bogs in the North Western Iberian Peninsula. Review of Palaeobotany and Palynology 141, 203–223.

Milanković, M., 1930. Mathematische Klimalehre und astronomische Theorie der Klimaschwankungen. Borntraeger.

Mohammed, M.U., Bonnefille, R., 1998. A late Glacial/late Holocene pollen record from a highland peat at Tamsaa, Bale Mountains, south Ethiopia. Global and Planetary Change 16–17, 121–129.

Monnin, E., Indermuhle, A., Dallenbach, A., Fluckiger, J., Stauffer, B., Stocker, T.F., Raynaud, D.a.B., J-M., 2001. Atmospheric CO2 concentrations over the last glacial termination. Science 291, 112–114.

Montoya, M., Crowley, T.J., von Storch, H., 1998. Temperatures at the last interglacial simulated by a coupled ocean-atmosphere climate model. Paleoceanography 13, 170–177.

Moon, P.A., Mason, D., 1967. The geology of 1/4° field sheets 129 and 131, Bompata S.W. and N.W. Ghana Geological Survey Bulletin 31.

Moore, P.D., Webb, J.A., Collinson, M.E., 1991. Pollen analysis, 2nd ed. Blackwell Scientific, Oxford.

Myers, N., Mittermeier, R.A., Mittermeier, C.G., da Fonseca, G.A.B., Kent, J., 2000. Biodiversity hotspots for conservation priorities. Nature 403, 853–858.

Nicholson, S.E., 2001. Climatic and environmental change in Africa during the last two centuries. Climate Research 17, 123–144.

Nicholson, S.E., 2009. A revised picture of the structure of the monsoon and land ITCZ over West Africa. Climate Dynamics 32, 1155–1171.

Nicholson, S.E., Grist, J.P., 2001. A conceptual model for understanding rainfall variability in the West African Sahel on interannual and interdecadal timescales. International Journal of Climatology 21, 1733–1757.

Nicholson, S.E., Tucker, C.J., Ba, M.B., 1998. Desertification, Drought, and Surface Vegetation: An Example from the West African Sahel. Bulletin of the American Meteorological Society 79, 815–829.

Nikolova, I., Yin, Q., Berger, A., Singh, U.K., Karami, M.P., 2012. The last interglacial (Eemian) climate simulated by LOVECLIM and CCSM3. Climate of the Past Discussions 8, 5293–5340.

Ning, S., Dupont, L., 1997. Vegetation and climatic history of southwest Africa: A marine palynological record of the last 300,000 years. Vegetation History and Archaeobotany 6, 117–131.

Odgaard, B.V., 1999. Fossil pollen as a record of past biodiversity. Journal of Biogeography 26, 7–17.

Olson, D.M., Dinerstein, E., Wikramanayake, E.D., Burgess, N.D., Powell, G.V.N., Underwood, E.C., D'Amico, J.A., Itoua, I., Strand, H.E., Morrison, J.C., Louks, C.J., Allnutt, T.F., Ricketts, T.H., Kura, Y., Lamoreux, J.F., Wettengel, W.W., Hedao, P., Kassem, K.R., 2001. Terrestrial ecoregions of the world: a new map of life on earth. Bioscience 51, 933–938.

Ostrom, N.E., Long, D.T., Bell, E.M., Beals, T., 1998. The origin and cycling of particulate and sedimentary organic matter and nitrate in Lake Superior. Chemical Geology 152, 13–28.

Otto, F.E.L., Jones, R.G., Halladay, K, Allen, M.R., 2013. Attribution of changes in precipitation patterns in African rainforests. Philosophical Transactions of the Royal Society 368.

Overpeck, J.T., Rind, D., Goldberg, R., 1990. Climate-induced changes in forest disturbance and vegetation. Nature 343, 51–53.

Paillard, D., Labeyrie, L., Yiou, P., 1996. Macintosh program performs time-series analysis. Eos, Transactions, American Geophysical Union 77, 379.

Peck, J.A., Green, R.R., Shanahan, T.M., King, J.W., Overpeck, J.T., Scholtz, C.A., 2004. A magnetic mineral record of Late Quaternary tropical climate variability from Lake Bosumtwi, Ghana. Palaeogeography Palaeoclimatology Palaeoecology 215, 37–57.

Peck, J., Heil, C., King, J.W., Scholz, C.A., Shanahan, T.M., Overpeck, J., Fox, P.A., Amoako, P.Y.O., Forman, S.L., Koeberl, C., Milkereit, B., 2005. The Lake Bosumtwi Drilling Project: A 1 Ma West African Paleoclimate Record. American Geophysical Union, Fall Meeting abstract #PP13C–02.

Peet, R.K. 1974. The measurement of species diversity. Annual Review of Ecological Systems 5, 285–307.

Petit, J.R., Jouzel, J., Raynaud, D., Barkov, N.I., Barnola, J.-M., Basile, I., Chappellaz, J., Davis, M., Delaygue, G., Melmotte, M., Kotlyakov, V.M., Legrand, M., Lipenkov, V.Y., Lorius, C., Pepin, L., Ritz, C., Sltzman, E., Stievenard, M., 1999. Climate and atmospheric history of the past 420,000 years from the Vostok ice core, Antarctica. Nature 399, 429–436.

Piperno, D.R., Flannery, K.V., 2001. The earliest archaeological maize (Zea mays L.) from highland Mexico: new accelerator mass spectrometry dates and their implications. Proceedings of the National Academy of Sciences 98, 2101–2103.

Pisias, N.G., Shackleton, N.J., 1984. Modelling the global climate response to orbital forcing and atmospheric carbon dioxide changes. Nature 310, 757–759.

Pokras, E.M., Mix, A.C., 1985. Eolian evidence for spatial variability of late Quaternary climates in tropical Africa. Quaternary Research 24, 137–149.

Pokras, E.M., Mix, A.C., 1987. Earth's precession cycle and Quaternary climatic change in tropical Africa. Nature 326, 486–487.

Power, M.J., Marlon, J., Ortiz, N., Bartlein, P.J., Harrison, S.P., Mayle, F.E., Ballouche, A., Bradshaw, R.H.W., Carcaillet, C., Cordova, C., Mooney, S., Moreno, P.I., Prentice, I.C., Thonicke, K., Tinner, W., Whitlock, C., Zhang, Y., Zhao, Y., Ali, A.A., Anderson, R.S., Beer, R., Behling, H., Briles, C., Brown, K.J., Brunelle, A., Bush, M., Camill, P., Chu, G.Q., Clark, J., Colombaroli, D., Connor, S., Daniau, A.-L., Daniels, M., Dodson, J., Doughty, E., Edwards, M.E., Finsinger, W., Foster, D., Frechette, J., Gaillard, M.-J., Gavin, D.G., Gobet, E., Haberle, S., Hallett, D.J., Higuera, P., Hope, G., Horn, S., Inoue, J., Kaltenrieder, P., Kennedy, L., Kong, Z.C., Larsen, C., Long, C.J., Lynch, J., Lynch, E.A., McGlone, M., Meeks, S., Mensing, S., Meyer, G., Minckley, T., Mohr, J., Nelson, D.M., New, J., Newnham, R., Noti, R., Oswald, W., Pierce, J., Richard, P.J.H., Rowe, C., Sanchez GoÃ±i, M.F., Shuman, B.N., Takahara, H., Toney, J., Turney, C., Urrego-Sanchez, D.H., Umbanhowar, C., Vandergoes, M., Vanniere, B., Vescovi, E., Walsh, M., Wang, X., Williams, N., Wilmshurst, J., Zhang, J.H., 2008. Changes in fire regimes since the last glacial maximum: An assessment based on a global synthesis and analysis of charcoal data. Climate Dynamics 30, 887–907.

Prell, W.L., Kutzbach, J.E., 1987. Monsoon variability over the past 150,000 years. Journal of Geophysical Research 92, 8411–8425.

Prentice, I.C., 1985. Pollen representation, source area, and basin size: Toward a unified theory of pollen analysis,. Quaternary Research 23, 76–86.

Punt, W., Hoen, P.P., Blackmore, S., Nilsson, S., Le Thomas, A., 2007. Glossary of pollen and spore terminology. Review of Palaeobotany and Palynology 143, 1–81.

QPG, 2008. Cambridge University Palynological Online Database, University of Cambridge.

Ramanathan, V., Feng, Y., 2008. On avoiding dangerous anthropogenic interference with the climate system: Formidable challenges ahead. Proceedings of the National Academy of Sciences.

Raynaud, D., Barnola, J.M., Souchez, R., Lorrain, R., Petit, J.R., Duval, P., Lipenkov, V., 2005. Palaeoclimatology: The record for marine isotopic stage 11. Nature 436, 39–40.

Rayner, P.J., Enting, I.G., Francey, R.J., Langenfelds, R., 1999. Reconstructing the recent carbon cycle from atmospheric CO2, δ13C and O2/N2 observations. Tellus B 51, 213–232.

Rebelo, A.G., Siegfried, W.R., 1990. Protection of Fynbos vegetation: Ideal and real-world options. Biological Conservation 54, 15–31.

Reille, M., 1995. Pollen et spores d'Europe et d'Afrique du Nord. Laboratoire de Botanique Historique et Palynologie.

Riollet, G., Bonnefille, R., 1976. Pollen des Amaranthacées du Lac Rodolphe (Afrique orientale). Déterminations générique et spécifique. . Pollen et Spore 18, 67–92.

Roberts, D.L., Karkanas, P., Jacobs, Z., Marean, C.W., Roberts, R.G., 2012. Melting ice sheets 400,000 yr ago raised sea level by 13 m: Past analogue for future trends. Earth and Planetary Science Letters 357–358, 226–237.

Rockström, J., Steffen, W., Noone, K., Persson, A., Chapin, F. S., Lambin, E., Lenton, T. M., Scheffer, M., Folke, H.S.C., Nykvist, B., De Wit, C. A., Hughes, T., van der Leeuw, S., Rodhe, H., Sörlin, S. Snyder, R. C. K., Svedin, U., Falkenmark, M., Karlberg, L., Corell, R.W., Fabry, V.J., Hansen, J., Richardson, K. Crutzen, P., Foley., J., 2009. Planetary boundaries: Exploring the Safe Operating Space for Humanity. Ecology and Society 14.

Rossignol-Strick, M., 1983. African monsoons, an immediate climate response to orbital insolation. Nature 304, 46–49.

Roubik, D.W., Moreno, P.J.E., 1991. Pollen and Spores of Barro Colorado Island. Monographs in Systematic Botany 36, Missouri Botanical Garden.

Ruddiman, W.F., 2006. Orbital changes and climate. Quaternary Science Reviews 25, 3092–3112.

Rull, V., 1987. A note on pollen counting in palaeoecology. Pollen et Spores XXIX, 471–480.

Salzmann, U., Hoelzmann, P., 2005. The Dahomey Gap: an abrupt climatically induced rain forest fragmentation in West Africa during the late Holocene. The Holocene 15, 190–199.

Salzmann, U., Hoelzmann, P., Morczinek, I., 2002. Late Quaternary Climate and Vegetation of the Sudanian Zone of Northeast Nigeria. Quaternary Research 58, 73–83.

Sarnthein, M., Tiedemann, R., 1989. Stable isotope record of ODP Sites 108–658 and 108–659, Proceedings of the Ocean Drilling Program Scientific Results, College Station, TX (Ocean Drilling Program), pp. 167–185.

Scholz, C.A., Johnson, T.C., Cohen, A.S., King, J.W., Peck, J.A., Overpeck, J.T., Talbot, M.R., Brown, E.T., Kalindekafe, L., Amoako, P.Y.O., Lyons, R.P., Shanahan, T.M., CastaÃ±eda, I.S., Heil, C.W., Forman, S.L., McHargue, L.R., Beuning, K.R., Gomez, J., Pierson, J., 2007. East African megadroughts between 135 and 75 thousand years ago and bearing on early-modern human origins. Proceedings of the National Academy of Sciences 104, 16416–16421.

Scholz, C.A., Karp, T., Brooks, K.M., Milkereit, B., Amoako, P.Y.O., Arko, J.A., 2002. Pronounced central uplift identified in the Bosumtwi impact structure, Ghana, using multichannel seismic reflection data. Geology 30, 939–942.

Scott, L., 1982. Late quaternary fossil pollen grains from the Transvaal, South Africa. Review of Palaeobotany and Palynology 36, 241–278.

Shackleton, N.J., 2000. The 100,000 year ice-age cycle identified and found to lag temperature, carbon dioxide and orbital eccentricity. Science 289, 1897–1902.

Shackleton, N.J., Sánchez-Goñi, M.F., Pailler, D., Lancelot, Y., 2003. Marine Isotope Substage 5e and the Eemian Interglacial. Global and Planetary Change 36, 151–155.

Shanahan, T.M., Beck, J.W., Overpeck, J.T., McKay, N.P., Pigati, J.S., Peck, J.A., Scholz, C.A., Heil Jr, C.W., King, J., 2012. Late Quaternary sedimentological and

climate changes at Lake Bosumtwi Ghana: New constraints from laminae analysis and radiocarbon age modeling. Palaeogeography, Palaeoclimatology, Palaeoecology 361–362, 49–60.

Shanahan, T.M., Overpeck, J.T., Anchukaitis, K.J., Beck, J.W., Cole, J.E., Dettman, D.L., Peck, J.A., Scholz, C.A., King, J.W., 2009. Atlantic forcing of persistent drought in West Africa. Science 324.

Shanahan, T.M., Overpeck, J.T., Scholz, C.A., Beck, J.W., Peck, J., King, J.W., 2008. Abrupt changes in the water balance of tropical West Africa during the late quaternary. Journal of Geophysical Research D: Atmospheres 113.

Shanahan, T.M., Overpeck, J.T., Sharp, W.E., Scholz, C.A., Arko, J.A., 2007. Simulating the response of a closed-basin lake to recent climate changes in tropical West Africa (Lake Bosumtwi, Ghana). Hydrological Processes 21, 1678–1691.

Shanahan, T.M., Overpeck, J.T., Wheeler, C.W., Beck, J.W., Pigati, J.S., Talbot, M.R., Scholtz, C.A., Peck, J., King, J.W., 2006. Paleoclimatic varitations in West Africa from a record of late Pleistocene and Holocene lake level stands of Lake Bosumtwi, Ghana. Palaeogeography Palaeoclimatology Palaeoecology 242, 287–302.

Shanahan, T.M., Peck, J.A., McKay, N., Heil Jr, C.W., King, J., Forman, S.L., Hoffmann, D.L., Richards, D.A., Overpeck, J.T., Scholz, C., 2013. Age models for long lacustrine sediment records using multiple dating approaches – An example from Lake Bosumtwi, Ghana. Quaternary Geochronology 15, 47–60.

Shi, N., Dupont, L., 1997. Vegetation and climatic history of southwest Africa: A marine palynological record of the last 300,000 years. Vegetation History and Archaeobotany 6, 117–131.

Shi, N., Schneider, R., Beug, H.-J., Dupont, L.M., 2001. Southeast trade wind variations during the last 135 kyr: evidence from pollen spectra in eastern South Atlantic sediments. Earth and Planetary Science Letters 187, 311–321.

Siegenthaler, U., Stocker, T.F., Monnin, E., Lüthi, D., Schwander, J., Stauffer, B., Raynaud, D., Barnola, J.-M., Fischer, H., Masson-Delmotte, V., Jouzel, J., 2005. Stable Carbon Cycle–Climate Relationship During the Late Pleistocene. Science 310, 1313–1317.

Sowunmi, M.A., 1973. Pollen grains of Nigerian plants. Grana Palynologica 13, 145–186.

Sowunmi, M.A., 1981. Aspects of Late Quaternary Vegetational Changes in West Africa. Journal of Biogeography 8, 457–474.

Stockmarr, J., 1972. Tablets with spores used in absolute pollen analysis. Pollen et Spore XIII, 615–621.

Stone, J.R., Westover, K.S., Cohen, A.S., 2011. Late Pleistocene paleohydrography and diatom paleoecology of the central basin of Lake Malawi, Africa. Palaeogeography, Palaeoclimatology, Palaeoecology 303.

Street-Perrott, F.A., Grove, A.T., 1976. Environmental and climatic implications of late Quaternary lake-level fluctuations in Africa. Nature 261, 385–390.

Street-Perrott, F.A., Perrott, R.A., 1993. Holocene variation, lake levels, and climate of Africa, In: Wright, H.E., Jr., Kutzbach, J.E., Webb, T., III, Ruddiman, W.F., Street-Perrott, F.A., Bartlein, P.J. (Eds.), Global Climates Since the Last Glacial Maximum. University of Minnesota Press, Minneapolis.

Stuiver, M., Reimer, P.J., 2005. CALIB 5.0. Program and documentation.

Talbot, M.R., 2002. Nitrogen Isotopes in Palaeolimnology, In: Last, W.M., Smol, J.P. (Eds.), Tracking Environmental Change Using Lake Sediments. Springer Netherlands, pp. 401–439.

Talbot, M.R., Delibrias, G., 1980. A new late Pleistocene-Holocene water-level curve for Lake Bosumtwi, Ghana. Earth and Planetary Science Letters 47, 336–344.

Talbot, M.R., Johannessen, T., 1992. A high resolution palaeoclimatic record for the last 27 500 years in tropical West Africa from the carbon and nitrogen isotopic composition of lacustrine organic matter. Earth & Planetary Science Letters 110, 23–37.

Talbot, M.R., Livingstone, D.A., Palmer, P.G., Maley, J., Melack, J.M., Delibrias, G., Gulliksen, S., 1984. Preliminary results from sediment cores from Lake Bosumtwi, Ghana. Palaeoecology of Africa 16, 173–192.

Tarasov, P.E., Webb Iii, T., Andreev, A.A., Afanas'eva, N.B., Berezina, N.A., Bezusko, L.G., Blyakharchuk, T.A., Bolikhovskaya, N.S., Cheddadi, R., Chernavskaya,

M.M., Chernova, G.M., Dorofeyuk, N.I., Dirksen, V.G., Elina, G.A., Filimonova, L.V., Glebov, F.Z., Guiot, J., Gunova, V.S., Harrison, S.P., Jolly, D., Khomutova, V.I., Kvavadze, E.V., Osipova, I.M., Panova, N.K., Prentice, I.C., Saarse, L., Sevastyanov, D.V., Volkova, V.S., Zernitskaya, V.P., 1998. Present-day and mid-Holocene biomes reconstructed from pollen and plant macrofossil data from the former Soviet Union and Mongolia. Journal of Biogeography 25, 1029–1053.

Tiedemann, R., Sarnthein, M., Ruediger, S., 1989. Climatic changes in the western Sahara: aeolo-marine sediment record of the last 8 million years (Sites 657–661). In: Ruddiman, W., Sarnthein M., et al. (Ed.), Climatic changes in the western Sahara: aeolo-marine sediment record of the last 8 million years . Proceedings of the Ocean Drilling Program, Scientific Results, College Station, TX (Ocean Drilling Program). pp. 241–277.

Tinner, W., Conedera, M., Gobet, E., Hubschmid, P., Wehrli, M., Ammann, B., 2000. A palaeoecological attempt to classify fire sensitivity of trees in the southern Alps. The Holocene 10, 565–574.

Tinner, W., Hofstetter, S., Zeugin, F., Conedera, M., Wohlgemuth, T., Zimmermann, L., Zweifel, R., 2006. Long-distance transport of macroscopic charcoal by an intensive crown fire in the Swiss Alps - implications for fire history reconstruction. The Holocene 16, 287–292.

Trauth, M.H., Larrasoaña, J.C., Mudelsee, M., 2009. Trends, rhythms and events in Plio-Pleistocene African climate. Quaternary Science Reviews 28, 399–411.

Tuenter, E., Weber, S.L., Hilgen, F.J., Lourens, L.J., 2003. The response of the African summer monsoon to remote and local forcing due to precession and obliquity. Global and Planetary Change 36, 219–235.

Turner, B.F., Gardner, L.R., Sharp, W.E., Blood, E.R., 1996. The geochemistry of Lake Bosumtwi, a hydrologically closed basin in the humid zone of tropical Ghana. Limnology and Oceanography 41, 1415–1424.

Tzedakis, P.C., Andrieu, V., De Beaulieu, J.-L., Crowhurst, S., Follieri, M., Hooghiemstra, H., Magri, D., Reille, M., Sadori, L., Shackleton, N.J., Wijmstra, T.A., 1997. Comparison of terrestrial and marine records of changing climate of the last 500,000 years. Earth and Planetary Science Letters 150, 171–176.

van de Berg, W.J., van den Broeke, M., Ettema, J., van Meijgaard, E., Kaspar, F., 2011. Significant contribution of insolation to Eemian melting of the Greenland ice sheet. Nature Geosci 4, 679–683.

van Zinderen Bakker, E.M., 1953. South African Pollen Grains and Spores. A. A. Balkema.

van Zinderen Bakker, E.M., 1956. South African Pollen Grains and Spores. A. A. Balkema.

Van Zinderen Bakker, E.M., Coetzee, J.A., 1959. South African Pollen Grains and Spores. A. A. Balkema.

Verschuren, D., Laird, K.R., Cumming, B.F., 2000. Rainfall and drought in equatorial east Africa during the past 1,100 years. Nature 403, 410–414.

Vizy, E.K., Cook, K.H., 2002. Development and application of a mesoscale climate model for the tropics: Influence of sea surface temperature anomalies on the West African monsoon. Journal of Geophysical Research: Atmospheres 107, ACL 2-1-ACL 2–22.

von Post, L., 1967. Forest tree pollen in south Swedish peat bog deposits. Pollen et Spore 9, 375–401 (Translation from 1916 lecture by M.B. Davis and K. Faegri, Introduction by K. Faegri and J. Iversen).

Walter, R.C., Buffler, R.T., Bruggemann, J.H., Guillaume, M.M.M., Berhe, S.M., Negassi, B., Libsekal, Y., Cheng, H., Edwards, R.L., von Cosel, R., Neraudeau, D., Gagnon, M., 2000. Early human occupation of the Red Sea coast of Eritrea during the last interglacial. Nature 405, 65–69.

Wang, G.L., Eltahir, E.A.B., 2000. Biosphere-atmosphere interactions over West Africa. II: Multiple climate equilibria. Quarterly Journal Of The Royal Meteorological Society 126.

Wang, Y., Cheng, H., Lawrence Edwards, R., He, Y., Kong, X., An, Z.,Wu, J., Kelley, M.J., Dykoski, A., Li, X., 2005. The Holocene Asian monsoon: links to solar changes and north Atlantic climate. Science 308, 854–857.

Weedon, G.P., 2003. Time Series Analysis and Cyclostratigraphy: Examining Stratigraphic Records of Environmental Cycles. Cambridge University Press.

Weijer, W., Maltrud, M.E., Hecht, M.W., Dijkstra, H.A., Kliphuis, M.A., 2012. Response of the Atlantic Ocean circulation to Greenland Ice Sheet melting in a strongly-eddying ocean model. Geophysical Research Letters 39, L09606.

Weldeab, S., Lea, D.W., Schneider, R.R., Andersen, N., 2007. 155,000 Years of West African Monsoon and Ocean Thermal Evolution. Science 316, 1303–1307.

White, F., 1983. The vegetation of Africa: a descriptive memoir to accompany the UNESCO/AETFAT/UNSO vegetation map of Africa. Natural Resources Research 20, 1–356.

Wikström, N., Savolainen, V., Chase, M.W., 2001. Evolution of the angiosperms: calibrating the family tree. Proceedings of the Royal Society of London. Series B: Biological Sciences 268, 2211–2220.

Williams, J.W., Shuman, B.N., Webb III, T., Bartlein, P., Leduc, P.L., 2004. Quaternary vegetation dynamics in north American: Scaling from taxa to biomes. Ecological Monographs 74, 309–334.

Wright, L.A., 1985. Geology and Mineral Resources of West Africa. Springer.

Ybert, J.P., 1979. Altas des pollens de Côte d'Ivoire. ORSTOM, Paris.

Zachos, J., Pagani, M., Sloan, L., Thomas, E., Billups, K., 2001. Trends, Rhythms, and Aberrations in Global Climate 65 Ma to Present. Science 292, 686–693.

Zhao, M., Dupont, L., Eglinton, G., Teece, M., 2003. n-Alkane and pollen reconstruction of terrestrial climate and vegetation for N.W. Africa over the last 160 kyr. Organic Geochemistry 34, 131–143.

Ziegler, M., Tuenter, E., Lourens, L.J., 2010. The precession phase of the boreal summer monsoon as viewed from the eastern Mediterranean (ODP Site 968). Quaternary Science Reviews 29, 1481–1490.